Assessment, Repair, and Replacement of Bridges Subjected to Fire

Final Report
August 2022

BRIDGE ENGINEERING CENTER

IOWA STATE UNIVERSITY
Institute for Transportation

Sponsored by
Iowa Department of Transportation
(InTrans Project 20-734)
Federal Highway Administration

About the Bridge Engineering Center

The mission of the Bridge Engineering Center (BEC) is to conduct research on bridge technologies to help bridge designers/owners design, build, and maintain long-lasting bridges.

About the Institute for Transportation

The mission of the Institute for Transportation (InTrans) at Iowa State University is to save lives and improve economic vitality through discovery, research innovation, outreach, and the implementation of bold ideas.

Iowa State University Nondiscrimination Statement

Iowa State University does not discriminate on the basis of race, color, age, ethnicity, religion, national origin, pregnancy, sexual orientation, gender identity, genetic information, sex, marital status, disability, or status as a US veteran. Inquiries regarding nondiscrimination policies may be directed to the Office of Equal Opportunity, 3410 Beardshear Hall, 515 Morrill Road, Ames, Iowa 50011, telephone: 515-294-7612, hotline: 515-294-1222, email: eooffice@iastate.edu.

Disclaimer Notice

The contents of this report reflect the views of the authors, who are responsible for the facts and the accuracy of the information presented herein. The opinions, findings and conclusions expressed in this publication are those of the authors and not necessarily those of the sponsors.

The sponsors assume no liability for the contents or use of the information contained in this document. This report does not constitute a standard, specification, or regulation.

The sponsors do not endorse products or manufacturers. Trademarks or manufacturers' names appear in this report only because they are considered essential to the objective of the document.

Quality Assurance Statement

The Federal Highway Administration (FHWA) provides high-quality information to serve Government, industry, and the public in a manner that promotes public understanding. Standards and policies are used to ensure and maximize the quality, objectivity, utility, and integrity of its information. The FHWA periodically reviews quality issues and adjusts its programs and processes to ensure continuous quality improvement.

Iowa DOT Statements

Federal and state laws prohibit employment and/or public accommodation discrimination on the basis of age, color, creed, disability, gender identity, national origin, pregnancy, race, religion, sex, sexual orientation or veteran's status. If you believe you have been discriminated against, please contact the Iowa Civil Rights Commission at 800-457-4416 or the Iowa Department of Transportation affirmative action officer. If you need accommodations because of a disability to access the Iowa Department of Transportation's services, contact the agency's affirmative action officer at 800-262-0003.

The preparation of this report was financed in part through funds provided by the Iowa Department of Transportation through its "Second Revised Agreement for the Management of Research Conducted by Iowa State University for the Iowa Department of Transportation" and its amendments.

The opinions, findings, and conclusions expressed in this publication are those of the authors and not necessarily those of the Iowa Department of Transportation or the U.S. Department of Transportation Federal Highway Administration.

Technical Report Documentation Page

1. Report No.	2. Government Accession No.	3. Recipient's Catalog No.
InTrans Project 20-734		

4. Assessment, repair, and replacement of bridges subjected to fire	5. Report Date
Assessment, Repair, and Replacement of Bridges Subjected to Fire	August 2022
	6. Performing Organization Code

7. Author(s)	8. Performing Organization Report No.
Justin M. Dahlberg (orcid.org/0000-0002-6184-4122) and Brent M. Phares (orcid.org/0000-0001-5894-4774)	InTrans Project 20-734

9. Performing Organization Name and Address	10. Work Unit No. (TRAIS)
Bridge Engineering Center Iowa State University 2711 South Loop Drive, Suite 4700 Ames, IA 50010-8664	11. Contract or Grant No.

12. Sponsoring Organization Name and Address		13. Type of Report and Period Covered
Iowa Department of Transportation 800 Lincoln Way Ames, IA 50010	Federal Highway Administration 1200 New Jersey Avenue, SE Washington, DC 20590	Final Report
		14. Sponsoring Agency Code Federal SPR Part II, CFDA 20.205

15. Supplementary Notes

Visit https://intrans.iastate.edu/ for color pdfs of this and other research reports.

16. Abstract

Although bridge fires are not frequent events, they pose impacts on safety, traffic flow, and the economy given bridge repairs or replacement can be costly. A lack of information and the tools needed to evaluate fire damage to concrete bridges and to aid in decisions for both immediate and long-term use of fire-damaged bridges was the impetus for this research.

On October 30, 2019, multiple items within a homeless encampment were set on fire beneath the I-29 northbound bridge over the Perry Creek conduit in Sioux City, Iowa. The fire was exacerbated when a propane tank became engulfed by the flames. The bridge girders and deck were particularly vulnerable to the ground fire because of the minimal ground clearance (about 6 ft) in comparison to that of most other bridges.

Despite this unfortunate incident, it provided an opportunity to learn more about the residual condition and strength of the bridge girders through a research study. The Iowa Department of Transportation (DOT) elected for the removal and replacement of the bridge, which allowed for girders to be removed and undergo testing.

Three fire-damaged girders were selected from the bridge, carefully removed, and transported to the Iowa DOT maintenance yard in Ames, Iowa. Each girder was visually assessed and selected based on the apparent level of damage incurred: one low-level, one mid-level, and one higher-level. The goal was to compare and contrast apparent levels of damage and assess the impacts each level of damage had on the serviceability and strength of the girder.

This report provides the results and recommendations resulting from the completed load testing. The results will assist in providing more technical information with respect to fire-damaged girders to help bridge owners to develop guidelines for assessment and repair.

17. Key Words	18. Distribution Statement
bridge condition assessment—bridge girder repair—bridge girder replacement—concrete beam bridges—concrete girder strength—economic analysis—fire-damaged girders—load test results	No restrictions.

19. Security Classification (of this report)	20. Security Classification (of this page)	21. No. of Pages	22. Price
Unclassified.	Unclassified.	176	NA

ASSESSMENT, REPAIR, AND REPLACEMENT OF BRIDGES SUBJECTED TO FIRE

Final Report
August 2022

Principal Investigator
Justin Dahlberg, Research Engineer
Bridge Engineering Center, Iowa State University

Co-Principal Investigator
Brent Phares, Bridge Research Engineer
Bridge Engineering Center, Iowa State University

Research Assistant
Rabia Afzal

Authors
Justin Dahlberg and Brent Phares

Sponsored by
Iowa Department of Transportation

Preparation of this report was financed in part
through funds provided by the Iowa Department of Transportation
through its Research Management Agreement with the
Institute for Transportation
(InTrans Project 20-734)

A report from
Bridge Engineering Center
Institute for Transportation
Iowa State University
2711 South Loop Drive, Suite 4700
Ames, IA 50010-8664
Phone: 515-294-8103 / Fax: 515-294-0467
https://intrans.iastate.edu/

TABLE OF CONTENTS

LIST OF FIGURES

LIST OF TABLES

ACKNOWLEDGMENTS

The authors would like to acknowledge the Iowa Department of Transportation (DOT) for sponsoring this research using state planning and research (Federal SPR Part II, CFDA 20.205) funding. They would also like to thank the Iowa DOT technical advisory committee members for their guidance on this project:

- James Hauber, Chief structural engineer
- Michael Nop, Bridge project development engineer
- Scott Neubauer, Bridge maintenance engineer
- Darwin Bishop, District construction engineer

Finally, they would like to thank the Iowa State University structures laboratory staff for their assistance:

- Douglas Wood
- Owen Steffens
- Andrew Goreczny

EXECUTIVE SUMMARY

Project Overview

The overall goal of this study was to determine the effects on girder strength and serviceability resulting from an actual fire below a concrete girder bridge and to determine potential repair options if replacement is not required.

Problem Statement

Although bridge fires are not frequent events, they pose impacts on safety, traffic flow, and the economy given bridge repairs or replacement can be costly. A lack of information and the tools needed to evaluate fire damage to concrete bridges and aid in decisions for both immediate and long-term use of fire-damaged bridges was the impetus for this research.

Project Background

On October 30, 2019, multiple items within a homeless encampment were set on fire beneath the I-29 northbound bridge over the Perry Creek conduit in Sioux City, Iowa. The fire was exacerbated when a propane tank became engulfed by the flames. The bridge girders and deck were particularly vulnerable to the ground fire because of the minimal ground clearance (about 6 ft) in comparison to that of most other bridges.

Despite this unfortunate incident, it provided an opportunity to learn more about the residual condition and strength of the bridge girders through this research study. The Iowa Department of Transportation (DOT) elected for the removal and replacement of the bridge, which allowed for three girders to be removed to undergo testing.

The stay-in-place polycarbonate deck forms caught on fire, which aided the spread of the fire along the deck. Spalling was extensive on the concrete prestressed girders where the fire was concentrated, resulting in the exposure of steel reinforcement strands and stirrups. Per the initial condition assessment, a loss of camber was observed in three girders.

Research Objectives

The objectives of this research study were as follows:

- Develop a greater understanding of the effects on prestressed concrete girders from fire events in order to develop recommended practices for bridge owners
- Conduct a condition assessment of three girders removed from an in-service fire-damaged bridge
- Evaluate the impact of fire on the serviceability and strength for the girders through load and materials testing

- Evaluate potential repair and replacement methods
- Provide recommendations for fire prevention measures or management strategies that can be implemented for bridges

Research Description

The Iowa DOT arranged for the removal of the three selected prestressed concrete girders from the I-29 Sioux City fire-damaged bridge. The girders were brought to a test site at the Iowa DOT maintenance yard in Ames to begin visual and nondestructive evaluation (NDE) condition assessment.

Visual Assessment

Visual assessment included documenting all visible fire damage using images, notes, and sketches. Girder length, deck width, deck thickness, concrete cracks, spalling, large areas of missing concrete, color changes, and any exposed reinforcement were documented in the notes prior to load testing.

Materials Testing

Materials testing was conducted from samples extracted from one girder. Several concrete core samples were obtained to undergo compression tests, and steel strands were obtained to undergo tension tests.

Each of the samples was taken from an area near the bottom of the girder, which is an area presumably more susceptible to greater heat-related damage. The goal was to capture stress-strain curves as well as ultimate strength values to understand the material properties of the more-damaged end of the girder.

Two-Point Bending Load Tests

The three concrete girders underwent load testing to compare their serviceability and strength to the calculated behavior of the non-fire-damaged girders. Each girder underwent a two-point bending test with deflection and strain transducers in place to compare the strain and deflection values from the applied load to the calculated strain and deflection values based on the girder properties. To set up the two-point bending test, four helical piles were installed to anchor the load frame to the ground.

Once the piles had been placed, four Dyckerhoff & Widmann AG (DYWIDAG) threaded bars were connected to each of the piles. Reaction beams were placed over the DYWIDAG bars 4 ft on either side of the girder cross-section midspan, leaving 8 ft between the two bars on either side of the girder. Each reaction beam across the girder had a hollow core hydraulic cylinder ram at each end.

The hydraulic rams were connected to a single hydraulic pump so that the load could be applied uniformly and incrementally. Two load cells were used to measure the induced force. One was placed on each reaction beam between the ram and a reaction plate. Below each reaction beam, a steel plate was centered on the girder providing a single point at which the girder would be loaded. This setup ensured a constant moment region in the middle 8 ft section of the girder.

Shear Capacity Load Testing

Upon completion of the bending tests, testing of the shear capacity was completed for one girder in the laboratory at Iowa State University. The end of the girder nearer the fire epicenter was used to evaluate if reductions in shear capacity resulted from the fire.

The end section of the girder was placed on two roller supports 10 ft apart on top of two reaction blocks. The two reaction beams were used similarly to those in the bending tests with a hollow core hydraulic cylinder ram at each end. Each reaction beam was placed 1.5 ft from midspan, resulting in a 3-ft distance between the two.

Deflection data were collected at midspan during loading of the girder. Visual observation for the formation of shear cracks was also completed.

During the third cycle, the goal was to fail the girder in shear; however, the hydraulic jacks did not have enough capacity to continue the test to that point. The girder was observed for cracking during each of the three cycles of shear testing. Although occasional audible pops could be heard, no cracks were observed.

Exploration of Girder Repairs

For the girders tested in this research project, it was shown that the strength and stiffness were not significantly reduced despite the apparent damage sustained, including concrete spalling along the girder length. Given that the structural integrity remained intact, the purpose of the repairs was to focus on protecting the remaining concrete and reinforcement to ensure service life is not lost rather than on restoring any lost capacity.

Of the three girders subjected to load testing, only one girder was used to undergo repair using three different methods. The loading of the girder in its previous test was limited to that which maintained its elastic properties throughout the girder length. (The other two girders were loaded past their yield points or even to failure and, thus, repairs would not have been suitable using them).

The repairs were evaluated for simplicity, the effectiveness of protecting the remaining girder, and durability under a sustained load. The following materials/methods were chosen for demonstration with each option occupying a 10 ft length of the girder near midspan:

- Self-consolidating concrete (SCC)
- Ultra-high performance concrete (UHPC)
- SCC in combination with fiber-reinforced polymer (FRP) wrap

In each case, forms were constructed around the bottom flange to create a cast around the most damaged portions of the girder. The three repair methods were completed near midspan to maximize the load effects when tested.

Economic Analysis for Girder Repair vs. Girder Replacement

Economic feasibility is a key factor when it comes to deciding how to approach repairing a fire-damaged bridge. Repairs or partial replacements exceeding the cost of complete removal and replacements are not practical. Therefore, to aid repair decision making, a breakdown of typical costs for different repairs and girder replacements were investigated and are documented in this final report.

Key Findings

The girders had varying levels of damage that coincided with the epicenter of the fire. At a minimum, each of the girders was soot-covered and experienced some spalling of the concrete. At worst, large concrete spalls that reached the depth of reinforcement, primarily from the bottom flange of the girder, were observed.

Each of the girders, despite the visual differences in levels of damage, performed nearly equally when tested in bending. The measured deflection and strain magnitudes were within an expected range as determined by analysis of plan-documented material properties and geometric configuration. Per visual observation and load testing, the effect of the fire on the girders appeared to have been limited to the surface-level concrete and to no greater depth than the reinforcement.

Samples of the primary strand reinforcement were selected for testing, and each sample was within specifications, indicating the material properties were not ill-effected by the temperatures achieved at that level.

The level of fire effect on the concrete strength was not conclusive. Concrete core samples taken from one of the girders showed a greater concrete strength than what was specified in the plan documents.

While two of the girders were loaded in bending beyond the elastic range, the load on the third girder was reduced to remain within the elastic range to accommodate the repair methods. The ultimate capacity of the girder end that was tested for shear capacity could not be determined, because the available equipment could not generate enough shear force. Despite this fact, the girder exhibited the shear capacity required to function in service.

The primary repairs completed were necessary along the bottom flange of the girder where spalling of concrete was most significant and reinforcement had become exposed. Each repair method performed sufficiently well to protect the remaining structure during the load test and limited time of evaluation.

The simpler repair option to complete was the use of SCC only when evaluated from the perspective of constructability. Cracking of the SCC repair resulted from a sustained high load, while service loads are not likely to cause the same cracks.

The completed UHPC protection resulted in a good, durable product, but the expense and additional construction efforts present some disadvantages.

The FRP wrap provided a means for additional protection and strength if that was required; however, the workability in an overhead application and the need for a very smooth surface for full adherence presented some challenges.

Girder replacement is more expensive than girder repair; however, new girders are accompanied with a well-known structural performance and service life. The cost can vary depending on the level of damage, location, construction risks, etc. However, the largest economic impact during bridge closure is due to traffic delays and detours. The cost of construction alone does not capture the total cost of a project.

Implementation Readiness and Benefits

Different levels of fire damage require different repair methods for prestressed concrete bridges. The severity of the damage a bridge has incurred from fire greatly varies and needs to be evaluated on a case-by-case basis. In situations where the extent of damage compromises the structural integrity of a concrete bridge, replacement of partial or all components of the bridge is needed.

The longevity of repairs or undetected structural degradation due to the fire provide a level of uncertainty for long-term performance. In the event of girder replacement, bridge owners and engineers should also consider the economic impact bridge closures can have on a city or state. This must be considered in the overall decision to repair or replace damaged girders.

Being proactive to put measures in place to prevent, assess, and repair damage in case of fire occurrence is recommended. An assessment of susceptibility to fire damage during initial design and construction is recommended for new bridge projects.

Also, an assessment of in-service bridges to determine high levels of vulnerability is a good idea. Where highly vulnerable bridges are identified, specific plans for permitting or re-routing of certain vehicle types can be established or plans for the removal of storage materials can be developed if storage of flammable materials is the cause of elevated vulnerability, for example.

A fire-damage-assessment team can be formed with the goal to create guiding documents and tools for the rapid assessment of fire-damaged bridges.

Recommended Fire and Damage Prevention Measures and Management Strategies

Based on review of previous literature and case studies, the following preventive measures and management strategies are recommended to prevent damage on bridges from fire:

- A risk assessment should be required during the design phase for bridges. This can include qualitative analysis methods, quantitative analysis methods, and relative risk ranking methods.

- Different factors (deck material, location, type of bridge, cause of fire, etc.) typically involved in bridge fires should be ranked in terms of damage levels that could occur during a fire. This can help engineers and bridge owners to design against fire damage early on (e.g., proper design of bridge drainage systems to prevent the accumulation of fuel from tanker-truck incidents).

- Due to high damage levels resulting from tanker-truck fires on bridges, coordination between bridge management, fire control, engineers, DOTs, and government officials should be required through the establishment of an emergency rescue group, with a specific focus on fire incidents.

- For certain vulnerable bridges, it is recommended that tanker-truck operators use designated lanes to reduce damage levels during an incident (e.g., center lanes so other bridge users may escape safely and quickly). Through logging and reporting, some trucks may be restricted from traveling over or under a specific bridge with high fire risks dependent on the amount or type of flammable materials carried. Detour routes for these cases should be established in a guide for truck drivers.

- Guidelines for storage near or under a bridge should be implemented prior to bridge service. This should include under-bridge parking of cars and construction equipment. These guidelines should also include safety management policies, such as specific locations, placement, and restrictions for different types of stored materials. Flammable materials should be forbidden at all times.

- For bridges in isolated locations, such as some historic bridges, routine maintenance should be coordinated to prevent the buildup of ignitable materials as well as provide routine measures for fire prevention (e.g., address vandalism and arson).

1 INTRODUCTION

1.1 Purpose

This project was undertaken to develop a greater understanding of the effects of fire on prestressed concrete bridge girders and to propose methods for repair and fire prevention strategies. This chapter briefly introduces the significant impacts that fire can have on prestressed concrete girders using the northbound I-29 Bridge in Sioux City, Iowa, that was damaged by a fire beneath it in the fall of 2019 as a case study. This research built and expanded on information and data collected through other published research studies.

1.2 Report Overview

This report consists of seven chapters given the multiple phases of this research.

Chapter 1 provides an introduction on the significance of this research, presents the I-29 Sioux City Bridge case study, and discusses research scope, goals, and objectives.

Chapter 2 provides a literature review of prestressed concrete girders that have had fire damage, especially through hydrocarbon fires. It also includes results from different case studies and the impacts that fires had on the serviceability and strength of the bridges. Additionally, fire prevention and policy recommendations for bridges are addressed.

Chapter 3 describes the test setup and instrumentation used for three prestressed concrete girders obtained from the I-29 Sioux City Bridge for load, shear, and materials testing.

Chapter 4 provides information from the visual condition assessments and nondestructive evaluations (NDEs) and presents results from the load and materials tests.

Chapter 5 describes the repair methods implemented on one of the three prestressed concrete girders.

Chapter 6 presents an economic analysis of partial girder repair or replacement for similar types of concrete bridges.

Chapter 7 provides conclusions and recommendations for future work.

1.3 Research Goals and Objectives

The primary goal of this research study is to increase available information related to the assessment, repair, and replacement of prestressed concrete girders that have been damaged by fire. The objectives of this research were as follows:

- Develop a greater understanding of the effects on prestressed concrete girders from fire events in order to develop recommended practices for bridge owners
- Conduct a condition assessment of three girders removed from an in-service fire-damaged bridge
- Evaluate the impact of fire on the serviceability and strength for the girders through load and materials testing
- Evaluate potential repair and replacement methods
- Provide recommendations for fire prevention measures or management strategies that can be implemented for bridges

1.4 Research Background and Scope

Although bridge fires are not frequent events (see Table 1), they pose impacts on safety, traffic flow, and the economy given that repairs or replacement can be costly.

Table 1. Causes of bridge failures by 10-year intervals

Causes of Failure	2000-2012	1990-2000	1980-1990	Total	Percent
Internal Causes	32	36	50	118	11.1%
Scour	53	92	55	200	18.8%
Collision	51	55	57	163	15.3%
Flood	40	154	107	301	28.3%
Overload	37	31	67	135	12.7%
Fire	12	10	8	30	2.8%
Wind	8	8	1	17	1.6%
Environmental Degradation	23	22	26	71	6.7%
Earthquake	1	11	8	20	1.9%
Others	2	3	2	7	0.7%
Total	259	422	381	1,062	100.0%

Lee et al. 2013, Multidisciplinary Center for Earthquake Engineering Research (MCEER), University at Buffalo, State University of New York

The technical information on fire damage is insufficient, and few tools are provided to evaluate fire damage to concrete bridges. Those in charge of making decisions for fire-damaged bridges do not have clearly defined tools to aid in their decisions for either immediate or long-term use and condition of a damaged bridge. Furthermore, guidance is lacking to make the most economical decisions for repairing or replacing structures identified as “too-damaged.” This report assists in providing more technical information with respect to fire-damaged girders and helping bridge owners to develop guidelines, both of which are needed nationally.

On October 30, 2019, multiple items within a homeless encampment were set on fire beneath the I-29 northbound bridge over the Perry Creek conduit in Sioux City, Iowa. The fire was exacerbated when a propane tank became engulfed by the flames. The bridge girders and deck were particularly vulnerable to the ground fire because of the minimal ground clearance (about 6 ft) in comparison to that of most other bridges.

The stay-in-place polycarbonate deck forms caught on fire, which aided the spread of the fire along the deck. Spalling was extensive on the concrete prestressed girders where the fire was concentrated, resulting in the exposure of steel reinforcement strands and stirrups. Per the initial condition assessment (HDR 2019), a loss of camber was observed in Girders D, E, and F. Images of the damages incurred by the bridge are shown in Figure 1 through Figure 5.

Figure 1. I-29 Bridge fire in Sioux City, Iowa (north side of bridge looking toward west abutment)

Figure 2. Concrete spalling on concrete girder

HDR 2019

Figure 3. Exposed steel reinforcement strands and stirrups on Beam E

Figure 4. Melted polycarbonate stay-in-place forms

HDR 2019

Figure 5. Melted polycarbonate formwork between Girders G and F

Figure 6 provides a drawing that notes the specific types and locations of damage.

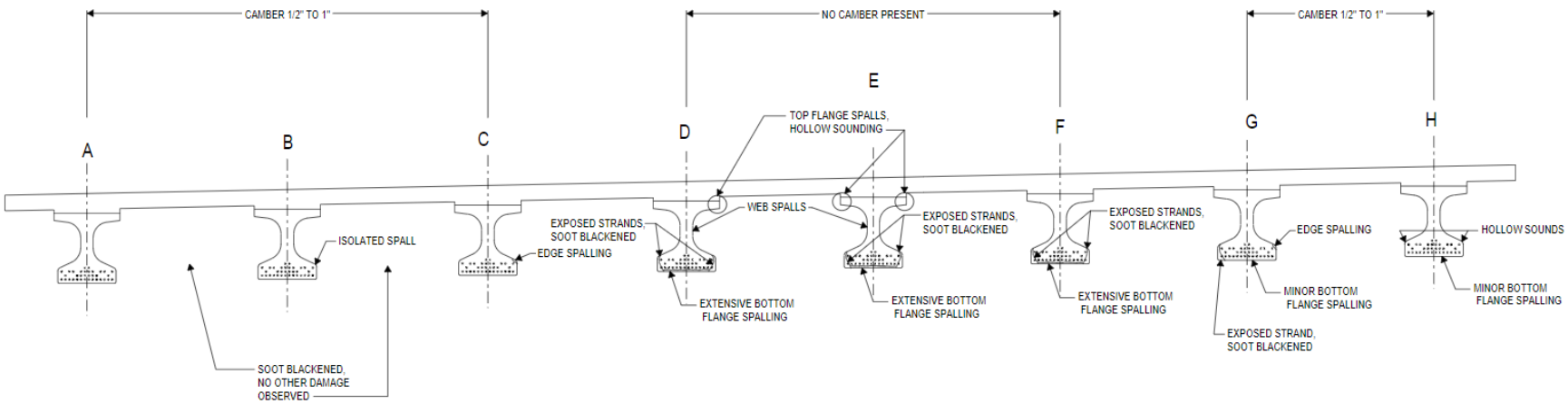

HDR 2019

Figure 6. Damage indicators on northbound bridge cross section looking upstation

Despite the unfortunate incident, an opportunity to learn more about the residual condition and strength of the bridge girders through a research study was provided. The Iowa Department of Transportation (DOT) elected for the removal and replacement of the bridge, which allowed for some components to undergo further testing. Three fire-damaged girders were selected from the I-29 Sioux City Bridge, carefully removed, and transported to the Iowa DOT maintenance yard in Ames, Iowa (see Figure 7 and Figure 8).

Figure 7. Girder transport from bridge site to Iowa DOT maintenance yard

Figure 8. Girders B, E, and G at Iowa DOT maintenance yard

Each girder was visually assessed and selected based on the apparent level of damage incurred: one low-level, one mid-level, and one higher-level. The goal was to compare and contrast apparent levels of damage and assess the impacts each had on the serviceability and strength of the girder. Girders B, E, and G were selected for this study because of the relative damage each incurred. Girder B was the least damaged, whereas Girders E and G incurred greater amounts of damage (e.g., bottom flange spalling). Figure 9 shows the approximate location of the fire epicenter based on the levels of damage observed.

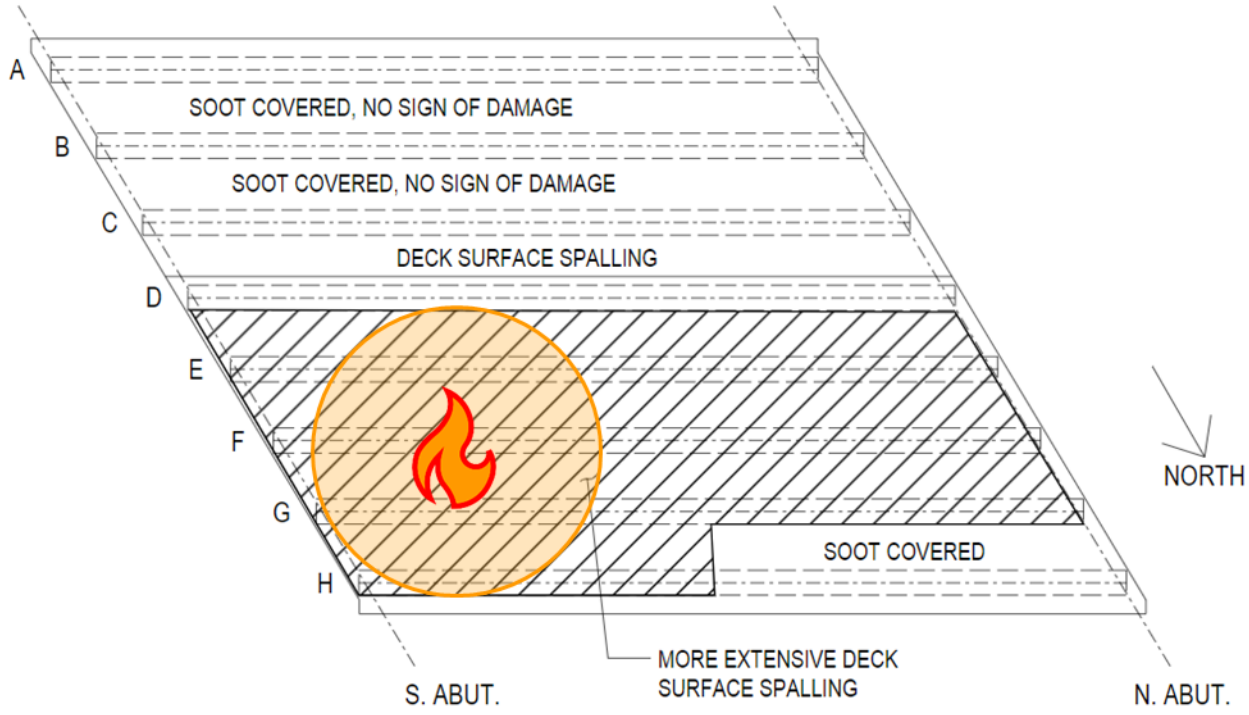

Adapted from HDR 2019

Figure 9. Bridge fire epicenter

Figure 10 shows the selected girders relative to other girders in the cross-sectional plan.

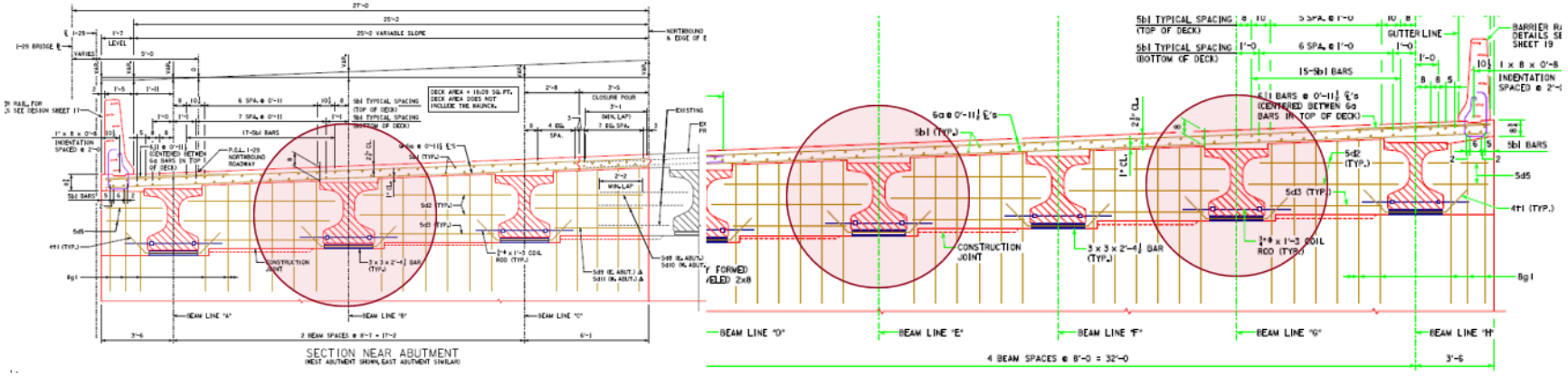

Adapted from contract plans

Figure 10. Section plan for I-29 Bridge showing Girders B, E, and G

2 LITERATURE REVIEW

2.1 Introduction

The purpose of this chapter is to present relevant literature reviewed for this research project. Much of the literature focused on the characteristics and performance of prestressed concrete girders subjected to fire. Condition assessment, load and materials testing, finite element analysis (FEA) for prestressed concrete girders subjected to fire, repair and replacement options, and the need for a guide or additional research in this area are discussed.

Furthermore, methods for fire prevention of bridge structures are discussed. Recommendations for policies that may be implemented through risk assessments, management strategies, and other preventive measures to aid in fire prevention for concrete bridges are provided. Policies that are not currently addressed or have limited research are discussed as suggestions for future work.

2.2 Condition Assessment

Although not an overly common occurrence, bridge fires can cause great damage to different structural components of a bridge. Garlock et al. (2012) conducted a review of several case studies of fire-damaged bridges and found that, not only is infrastructure impacted significantly, but the damage can also lead to major economic and public loses.

As the development of infrastructure expands and traffic numbers continue to increase, the probability is greater that bridge fires will become more common. Specifically, hydrocarbon fires are a large concern due to their severe impacts. Several case studies have noted the severity of these types of fires (e.g., Garlock et al. 2012, Davis et al. 2008, Stoddard 2004).

Garlock et al. (2012) define hydrocarbon fires through the characterization of extremely high temperatures and fast heating rates. Although hydrocarbon fires are far more severe than other types of fires (e.g., arson, wildfires, homeless encampments), the characteristics of the damage are similar in many cases.

A condition assessment is required to note the different categories of damage. Typically, a condition assessment will begin with visual inspection of the damaged girders. Garlock et.al (2012) recommended documenting color changes in the concrete, excessive cracking, spalling of concrete, and the loss of larger chunks of concrete. The researchers also mentioned how a cross-section of a beam can provide a temperature depth for the concrete alone through color responses of aggregates in the concrete (see Table 2).

Table 2. Correlation between temperature and fire-damaged concrete color

Color	Probable maximum temperature	
No discoloration	<315°C	<599°F
Pink	315–593°C	599–1,099°F
Whitish-grey	>593°C	>1,099°F
Buff (light tan)	>927°C	>1,701°F

Source: Garlock 2012

Davis et al.'s (2008) analysis of the July 2006 tanker incident on the Bill Williams River Bridge in Arizona provides a brief explanation of the methods used in condition assessment. For this study, a detailed inspection was conducted by HDR Engineering, Inc. for the fire-damaged sections. This included Spans 8, 9, and 10 and all barriers, girders, pier caps, columns, and both the tops and bottoms of the deck sections (see Figure 11).

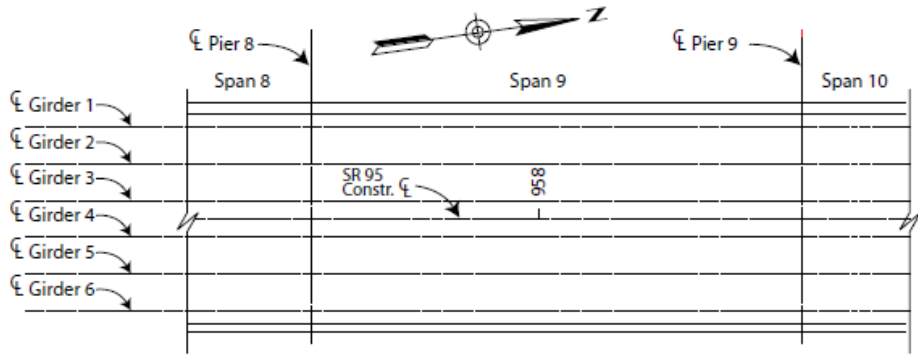

Davis et al. 2008, National Council of Structural Engineers Associations (NCSEA)

Figure 11. Bill Williams River Bridge plan view

Visual inspection consisted of noting spalled locations in the concrete and any exposed reinforcement. A key component of the inspection included a hammer test. This involved sounding a hammer to detect locations of delamination in the concrete. Davis et al. noted that much of the damage occurred on the underside of the bridge due to diesel fuel leaking through the deck drains, and specifically the drain locations on Girders 1, 2, and 6 (see Figure 12).

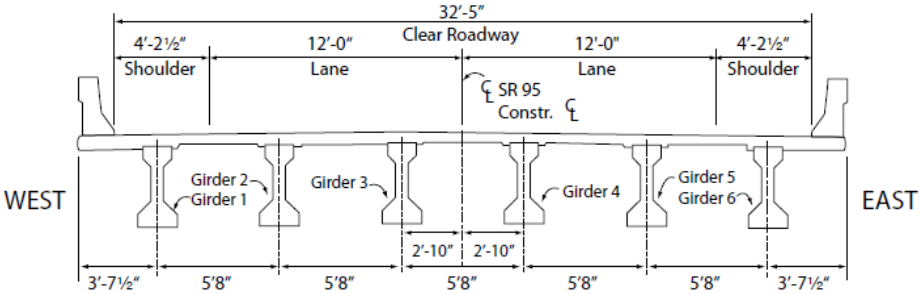

Davis et al. 2008, National Council of Structural Engineers Associations (NCSEA)

Figure 12. Typical section view

These areas had larger amounts of spalled and delaminated concrete.

Davis et al. (2008) stated that the fire-damaged girders did not show any visible signs of loss of prestressing force due to no sagging or flexural cracks being present. However, the great amount of spalling and dull tones from the hammer test indicated a significant amount of delamination. This is important to note as spalling and delamination together can indicate a loss of internal strength properties through significant exposure of reinforcement. Figure 13 shows the reduced girder section.

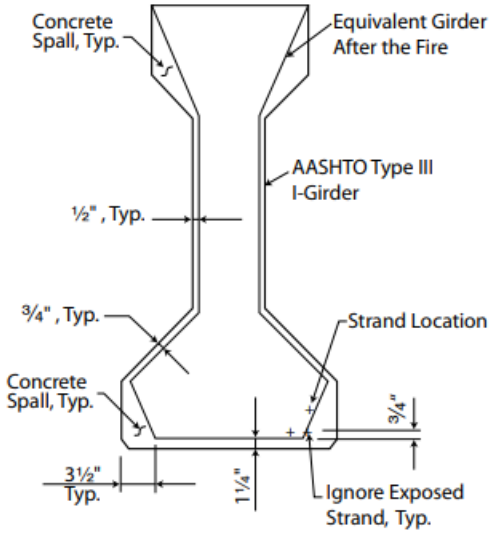

Davis et al. 2008, National Council of Structural Engineers Associations (NCSEA)

Figure 13. Girder cross section after fire damage

Color changes of concrete exposed to fire are visual indications of temperature effects, with lighter colors indicating greater damage (Stoddard 2004). Different colors also help indicate the location of the fire and which sections experienced the most intense temperatures. Stoddard (2004) discusses significant color changes found after the Puyallup River Bridge railroad tanker fire incident that occurred in Washington on December 11, 2002 (see Figure 14).

Stoddard 2004, Washington State DOT

Figure 14. Tanker fire on Puyallup River railroad bridge

Span 8 was where most of the damage occurred as the fire fully engulfed this section for an hour. Stoddard (2004) noted four concrete color variations on the bottom flanges of the girders in Span 8. These color variations correspond to changes in concrete condition states, as illustrated in Figure 15.

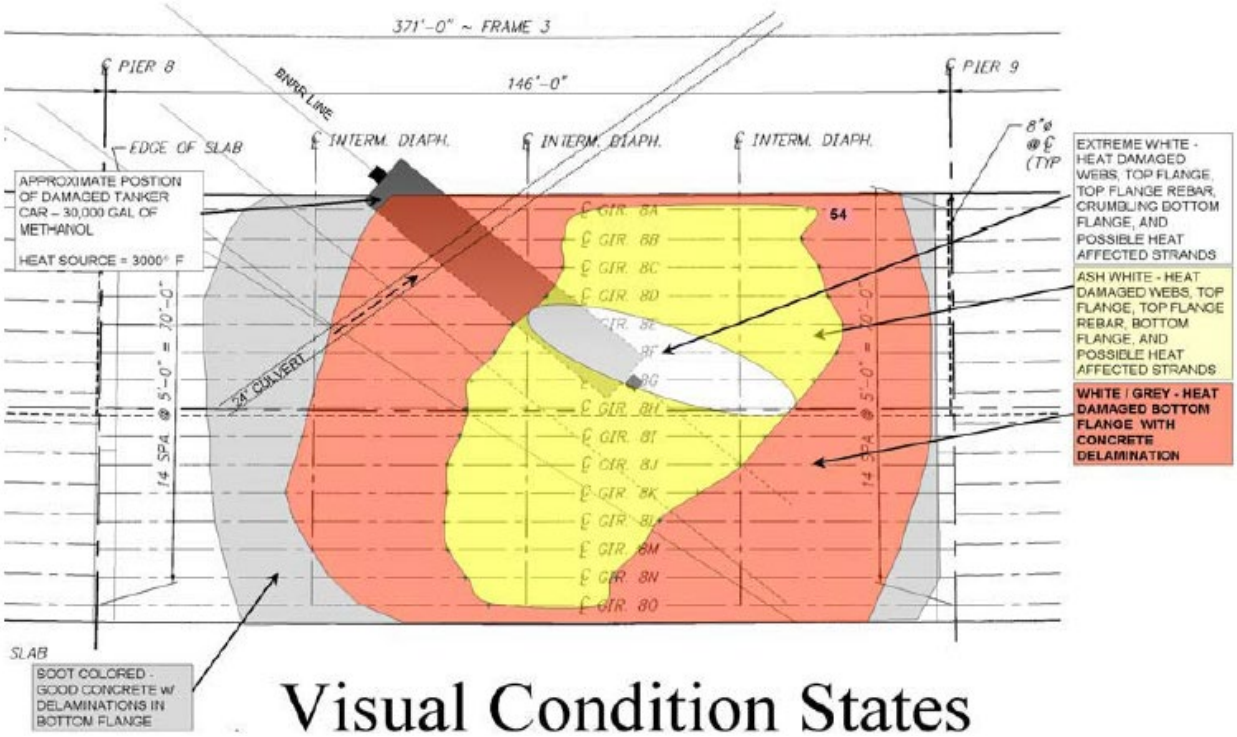

Stoddard 2004, Washington State DOT

Figure 15. Fire induced color regions

The colored regions are described as extreme-white, ash-white, white-gray, and soot.

Stoddard (2004) found that extreme-white represents exposure to the most intense heat over the fire source. This color covered about 10% of Span 8 and crumbled when sounded with a rock hammer. Larger amounts of spalling were indicated on the soffit, webs, and top flanges. The steel had deformed due to the intense heat, and the nylon reinforcing chairs burned during the fire, “leaving deep pockets in the flange soffit” (Stoddard 2004, pg.6).

The ash-white area was about 30% of Span 8 and crumbled when sounded with the rock hammer. Spalling had occurred in the webs and top flanges and only on part of the webs that were close to the fire. The nylon reinforcing chairs indicated some melting during the fire through stalactites and some pockets of charred nylon (Stoddard 2004).

White-gray encompassed 30% of Span 8. Stoddard (2004) concluded that this area could be characterized through delamination sounds in the bottom flanges during the hammer test. Although the concrete did not crumble, spalling could be produced when hit with a rock hammer. The spalled pieces were about 6 to 12 in. in size. Soot was visible on the top flanges and web, but the concrete was not damaged. More nylon stalactites had formed in this area from the heat.

The soot colored area covered 20% of Span 8. The concrete seemed to look intact; however, when struck with a rock hammer, delamination sounds were produced indicating some damage. The nylon reinforcing chairs had melted, but no stalactites were visible.

In addition to noting color changes, another way to determine the effect of varying temperatures from a fire is through observation of concrete cracking. Severe cracking can lead to large pieces of concrete falling off and exposure of the reinforcement. This exposure leads to the corrosion of prestressing strands, which in turn reduces the strength of a beam.

Chaowei et.al (2019) provided evidence for the impact of concrete cracking on beam strength through research on the material properties of prestressed concrete girders after fire exposure. The authors verified that concrete exposed to high temperatures results in large losses to concrete sections. Table 3 provides a summary of the effect of varying temperatures on the burning thickness of a concrete member.

Table 3. Relationship between fire temperature and thickness of concrete sparse layer

Burning thickness		Field temperature	
mm	in.	°C	°F
1~2	3/64~5/64	<700	<1,292
2~3	5/64~1/8	700~800	1,292~1,472
3~4	1/8~5/32	800~850	1,472~1,562
4~5	5/32~13/64	850~900	1,562~1,652
5~6	13/64~15/64	900~1,000	1,652~1,832
>6	>15/64	>1,000	>1,832

Source: Chaowei et al. 2019

The researchers stated that "when the spalling depth is less than a third of the net protective layer of the steel strand, the strength reduction coefficient is 0.85, and when the spalling depth is more than two-thirds of the net protective layer, the strength reduction factor coefficient is 0.68 in. (Chaowei et al. 2019, p.5).

Chaowei et al. (2019) also found that when temperatures exceeded 932°F (500°C), the strength of prestressing strands significantly decreased. Overall, the researchers concluded that concrete cracking can lead to strength reduction in a beam, which then leads to a reduction of the capacity (Chaowei et al. 2019, p.1).

A study conducted at Purdue University on the post-fire assessment of prestressed concrete bridges discusses temperature profiles through concrete depth on four different test specimens (PS1, PS2, PS3, and PS4) (Varma et al. 2021). Table 4 and Table 5 provide the maximum depth temperatures for all four specimens for different heating duration tests.

Table 4. PS1 and PS2 maximum through depth temperatures

Location	PS1-40-Minute Heating		PS2-80-Minute Heating	
	Maximum Temperature (°F[°C])	Time at Max. Temperature (min.)	Maximum Temperature (°F[°C])	Time at Max. Temperature (min.)
Surface	1121 [605]	40	1323 [717]	80
0.25 in.	803 [428]	41	1123 [606]	81
0.5 in.	531 [277]	43	871 [466]	81
0.75 in.	446 [230]	49	823 [439]	82
1 in.	414 [212]	47	702 [372]	82
1.5 in.	339 [171]	51	577 [303]	84
2 in.	287 [142]	58	473 [245]	90

Source: Varma et al. 2021, Joint Transportation Research Program, Purdue University

Table 5. PS3 and PS4 maximum through depth temperatures

Location	PS3-80-Minute Heating		PS4-30-Minute Heating	
	Maximum Temperature (°F[°C])	Time at Max. Temperature (min.)	Maximum Temperature (°F[°C])	Time at Max. Temperature (min.)
Surface	1485 [807]	80	899 [482]	29
0.25 in.	976 [524]	80	647 [342]	31
0.5 in.	842 [450]	80	489 [254]	31
0.75 in.	759 [404]	82	427 [219]	33
1 in.	703 [373]	82	372 [189]	33
1.5 in.	598 [314]	87	298 [148]	36
2 in.	449 [232]	98	297 [147]	95

Source: Varma et al. 2021, Joint Transportation Research Program, Purdue University

The results from this study indicated that the temperature profile through the thickness of the concrete is determined from the fire/heating duration. The researchers explain that the depth of the damage is a function of the period of time the girder is exposed to the fire. Concrete does not conduct heat quickly in comparison to steel. However, internal temperatures can increase significantly during long lasting fires.

While visual observation can help map different regions of deterioration and distress while providing a general indication of the severity of damage, this alone is not enough to determine the serviceability and strength of a bridge. To fully understand the performance of concrete girders subjected to fire damage, load and materials tests are necessary.

2.3 Serviceability and Strength

Testing and further analysis (i.e., finite element [FE] thermal analysis) of fire-damaged girders in addition to condition assessment allows for a deeper understanding of the damaged incurred by the girders in different situations. Prolonged exposure to high temperatures can lead to loss of strength and affect the structural performance of the overall bridge. When checking the strength

and serviceability of a structure, both flexural and shear checks must be considered (Masetti et al. 2018).

Graybeal (2007) discusses tests conducted on a US 7 box-beam bridge in southwestern Connecticut after a gasoline tanker fire, focusing on the flexural capacity of the box beams to determine if the bridge could have remained in service (see Figure 16 and Figure 17).

Graybeal 2007, FHWA

Figure 16. Tanker truck remains on US 7 Bridge in southwestern Connecticut after fire

Graybeal 2007, FHWA

Figure 17. US 7 Bridge fascia after fire

Visual examination and lack of nondestructive means to determine the strength of the prestressing strands deemed the bridge to be insufficient; therefore, the Connecticut DOT (CTDOT) made the decision to replace all of the beams in the superstructure.

A flexure test was conducted on the damaged girders to fully determine the structural capacity remaining in the beams. A two-point load test was set up to keep a constant moment in the midspan of the beam. Both ends of the beam were supported by roller supports and loads were applied to each beam through a 12 in. wide steel plate spanning the width of the beam (Graybeal 2007). Four load cells measured the load applied to the beam at the two load points. Eleven strain gauges were placed on each beam to measure the strains throughout the tests and seven string potentiometers were used to measure the vertical deflections. Figure 18 and Figure 19 show the setup and cross-section of the beam tests.

Graybeal 2007, FHWA

Figure 18. US 7 box beam flexural loading

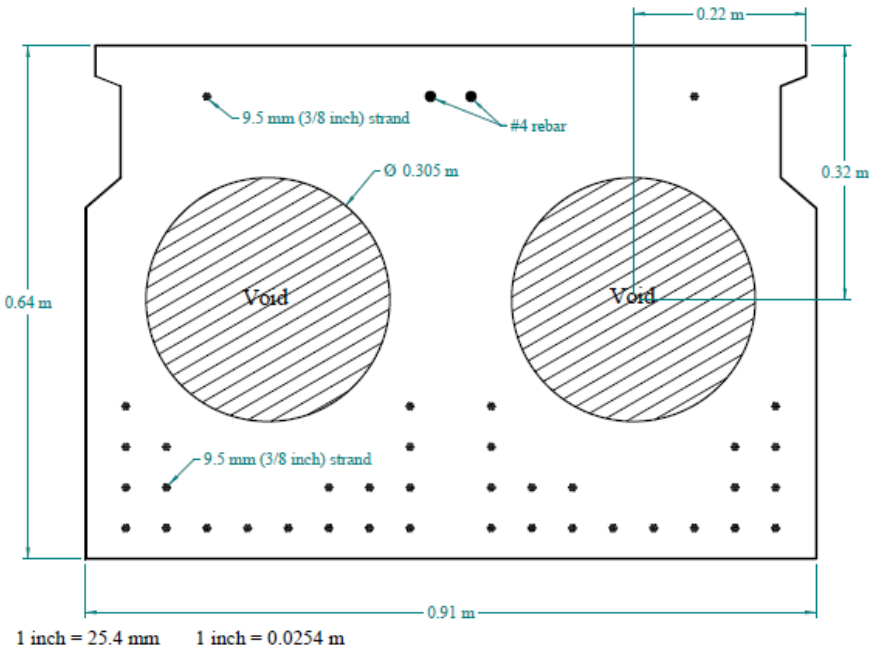

Graybeal 2007, FHWA

Figure 19. US 7 cross-section of box beam

Graybeal (2007) reported the use of an incremental increase in the applied load during each test. The midspan deflection was paused at different intervals to record the flexural stiffness of each beam. About 80% of the peak load was released each time the testing was paused and reloaded by 10kN increments back to the peak load (Graybeal 2007). The loading was also paused at the different intervals to map any cracks formed during the load test. Figure 20 shows an example of one beam loaded until failure.

Graybeal 2007, FHWA

Figure 20. US 7 Beam #14 failure

Graybeal (2007) concluded that all four beams (Beam #3, #4, #7, and #14) exhibited similar behavior when it came to flexural capacity, elasticity, and midspan deflection at flexural failure (see Figure 21).

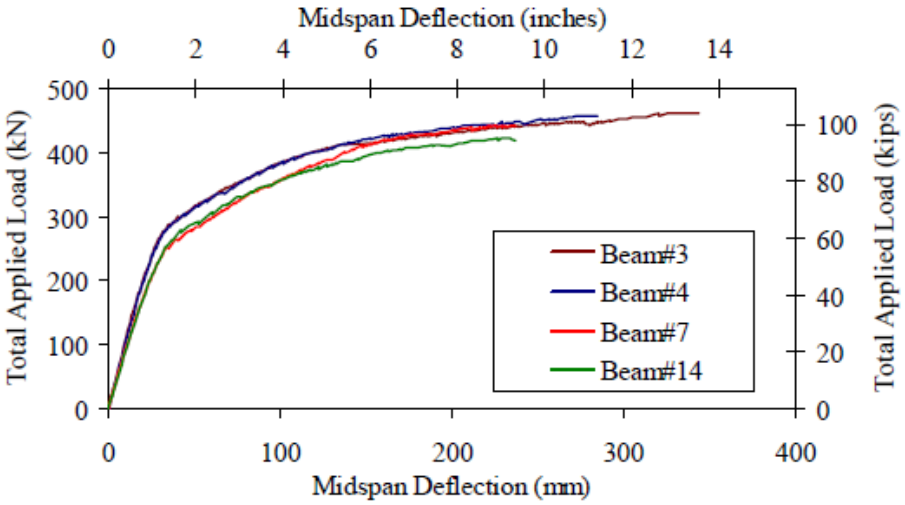

Graybeal 2007, FHWA

Figure 21. Load vs. midspan deflection curve for US 7 beams

The compression flange microstrain was similar in all the beams as well (see Figure 22).

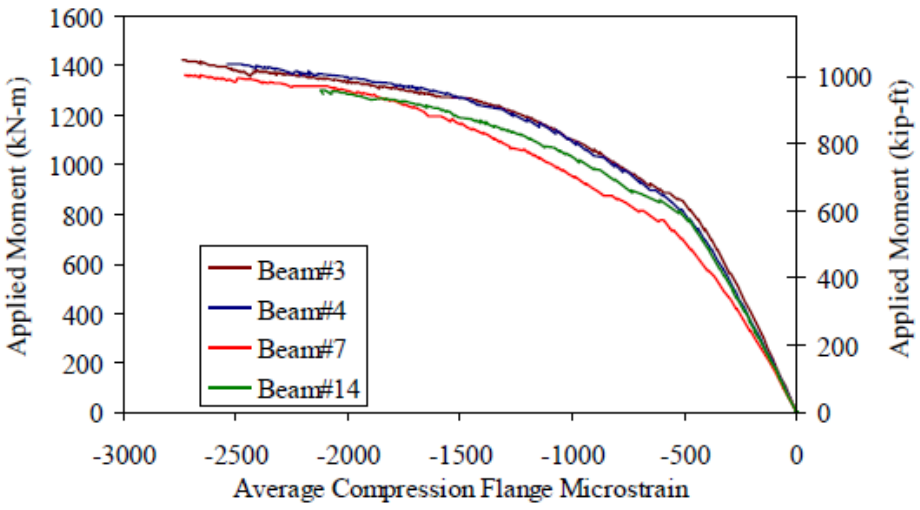

Graybeal 2007, FHWA

Figure 22. Applied moment vs. average compression flange microstrain for US 7 beams

Graybeal found that, even though each beam was located at a different location of the bridge, all had a similar level of degradation. The weakest beam, Beam #14, still had an ultimate flexural capacity that was 10% greater than the calculated capacity, meaning the beams had not been significantly damaged during the fire. However, Graybeal (2007) states that their long-term flexural behavior was still unknown. The significant damage to the bottom flange concrete in all beams could lead to faster degradation and a long-term decrease in the flexural capacities.

Varma et al.'s (2021) study conducted load tests for both ambient and post-fire conditions on decommissioned American Association of State and Highway Transportation Officials (AASHTO) Type I girders for flexure-controlled and shear-controlled tests. Two tests were conducted for each condition, and three different girders were selected for the tests. C2, C5, and C7 were selected from the I-469 Bridge over Feighner Road in Indiana, as documented in Table 6 and Figure 23.

Table 6. I-469 Bridge over Feighner Road AASHTO Type I girders test matrix

Test Specimens	North Overhang (in.)	South Overhang (in.)	Shear Span to Depth Ratio	Stirrup Spacing at Loading Point (in.)	Specimen Condition	Expected Failure Mode
C2-Flexure	102	48	1.59	6	Unburned	Flexural
C2-Shear	138	48	1.59	9	Unburned	Shear
C7	102	48	1.59	6	Burned	Flexural
C5	138	48	1.59	9	Burned	Shear

Source: Varma et al. 2021, Joint Transportation Research Program, Purdue University

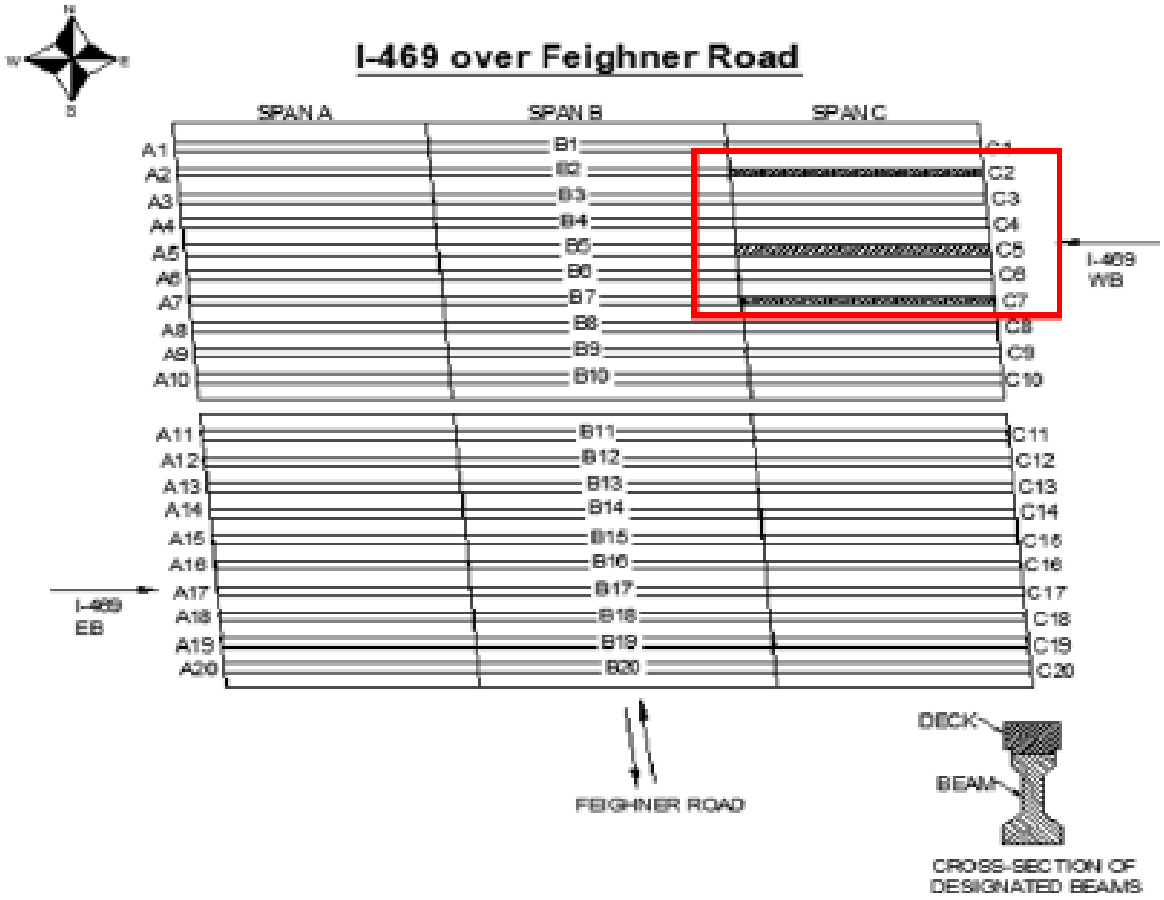

Varma et al. 2021, Joint Transportation Research Program, Purdue University

Figure 23. Selected specimen plan view for I-469 Bridge over Feighner Road

The ambient condition test portion was conducted, followed by the pool-fire test portion, in which the girders were subjected to fire for 43 minutes. The specimens were left to cool to an ambient temperature before testing for flexure and shear.

For the flexure-controlled ambient load test, vertical flexural cracks were observed near the loading point at a load of 140 kips. As the load increased, more flexural cracks developed. The shear-controlled ambient load test had an observed shear crack at 160 kips and additional shear cracks developed as the load increased. For the pool-fire flexure-controlled and shear-controlled load tests, spalling occurred due to the fire before testing began. However, additional cracks developed during loading as seen in Figure 24.

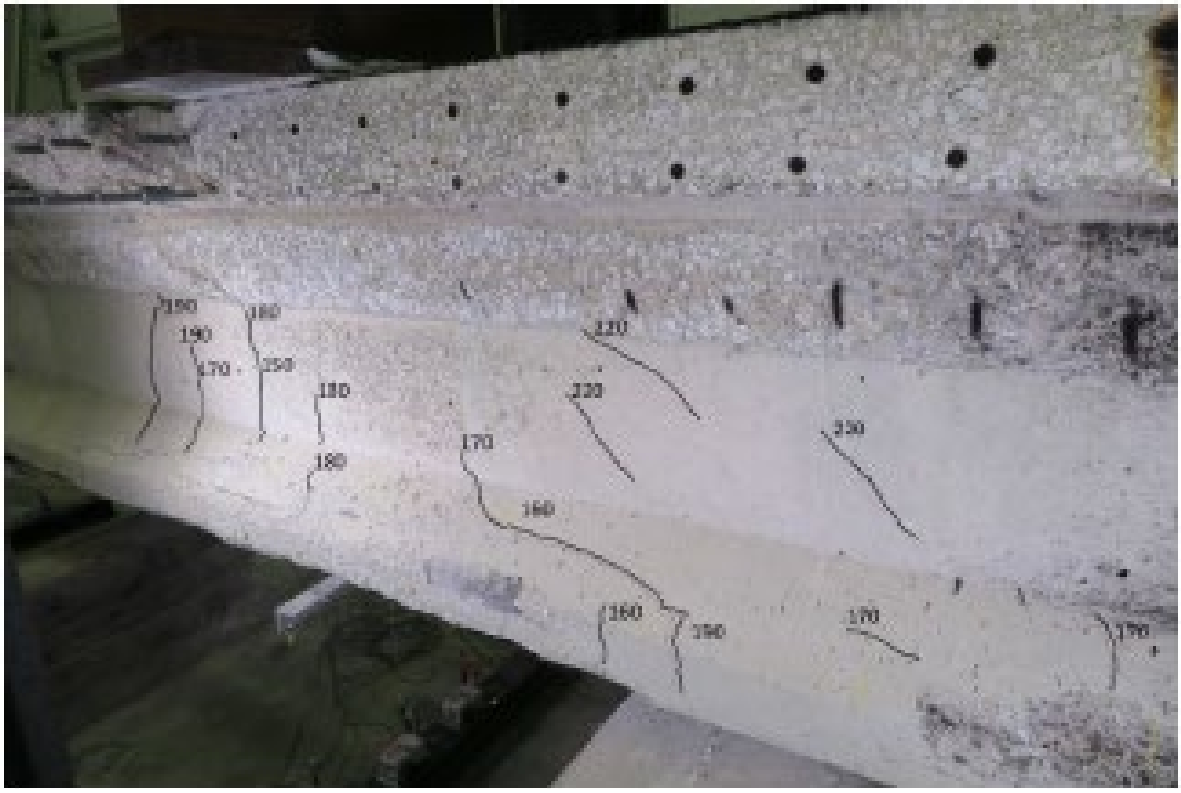

Varma et al. 2021, Joint Transportation Research Program, Purdue University

Figure 24. Beam C7 cracking at 220 kips for I-469 Bridge over Feighner Road

Varma et al. (2021) provided load-deflection plots for each condition, as shown in Figure 25 and Figure 26.

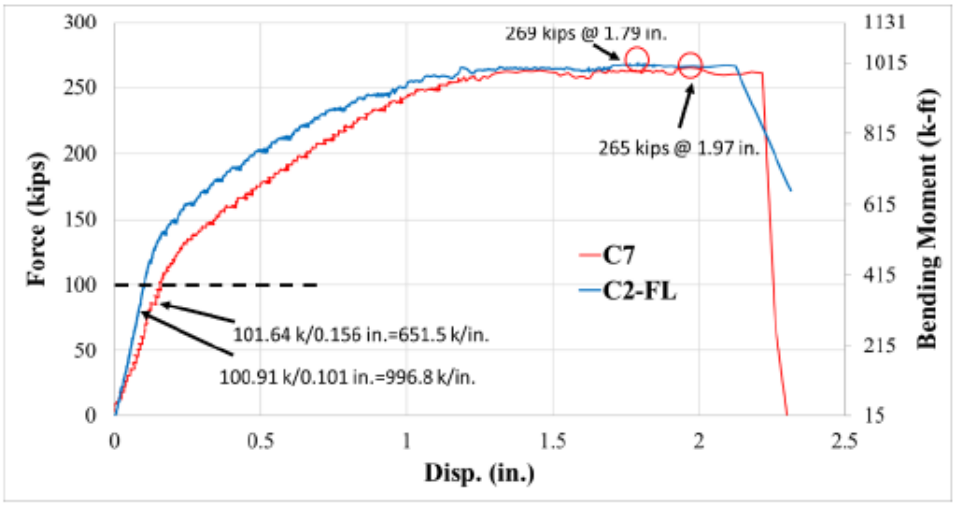

Varma et al. 2021, Joint Transportation Research Program, Purdue University

Figure 25. Load-deflection curves for I-469 Bridge over Feighner Road flexure-controlled tests

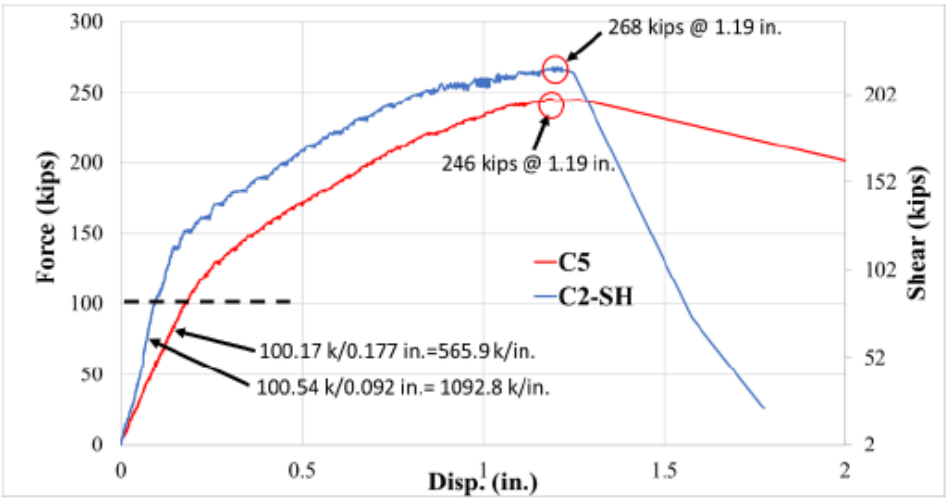

Varma et al. 2021, Joint Transportation Research Program, Purdue University

Figure 26. Load-deflection curves for I-469 Bridge over Feighner Road shear-controlled tests

For flexure-controlled testing, the researchers found that the initial stiffness of the fire-damaged girders was much less than those girders in the ambient condition. However, they did not find a difference at the load plateau and also found that the maximum displacements were similar in both cases. For shear-controlled testing, the researchers again found a reduction in the initial stiffness for the fire-damaged girder. The overall behaviors of the girders as seen in the load-deflection plots are relatively similar in this case as well.

Besides load testing, materials testing is also a good indicator of the extent of damage a girder has sustained. Masetti et al. (2018) reviewed the effects of high temperatures on concrete members in a study of double-T beams through physical testing (i.e., destructive and nondestructive) and use of analysis techniques.

One method of destructive laboratory testing discussed is called petrographic examination. The researchers state that, to determine the residual structural capacity of the damaged members, the temperature at which the concrete members and steel reinforcement was heated must first be estimated. The maximum temperature that the steel reinforcement reaches is usually determined through FE thermal analysis (discussed further in Section 2.3.1). Concrete members are examined by extracting core samples and observing changes through a microscopic lens. The color, along with mineralogical and physical changes, are key indicators in estimating the residual mechanical properties of the materials in the structure, maximum temperature reached, and duration of exposure.

Chloride testing is another method of destructive testing discussed by Masetti et al. (2018). Chloride tests can help determine the long-term durability of a structure through the examination of elevated chloride levels (if present). Masetti et al. (2018) explain that accidental chlorides can be introduced during the construction of a beam or when in service through deicing salts or salts in the atmosphere. The researchers state that when certain plastics (e.g., polyvinyl chloride

[PVC] plastics) are embedded into the concrete structure and then burned during the fire, the resulting vapor forms hydrochloric acid, which deposits chlorides into the structure; this then increases the risk of long-term corrosion of the steel reinforcement (Masetti et al. 2018). Chloride-content testing on the samples extracted from the damaged beams can determine if levels are elevated.

Typical materials tests include compression tests for concrete and tension tests for the steel strands. De Melo et al. (2014) describe materials tests carried out for a bridge subjected to an arson fire. The researchers used deep concrete core samples of at least 7 7/8 in. (200 mm) in length for compression tests to determine the strength of the concrete. In addition, steel samples were taken to be tested for tensile strength.

De Melo et al. (2014) reported that the laboratory results showed the reinforcement and prestressing wire material properties were not significantly damaged during the fire. Stress-strain plots were recorded for the tensile tests for the reinforcing bars; however, they were not recorded for the prestressed wires to avoid further damage during the test.

Given that load and materials testing can provide a clearer image of the damages that occurred on these bridge structures, advanced analysis can be done through different means of computational analysis methods. Specifically, FE thermal analysis is very useful in determining the damaging effects on the reinforcement.

2.3.1 Finite Element Analysis

Masetti et al. (2018) continued their study of prestressing strand temperature through FE thermal analysis. The researchers discuss how, although concrete displays significant physical changes after exposure to high temperatures from a fire, steel reinforcement does not always have visible changes. It is not considered practical to remove embedded steel from a beam for any physical testing as this would be too destructive to yield appropriate samples. Therefore, FE thermal analysis of the overall structure is key to understanding the effects of fire on the reinforcement.

Masetti et al. (2018) provide further details on the temperature effects on relaxation of untreated cold-drawn prestressing wire. Overall, they conclude that exposure of any prestressing steel to high temperatures greater than 392°F (200°C) can result in the elongation of the strands as well as a reduction in the ultimate tensile strength. For every 176°F (80°C) increase beyond 392°F (200°C), a 10% linear reduction is seen in the ultimate tensile strength.

2.4 Repair and Replacement Options

Once a bridge structure has been exposed to fire, the options are limited: repair or replace significantly damaged structural components or replace the entire bridge. Following these options, Stoddard (2004) presents three repair strategies: encasement, hydro-blast/preload/pour-back, and hydro-blast/prestress/pour-back.

Encasement involves constructing some sort of confinement around any damaged girders to prevent any more deterioration. Some of the encasement alternatives include shotcrete and wire-mesh, stay-in-place steel forms with pressurized epoxy grout, and removable forms with epoxy grout.

Hydro-blast/preload/pour-back involves removing and replacing all the damaged concrete while adding a vertical preload to the bridge deck prior to placing the concrete. The preload is then removed to compress the pour-back concrete.

Hydro-blast/prestress/pour-back is similar except prestress is used instead of preload. The prestress strands are placed above and below an existing bottom flange.

Although Stoddard (2004) discusses realistic repair or replacement approaches, these methods may not always apply to other situations. A survey questionnaire was given to numerous state DOTs by the Indiana DOT (INDOT) in regards to post-fire prestressed girder repair and replacement. The results from the survey mentioned multiple materials that could be used for such repairs, like carbon fiber-reinforced polymer (CFRP) wrap, high-strength epoxy, cementitious repair concrete, and strand splicers (personal communication from Tommy Nantung with INDOT January 21, 2021).

Varma et al. (2021) provide a checklist for recommended practices from inspection to repairs post fire. Table 7 shows this step-by-step guide on how to begin the assessment/repair process.

Table 7. Recommended practices checklist

Step	Title	Content
1	Visual Inspection	Inspect and record concrete color change at different locations. Record the distribution of concrete cracking and spalling. Develop a concrete color/surface temperature contour map for the damaged girder. If available, record the method used to extinguish the fire.
2	Nondestructive Testing	Use Schmidt Hammer to test concrete hardness. Establish a concrete hardness contour map for the damaged girder. Compare the concrete hardness and color contour maps.
3	Concrete Sample Coring (optional)	Take concrete samples using coring equipment for material analysis. The diameter of the core should not be greater than 2 in. The core depth need not be greater than 1 in. unless the fire duration was >1 hour.
4	Material Analysis (optional)	Conduct material evaluation on cored samples. These can include one or more of the following: scanning electron microscopy (SEM), energy dispersive spectroscopy (EDS), and differential scanning calorimetry (DSC).
5	Damaged Concrete Removal	Remove loose and damaged concrete using manual procedures or appropriate equipment/tools as needed.
6	Mesh Protection	Use protective mesh to cover the damaged regions and protect vehicles and personnel from concrete debris.
7	Short-Term Repair Plans	Develop short-term repair plans for prestressed girders. These can consist of removing and replacing fire-damaged concrete (up to depth of 1 in.) with fresh concrete or mortar.

Source: Varma et al. 2021, Joint Transportation Research Program, Purdue University

Varma et al. (2021) also discuss potential long-term repair strategies. The authors mention how "an appropriate repair method should restore the load-carrying capacity, long-term serviceability, and durability of the bridge" (pg.148). Similar methods, as mentioned in Stoddard (2004), such as hydro-blast methods to remove loose concrete before any other repairs begin, are discussed. Varma et al. (2021) state that if the damage has occurred in the prestressing strands, new prestressing strands should be installed, or a prestressing force could be introduced by applying a vertical preload. The authors explain how a bonding agent can then be used between new and old concrete to provide an adhesive bond. Then, the preload/prestress can be released to compress the new concrete provided.

Other materials, such as fiber-reinforced polymer (FRP), can be used afterwards to wrap the replaced concrete material. This allows for the addition of stiffness and strength to the repaired girders (Varma et al. 2021, pg.148).

Because the strategies provided from this study are just examples for one case, repair methods/strategies should be specifically designed for each fire-damage situation.

Other studies specifically focus on putting preventive measures such as CRFP coating or fireproofing in place as an alternative. For example, Beneberu and Yazdani (2018, 2019) discuss this topic and report that girders without fireproofing are at high risk of failure, especially during hydrocarbon fires. However, it is neither economical nor practical to apply fireproofing on all bridges because risk levels vary.

To efficiently approach the repair or replacement of a concrete structure, more research is needed in a variety of areas, such as the preventive measures like CFRP coating, FEA, long-term repair strategies, and so forth. Current standards do not provide enough guidance when it comes to different fire scenarios considered for bridges (Garlock et al. 2012). A more definitive guide is required to help assess, repair, or replace fire-damaged bridge structures in the most efficient and economical way possible.

2.5 Relevance of Fire Safety for Bridges

Bridge fires are most commonly caused by tanker-truck incidents as previously mentioned, and additional causes have not been fully considered when it comes to fire safety. In fact, designs or policies to prevent or limit fire damage are mostly limited to building design and are barely considered for bridge design (Giuliani et al. 2012). Although bridge fires are not as common as other damage causes, the consequences, such as reduced safety and economic impacts for bridge users, can be significant.

In addition to car/truck accidents, bridge fires can be caused by earthquakes, ship collisions, and increased shipping of flammable materials in all forms of transportation (Kim et al. 2020). This has increased the total number of fire-damaged bridges, resulting in greater losses and, in some cases, complete collapse of a bridge (Kim et al. 2020). Some other causes of bridge fires include

under-bridge parking (construction equipment or cars), storage of materials underneath a bridge, arson, forest fires, and homeless encampments, as was the case for the bridge in this study.

A risk assessment is recommended to determine which bridges may have a higher risk of fire-related damages. Some methods to evaluate fire risk of structures include the following: qualitative analysis methods, quantitative analysis methods, and relative ranking methods (Kim et al. 2020). Preventing reoccurrence of fire incidents must require special management regulations as well as strategies for fires igniting under a bridge (Park et al. 2018). Fire risk assessment and prevention methods from multiple research studies are discussed in the next section.

2.6 Case Studies for Fire Prevention and Policy Implementation

The case studies presented in this section help show how some governments and other agencies have aimed to prevent fire damage on bridge structures. These efforts were a result of significant economic losses resulting from previous fire incidents. Included in these case studies are proposed policy recommendations or management strategies for preventing fire damage.

2.6.1 Bucheon Viaduct in South Korea

Park et al. (2018) discuss a tanker-truck fire that occurred under the Bucheon viaduct in South Korea (2010) and led to severe damage to an urban bridge. The fire severity was a result of the materials being stored under the bridge (e.g., plastic pallets). The authors state that the South Korean Government spent about $13 million to restore the bridge in three months. However, the total economic loss was about $200 million.

Because of such a large economic loss, the Korea Expressway Corporation modified practices and manuals for fire prevention management under bridges. Park et al. utilized the lessons learned from similar cases in South Korea for strategy development. The authors introduce several strategies for fire risk management through exploration of fire simulations for materials stored under bridges. Specifically, their focus was on the I-85 Overpass incident in Atlanta, Georgia.

2.6.2 I-85 Overpass in Atlanta, Georgia

A section of the I-85 overpass in Atlanta, Georgia, collapsed after a fire ignited in a state-owned storage lot for construction materials under the bridge (Park et al. 2018). The materials found under the bridge were high-density polyethylene (HDPE) conduits. No injuries were reported, but this incident resulted in a total loss of $16.6 million (including removal of damaged components and contractor incentives) to replace the bridge for the Georgia DOT (GDOT) (Park et al. 2018). The indirect inconvenience cost of the 220,000 daily commuters was not added. However, traffic congestion was greatly increased due to the bridge closure (Park et al. 2018).

Park et al. (2018) discuss how the Standard Specifications Construction of Transportation Systems states that inflammable materials and chemicals should be placed at least 200 ft away from the structure or roadway. However, it is unclear which materials are referred to as "inflammable." In addition, GDOT uses a Design Policy Manual for standard fire codes that does not clearly define a management policy for materials stored under a bridge. Due to the lack of clarity for policies or recommendations regarding storage of materials underneath or near bridges, Park et al. conducted fire simulations for HDPE conduits under a concrete bridge. Various distances between the bridge structures and materials placed nearby were used to present guidelines for this study.

Park et al. (2018) used the Fire Dynamic Simulator (FDS) from the National Institute of Standards and Technology (NIST) to prepare the various simulations for different locations and heights of the stored materials. The following cases presented in Table 8 were used to determine optimal management methods.

Table 8. Cases for fire simulation of stored materials

Case Number	Distance from Column		Height Distance from Deck	
	(m)	(ft)	(m)	(ft)
Case 1	0	0	3	9.8
Case 2	2	6.6	5	16.4
Case 3	0	0	5	16.4
Case 4	2	6.6	5.5	18

Source: Park et al. 2018

Figure 27 illustrates the different cases modeled using the FDS.

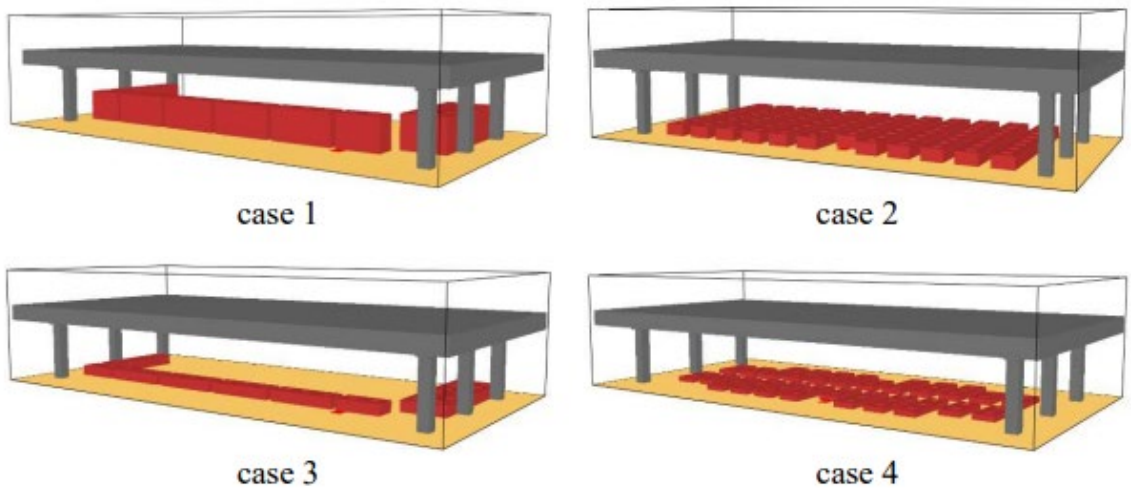

Park et al. 2018, © ASCE, used with permission

Figure 27. Case models using the FDS

Table 9 presents the thermal properties of the materials.

Table 9. Thermal properties for case study

	Materials	
Properties	**Concrete**	**HDPE**
Density (kg/m^3)	2,400	959
Specific heat (kJ/kg/K)	0.75	2.0
Conductivity (W/m K)	1.28	0.43
Emissivity	1.0	0.92
Reference temperature (ºC)		471
Heat of reaction (kJ/kg)		220
Heat of combustion (kJ/kg)		44,000

HDPE = high-density polyethylene

Source: Park et al. 2018

The critical temperature used to evaluate the results was 1,000°F (538°C) based on the yield strength reduction of ASTM A36 steel to 60% at this temperature (Park et al. 2018). The results from the study state that the fire on the HPDE conduits grew rapidly within 10 minutes and peaked at about 30 minutes (Park et al. 2018). Firefighting work was simulated by modeling virtual nozzles under the deck. It was determined that the fire could not be contained when limiting the water outflow to 1,000 gal. (3,785 liters) per minute due to flames exceeding the height of the bridge after 10 minutes (Park et al. 2018). Figure 28 illustrates the fire simulation results.

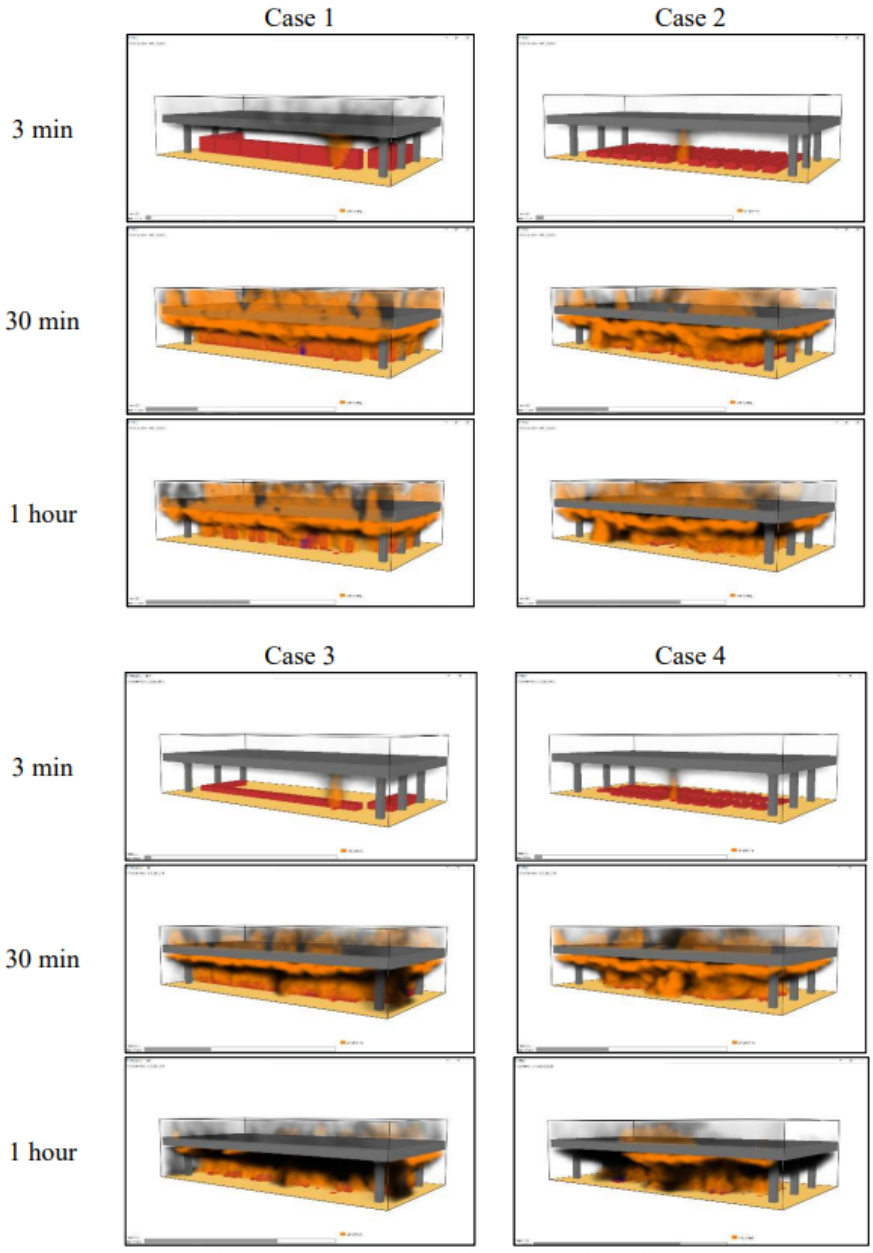

Park et al. 2018, © ASCE, used with permission

Figure 28. Fire growth during simulation

All cases had exceeded the critical temperature, but the researchers concluded that the temperature of a structure can be lowered by reducing the height of stored materials. From the results, the researchers recommend that HDPE materials are stored more than 6.6 ft (2 m) away from bridge columns and at least 18 ft (5.5 m) from the bridge deck. The authors state this study strictly applies to HDPE conduits only, but they discuss the need for guidelines of fire safety management for other stored materials under bridges. Guidelines should include location and placement of the stored materials (Park et al. 2018).

2.6.3 Evaluation of Fire-Damaged Components of Historic Covered Bridges

Kukay et al. (2016) reported on existing and exploratory approaches that can be used for general guidance on fire-damaged bridges. The authors discuss several different case studies of historic bridges that have been subjected to fire. From the case studies, the authors discuss designs for fire prevention and control that can be applicable to all bridges.

Risk-associated strategies for fire containment, such as fire-retardant treatments, help prevent bridges from collapsing but not from the fire occurring in the first place (Kukay et al. 2016). The authors state that design considerations such as site-specific conditions and proximity to resources related to fire prevention and extinguishment programs should incorporate serviceability, preservation, and aesthetics (Kukay et al. 2016).

A recommendation from this report is to provide constant maintenance to reduce ignitable or other materials that can contribute to fire intensity. Some of the historic bridges mentioned are in isolated locations that are more likely to be vandalized or damaged due to arson. Because of this, Kukay et al. (2016) further recommend routine operation and maintenance for necessary fire prevention.

2.7 Analysis of Bridge Fire Causes and Damage Levels

Peris-Sayol et al. (2017) present a research study consisting of 154 bridge fire cases (from previous literature) analyzed to develop fire damage levels and describe main factors involved in bridge fires. Some of the main factors involved include types of vehicles, position of vehicle, clearance height of the bridge, and type of deck material used. All 154 bridge fire cases were put into a database with different variables, as presented in Table 10.

Table 10. Field details

Variable	Details
Bridge site	Rural, Urban, Suburban
Deck material	Prestressed concrete, Steel, Composite steel-concrete, Wooden structures
Structural system	Cable-stayed bridges, Suspension bridges, Arch bridges, Truss bridges, Box girder bridges, I-girder bridges
Bridge span and width	Obtained from data collected from accident investigations or Google Earth (estimation)
Causes of fire	Cars, Trucks, Tanker trucks, Electrical problems, Stored materials, Forest fires, Others (such as formwork fires)
Fuel types	Gasoline, Diesel fuel, Other hydrocarbons, Alcohol-based liquids, tires, plastics and other solids
Position of tanker truck	Tanker truck on bridge (no fuel spillage on lower sections), Tanker truck under bridge, Tanker truck (fuel spillage causing fire on lower sections), Tanker truck near bridge (no contact with bridge)
Damage levels	Level 1: Superficial damage, Level 2: Slight damage, Level 3: Partial damage, Level 4: Massive damage, Level 5: Structural collapse

Source: Peris-Sayol et al. 2017

To analyze the data from the bridge fire cases, the authors used the analysis of variance (ANOVA) statistical test. Peris-Sayol et al. (2017) state that the test compares three or more groups in response to one or several variables. The test helps to determine the impact of independent variables (such as deck material) on dependent variables (such as damage levels) in a regression analysis through a coefficient known as the p-value (with more details on the ANOVA test found in the research paper) (Peris-Sayol et al. 2017). Table 11 provides the damage level mean and range for various independent variables.

Table 11. Damage level ANOVA statistical test results

Category	Type	Low	Mean	High
Deck Material	Concrete	2.0	2.4	2.8
	Composite	2.2	2.6	3.0
	Steel	1.6	2.0	2.4
	Timber	4.2	4.8	4.4
Cause of Fire	Car	0.4	1.1	1.8
	Heavy Goods Vehicle	1.2	1.6	2.0
	Tanker	2.7	3.1	3.5
	Electric	0.0	1.2	2.4
	Storage	1.4	2.0	2.6
	Other	2.0	2.7	3.4
Fuel Type	Gasoline	3.2	3.6	4.0
	Diesel	2.0	2.8	3.6
	Alcohol	2.0	3.0	4.0
	Other Hydrocarbon	1.7	2.4	3.1
Tanker Truck Position	On the Bridge	1.4	2.2	3.0
	Under the Bridge	3.0	3.4	3.8
	On the Bridge with Significant Oil Spillage	2.6	3.2	4.0
	Near the Bridge	0.6	1.8	3.0

Source: Peris-Sayol et al. 2017

Peris-Sayol et al. (2017) concluded that wooden bridges perform worse than concrete, composite, or steel bridges during a fire, as seen in the table. For fire causes, the authors found that tanker trucks caused the most damage; whereas, fires from cars or heavy-goods vehicles caused slight damage. Materials stored underneath the bridge can also cause severe damage if the volume of the materials is high along with a low clearance height between the fire and the bridge deck. Other causes (e.g., gas pipe fracture) were considered in the high damage level as well (Peris-Sayol et al. 2017).

Because tanker-truck fires cause the most damage, the types of fuel carried by these trucks were also taken into consideration for different damage levels (Peris-Sayol et al. 2017). Gasoline and alcohol-based fuels had higher damage levels than diesel and other hydrocarbons. This is because gasoline has a higher heat release rate than other types of fuels and is highly flammable at ambient temperatures (Peris-Sayol et al. 2017).

Lastly, the position of tanker trucks made a significant difference in damage levels for a bridge. Tanker trucks under the bridge or on the bridge with significant fuel spillage caused the highest damage levels (Peris-Sayol et al. 2017).

A fire-risk prevention plan (e.g., fire-retardant design) should be implemented for timber bridges, specifically, given they pose a higher risk of collapse during a fire. Tanker trucks on bridges pose the greatest risk for bridge fires, so the following measures should be implemented to prevent incidents (Peris-Sayol et al. 2017):

- Proper design and maintenance of bridge drainage systems (preventing fuel spills from accumulating under the bridge)
- Materials storage (especially flammable materials) should be forbidden at all times but most importantly when the bridge clearance is low
- More research should be done to ensure adequate response of a bridge from authorities

Peris-Sayol et al. (2017) concluded that the preventive measure discussed can be used for other scenarios by engineers in charge of fire risk management.

2.8 Tanker-Truck Risk Prevention Measures

Another study on risk prevention measures is discussed in this section. The study presents additional ideas for implementing management measures regarding tanker-truck bridge use.

Liu et al. (2014) discuss risk prevention measures for fires underneath bridges. Specifically, a traffic reporting system was set up in a study for the Yingwuzhou Yangtze River bridge (a three-tower, four-span suspension bridge) in China to determine reports of tanker-truck incidents. Liu et al. (2014) state that fires caused by vehicles loaded with flammable materials happens often, and, in response, tanker trucks on bridges should be carried out using registration logging reporting.

The authors suggest that tanker/heavy trucks should be driven under the guidance of bridge management departments as well as be restricted to the middle lane of the bridge. This helps allow other vehicle operators to rapidly escape from a fire hazard. Another recommendation mentioned is that “Department of public security, fire control, transportation, bridge management center, and other departments should get together to establish an accident emergency rescue leading group” (Liu et al. 2014).

Although these measures were suggested and implemented for the Yingwuzhou Yangtze River bridge, they can apply internationally for other cases. Not only can these tanker-truck fire prevention measures be used for suspension bridges but for all other types of bridges (e.g., concrete bridges).

2.9 Recommended Fire Prevention Measures and Management Strategies

The lack of clarity from design manuals for bridges regarding risks from fire can cause serious consequences for bridge users and the economy. Based on reviewing previous literature and case studies, the following preventive measures and management strategies are recommended to prevent bridge damage from fires:

- A risk assessment should be required during the design phase for bridges. This assessment can include qualitative analysis methods, quantitative analysis methods, and relative risk ranking methods.

- Different factors (deck material, location, type of bridge, cause of fire, etc.) typically involved in bridge fires should be ranked in terms of damage levels that could occur during a fire. This helps engineers and bridge owners to design against fire damage early on (e.g., proper design of bridge drainage systems to prevent the accumulation of fuel from tanker-truck incidents).

- Due to high damage levels resulting from tanker-truck fires on bridges, coordination between bridge management, fire control, engineers, DOTs, and government officials should be required through the establishment of an emergency rescue group, with a specific focus on fire incidents.

- For certain vulnerable bridges, it is recommended that tanker-truck operators use designated lanes to reduce damage levels during an incident (e.g., center lanes so other bridge users may escape safely and quickly). Through logging and reporting, some trucks may be restricted from traveling over or under a specific bridge with high fire risks dependent on the amount or type of flammable materials carried. Detour routes for these cases should be established in a guide for truck drivers.

- Guidelines for storage near or under a bridge should be implemented prior to bridge service. This should include under-bridge parking of cars and construction equipment. These guidelines should also include safety management policies, such as specific locations, placement, and restrictions for different types of stored materials. Flammable materials should be forbidden at all times.

- For bridges in isolated locations, such as some historic bridges, routine maintenance should be coordinated to prevent the buildup of ignitable materials as well as provide routine measures for fire prevention (e.g., address vandalism and arson).

2.9.1 Future Work for Additional Fire Prevention Measures or Policies for Bridges

Although previous literature takes into consideration a variety of fire prevention measures for different cases, additional research could help with other situations. For example, homeless

encampments, which was the case with this Sioux City bridge study, is one situation that did not have preventive measures in place. Because homeless encampment policies regarding bridge use have not been fully addressed, further research is needed.

A guide should be developed for implementing policies related to homeless encampments underneath bridges that can assist in preventing fires. This may involve deterring encampments from state transportation rights-of-way (ROWs). Coordination with agencies, government officials, DOTs, construction managers, and bridge owners will be necessary to create policies related to the tolerance of homeless encampments (NCHRP 2022).

3 CONDITION ASSESSMENT, TEST PROCEDURES, AND INSTRUMENTATION

This chapter discusses the condition assessment, test procedures, and instrumentation of the fire-damaged, prestressed, concrete girders from the northbound I-29 Bridge in Sioux City, Iowa.

3.1 Condition Assessment

The Iowa DOT arranged for the removal of the three selected prestressed concrete girders from the I-29 Sioux City fire-damaged bridge. The girders were brought to a test site at the Iowa DOT maintenance yard in Ames to begin visual and NDE condition assessment. Visual assessment included documenting all visible fire damage using images, notes, and sketches. Girder length, deck width, deck thickness, concrete cracks, spalling, large areas of missing concrete, color changes, and any exposed reinforcement were documented in the notes prior to load testing. Cross-sections of the BTB85 beam, along with the section properties, are shown in Figure 29 and Figure 30.

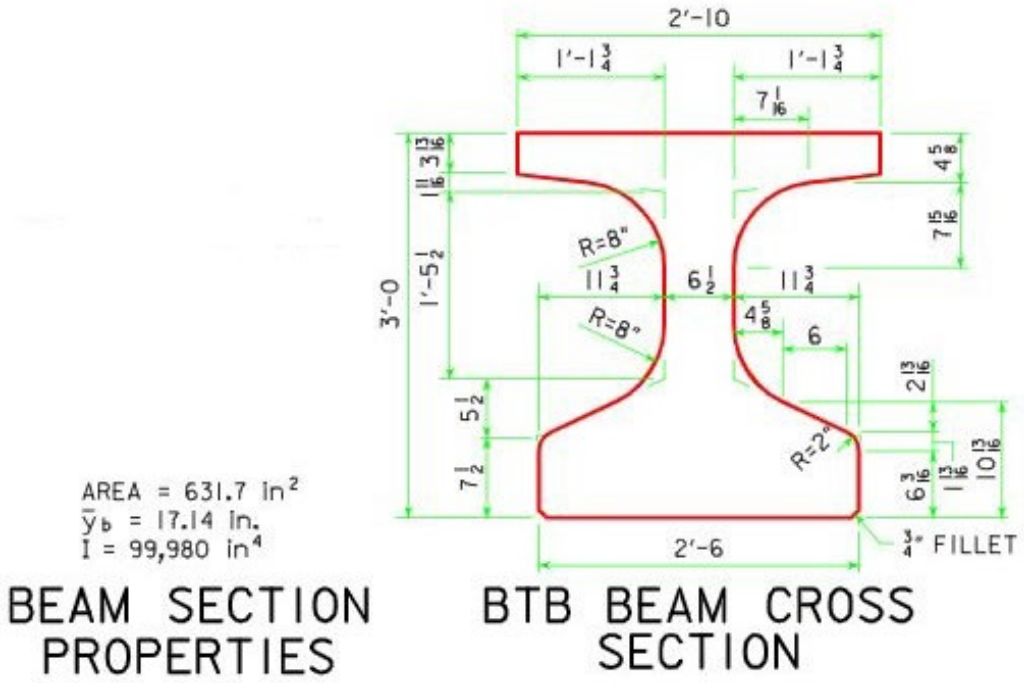

From contract documents

Figure 29. Girder cross-section detail

Strand reinforcement plans are shown in Figure 31.

The locations labeled A, B, C, D, and E in Figure 32 were used for testing, assessment, and calculations and are referred to through the remainder of this report.

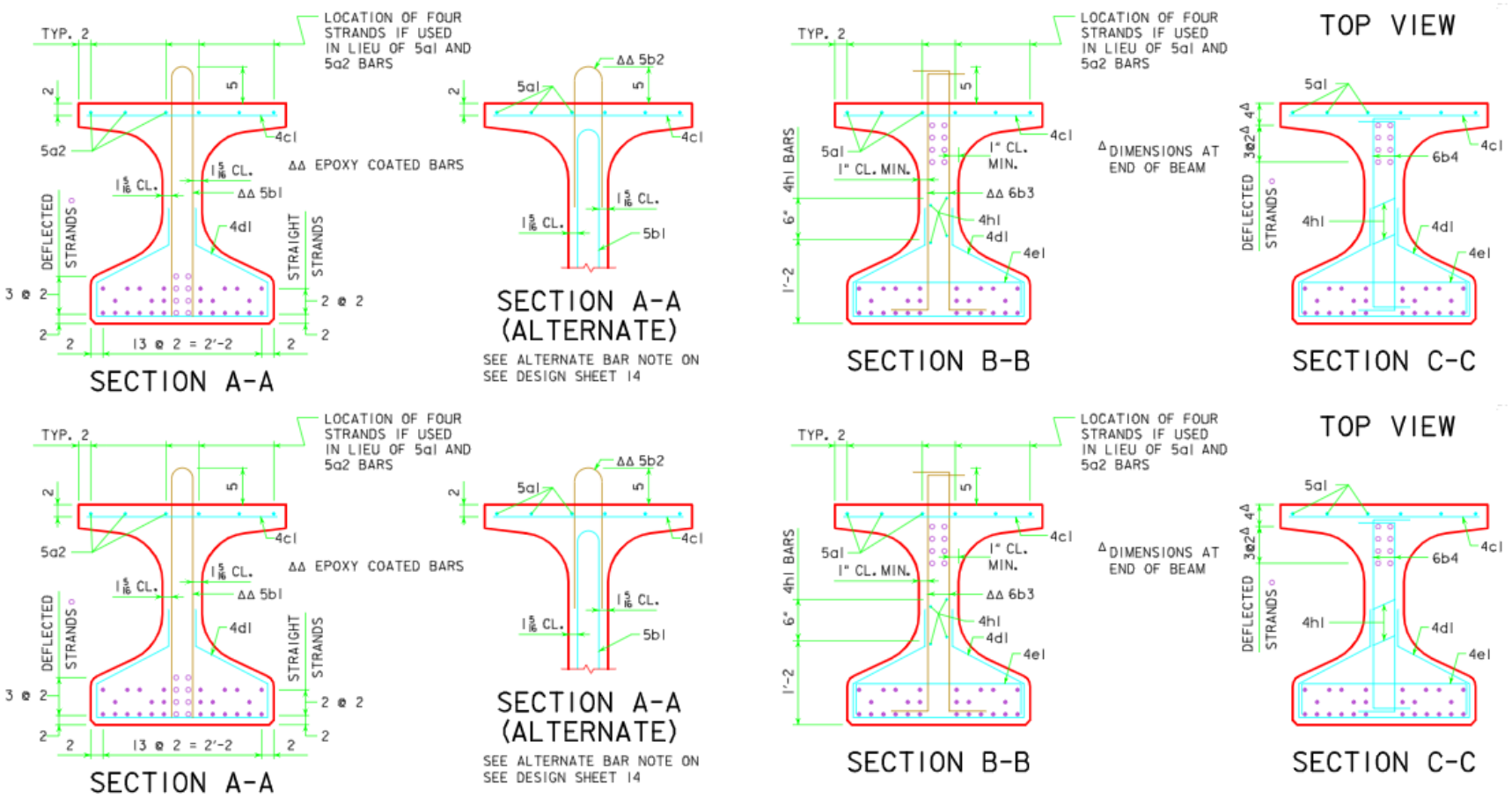

From contract documents

Figure 30. Girder cross-sections at Sections A, B, and C

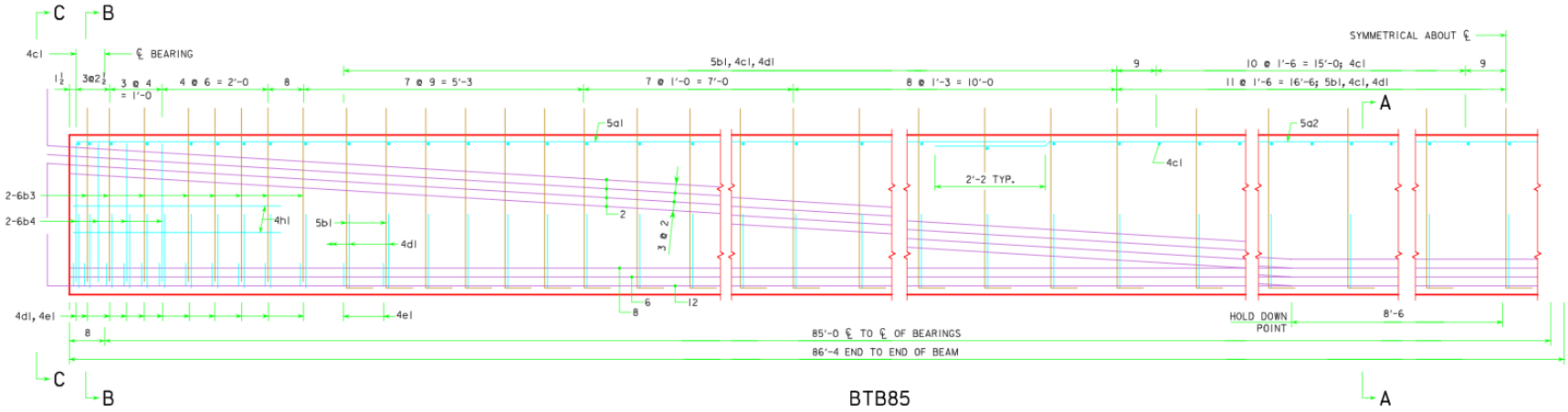

From contract plans

Figure 31. Girder strand and stirrup reinforcement

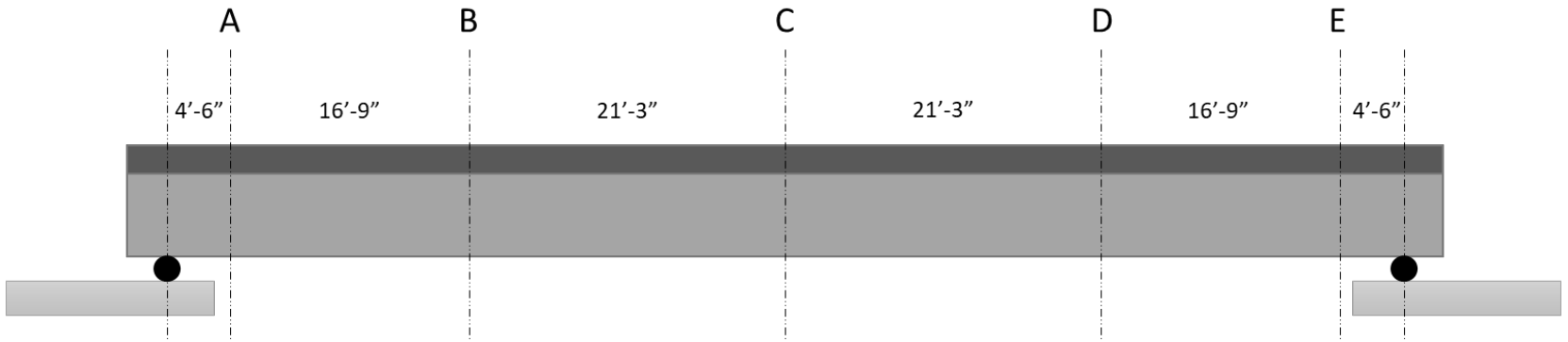

Figure 32. Defined girder points

3.2 Materials Testing

Materials testing was conducted from samples extracted from Girder B. Several concrete core samples were obtained to undergo compression tests, and steel strands were obtained to undergo tension tests. Each of the samples was taken from an area near the bottom of the girder, which is an area presumably more susceptible to greater heat-related damage. The goal was to capture stress-strain curves as well as ultimate strength values to understand the material properties of the more-damaged end of Girder B.

3.2.1 Materials Test Setup and Instrumentation

The two test configurations are separately discussed in detail below. Concrete compression tests are used to verify the strength of the concrete mix used in a particular project. Steel strand tensile tests are used to define the ultimate strength and performance of the material. Steel strand tensile tests are used to determine yield strength, ultimate tensile strength, Young's modulus, and Poisson's ratio.

Three different concrete core samples were collected from Girder B. All three samples had 3 in. diameters and were of varying heights (Figure 33).

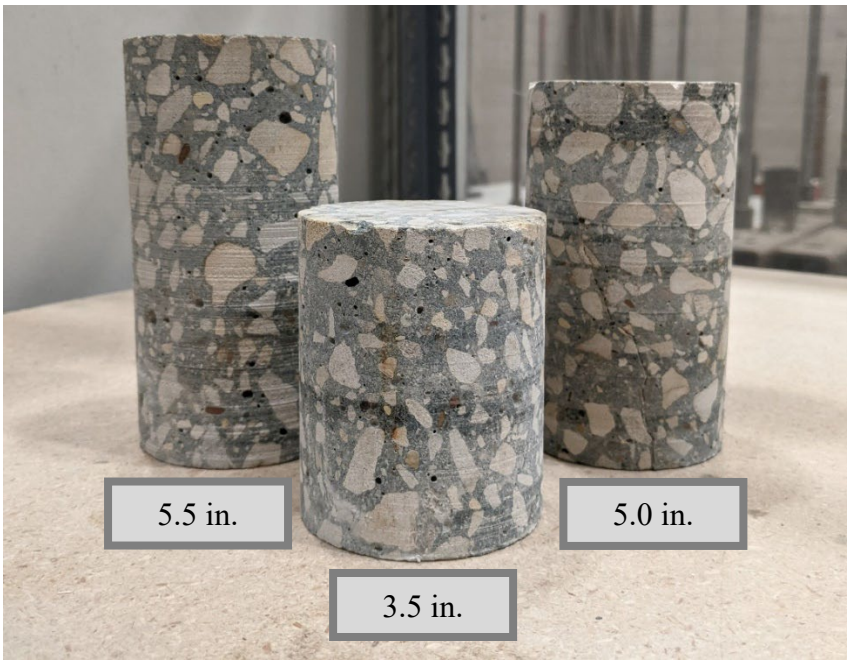

Figure 33. Concrete cylinder core samples for compression tests

The first sample was 3.5 in. tall, and the second and third samples were 5 in. and 5.5 in. tall, respectively. Apparent cracking was observed in the 5 in. cylinder prior to testing.

Each sample was placed in a static servo-hydraulic SATEC universal testing machine (UTM) to undergo the compression test. All samples were loaded at an approximate rate of 14.3 kips per minute.

Three different prestressing steel strands were used for the tensile tests (Figure 34).

Figure 34. Steel strand samples for tensile tests

Each bar was a 270 ksi, seven-strand configuration cut to 53.5 in. in length. The distance between grips on the UTM was 35.75 in., 37 in., and 36.5 in. for the first, second, and third specimens, respectively. All steel strands were pulled at 0.75 in. per minute.

3.3 Two-Point Bending Load Tests

The three concrete girders underwent load testing to compare their serviceability and strength to the calculated behavior of the non-fire-damaged girders. Each girder underwent a two-point bending test with deflection and strain transducers in place to compare the strain and deflection values from the applied load to the calculated strain and deflection values based on the girder properties. Test preparation and setup is discussed below.

To prepare the girders for the two-point bending tests, 12 4.72 in. strain gauges (from Tokyo Measuring Instruments Laboratory Co., Ltd.) were placed at three 21.5 ft intervals on the top and bottom flanges of both sides of each girder. The concrete surface at which each strain gauge would be placed was first prepared with a grinder to remove surface irregularities. Once the concrete was prepared, a layer of epoxy (about 6 in. in length) was placed at each strain gauge location and left to cure. After curing, the epoxy was sanded with fine grit sandpaper to attain a very smooth surface. Adhesive was then used to adhere the strain gauges to the girders and covered with butyl rubber to protect against harsh weather conditions (see Figure 35).

Figure 35. Girder B – Strain gauges at Section B bottom on south side

Each strain gauge was connected to the data acquisition system and labeled, as shown in Figure 35, as follows: B, E, or G (for girder identification), A, B, C, D, or E (for cross-section location), S (for strain gauge), T or B (for top or bottom), and 1 for south side or 2 for north side.

Following the placement of the strain gauges, deflection transducers were placed beneath each girder at each quarter-point cross-section location (see Figure 36).

Figure 36. Deflection transducer

Each strain gauge and deflection transducer was connected to the data acquisition system.

To set up the two-point bending test, four helical piles were installed to anchor the load frame to the ground (see Figure 37).

Figure 37. Installation of helical piles

Once the piles had been placed, four Dyckerhoff & Widmann AG (DYWIDAG) threaded bars were connected to each of the piles. Each pile and DYWIDAG bar connection was designed to accept a minimum tensile reaction of 80 kips.

Reaction beams were placed over the DYWIDAG bars 4 ft on either side of cross-section C (girder midspan), leaving 8 ft between the two bars on either side of the girder. Each reaction beam across the girder had a hollow core hydraulic cylinder ram at each end (see Figure 38).

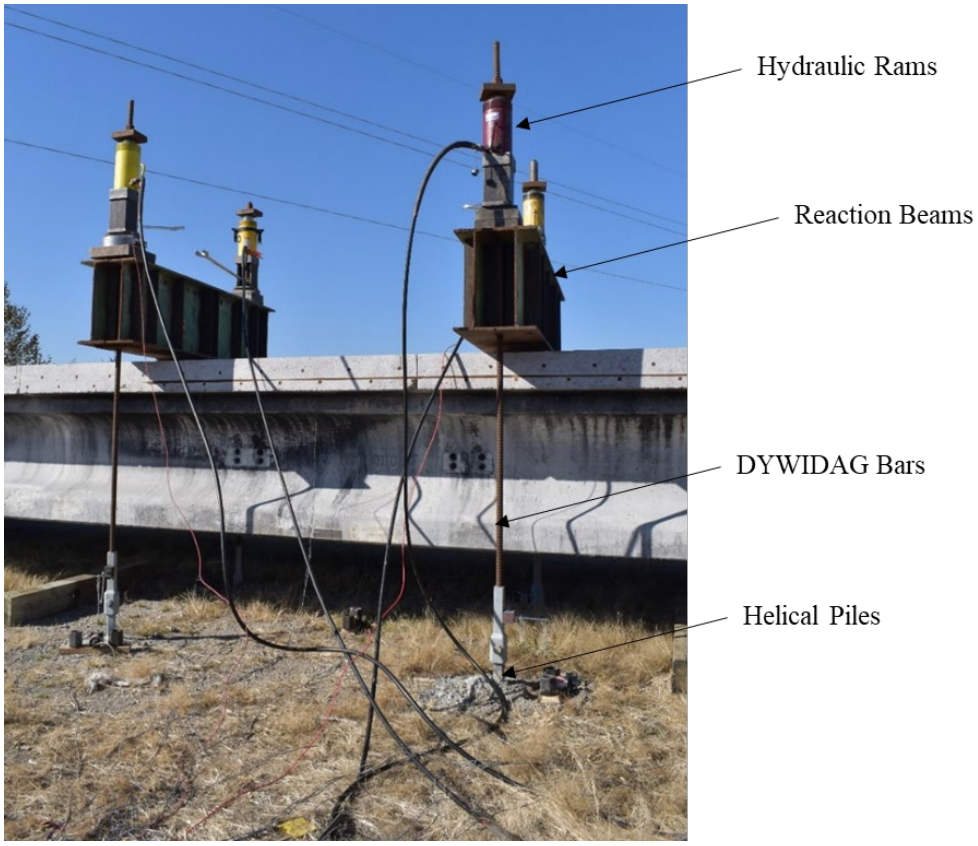

Figure 38. Reaction frame

The hydraulic rams were connected to a single hydraulic pump so that the load could be applied uniformly and incrementally. Two load cells were used to measure the induced force. One was placed on each reaction beam between the ram and a reaction plate. Below each reaction beam, a steel plate was centered on the girder providing a single point at which the girder would be loaded. This setup ensured a constant moment region in the middle 8 ft section of the girder. Figure 39 through Figure 41 show additional details of the load test setup.

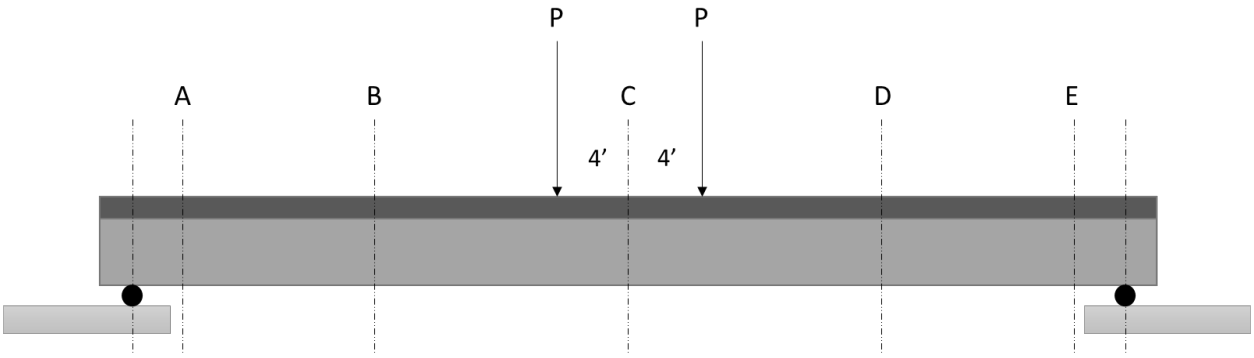

Figure 39. Locations of applied point loads

Figure 40. Hydraulic pump with four-hose manifold

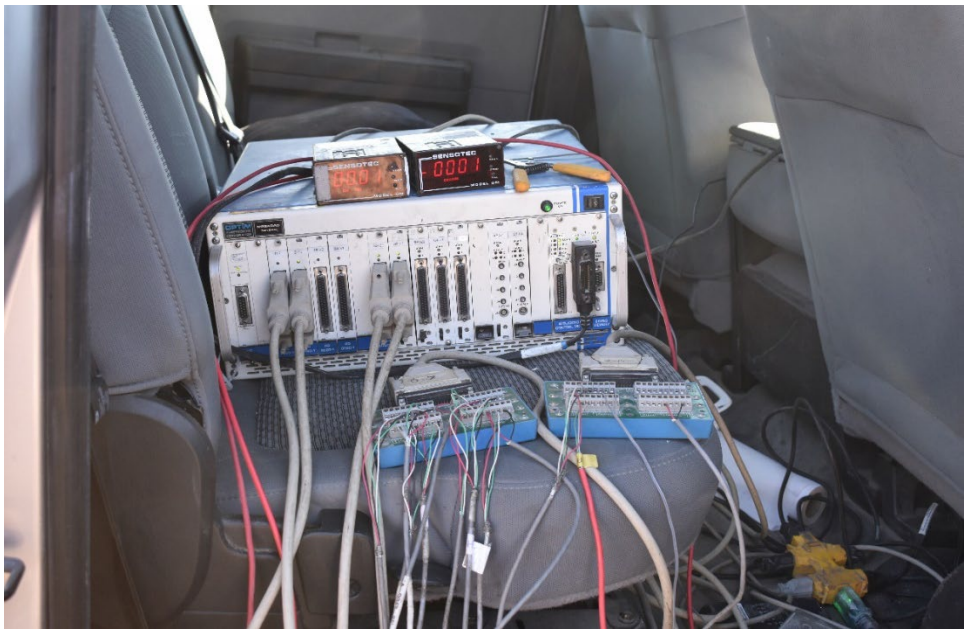

Figure 41. Fully connected data acquisition system

A total of three load cycles were completed with the objective of the first two cycles being to collect deflection and strain data within the elastic range and to ensure all instrumentation was properly functioning. For the first cycle of Girder B, a 20-kip load was produced at each hydraulic ram, totaling 80 kips of applied load combined between the two reaction beams. The load was removed, and the process was repeated a second time before the final cycle, which increased the total load to about 250 kips.

For Girder E, the first two cycles were completed in the same manner as Girder B up to 80 kips, while, for the last cycle, the girder was loaded until failure, exceeding 250 kips total.

Girder G was loaded to about 130 kips for each of the three cycles, which is slightly below the load required to reach the elastic limit. This ensured no additional damage occurred before the girder could be used for the demonstration of repair methods and a final load test.

3.4 Shear Capacity Load Testing

Upon completion of the bending tests, testing of the shear capacity was completed for Girder B. The end of the girder nearer the fire epicenter was used to evaluate if reductions in shear capacity resulted from the fire. The shear test setup and instrumentation are discussed below.

The shear test for Girder B took place in the Wallace W. and Julia B. Sanders Structural Laboratory in the Town Engineering Building at Iowa State University. The end section of the girder was placed on two roller supports 10 ft apart on top of two reaction blocks (see Figure 42).

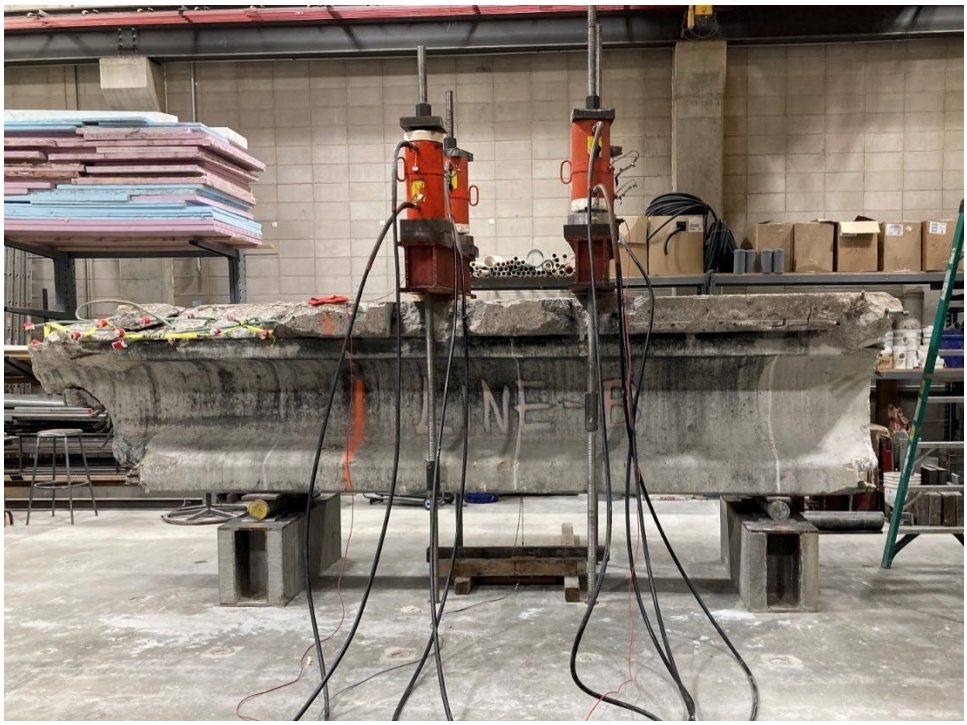

Figure 42. Girder end shear test configuration

Two reaction beams were used similarly to the bending tests with a hollow core hydraulic cylinder ram at each end. Each reaction beam was placed 1.5 ft from midspan, resulting in a 3-ft distance between the two. Deflection data were collected at midspan during loading of the girder. Visual observation for the formation of shear cracks was also completed.

For the first two cycles, a total load of 600 kips between the two reaction points was applied in 100-kip increments per reaction beam. During the third cycle, the goal was to fail the girder in shear; however, the hydraulic jacks did not have enough capacity to continue the test beyond the 840-kip total load. The girder was observed for cracking during each of the tests. Although occasional audible pops could be heard, no cracks were observed.

4 TEST RESULTS

4.1 Condition Assessment Documentation

This section discusses the condition of all girders post fire. Before any load testing occurred, a condition assessment of any cracks, spalling, color changes, etc. was documented. The Appendix provides additional documentation of the condition assessments for Girders B, E, and G.

4.1.1 Girder B

A visual assessment indicated that Girder B was least effected by the fire. Cracks observed on the deck surface were documented, but they were not considered to be a result of the fire. Rather, they appeared to be a result of concrete shrinkage typically observed on bridge decks. Figure 43 shows an example of the typical transverse cracks observed (annotated for clarity).

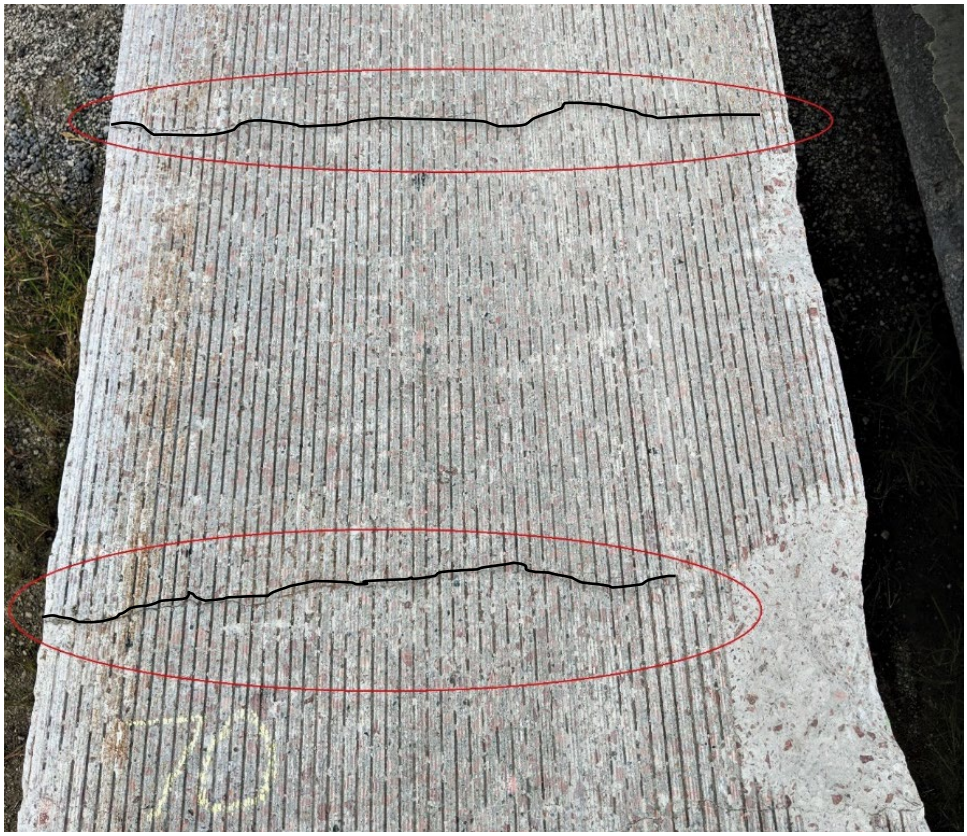

Figure 43. Typical deck surface cracking observed on Girder B

Areas of spalling were present on each side and bottom of the girder although it was in better condition than Girder E or G. An example of spalling near the midspan of Girder B at the bottom flange concrete is shown in Figure 44 and Figure 45 (annotated for clarity).

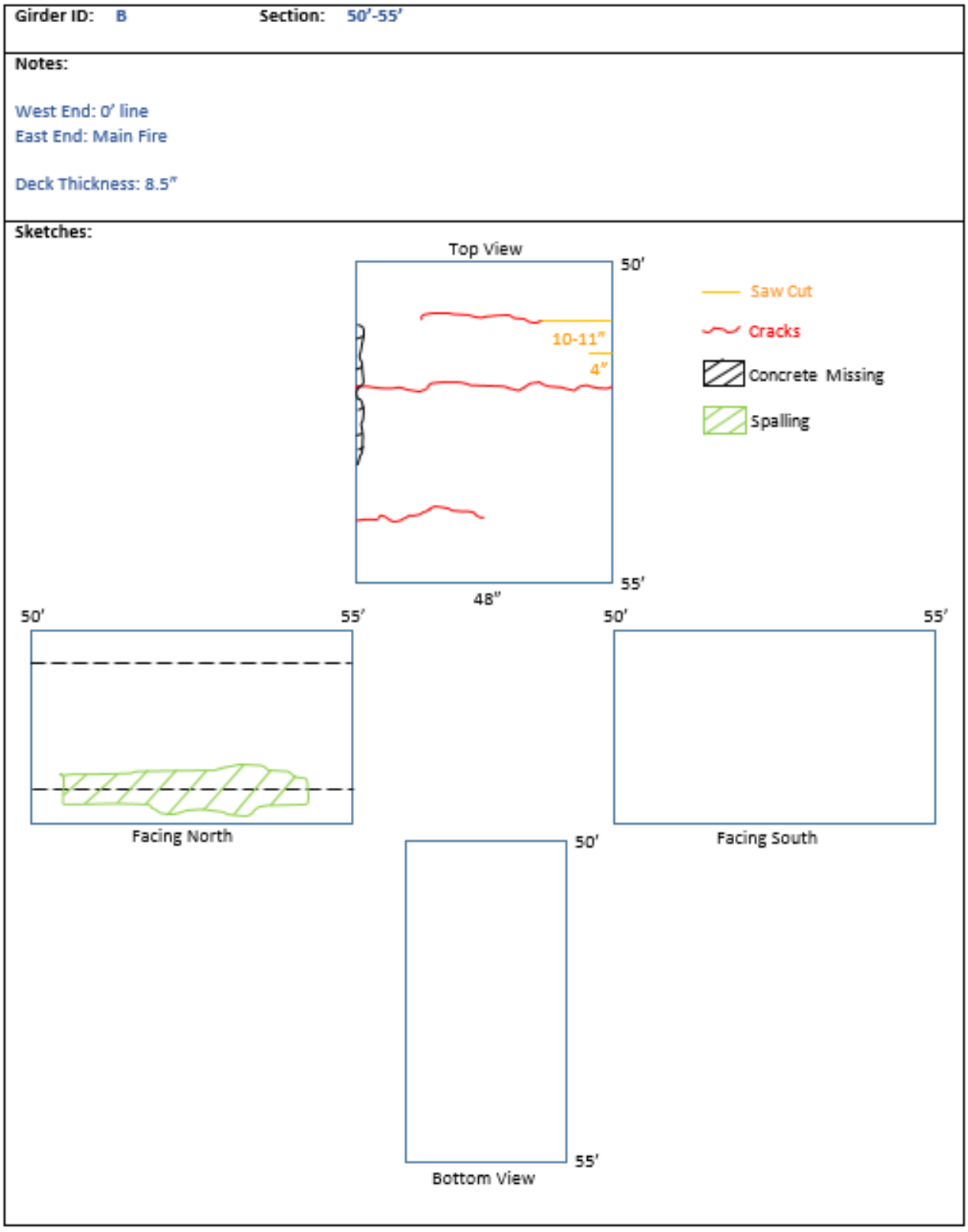

Figure 44. Example showing digitized condition assessment for Girder B

Figure 45. Spalled area on bottom flange near Girder B midspan

The full set of digitized condition assessment documents is provided in the Appendix.

4.1.2 Girder E

Visual observation of Girder E indicated a greater level of damage than Girder B (see Appendix). An increased area and depth of spalling was present compared to that for Girder B. The spalling occurred throughout the bottom flanges and at several areas on the web. Areas of steel reinforcement were exposed as shown in Figure 46 and Figure 47.

Figure 46. Bottom flange spalling on Girder E

Figure 47. Web spalling on Girder E

Extensive spalling on the bottom side of the girder is shown in Figure 48.

Figure 48. Bottom side spalling on Girder E

The top surface cracks observed were similar to what was seen on Girder B and not likely a result of the fire.

4.1.3 Girder G

The condition of Girder G was similar to what was observed on Girder E (see Appendix), although the overall area of concrete damage was greater. The bottom flanges and bottom side of the girder had extensive spalling (see Figure 49), which resulted in the exposure of steel strands and shear reinforcement (see Figure 50).

Figure 49. Spalling of concrete on bottom side of Girder G

Figure 50. Exposure of steel reinforcement as a result of concrete spalling on Girder G

4.2 Bending Test Results

In this section, the results from the two-point bending test are presented for each girder. Prior to the tests being completed, theoretical calculations were completed to determine the expected deflections of a non-damaged girder. These calculations were used to assess the effects of the fire on girder stiffness.

4.2.1 Calculated Deflections

Total deflection values for Girders B, E, and G were calculated using the equations provided in Figure 51 for two equal concentrated loads symmetrically placed about the girder midspan.

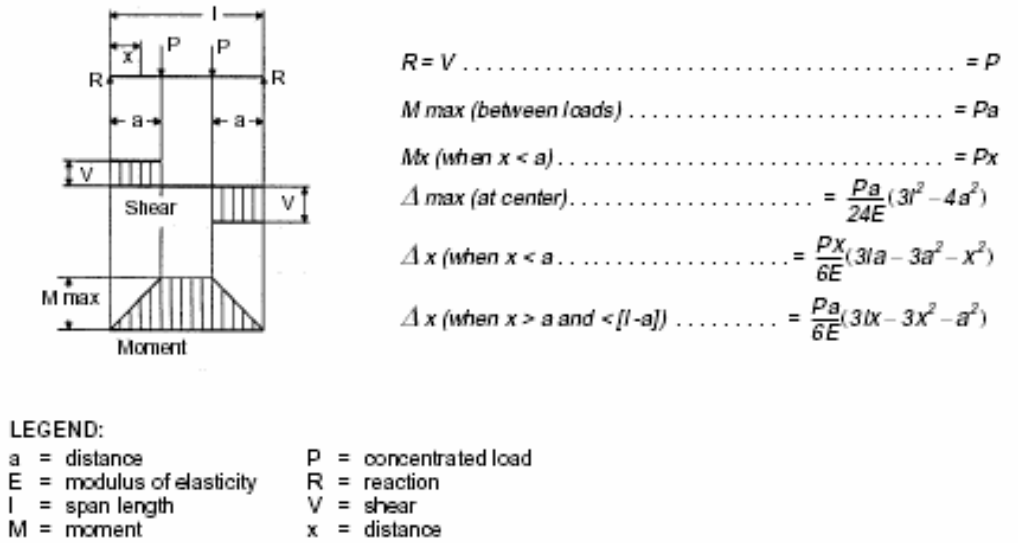

Figure 51. Deflection of simple beam with two equal concentrated loads

The material properties and girder geometry provided in the plan documents were used in these calculations. Deflection values at each cross-section (A, B, C, D, and E) were determined and are provided in Table 12.

Table 12. Girder cross-section locations

Cross-Section Location	Distance to Nearest Bearing Point	Location
A	4 ft 6 in.	Near End Span
B	21 ft 3 in.	Quarter Span
C	42 ft 6 in.	Mid-Span
D	21 ft 3 in.	Quarter Span
E	4 ft 6 in.	Near End Span

4.2.2 Girder B Bending Test Results

Girder B remained in an elastic state until the load reached about 70 kips at each load point location, or 140 kips total. This resulted in a midspan moment of about 2,700 kip-ft. Once this load magnitude was exceeded, yielding of the tensile reinforcement ensued at the extremities of the midspan, and flexural cracks in the concrete began to form at the bottom flange extending into the web. An example of the crack pattern is shown in Figure 52.

Figure 52. Crack patterns at midspan of Girder B

The strain data collected at midspan corroborated the observation of crack initiation at this point of loading. As shown in Figure 53, the tensile strain data at the bottom flange consistently

increased, and the compression strain data at the top flange consistently decreased, up until the point of the girder yielding.

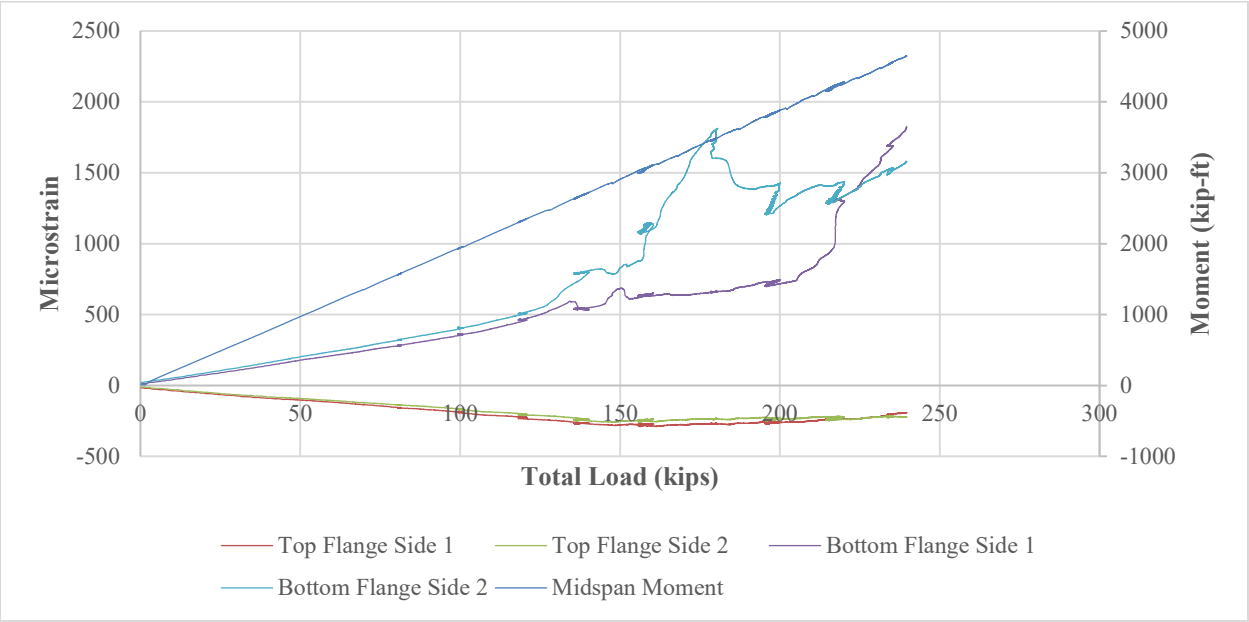

Figure 53. Midspan strain data for Girder B bending load test

The maximum tensile strain achieved prior to the data becoming inconsistent was about 500 microstrain at the bottom flange.

The deflection curves for Girder B at each point (A, B, C, E, and D) are shown in Figure 54, along with the predicted (elastic range only) deflection values using the plan dimensions and material properties.

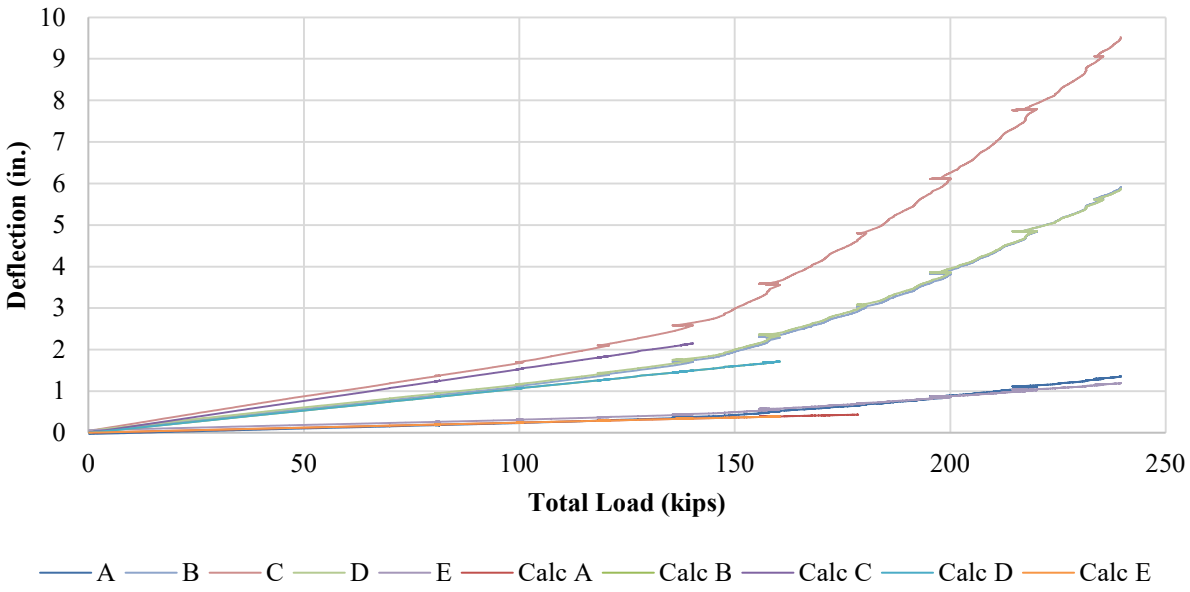

Figure 54. Actual vs. predicted deflection of Girder B

The actual and predicted deflection values were nearly matched through the elastic range of loading. This is also shown in Figure 55, which compares the measured deflection to the predicted values at a total load of 100 kips or moment of 1,925 kip-ft.

Figure 55. Girder B measured vs. predicted deflection at total load = 100 kip, M = 1,925 kip-ft

This value was chosen to ensure all sections were within the elastic range. The load test was ceased after reaching a midspan moment of about 4,600 kip-ft and a total midspan deflection of 9.5 in. or L/107. The deflected shape is shown in Figure 56 and can be contrasted with that of the adjacent girder.

Figure 56. Deflected shape of Girder B at max loading

4.2.3 Girder E Bending Test Results

The load test of Girder E differed from that for Girder B in that the load was increased to the point of girder failure. The measured strain and deflection behavior were consistent with what was observed during the Girder B test, despite the evidence of more extensive damage (increased areas and depth of concrete spalling). Figure 57 shows the observed crack pattern near midspan prior to full failure of Girder E.

Figure 57. Cracking of Girder E bottom flange and web

Cracks emanated from the bottom flange through the web. The angle of the cracks increased in slope the farther from midspan they appeared, with the tops of the cracks directed toward midspan.

Similar to Girder B, Girder E remained in an elastic state until the load reached about 70 kips at each load point location or 140 kips total. This resulted in a midspan moment of about 2,700 kip-ft. Once this load magnitude was exceeded, yielding of the tensile reinforcement at the extremities ensued at midspan, and flexural cracks in the concrete began to form at the bottom flange extending into the web.

The final failure was a result of deck buckling. Capacity of the deck portion of the composite section was quickly lost upon buckling, resulting in all of the load being directed into the girder and exceeding the girder ultimate capacity. Figure 58 shows the initiation of the deck buckling near one of the points of loading, and Figure 59 shows the girder after failure occurred at a total load of 260 kips or a midspan moment of about 5,000 kip-ft

Figure 58. Initiation of deck cracking at Girder E midspan

Figure 59. Girder E after failure at midspan

The strain data collected at midspan corroborated the observation of crack initiation at this point of loading. As shown in Figure 60, the tensile strain data at the bottom flange consistently

increased and the compression strain data at the top flange consistently decreased up until the point of the girder yielding.

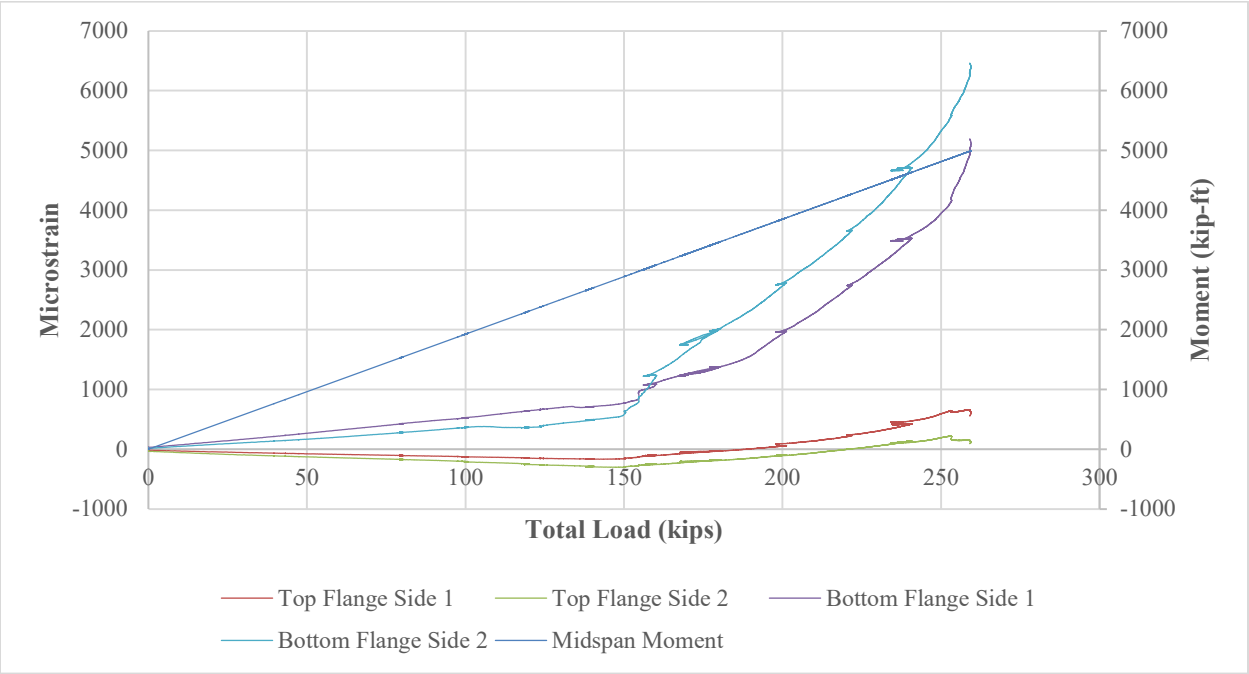

Figure 60. Midspan strain data for Girder E bending load test

The maximum tensile strain achieved prior to the data becoming inconsistent ranged from about 500 to 600 microstrain at the bottom flange depending on the side of the girder observed.

The deflection curves for Girder E at each point (A, B, C, E, and D) are shown in Figure 61, along with the predicted (elastic range only) deflection values using the plan dimensions and material properties.

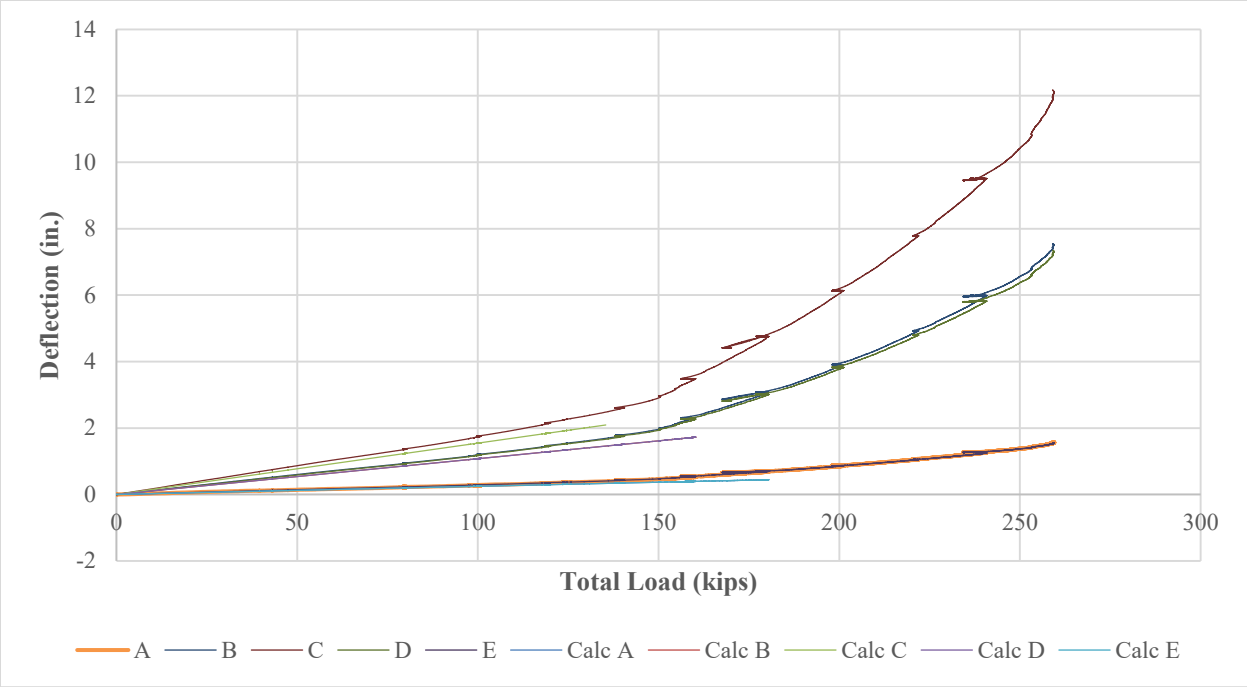

Figure 61. Actual vs. predicted deflection of Girder E

The actual and predicted deflection values were nearly matched through the elastic range of loading. This is also shown in Figure 62, which compares the measured deflection to the predicted values at a total load of 100 kips or moment of 1,925 kip-ft.

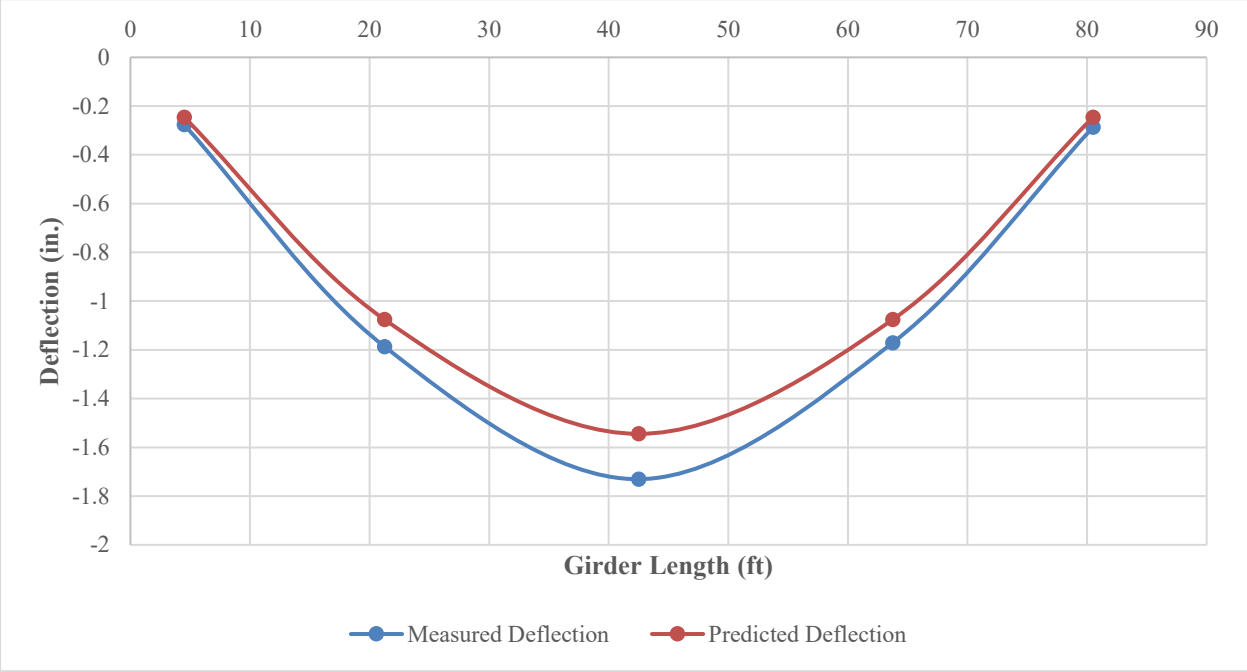

Figure 62. Girder E measured vs. predicted deflection at total load = 100 kip, M = 1,925 kip-ft

This value was chosen to ensure all sections were within the elastic range. The load test was ceased at the point of failure, which occurred after reaching a midspan moment of about 5,000 kip-ft and a total midspan deflection of 12.2 in. or L/84.

4.2.4 Girder G Bending Test Results

It was known that Girder G would be used for completing repair methods, so the load test was limited to loading that allowed the girder to remain within the elastic range given the research team did not want to induce additional permanent damage. The load test was performed to establish baseline data and performance before any repair methods were undertaken and to compare the results to the previous load test results up to the limit of loading.

The maximum load on the girder before concluding the test was about 130 kips, resulting in a midspan moment of 2,500 kip-ft. After the initial test and analysis, the researchers anticipated the elastic limit of Girder G would be very close to what was observed for Girder B and Girder E. Figure 63 shows the load test of Girder G being performed.

Figure 63. Girder G bending load test

The strain data collected at midspan were consistent with the strain behavior observed for Girders B and E. As shown in Figure 64, the tensile strain data at the bottom flange consistently increased and the compression strain data at the top flange consistently decreased.

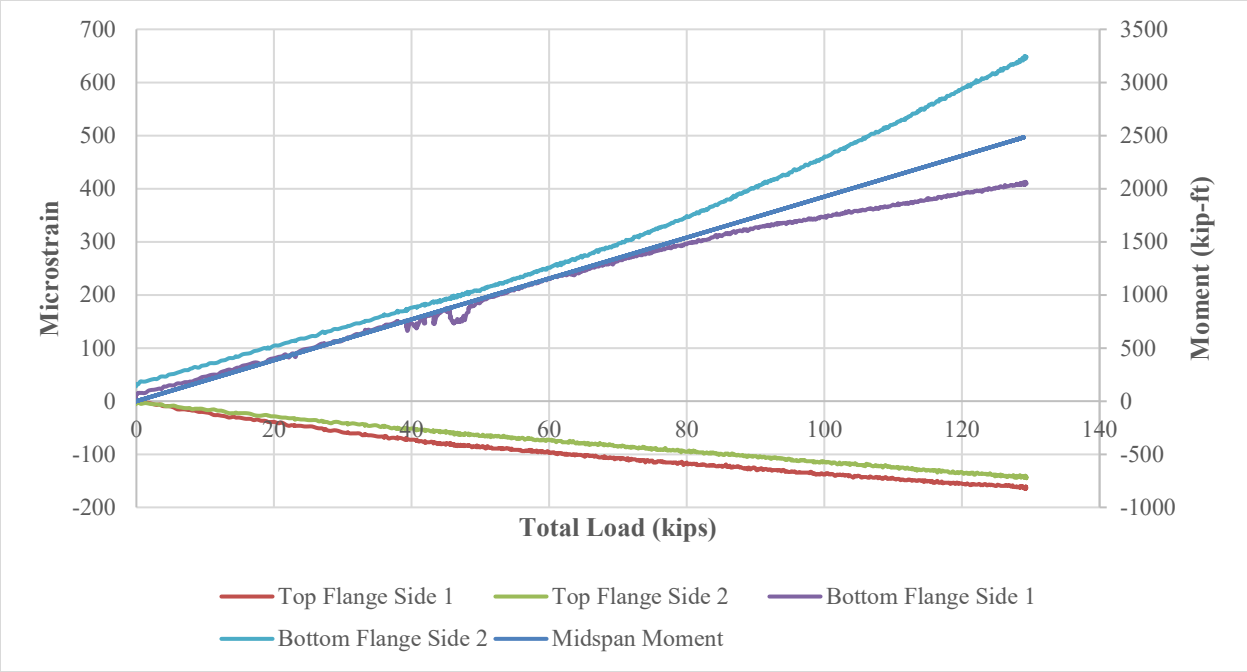

Figure 64. Measured vs. predicted deflection of Girder G

The maximum tensile strain achieved prior to the test data becoming inconsistent ranged from about 400 to 600 microstrain at the bottom flange, depending on the side of the girder observed. This deviation could be a result of specific localized damage to the girder or slight rotation of the girder upon continued loading.

The deflection curves for Girder E at each point (A, B, C, E, and D) are shown in Figure 65, along with the predicted deflection values using the plan dimensions and material properties.

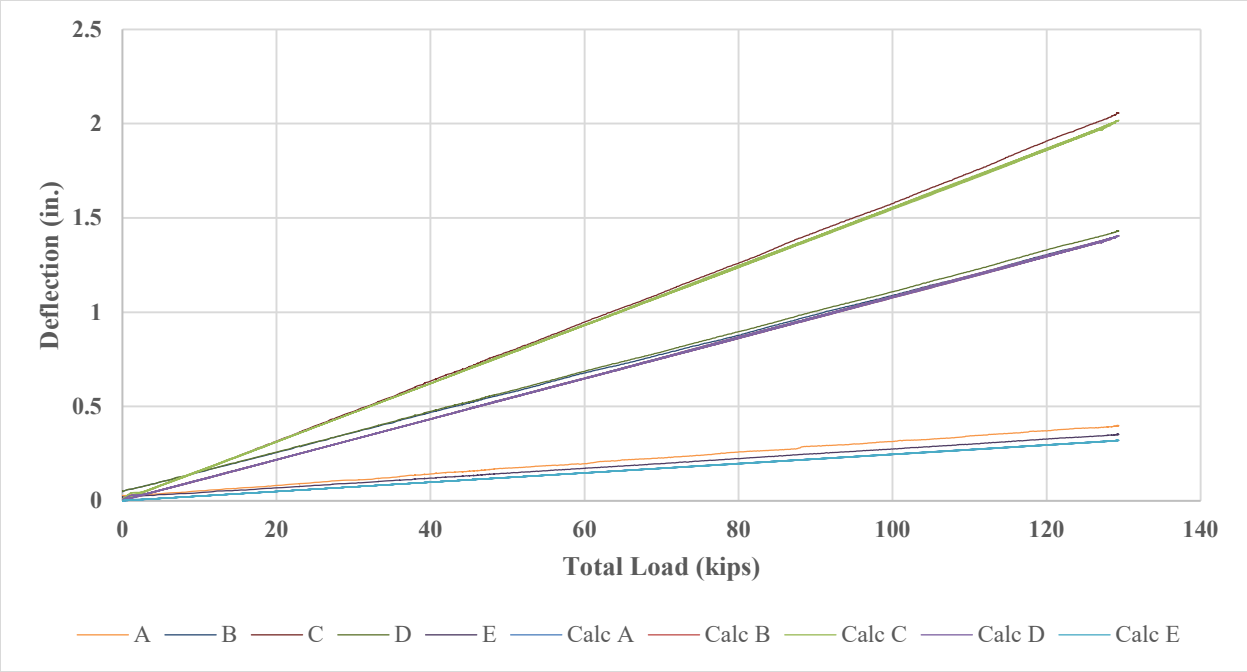

Figure 65. Measured vs. predicted deflection of Girder G at each point

The actual and predicted deflection values were nearly matched through the elastic range of loading. This is also shown in Figure 66, which compares the measured deflection to the predicted values at a total load of 100 kips or moment of 1,925 kip-ft.

Figure 66. Girder G measured vs. predicted deflection at total load = 100 kip, M = 1,925 kip-ft

This value was chosen to ensure all sections were within the elastic range. The load test was ceased prior to yielding of the girder when the midspan moment of about 2,500 kip-ft and a total midspan deflection of 2.0 in. or L/510 was reached.

4.2.5 Combined Girder Load Test Results

Figure 67 shows the combined strain results at midspan for the corresponding total load and midspan moment for each of the three girder bending tests.

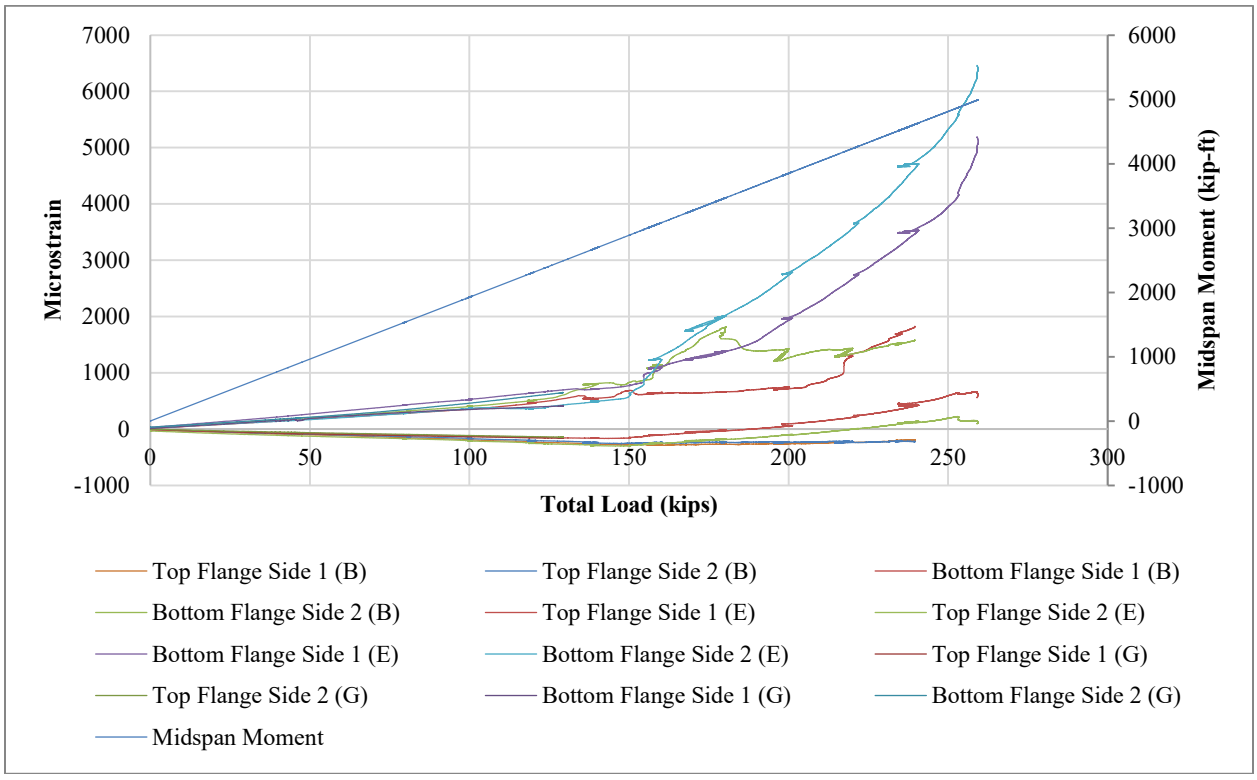

Figure 67. Combined strain results for Girders B, E, and G

Despite the apparent varying levels of damage between the girders (area and depth of concrete spalls), the tensile and compressive strain values were relatively consistent between tests up to the point of yielding.

Figure 68 shows the combined measured deflection at midspan versus the total load applied.

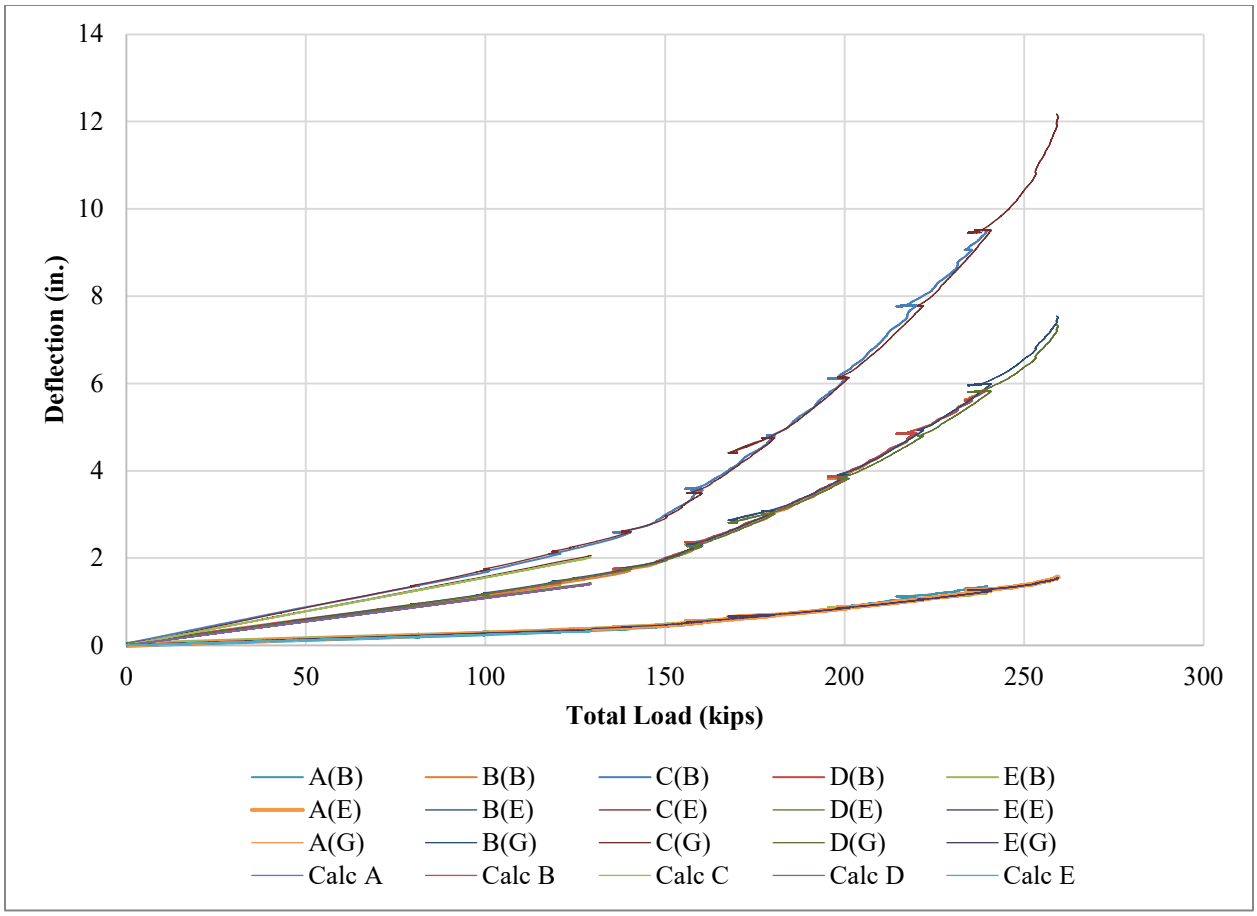

Figure 68. Combined deflection results for Girders B, E, and G

The measured deflection values for each of the three load tests were very nearly equal despite their varied conditions, similar to those for the measured strain values.

The primary objective of the load tests was to determine whether a clear difference existed in structural performance of each girder that could be correlated to their visual conditions. Despite the differences in area and depth of spalls, especially between Girder B and Girders E and G, the performance of each girder was nearly replicated from one test to another.

Furthermore, the deflection values calculated per the plan-based material properties and girder geometry produced results that coincided with their actual measured behavior. This indicates that the damage was limited to the surface concrete, which sufficiently insulated the steel reinforcement from extreme temperatures that would have materially affected girder performance. Therefore, a properly completed repair to ensure the protection and performance of the remaining structure could have been an option for this particular bridge.

4.3 Shear Test Results

The shear test on the end of Girder B was completed by applying load in three total cycles. The total load was increased to 600 kips for the first and second cycles and then to about 840 kips for the third and final cycle, resulting in a maximum shear force of 420 kips. The load effects for the first cycle resulted in a portion of the specimen becoming inelastic, as the specimen did not return to its pre-loaded deflection values. The specimen further yielded during the final cycle. The maximum deflection was 0.21 in. at the max load over the 10 ft clear span length. The results are shown in Figure 69.

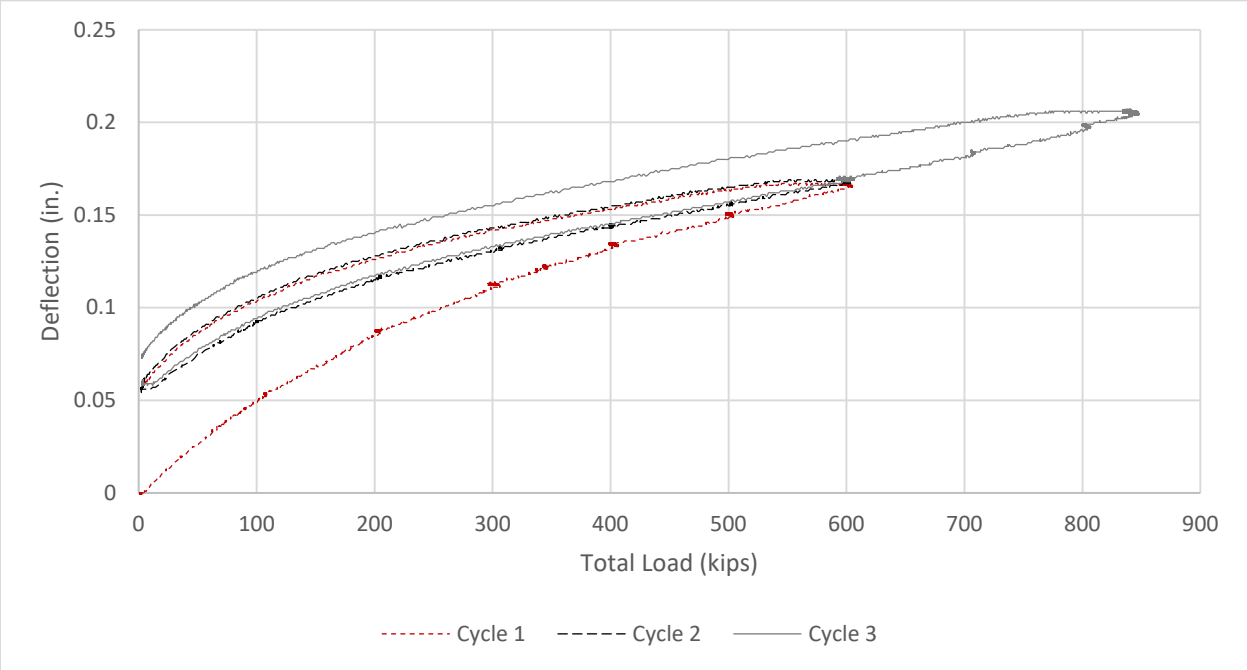

Figure 69. Deflection vs. total load for girder end shear test

Cracking noises could be heard during the last cycle as the load increased, but no visible cracks appeared anywhere on the girder. Despite the ultimate capacity not being determined, the girder exhibited shear capacity beyond what could be foreseeably seen in service.

4.4 Materials Test Results

This section discusses in detail the results for both the concrete compression and steel strand tensile test results. The results were used to determine any clear changes in the concrete and steel material properties due to the heat of the fire and to compare the results against those for the assumed properties used for theoretical deflection calculations.

4.4.1 Compression Test Results

The compressive strength for each of the concrete cylinder specimens is provided in Figure 70.

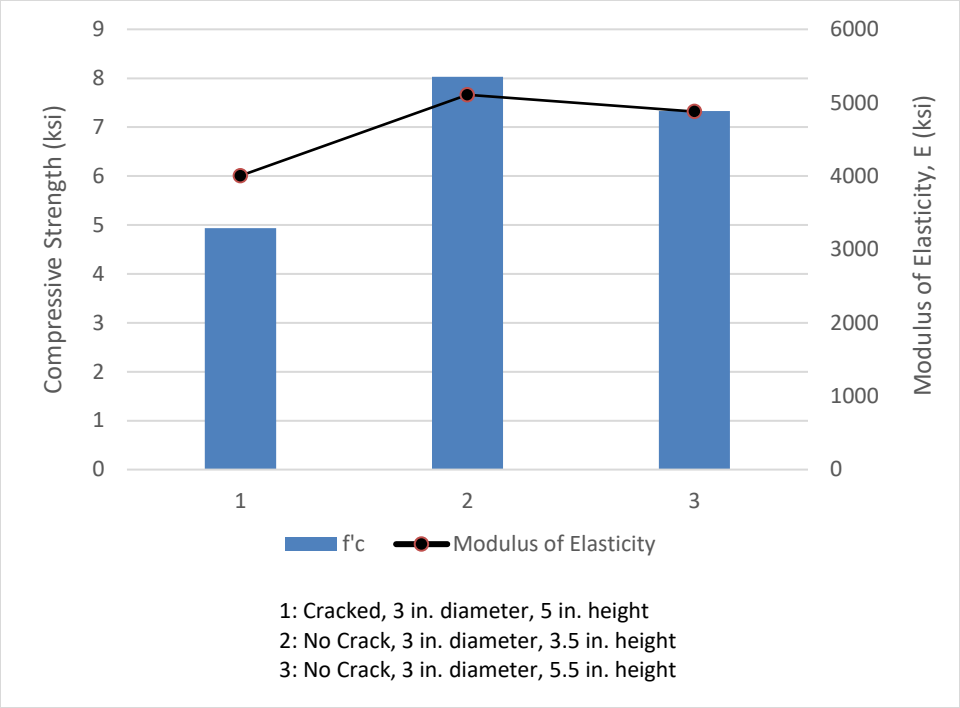

Figure 70. Concrete cylinder test results

The corresponding modulus of elasticity (E) was calculated using the following equation:

$$E = 57{,}000\sqrt{f'_c}$$

The results from each test were varied, which may have been a function of several variables, such as the size of specimen, the location from which the core was obtained, the concrete condition, and so forth. The number of samples tested did not provide sufficient evidence to conclusively state the concrete strength was significantly affected beyond that at the immediate fire-exposed surface.

Nonetheless, these samples showed the strength of the concrete was very likely greater than that specified in the plan documents. The researchers still calculated the modulus of elasticity (E) for each sample using the previous equation.

4.4.2 Tensile Test Results

The stress versus strain results for the steel strand tensile tests are shown in Figure 71.

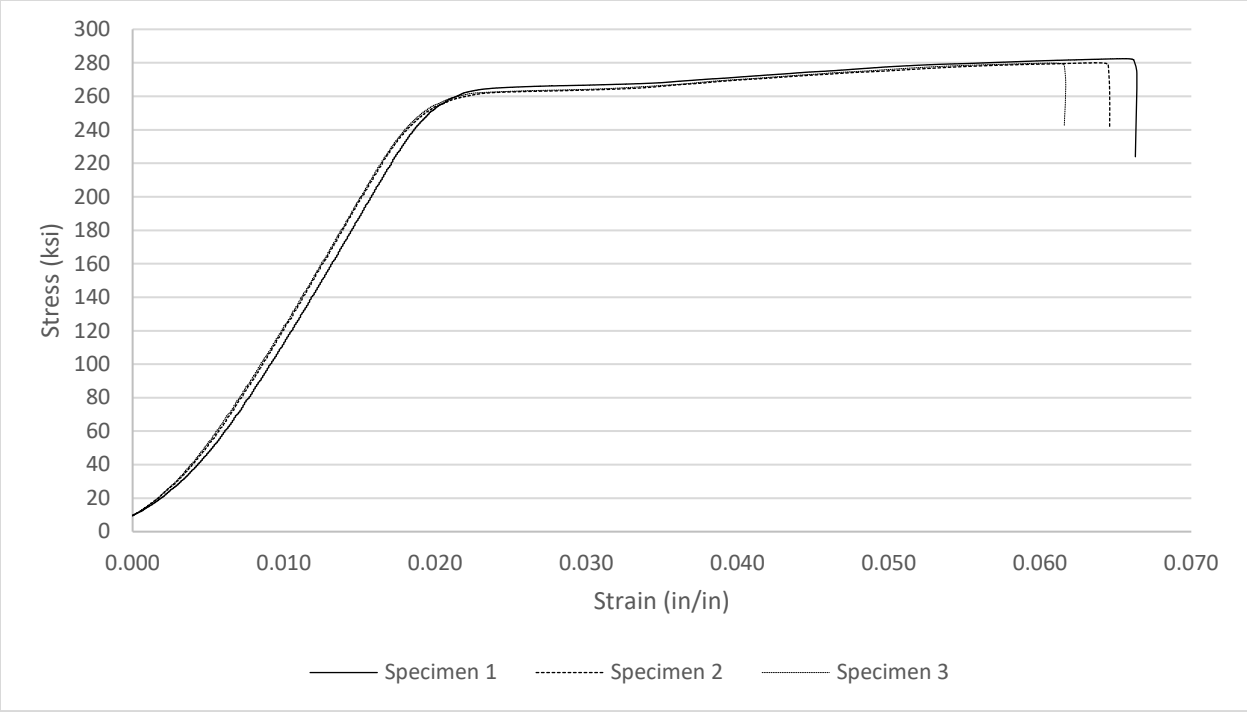

Figure 71. Reinforcement strand test results

The ultimate tensile strength for the prestressing steel strands per the contract documents was specified as 270 ksi. As shown in the graph, the strands performed consistently among the specimens with a yield strength of about 255 ksi and an ultimate tensile stress of about 280 ksi. This indicates that the prestressing steel reinforcement still achieved the specified strength requirements despite any possible effects from the fire.

5 GIRDER REPAIRS

5.1 Purpose of Repair Exploration

With respect to bridges, fire damage is not as common as other types of damage; however, finding suitable solutions for the repair of fire-damaged bridge elements is important. For the girders tested in this research project, it was shown that the strength and stiffness were not significantly reduced despite the apparent damage sustained, including concrete spalling along the girder length. Given that the structural integrity remained intact, the purpose of the repairs was to focus on protecting the remaining concrete and reinforcement to ensure service life is not lost rather than on restoring any lost capacity.

5.2 Repair Methods

This section explores a few different repair methods for fire-damaged girders. Of the three girders subjected to load testing, only Girder G was used to undergo repair using three different methods. The loading of the girder in its previous test was limited to that which maintained its elastic properties throughout the girder length. (Girders B and E were loaded in bending beyond their yield points or even to failure and, thus, repairs would not have been suitable using those girders).

The repairs were evaluated for simplicity, the effectiveness of protecting the remaining girder, and durability under a sustained load. The following materials/methods were chosen for demonstration with each option occupying a 10 ft length of the girder near midspan:

- Self-consolidating concrete (SCC)
- Ultra-high performance concrete (UHPC)
- SCC in combination with FRP wrap

In each case, forms were constructed around the bottom flange to create a cast around the most damaged portions of the girder.

5.2.1 SCC Girder Repair

SCC is defined as a “highly flowable, non-segregating concrete with a slump flow of 20 to 30 in. that can spread into place, fill the formwork, and encapsulate the reinforcement without any mechanical consolidation” (ACI 2015). Some advantages of SCC over regular concrete are that it has better hardening properties, can be flexible, has smoother surfaces, is self-leveling, and reduces labor and equipment usage (ACI 2015).

SCC was chosen because it can more easily spread into the formwork, into smaller voids, and around the reinforcement where space is limited and without the need for mechanical vibration.

A highly flowable concrete mix maximizes the potential for any exposed reinforcement to be fully covered once placement is completed.

5.2.2 UHPC Girder Repair

UHPC is "a cementitious composite material composed of an optimized gradation of granular constituents, a water-to-cementitious materials (w/cm) ratio less than 0.25, and a high percentage of discontinuous internal fiber reinforcement" (FHWA 2022). UHPC has gained popularity in new construction and also become more commonly used as a repair material for concrete bridge elements. In fact, the first UHPC prestressed concrete bridge built in the United States is located in Wapello County, Iowa (FHWA 2022).

This type of concrete has been shown to increase strength and durability and can lengthen the design life of structures. The material properties of UHPC lend well to the repairs of Girder G and the required encapsulation of existing elements.

UHPC can be relatively costly, although its material advantages may be worth the increased cost and may serve well for repairs of this nature where the quantity is proportionally small. The UHPC concrete used for this project has the following material properties per the supplier (see Table 13).

Table 13. Typical UHPC material properties

Property	Value
Compressive Strength: 1 day	≥ 11 ksi (76 MPa)[1]
7 days	≥ 19 ksi (131 MPa)
13 days	≥ 21 ksi (145 MPa)
28 days	≥ 23 ksi (159 MPa)
56 days	≥ 25 ksi (172 MPa)
Sustained Post-Cracking Tensile Strength (Graybeal and Baby 2019)	1.07 ksi (7.38 MPa) minimum; 1.50 ksi (10.34 MPa) average
Static Modulus of Elasticity	8,250 ksi (57 GPa)
Chloride Ion Penetration (ASTM C1202)	49 coulombs at 56 days
Flow (adjustable per project needs)	6 in. (15 cm) to 13 in. (33 cm) diameter
Working Time	As needed[2]
Set Time (minimum values)	75 minutes initial; 87 minutes final[2]

According to ASTM C1856/C1856M except where noted otherwise; 70°F (21°C) curing temp, 2% load of 0.5 in. × 0.008 in. (13 mm × 0.2 mm) steel fiber with 435 ksi (3 GPa) tensile strength

[1] Steelike® UHPC can be modified to reach 14 ksi compressive strength in as little as 12 hours

[2] Set times and working times can be customized according to project needs

Source: © Steelike Inc. 2022, used with permission

5.2.3 SCC and FRP Wrap Girder Repair

An FRP system can be made out of many different materials. The most common FRP system for strengthening concrete is CFRP due to its high tensile strength, stiffness, and durability

(Alkhrdaji 2015). Similar systems made with glass fibers can be a good option when the repair needs are satisfied, because it is often more cost effective.

Whether carbon fiber or glass fiber, the material is woven into a fabric matrix that can easily be wrapped around different profile types and provide additional tensile reinforcement to increase the flexural strength. Typically, FRP wrapping is used in combination with concrete and epoxy to repair or strengthen structurally insufficient elements.

For Girder G, the FRP wrap was used in combination with SCC cast of the bottom flange. The FRP wrap was SikaWrap Hex-106 G, a bi-directional E-glass fiber fabric from Sika Corporation (see Table 14 for technical information).

Table 14. SikaWrap Hex-106 G product information

TECHNICAL INFORMATION

Nominal Ply Thickness	**Average Ultimate Value**	**Design Value**	-
	-	0.007 in. (0.18 mm) each fiber direction	
Tensile Strength	**Average Ultimate Value**	**Design Value**	(ASTM D-3039) 73 °F (23 °C) 50 % R.H.
	76.7 ksi (529 MPa)	65.6 ksi (452 MPa)*	
	* Average ultimate value minus 3 standard deviations		
	Average Ultimate Value	**Design Value**	(ASTM D-7565) 73 °F (23 °C) 50 % R.H.
	-	0.5 kips/in./ply	
Tensile Modulus	**Average Ultimate Value**	**Design Value**	(ASTM D-3039) 73 °F (23 °C) 50 % R.H.
	-	4.24 msi (29.2 GPa)(E_f)	
	* Average ultimate value minus 3 standard deviations		
Tensile % Elongation	**Average Ultimate Value**	**Design Value**	(ASTM D-3039) 73 °F (23 °C) 50 % R.H.
	1.81 %	1.45 %*	
	* Average ultimate value minus 3 standard deviations		
Tensile Stiffness	**Average Ultimate Value**	**Design Value**	(ASTM D-7565) 73 °F (23 °C) 50 % R.H.
	-	29.7 kips/in./ply (E_f*A)	

Sika 2018

The wrap was used in conjunction with a two-part high-modulus, high-strength, impregnating resin Sikadur Hex-300, also from Sika Corporation.

5.3 Repair Implementation/Methodology

The three repair methods were completed near midspan to maximize the load effects when tested. Figure 72 shows the configuration of the repair materials with respect to the bottom flange of the girder.

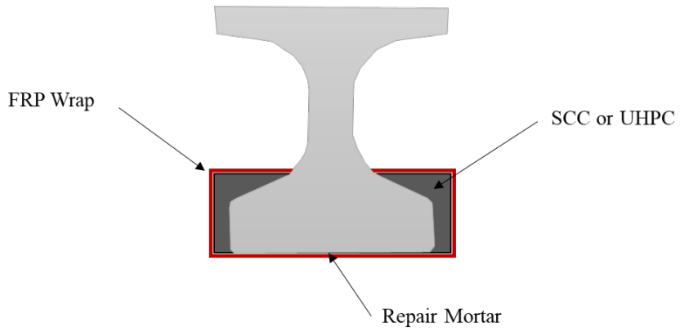

Figure 72. Repair methods for fire-damaged girder

Note that each repair method is shown in one graphic, not each unique repair. In total, a 30 ft section at midspan was repaired, consisting of three 10 ft sections for each repair method. Prior to any of the repairs being completed, any loose or delaminated concrete was removed, as shown in Figure 73 and Figure 74, to ensure a sound bonding surface for each repair material.

Figure 73. Removal of loose bottom flange concrete

Figure 74. Bottom flange after loose concrete removal

Tapcon concrete screw anchors (1/4 × 2 1/2 in.) were placed along the 10 ft spans in multiple rows at about 12 in. spacing (see Figure 75), and #3 reinforcing steel bar was tied to the anchors along the girder length, as shown in Figure 76.

Figure 75. Concrete anchors into bottom flange

Figure 76. Tapcon concrete anchors and #3 rebar

Steel forms were then placed vertically along the bottom flanges of the girder with plywood panels abutted to the bottom surface (see Figure 77).

Figure 77. Steel and plywood formwork

The concrete mix was then poured (see Figure 78) and allowed to harden before removing the formwork.

Figure 78. Placement of the SCC mix around the bottom flange

The UHPC repair section required the materials to be batched on site. A mixer and the pre-measured material quantities were trailered to the site as shown in Figure 79.

Figure 79. UHPC materials and mixer

Once the mixing protocol was completed, the UHPC was poured into the forms either directly from the mixer or by using 5 gal pails (see Figure 80).

Figure 80. Placement of the UHPC section of repair

The consistency of the UHPC allowed the forms to be simply filled without the need for mechanical vibration. Even so, the material can present some challenges while mixing due to the precision of mix ingredient quantities and the timeliness required before hardening begins. It is expected that the challenges presented for a repair of this nature on an in-service bridge are simply mitigated by off-site batching and experienced work crews.

Figure 81 and Figure 82 show the completed SCC and UHPC repairs and their dimensions after the formwork was removed.

Figure 81. UHPC and SCC repair sections fully cast

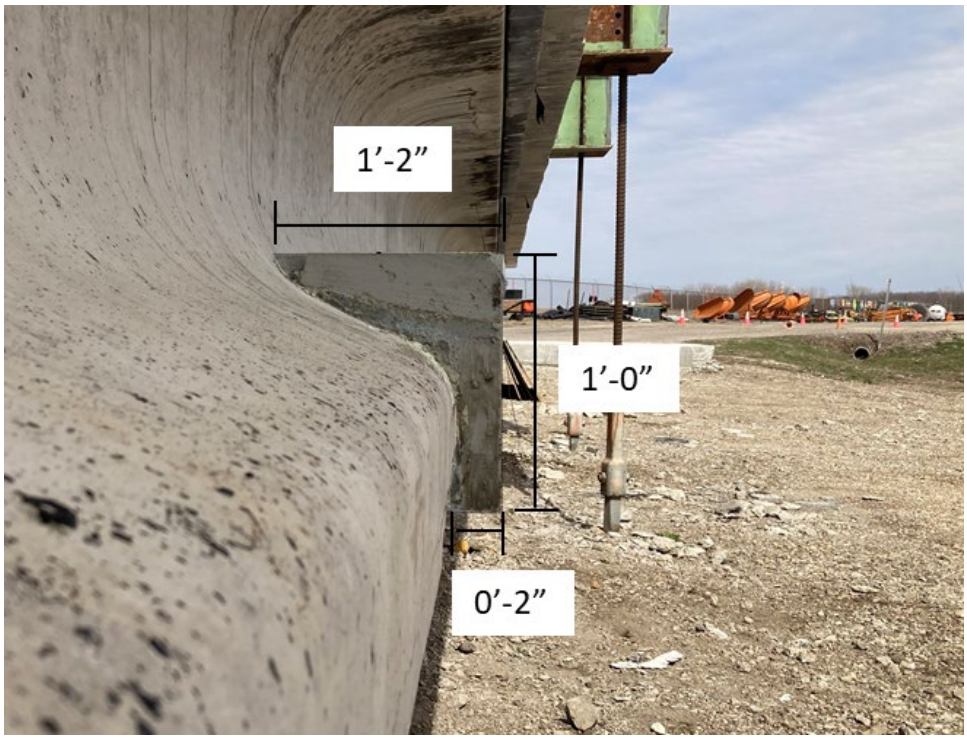

Figure 82. Dimensions of SCC and UHPC bottom flange repair

Once the SCC and UHPC sections were fully cast and allowed to cure, the spalling along the bottom of the girder was repaired using SikaQuick vertical and overhead (VOH) repair mortar, which is intended for vertical and overhead use. The spalls were relatively shallow in comparison to the bottom flange tips; thus, a repair mortar was sufficient to restore the surface to its pre-damage plane. The spall condition prior to the repair condition is shown in Figure 83, and the condition after the repair was completed is shown in Figure 84.

Figure 83. Bottom of girder spalls prior to repair

Figure 84. Bottom of girder spalls after repair mortar application

For the middle 10 ft section, the SCC repair was combined with an FRP wrap. The objective of this repair was to evaluate the constructability of the FRP wrap with a secondary objective to

provide a duplex option in the event it was determined additional concrete strength or protection was desired. FRP wrap is known to be able to be used on complex shapes due to its flexibility and light weight.

To begin the installation process, the resin was mixed and applied to the girder using a 3/8 in. nap paint roller (see Figure 85).

Figure 85. Preparation for mixing the FRP resin

The FRP fabric was then placed into the resin and rolled flat to the surface (see Figure 86).

Figure 86. FRP wrap application on bottom flange repair

A couple of specific observations were noted with respect to the FRP wrap installation process. First, the resin product did not provide sufficient tack to hold the FRP in place in an overhead position upon initial installation; continuous rolling with additional resin was required. Secondly, the surface, although relatively smooth, requires a high-level of smoothness to bond the FRP wrap. Any surface deviation was spanned by the FRP wrap leaving a small pock of un-adhered FRP wrap. Thirdly, the FRP wrap is highly flexible, but enough rigidity remained that wrapping around 90-degree corners was difficult. Void space between the FRP was observed immediately at the corners. Some of these problematic areas are shown in Figure 87.

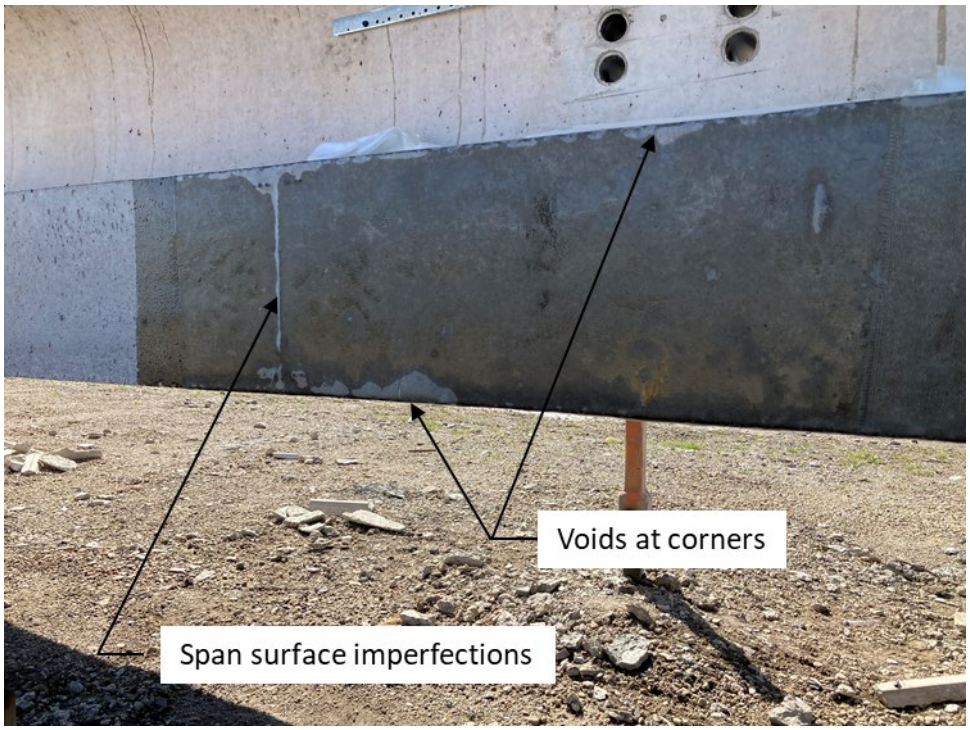

Figure 87. Problematic areas of FRP installation

After all repair methods were completed, a two-point load test was performed in the same manner as the previous girder tests. The load test setup is shown in Figure 88.

Figure 88. Load test of repaired girder

Deflection transducers were placed at each of the five defined points (A, B, C, D, and E) to measure deflection. However, for this test, the loading was locked off at 130 kips total load (close to its elastic limit) and maintained for an extended time period. The purpose of this was to see how the girder performed under sustained loading and how this impacted the stress on the repairs.

The measured deflection results were compared to those from the initial pre-repaired girder test as presented in Figure 89.

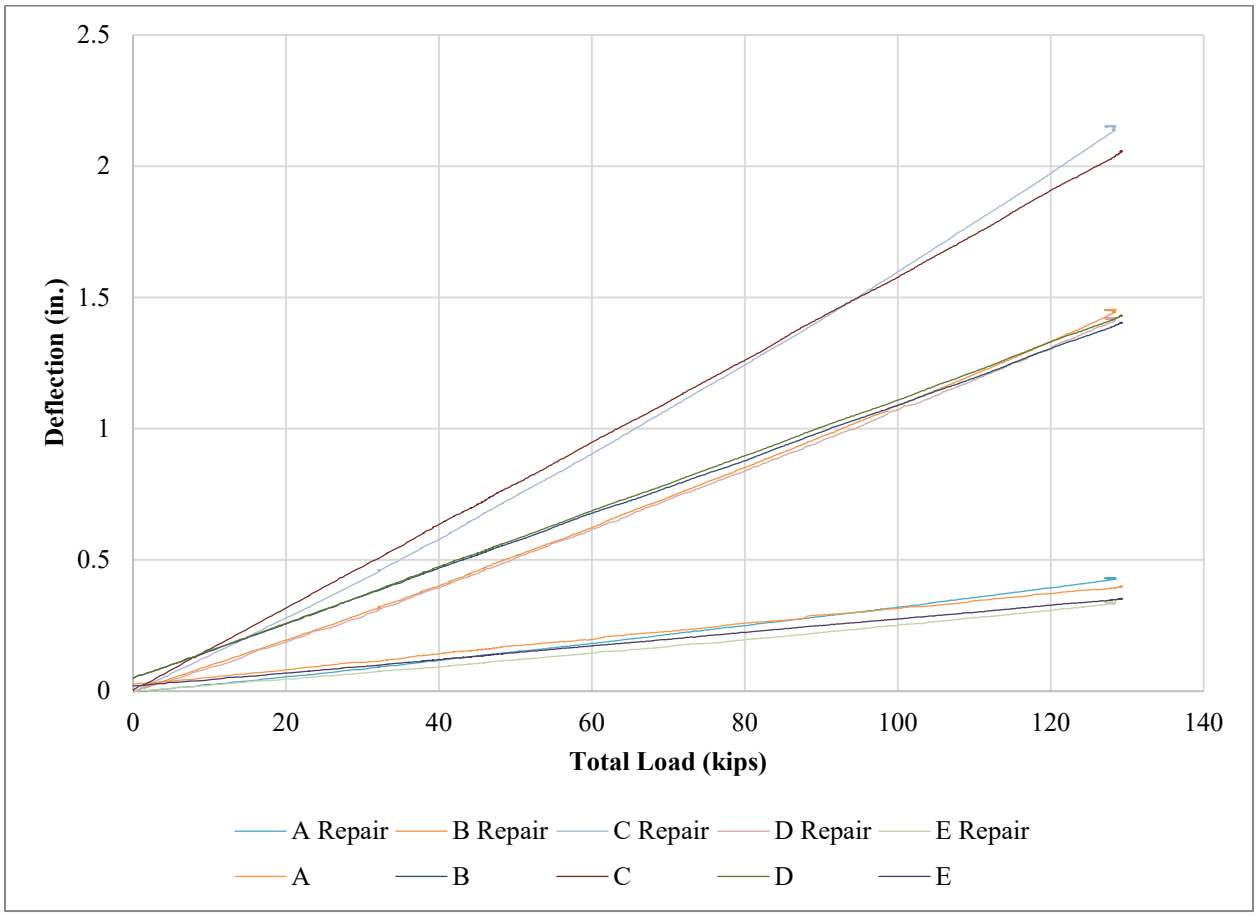

Figure 89. Comparison of repaired vs. pre-repaired Girder G deflection results

Despite the added concrete sections at midspan, the repair was not anticipated to increase the stiffness in any appreciable way. The deflection results bear this out as the results from the pre-repaired and repaired girder do not deviate in any significant way.

Within weeks of the sustained load being applied to the girder, vertical cracks formed in the SCC repaired sections as shown in Figure 90 and Figure 91.

Figure 90. Vertical cracks in SCC/FRP repair section

Figure 91. Closeup of vertical cracks in SCC/FRP repair section

These cracks were especially evident in the FRP repaired sections given the epoxy debonded from the concrete at the crack locations.

Cracks were not observed in the UHPC section.

The moment at midspan was about 5,000 kip-ft resulting from two-point loads of nearly 65 kips. It is unknown through load testing what reduction in load would be required to eliminate the cracking, although it can be surmised that the non-prestressed SCC would crack once the strain magnitude reaches about 130 microstrain. The non-repaired girders reached this level of strain when the two-point loads reached about 15 kips each.

This load scenario is likely still more than what a girder would experience on an in-service bridge, accounting for load distribution among adjacent girders. Furthermore, crack reduction or elimination could be accomplished through preloading the girder prior to concrete placement such that the concrete is placed in compression upon removal of the load.

6 ECONOMIC ANALYSIS FOR GIRDER REPAIR VS. GIRDER REPLACEMENT

6.1 Introduction

The purpose of this chapter is to present an economic analysis for girder repairs and partial girder replacement. Economic feasibility is a key factor when it comes to deciding how to approach repairing a fire-damaged bridge. Repairs or partial replacements exceeding the cost of complete removal and replacements are not practical. Therefore, to aid repair decision making, a breakdown of typical costs for different repairs and girder replacements are presented below.

6.2 Girder Repairs

Different levels of fire damage require different repair methods for prestressed concrete bridges. The severity of the damage a bridge has incurred from fire greatly varies and needs to be evaluated on a case-by-case basis.

Replacement of a girder can be costly and time consuming. Average girder replacement can cost $8,000 per ft and take one to two months to complete (Jones 2015). Hence, girder repairs are the first option to consider for low-to-mid levels of damage. The following cost estimates discussed in this section are typical costs for general girder repairs, which can apply to fire-damaged girders.

Typically, prestressed concrete girders are replaced if damaged (Enchayan 2010). The repairs can be costly, cause traffic delays, and produce cold joints on the bridge deck (Enchayan 2010). Enchayan (2010) mentions that girder repair with strand splicing is a good option to consider initially along with using compatible grout to repair spalled concrete. The author also states that repair costs are usually less than 70% of girder replacement, encouraging repairs to be considered first.

Another study discussing repair methods for prestressed concrete bridge members states that "repair-in-place techniques may cost 30% of the cost for replacement" (Shanafelt and Horn 1980).

The first repair option utilized in the research for this project was SCC. SCC is $10 to $15 per cubic yard (and sometimes up to $30 per cubic yard) and more expensive than normal concrete (Concrete Questions 2022). Bill Bundschuh, president of PRETECH Corp. of Kansas City, Kansas, has said that although there may be a surcharge of $20 per cubic yard for SCC, the extra cost can be mitigated due to the cost savings in labor, vibrator repair, and safety (McCraven 2010).

Another repair option, using UHPC to patch areas of spalled concrete, was evaluated. The typical cost of UHPC is about $2,000 per cubic yard, which includes material cost of the proprietary mix, fiber reinforcement, and labor/delivery costs (ODOT 2020). However, a non-proprietary blend can cost under $1,000 per cubic yard with domestic materials (ODOT 2020). Although

there is a potential for savings when selecting a non-proprietary mix over a proprietary mix, UHPC is still a much more expensive concrete to use. Despite this fact, UHPC may be more beneficial due to its high compressive strength in situations where a girder has had a loss of strength.

The third repair method considered during this research was combining SCC with FRP wraps. Specifically, glass fiber-reinforced polymer (GFRP) wraps were used for the girder repair. The following two tables, Table 15 and Table 16, provide a summary of repair costs in 2006 using CFRP, which is a very similar product.

Table 15. Labor summary (hours) for AASHTO girder repairs using CFRP

Task Description	AASHTO1	AASHTO2	AASHTO3	AASHTO2R
Chipping damaged concrete	4	4	4	4
Applying rust inhibitors	2.5	2.5	2.5	2.5
Constructing and installing formwork	3.2	3.2	3.2	3.2
Pouring concrete	19.83	8	8	8
Epoxy injection	5	5	5	5
Grinding	20	20	20	20
Sandblasting	9	8	8	6
Cutting fiber	3	5	5	8
Installing longitudinal CFRP reinforcement	15	15	15	10
Installing U-wrap CFRP reinforcement	12	13	13	22
Total hours / girder	93.53	83.7	83.7	88.7
Total hours / ft*	3.23*	2.89*	2.89*	8.87**

* length of repair = 28.9 ft.
** length of repair = 10 ft.

Rizkalla et al. 2007, North Carolina State University

Table 16. Cost analysis for AASHTO girder repairs using CFRP

System Designation	AASHTO1	AASHTO2	AASHTO3	AASHTO2R
Repair system	EB CFRP sheets	EB CFRP sheets	EB CFRP sheets	EB CFRP sheets
Repair Mortar	500	500	500	500
Rust Inhibitors	60	60	60	60
Epoxy Injection	100	100	100	100
Formwork Materials	700	700	700	700
Main Longitudinal CFRP	456	67.5	67.5	45
Tension strut CFRP	391.5	58.5	58.5	99
CFRP U-wraps	564	376.65	376.65	399.15
Equipment	265.5	265.5	265.5	265.5
Labor total ($45/hour)	4208.85	3762.2	3762.2	3987.0
Total cost	7245.85	5890.4	5890.4	6155.6
Total cost / ft*	249.91*	203.09*	203.09*	1373.19**

* length of repair = 28.9 ft.
** length of repair = 10 ft.

Rizkalla et al. 2007, North Carolina State University

Other materials, such as epoxy injections and shotcrete, may be used to aid in girder repairs. The typical costs for epoxy injections are about $100 per linear ft (Palmer Engineering 2019). Shotcrete can cost about $125 per yard and is useful in situations for difficult projects where vertical or overhead applications may be required (Concrete Questions 2022). Finally, after a cost estimation of repairs has been made, a 5 to 25% contingency is planned, depending on the extent of repairs and the labor required.

A research study conducted by Chaudhary et al. (2022) discusses the cost of repairs for fire-damaged concrete and steel structures. Table 17 and Table 18 present repair strategies as well as repairability criteria needed for fire-damaged structures.

Table 17. Damage states for concrete structures subjected to fire

Damage state	Thermal damage	Repair	Mechanical damage	Repair
DS0	D300 ≅ 0	No repair required	$\Delta s/l < 1/240$	Repair for thermal damage, if necessary
DS1	D300 < $c/10$	Clean damaged surface	$1/240 \leq \Delta s/l < 1/120$	
DS2	$c/10 \leq$ D300 < $d/2$	Clean damaged surface; replace damaged concrete	$1/120 \leq \Delta_s/l < 1/60$	Slab needs to be demolished and reconstructed
DS3	$d/2 \leq$ D300	Slab needs demolished and reconstructed	$1/60 \leq \Delta_s/l$	Whole floor system (slab and beams) needs demolished and reconstructed

D300 = maximum depth of section with temperature greater than 300°C (572°F); c = concrete cover to reinforcement; d = depth of slab; Δ_s = residual vertical deflection at center of slab; l = square root of $l_1 l_2$, where l_1 and l_2 = spans of slabs in adjacent directions

Source: Chaudhary et al. 2022 (who adapted from Ni and Gernay 2021)

Table 18. Damage states for steel structures subjected to fire

Damage state	Thermal damage	Repair	Mechanical damage	Repair
DS0	$T_{max} < 300$°C	No repair required; re-painting if necessary	$\varepsilon_s = \varepsilon_{s,amb}$	No repair required
DS1	$300 \leq T_{max} < 900$°C	Remove and re-apply steel protection insulation and paint	$\varepsilon_y \leq \varepsilon_s \leq 15\varepsilon_y$	Heat-straightening of steel member
DS2	900°C $\leq T_{max}$	Steel members need replaced	$15\varepsilon y \leq \varepsilon_s$	Steel members need replaced

T_{max} = maximum temperature in steel members; 300°C = 572°F; 900°C = 1,652°F; ε_s = maximum residual strain in steel members; $\varepsilon_{s,amb}$ = maximum residual strain in steel members at ambient condition; ε_y = yield strain in steel member

Source: Chaudhary et al. 2022

DS0 and DS1 is repair for thermal damage only. DS2 indicates the structure or structural member must be replaced. DS3 indicates the entire structure must be demolished and reconstructed.

As seen in both tables, the level of thermal damage determines the required repair. Chaudhary et al. (2022) used an RSMeans (2019) database for building and construction costs to determine repair costs for concrete structures. The following equations from Chaudhary et al. present a way to determine the repair cost for a fire-damaged concrete slab ($l_1\ m \times l_2\ m$) with steel members in a *DS*1 or *DS*2 damage state.

*DS*1 *repair cost for concrete member* [$] =
12.58 [$/$m^2$] × $l_1 l_2$[m^2]

*DS*2 *repair cost for concrete member* [$] =
25.52 [$/$m$] × ($l_1 + l_2$) [$m$] + 101.83 [$/m^2] × $l_1 l_2$[m^2] + 1027.18 [$/$m^3$] × ($l_1 l_2$ [m^2] × *D*300 [m])

where, *D*300 represents the depth of thermal damage in concrete cross-section.

The following equations from Chaudhary et al. (2022) provide additional formulas to estimate repair for steel structures in *DS*1 or *DS*2 damage states.

*DS*1 *thermal damage repair cost for steel members* [$] =
$$\left(19.68\ \left[\frac{\$}{m^2}\right] + 0.52\left[\frac{\frac{\$}{m^2}}{mm}\right] \times t\ [mm]\right) \times s\ \ [m^2]$$

where, *s* refers to the surface area of the steel beams where insulation and paint is applied, and *t* is the thickness of the steel protection insulation.

*DS*1 *mechanical damage repair cost for steel members* [$] =
(0.10 + (0.65 – 0.10)/0.55) × (15$\varepsilon_y - \varepsilon_s$) × (*member rebuilding cost* [$])

Table 19 shows the breakdown of repair costs for both concrete and steel structural members.

Table 19. Repair costs per unit for concrete and steel structures

Particulars	Cost (RSMeans)	Cost (metric unit)	Units example slab (l_1 [m] × l_2 [m] × D300 [m])	Cost example slab ($)
Concrete slab				
Locating damaged area	0.29 $/ft^2	3.12 $/m^2	$l_1 l_2$ m^2	3.12 × $l_1 l_2$
Marking damaged perimeter	3.89 $/ft	12.76 $/m	2(l_1 + l_2) m	25.52 × (l_1 + l_2)
Cleaning by high-pressure water	1.13 $/ft^2	12.15 $/m^2	$l_1 l_2$ m^2	12.15 × $l_1 l_2$
Blowing off dust-debris	0.04 $/ft^2	0.43 $/m^2	$l_1 l_2$ m^2	0.43 × $l_1 l_2$
Removing damaged concrete	6.85 $/ft^2	73.66 $/m^2	$l_1 l_2$ m^2	73.66 × $l_1 l_2$
Concrete material	141 $/yd^3	184.42 $/m^3	$l_1 l_2$ m2 × D300	184.42 × $l_1 l_2$ × D300
Concrete mixing	11.20 $/ft^3	395.76 $/m^3	$l_1 l_2$ m2 × D300	395.76 × $l_1 l_2$ × D300
Placing repair material	12.65 $/ft^3	447 $/m^3	$l_1 l_2$ m^2 × D300	447 × $l_1 l_2$ × D300
Curing and finishing	1.16 $/ft^2	12.47 $/m^2	$l_1 l_2$ m^2	12.47 × $l_1 l_2$
Total cost thermal damage state DS1	(12.15 + 0.43) × $l_1 l_2$			
Total cost thermal damage state DS2	25.52 × (l_1 + l_2) + 101.83 × $l_1 l_2$ + 1027.18 × ($l_1 l_2$ × D300)			
Steel beams			**Unit example steel beams**	**Cost example steel beams ($)**
Cost of steel protection insulation	1.23 $/ft^2 per in. thick	0.52 $/m^2 per mm thick	s m^2 (surface area) per t mm thick	0.52 × s × t
Cost of painting (water-based)	1.83 $/ft^2	19.68 $/ m^2	s m^2 (surface area)	19.68 × s
Heat straightening	10%–65% of member demolition and reconstruction cost, 65% for limit of irreparability (15ε_y), and 10% as minimum cost			
Total cost (thermal) damage state DS1	(19.68 + 0.52 × t) × s			
Total cost (mechanical) damage state DS1	(0.10+(0.65–0.10)/0.55) × (15ε_y-ε_s)) × (member replacement cost)			

l_1 and l_2 = spans of slabs in adjacent directions; D300 = depth of thermal damage in concrete cross-section; s = surface area of steel beams where insulation and paint applied; t = thickness of steel protection insulation; ε_y = yield strain in steel member; ε_s = maximum residual strain in steel members

Source: Chaudhary et al. 2022

6.3 Girder Replacement

In situations where the extent of damage compromises the structural integrity of a concrete bridge, replacement of partial or all components of the bridge is needed. The cost can vary depending on the level of damage, location, construction risks, etc. For preliminary replacement cost estimation of an entire bridge, the Iowa DOT (2022) provides a table of unit costs for different bridges as well as costs for bridge removals, widening, aesthetics, etc. (see Table 20).

Table 20. Iowa DOT unit costs for bridge replacement July 2020

Cost Item	Unit Cost (1), (2)
New continuous concrete slab (CCS) bridge	\$110/ft^2
New pretensioned prestressed concrete beam (PPCB) bridge	\$115/ ft^2
New rolled steel beam three-span standard bridge	\$120/ ft^2
New continuous welded plate girder (CWPG) bridge	\$140/ ft^2
Complex bridges: variable width, urban area such as Des Moines, construction over traffic	Add for each item: \$10/ ft^2
Staged bridges	Add 10%
Cofferdam for pier construction	\$25,000 per pier
Detour Bridge	(6)
Bridge removal	\$10/ ft^2
Bridge widening, including removal and staging	\$ 200/ ft^2
Bridge aesthetics	Add 3% (5)
Cast-in-place (CIP) reinforced concrete box (RCB) culvert, in close proximity or corridor projects	\$850/ yd^3 (4)
CIP RCB culvert, individual projects or extensions	\$900/yd^3 (4)
Revetment	\$50/ton (7)
Mobilization	10%
Contingency	B0 =20% (3); D0, B1, D2 = 15%; B2= 5%

(1) Unit costs for new construction do not include mobilization, removal of an existing structure, extensive river or stream channel work, large quantities of riprap, clearing and grubbing, approach slabs, and other construction work not part of the bridge.
(2) Unit costs were current as of July 2020.
(3) Event codes: B0, B1 = Bridges and Structures Bureau concept, layout, respectively; B2 = structural/hydraulic design plans to Design Bureau; D0, D2 = predesign concept, design field exam respectively.
(4) Unit cost includes concrete, reinforcing bars, minor grading and construction.
(5) Additional aesthetic costs should be considered for gateway or signature structures. See the Draft Aesthetic Guidelines for more information.
(6) The state-owned detour bridge components are no longer being used. Detour bridges are rented on a case-by-case basis and budgeting costs should be obtained from the venders.
(7) Include revetment costs with bridge and RCB culvert estimates. After B1 completion, revetment costs for RCB culverts are included with the roadway estimate.

Source: Iowa DOT 2022, Table 3.8

The Washington DOT (WSDOT) Bridge Design Manual (2020) similarly provides unit costs for structural estimations and construction costs. Table 21 presents unit costs for different types of girders including removal, widening, traffic barriers, and other bridge components.

Table 21. Replacement unit cost for bridge/bridge members

	UNIT	LOW	MEDIAN	HIGH ΔΔ
Prestressed Concrete Girders — Span 50 - 175 FT.				
Water Crossing w/piling	SF	$250.00	$300.00	$350.00
Water Crossing w/spread footings	SF	$200.00	$240.00	$270.00
Dry Crossing w/piling	SF	$230.00	$270.00	$320.00
Dry Crossing w/spread footings	SF	$180.00	$220.00	$250.00
Reinforced Concrete And Post-Tensioned Concrete Box Girder — Span 50 - 200 FT.				
Water Crossing w/piling	SF	$280.00	$320.00	$350.00
Water Crossing w/spread footings	SF	$230.00	$270.00	$300.00
Dry Crossing w/piling	SF	$260.00	$300.00	$330.00
Dry Crossing w/spread footings	SF	$210.00	$250.00	$280.00
Reinforced Concrete Flat Slab — Span 20 - 60 FT.	SF	$230.00	$280.00	$330.00
Prestressed Concrete Slabs — Span 13 - 69 FT.	SF	$200.00	$250.00	$300.00
Prestressed Concrete Decked Bulb -Tee Girder — Span 40 - 115 FT.	SF	$220.00	$270.00	$320.00
Steel Girder — Span 60 - 400 FT.	SF	$230.00	$270.00	$330.00
Steel Box Girder — Span 300 - 700 FT.	SF		$350.00	
Steel Truss — Span 300 - 700 FT.	SF		$380.00	
Steel Arch — Span 30 - 400 FT.	SF		$450.00	
Precast Reinforced Concrete Box Culvert (Interior Surface Area) 20 Foot Span and Greater	SF	$50.00	$65.00	$80.00
Precast Reinforced Concrete Split Box Culvert (Interior Surface Area) 20 Foot Span and Greater	SF	$45.00	$70.00	$90.00
Precast Reinforced Concrete Three Sided Structure (Interior Surface Area) 20 Foot Span and Greater	SF	$50.00	$75.00	$100.00
Bridge Approach Slab	SY		$250.00	
Concrete Bridge Removal	SF	$20.00	$35.00	$50.00
Widening Existing Concrete Bridges (Including Removal)	SF	$175.00	$200.00	$300.00
Railroad Undercrossing — Single Track	LF	* $9,000.00 (Steel Underdeck Girder) * $11,000.00 (Steel Thru-Girder)		
Railroad Undercrossing — Double Track	LF	* $14,000.00		
Pedestrian Bridge — Reinforced Concrete	SF	$400.00	$550.00	$700.00
Reinforced Concrete Rigid Frame (Tunnel)	SF		* $100.00	
Replace Existing Curbs & Barrier With Safety Shape Traffic Barrier (Including Removal)	LF	$220.00	$280.00	$350.00
Reinforced Concrete Retaining Wall (Exposed Area)	SF	$55.00	$75.00	$90.00

WSDOT 2020

6.4 Repair vs. Replacement and Economic Impact

As presented in this chapter, girder replacement has shown to be more expensive than girder repairs; however, new girders are accompanied with a well-known structural performance and service life. The longevity of repairs or undetected structural degradation due to the fire provide a level of uncertainty for long-term performance. This must be considered in the overall decision to repair or replace damaged girders.

In the event of girder replacement, bridge owners and engineers should also consider the economic impact bridge closures can have on a city or state. The largest economic impact during bridge closure is due to traffic delays and detours. The cost of construction alone does not capture the total cost of a project. Table 22 from the Oregon DOT (ODOT) Bridge Design Manual (2020) presents the costs for maintenance and control of traffic during bridge construction or detours.

Table 22. Traffic delay/detour unit costs

Detour Mileage Cost (DMC) = Duration * Length Detour (L) * Cost/Length (CpL) *ADT Sample Bridge Project (Br # 00138)	
Duration of facility for construction (D) in days	365
Detour length (L) in km	26
Cost per Mile per Vehicle driven of detour length (CpL)/km	$0.27
Annual Average Daily Traffic (AADT)	330
Time cost per person (TcP)/hr	$16.31
Occupancy rate (person) per vehicle (O)	1.56
Time cost per truck (TcT)/hr	$29.50
ADTT (Truck Traffic as a percentage of AADT; i.e. 10% this case)	.10
Speed of Traffic on Detour (DS) in km/hr	64
Detour Mileage Cost (DMC) = D*L*CpL*ADT	$845,600
Detour Time Cost (DTC) = D*L*[(O*TcP)*(1-ADTT)+(ADTT*TcT)]	$1.265 M
Total Community Cost associated with bridge closure $T1_{cost}$=DTC+DMC	$2.11 M

ODOT 2020 pg. 2-22

ODOT has utilized software called HYRISK for a sample bridge to assess economic losses in a community. The detour lengths and annual average daily traffic (AADT) are taken from the national bridge inventory data and an assumed project timeline is estimated to be one year. A cost of $0.44 per mile (from 2008) was used in the cost estimation.

To effectively reduce costs for a bridge project, an efficient construction plan and preliminary cost estimation are essential for both repairs and replacements. Bridge replacement or partial replacement is more expensive than repairs but necessary in situations where the cost of repairs exceeds the replacement costs.

Safety is the top priority; however, economic feasibility and public perception (e.g., aesthetics of a bridge) should be considered in repair decision making for bridge owners. This involves thoroughly evaluating the damage (e.g., condition assessments and FEA models), considering the cost of repairs versus replacements (pre/post estimations), and including the economic impact traffic detours or delays have during the project.

7 SUMMARY, CONCLUSIONS, AND RECOMMENDATIONS

7.1 Summary

The purpose of this research study was to present methods and ideas on assessment, repair, and replacement of concrete bridges that have been subjected to fire. Bridge fires are not as common as other causes of bridge damage or failure; however, the impact of bridge fires can be significant with respect to public safety and economic effects.

Although previous research studies regarding the impacts of bridge fires, technical information or guidance about the performance of prestressed concrete bridges and efficient repair methods for fire-damaged concrete and steel members is lacking. The objectives of this research study were as follows:

- Develop a greater understanding of the effects on prestressed concrete girders from fire events in order to develop recommended practices for bridge owners
- Conduct a condition assessment of three girders removed from an in-service fire-damaged bridge
- Evaluate the impact of fire on the serviceability and strength for the girders through load and materials testing
- Evaluate potential repair and replacement methods
- Provide recommendations for fire prevention measures or management strategies that can be implemented for bridges

7.2 Conclusions

The girders from the I-29 Sioux City Bridge had varying levels of damage that coincided with the epicenter of the fire. At a minimum, each of the girders was soot-covered and experienced some spalling of the concrete. At worst, large concrete spalls that reached the depth of reinforcement, primarily from the bottom flange of the girder, were observed. The level to which the strength and serviceability of the bridge was affected was determined through load and materials testing.

Each of the girders, despite the visual differences in levels of damage, performed nearly equally when tested in bending. The measured deflection and strain magnitudes were within an expected range as determined by analysis of plan-documented material properties and geometric configuration. Per visual observation and load testing, the effect of the fire on the girders appears to have been limited to the surface-level concrete and to no greater depth than the reinforcement.

Samples of the primary strand reinforcement were selected for testing, and each sample was within specifications, indicating the material properties were not ill-effected by the temperatures achieved at that level. The level of fire effect on the concrete strength was not conclusive. Concrete core samples taken from one of the girders showed a greater concrete strength than what was specified in the plan documents.

In each case, the girders remained in the elastic range until the load-induced midspan moment reached about 2,700 kip-ft, resulting from a total load near midspan of about 140 kips. The total deflection at this point of loading at midspan was between 2.4 and 2.5 in.

One of the girders was tested until failure occurred. The load-induced midspan moment, total load, and deflection were 5,000 kip-ft, 260 kips, and 12.2 in., respectively.

One end of a girder was tested for shear capacity. The ultimate capacity could not be determined, because the available equipment could not generate a shear force exceeding 420 kips. Despite this fact, the girder exhibited the shear capacity required to function in service.

Three repairs methods were proposed and completed for one of the girders. The goal for these repairs was to restore sufficient protection to the remaining concrete and steel reinforcement that exhibited good condition and structural performance. The primary repairs were necessary along the bottom flange of the girder where spalling of concrete was most significant and reinforcement had become exposed. The three repair methods were as follows:

- Re-casting around the bottom flange using SCC
- Re-casting around the bottom flange using UHPC
- Re-casting around the bottom flange using SCC in combination with a FRP wrap

Each option performed sufficiently well to protect the remaining structure during the load test and limited time of evaluation.

The simpler method to complete was the use of SCC only when evaluated from the perspective of constructability. Cracking of the SCC repair resulted from a sustained high load, while service loads are not likely to cause the same cracks.

The completed UHPC protection resulted in a good, durable product, but the expense and additional construction efforts present some disadvantages.

The FRP wrap provided a means for additional protection and strength if that was required; however, the workability in an overhead application and the need for a very smooth surface for full adherence presented some challenges.

Through available resources, in general, girder replacement was shown to be more expensive than girder repairs; however, new girders are accompanied with a well-known structural performance and service life. The longevity of repairs or undetected structural degradation due to the fire provide a level of uncertainty for long-term performance. This must be considered in the overall decision to repair or replace damaged girders. Furthermore, consideration should be given to the user costs incurred by any repair or replacement project to fully evaluate the economic impact.

The lack of clarity from design manuals for bridges regarding risks from fire can cause serious consequences for bridge users and the economy. Based on review of previous literature and case studies, the following preventive measures and management strategies are recommended to prevent damage on bridges from fire:

- A risk assessment should be required during the design phase for bridges. This can include qualitative analysis methods, quantitative analysis methods, and relative risk ranking methods.

- Different factors (deck material, location, type of bridge, cause of fire, etc.) typically involved in bridge fires should be ranked in terms of damage levels that could occur during a fire. This can help engineers and bridge owners to design against fire damage early on (e.g., proper design of bridge drainage systems to prevent the accumulation of fuel from tanker-truck incidents).

- Due to high damage levels resulting from tanker-truck fires on bridges, coordination between bridge management, fire control, engineers, DOTs, and government officials should be required through the establishment of an emergency rescue group, with a specific focus on fire incidents.

- For certain vulnerable bridges, it is recommended that tanker-truck operators use designated lanes to reduce damage levels during an incident (e.g., center lanes so other bridge users may escape safely and quickly). Through logging and reporting, some trucks may be restricted from traveling over or under a specific bridge with high fire risks dependent on the amount or type of flammable materials carried. Detour routes for these cases should be established in a guide for truck drivers.

- Guidelines for storage near or under a bridge should be implemented prior to bridge service. This should include under-bridge parking of cars and construction equipment. These guidelines should also include safety management policies, such as specific locations, placement, and restrictions for different types of stored materials. Flammable materials should be forbidden at all times.

- For bridges in isolated locations, such as some historic bridges, routine maintenance should be coordinated to prevent the buildup of ignitable materials as well as provide routine measures for fire prevention (e.g., address vandalism and arson).

7.3 Recommendations

Bridges fires are relatively uncommon events. Even so, being proactive to put measures in place to prevent, assess, and repair damage in case of occurrence is recommended. An assessment of susceptibility to fire damage during initial design and construction is recommended for new bridge projects.

Also, an assessment of in-service bridges to determine high levels of vulnerability is a good idea. Where highly vulnerable bridges are identified, specific plans for permitting or re-routing of certain vehicle types can be established, or plans for the removal of storage materials can be developed if storage of flammable materials is the cause of elevated vulnerability, for example. A fire-damage-assessment team can be formed with the goal to create guiding documents and tools for the rapid assessment of fire-damaged bridges.

REFERENCES

ACI. 2015. What is Self-Consolidating Concrete? American Concrete Institute, Farmington Hills, MI.

Alkhrdaji, T. 2015. Strengthening of Concrete Structures Using FRP Composites. *STRUCTURE magazine*.

Beneberu, E. and N. Yazdani. 2018. Performance of CFRP-Strengthened Concrete Bridge Girders under Combined Live Load and Hydrocarbon Fire. *Journal of Bridge Engineering*, Vol. 23, No. 7, pp. 4018042-1–4018042-16.

Beneberu, E. and N. Yazdani. 2019. Residual Strength of CFRP Strengthened Prestressed Concrete Bridge Girders after Hydrocarbon Fire Exposure. *Engineering Structures*, Vol. 184, pp. 1–14.

Chaowei, H., L. Kang, L. Hongyin, and W. Laiyong. 2019. Research on the Material Properties of Prestressed Concrete Girder Bridge after Exposed to Fire. *IOP Conference Series: Earth and Environmental Science*, Vol. 371, No. 4, 42027.

Chaudhary, R. K., A. Lucherini, T. Gernay, and R. Van Coile. 2022. Evaluation of Anticipated Post-Fire Repair Cost for Resilient Design of Composite Slab Panels. *Journal of Building Engineering*, Vol. 52, No. 104460.

Concrete Questions. 2022. Concrete Pricing Guide: All the Facts and Figures. https://concretequestions.com/concrete-pricing-guide-all-the-facts-and-figures/.

Davis, M., P. Tremel, and A. Pedrego. 2008. Bill Williams River Concrete Bridge Fire Damage Assessment. *STRUCTURE magazine*, pp. 30–32.

de Melo, M., R. Wheatley, N. Gibbin, M. Gonzalez-Quesada, and K. Harwood. 2014. Assessment and Repair of a Fire-Damaged Prestressed Concrete Bridge. *Structural Engineering International*, Vol. 24, No. 3, pp. 408–413.

Enchayan, R. 2010. *Repair of Damaged Prestressed Concrete Girder.* AASHTO Midwest Bridge Preservation Conference, October 13, Detroit, MI.

FHWA. 2022. Ultra-High Performance Concrete. https://highways.dot.gov/research/structures/ultra-high-performance-concrete/ultra-high-performance-concrete.

Garlock, M., I. Paya-Zaforteza, V. Kodur, and L. Gu. 2012. Fire Hazard in Bridges: Review, Assessment and Repair Strategies. *Engineering Structures*, Vol. 35, pp. 89–98.

Giuliani, L., C. Crosti, and F. Gentili. 2012. Vulnerability of Bridges to Fire. In *Bridge Maintenance, Safety, Management, Resilience and Sustainability*. Taylor & Francis Group, London, UK.

Graybeal, B. A. 2007. *Flexural Capacity of Fire-Damaged Prestressed Concrete Box Beams*. FHWA-HRT-07-024. Federal Highway Administration, Turner-Fairbank Highway Research Center, McLean, VA.

Graybeal, B. A. and F. Baby. 2019. *Tension Testing of Ultra-High Performance Concrete*. FHWA-HRT- 17-053. Federal Highway Administration, Turner-Fairbank Highway Research Center, McLean, VA.

HDR. 2019. *Interstate 29 Northbound Bridge over the Perry Creek Conduit – Sioux City, Iowa*. Fire Damage Inspection report. Iowa DOT, Ames, IA. https://www.siouxlandproud.com/news/local-news/officials-release-report-of-damages-to-northbound-i-29-bridge-after-fire/.

Iowa DOT. 2022. *Load and Resistance Factor Design (LRFD) Bridge Design Manual*. Iowa Department of Transportation Bridges and Structures Bureau, Methods Unit, Ames, IA.
Jones, M. S. 2015. *Repair of Impact-Damaged Prestressed Bridge Girders with Strand Splices and Fabric Reinforced Cementitious Matrix Systems*. MS thesis. Virginia Polytechnic Institute and State University, Blacksburg, VA.
Kim, M. O., K. Kim, J. H. Yun, and M. K. Kim. 2020. Fire Risk Assessment of Cable Bridges for Installation of Firefighting Facilities. *Fire Safety Journal*, Vol. 115, No. 103146.
Kukay, B., C. Todd, T. Jahn, J. Sannon, L. Dunlap, R. White, and M. Dietenberger. 2016. *Evaluating Fire-Damaged Components of Historic Covered Bridges*. FPL-GTR-243. USDA Forest Service, Forest Products Laboratory, Madison, WI.
Lee, G. C., S. B. Mohan, C. Huang, and B. N. Fard. 2013. *A Study of US Bridge Failures (1980–2012).* Multidisciplinary Center for Earthquake Engineering Research (MCEER), University at Buffalo, State University of New York, Buffalo, NY.
Liu, M. Y., W. Tian, Y. Wang, W. Jing, and X. Chen. 2014. Risk Prevention Measures for Three-Tower and Four-Span Suspension Bridge under Vehicle Fire. *Advanced Materials Research*, Vols. 919–921, pp. 590–597.
Masetti, F., G. A. Martinez, and S. M. O'Brien. 2018. Evaluation of Fire Effects on Precast, Prestressed Concrete Members. *Forensic Engineering 2018: Forging Forensic Frontiers*. Eighth Congress on Forensic Engineering, November 29–December 2, Austin, TX. pp. 396–407.
McCraven, S. 2010. Working with SCC Needn't Be Hit or Miss. *Precast, Inc. Magazine*. National Precast Concrete Association.
NCHRP. 2022. NCHRP 20-129 [Pending]: Guide for Addressing Encampments on State Transportation Rights-of-Way. National Cooperative Highway Research Program, Washington, DC.
Ni, S. and T. Gernay. 2021. A Framework for Probabilistic Fire Loss Estimation in Concrete Building Structures. *Structural Safety*, Vol. 88, No. 102029.
ODOT 2020. *Oregon Department of Transportation Bridge Design Manual*. Bridge Engineering Section, Salem, OR.
Palmer Engineering. 2019. Appendix J: Individual Bridge Repair Cost Estimates, *I-65 Bridges from I-264 to Kennedy Interchange Planning Study: Jefferson County, KY*. Kentucky Transportation Cabinet (KYTC), Frankfort, KY.
Park, J., Y. K. Cho, and J. Shim. 2018. Resilient Fire Prevention and Management Strategies for Structures and Materials Stored under Urban Bridges. *Construction Research Congress 2018*, pp. 584–593. April 2–4, New Orleans, LA.
Peris-Sayol, G., I. Paya-Zaforteza, S. Balasch-Parisi, and J. Alós-Moya. 2017. Detailed Analysis of the Causes of Bridge Fires and Their Associated Damage Levels. *Journal of Performance of Constructed Facilities*, Vol. 31, No. 3, pp. 04016108-1–04016108-9.
Rizkalla, S. H., O. Rosenboom, A. Miller, and C. Walter. 2007. *Value Engineering and Cost Effectiveness of Various Fiber Reinforced Polymer (FRP) Repair Systems, Phase II*. North Carolina State University, Raleigh, NC.
Shanafelt, G. O. and W. B. Horn. 1980. *NCHRP Report 226: Damage Evaluation and Repair Methods for Prestressed Concrete Bridge Members*. National Cooperative Highway Research Program, Washington, DC.
Sika. 2018. *SikaWrap Hex-106 G Product Data Sheet*. Sika Corporation. Lyndhurst, NJ.

Steelike. 2022. *Steelike® Concrete: Ultra-High Performance Concrete*. Steelike, Inc., Springfield, VA. https://steelike.com/product/product-data-sheet/.
Stoddard, R. *Inspection and Repair of a Fire Damaged Prestressed Girder Bridge*. Washington State DOT, Olympia, WA.
Varma, A. H., J. Olek, C. S. Williams, T.-C. Tseng, S. Wang, D. Huang, and T. Bradt. 2021. *Post-Fire Assessment of Prestressed Concrete Bridges in Indiana*. Joint Transportation Research Program, Purdue University, West Lafayette, IN.
WSDOT. 2020. Chapter 12, Appendix 12.3-A1, *WSDOT Bridge Design Manual*. Washington State DOT, Olympia, WA.

APPENDIX: DIGITIZED GIRDER CONDITION DOCUMENTATION

Girder B Condition Sheets

Girder ID: B **Section:** 0′-5′

Notes:

West End: 0′ line
East End: Main Fire

Deck Thickness: 9″

Sketches:

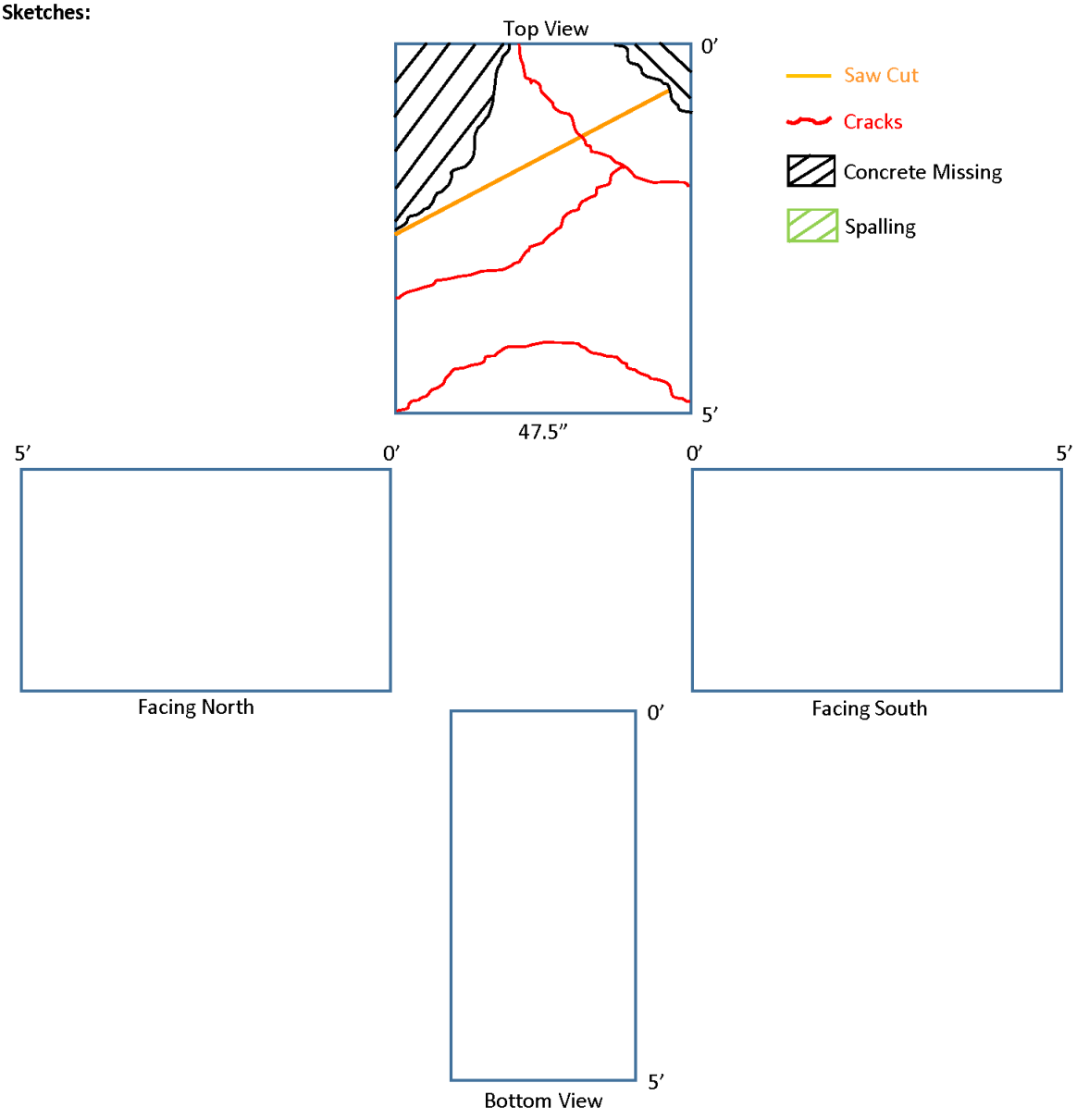

Girder ID: B **Section:** 5’-10’

Notes:

West End: 0’ line
East End: Main Fire

Deck Thickness: 8.5”

Sketches:

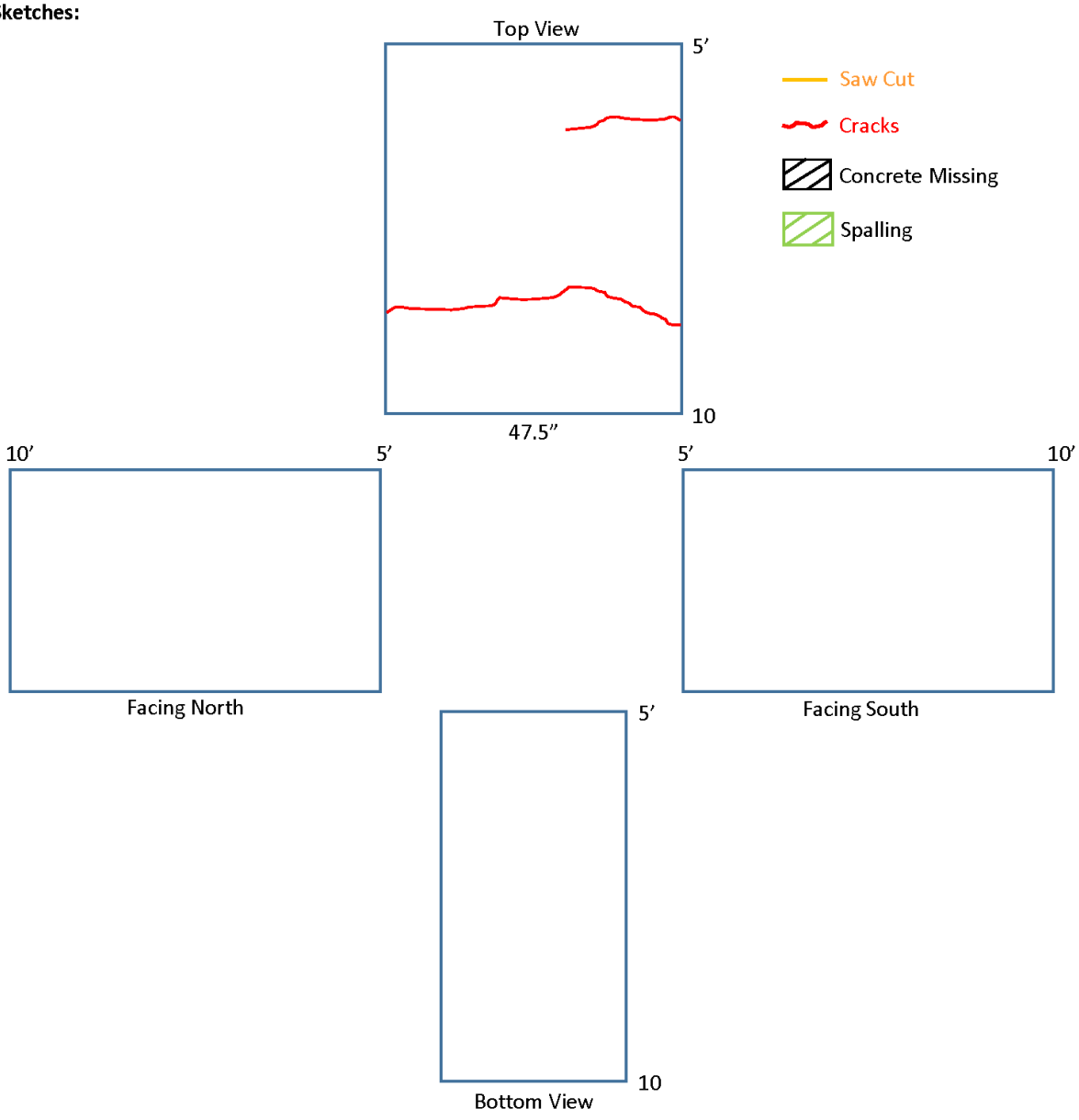

Girder ID: B **Section:** 10’-15’

Notes:

West End: 0’ line
East End: Main Fire

Deck Thickness: 8.5”

Sketches:

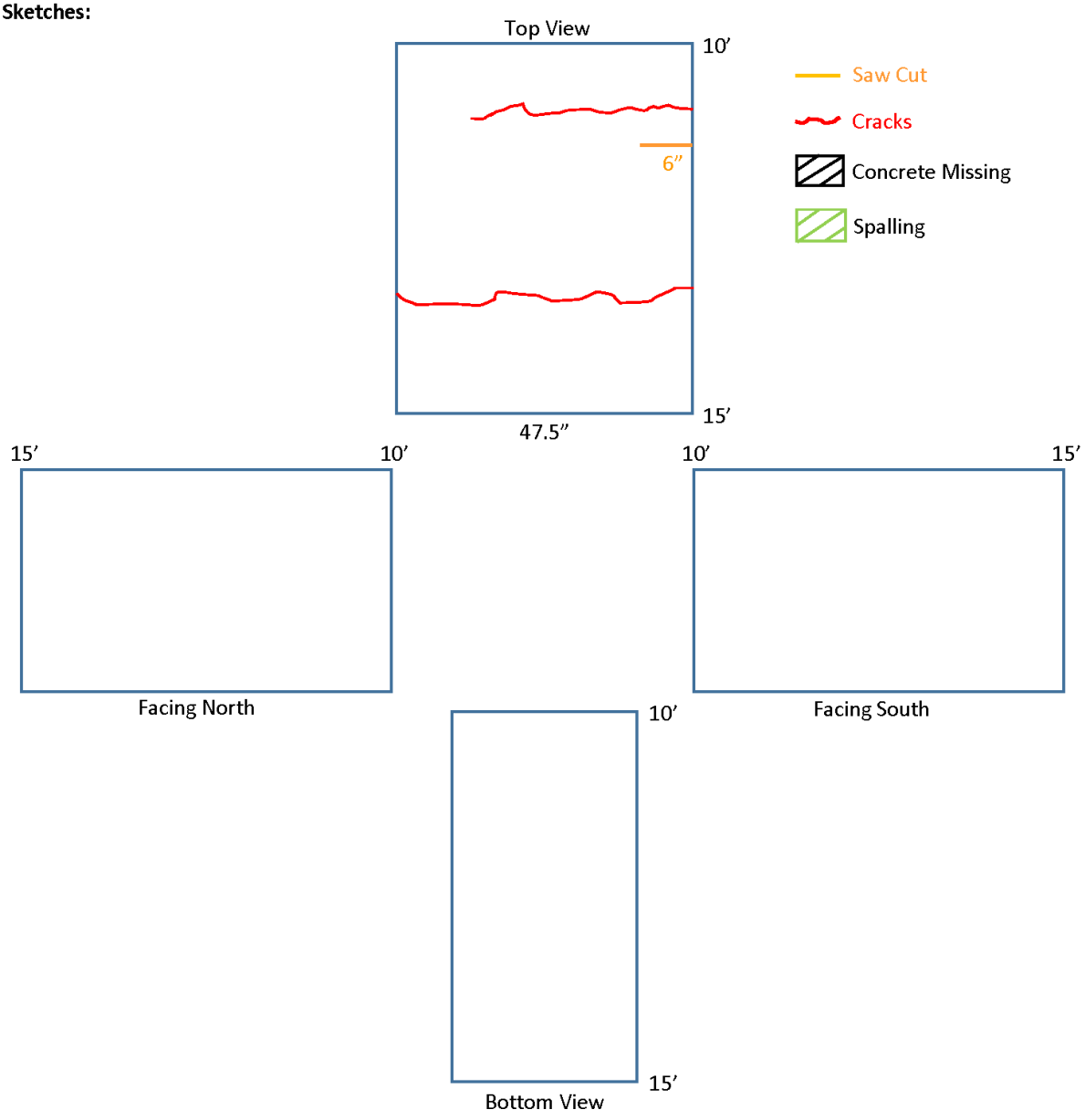

Girder ID: B **Section:** 15’-20’

Notes:

West End: 0’ line
East End: Main Fire

Deck Thickness: 8”

Sketches:

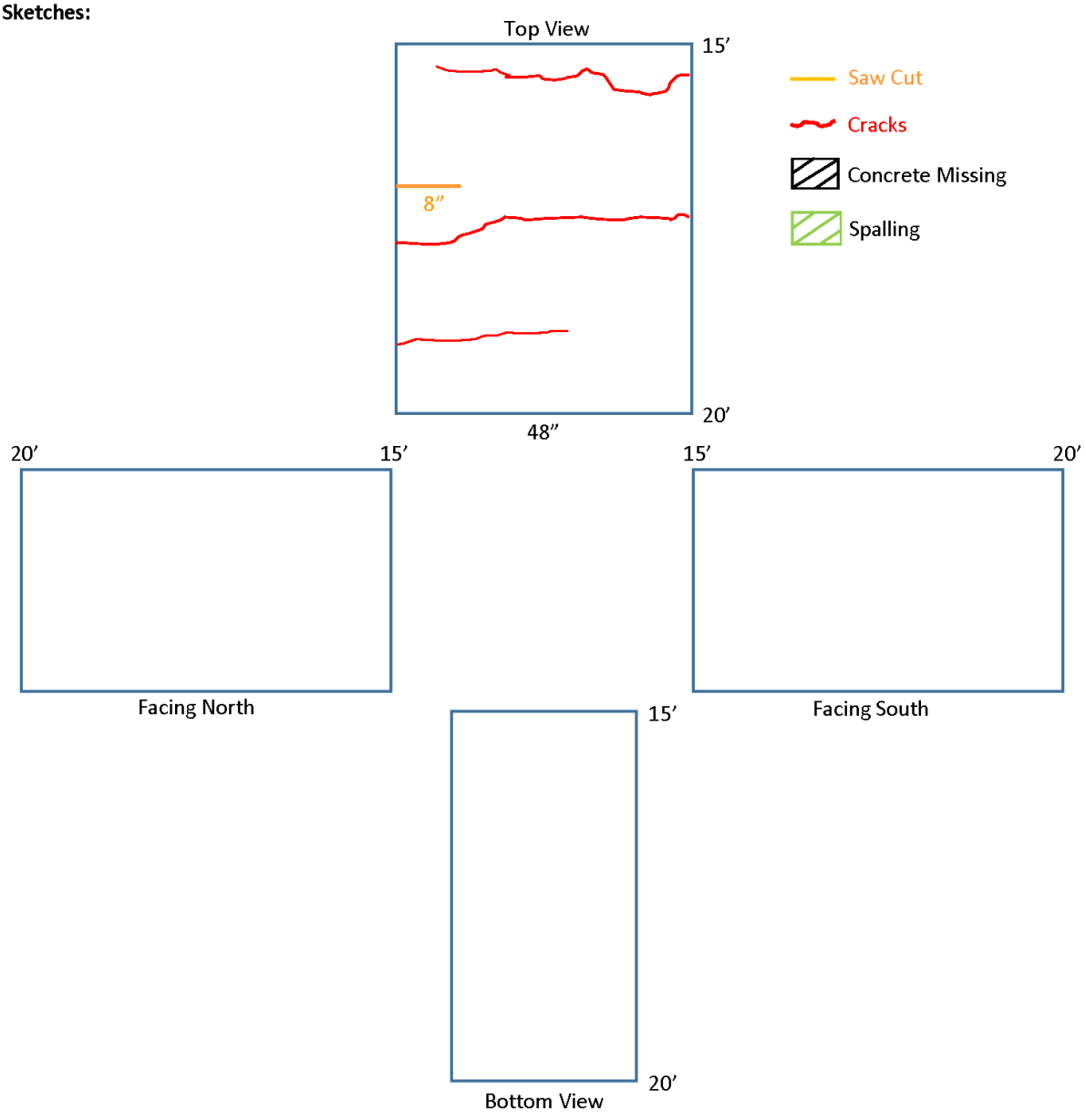

Girder ID: B **Section:** 20'-25'

Notes:

West End: 0' line
East End: Main Fire

Deck Thickness: 8"

Sketches:

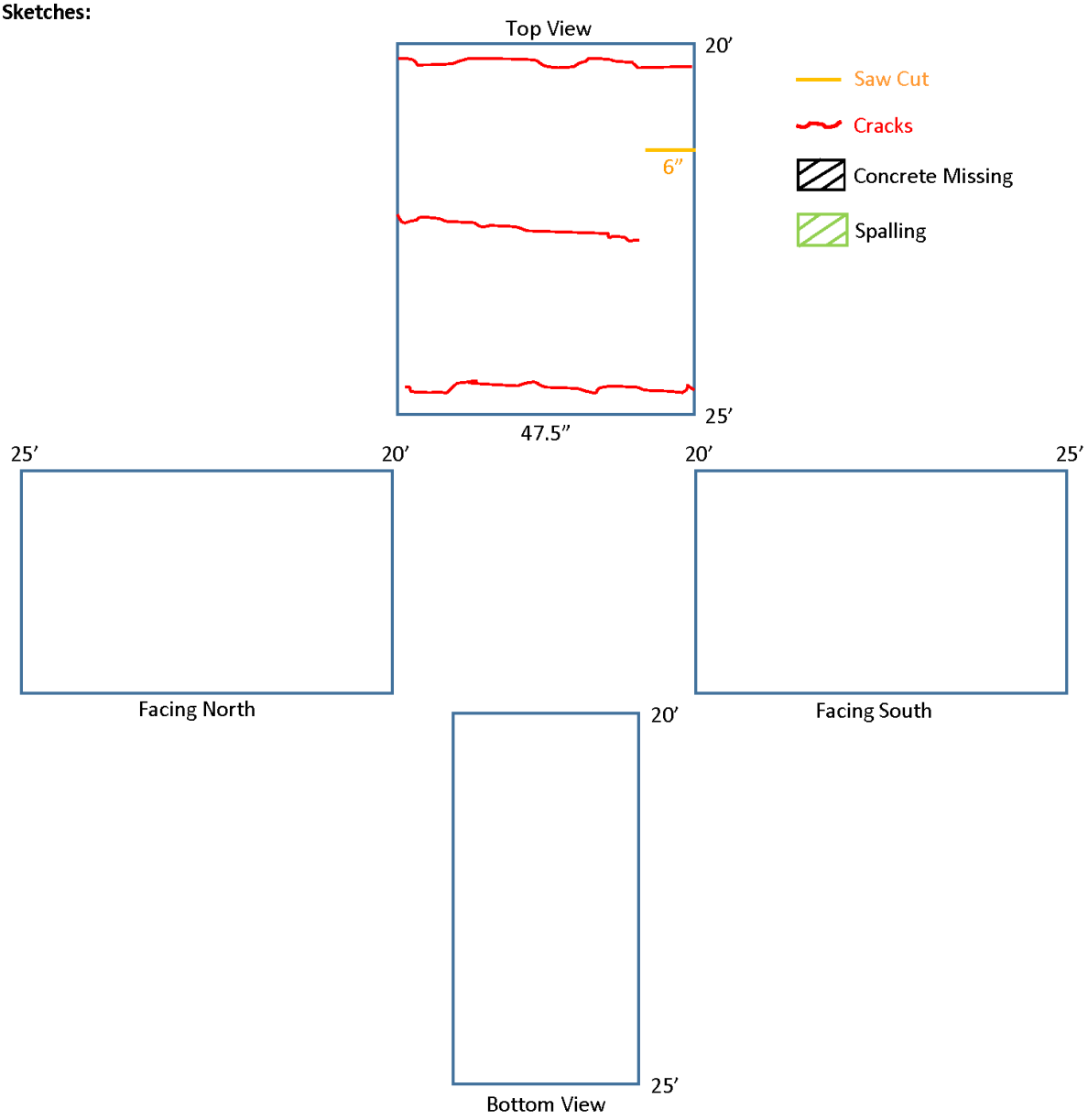

Girder ID: B **Section:** 25'-30'

Notes:

West End: 0' line
East End: Main Fire

Deck Thickness: 8"

Sketches:

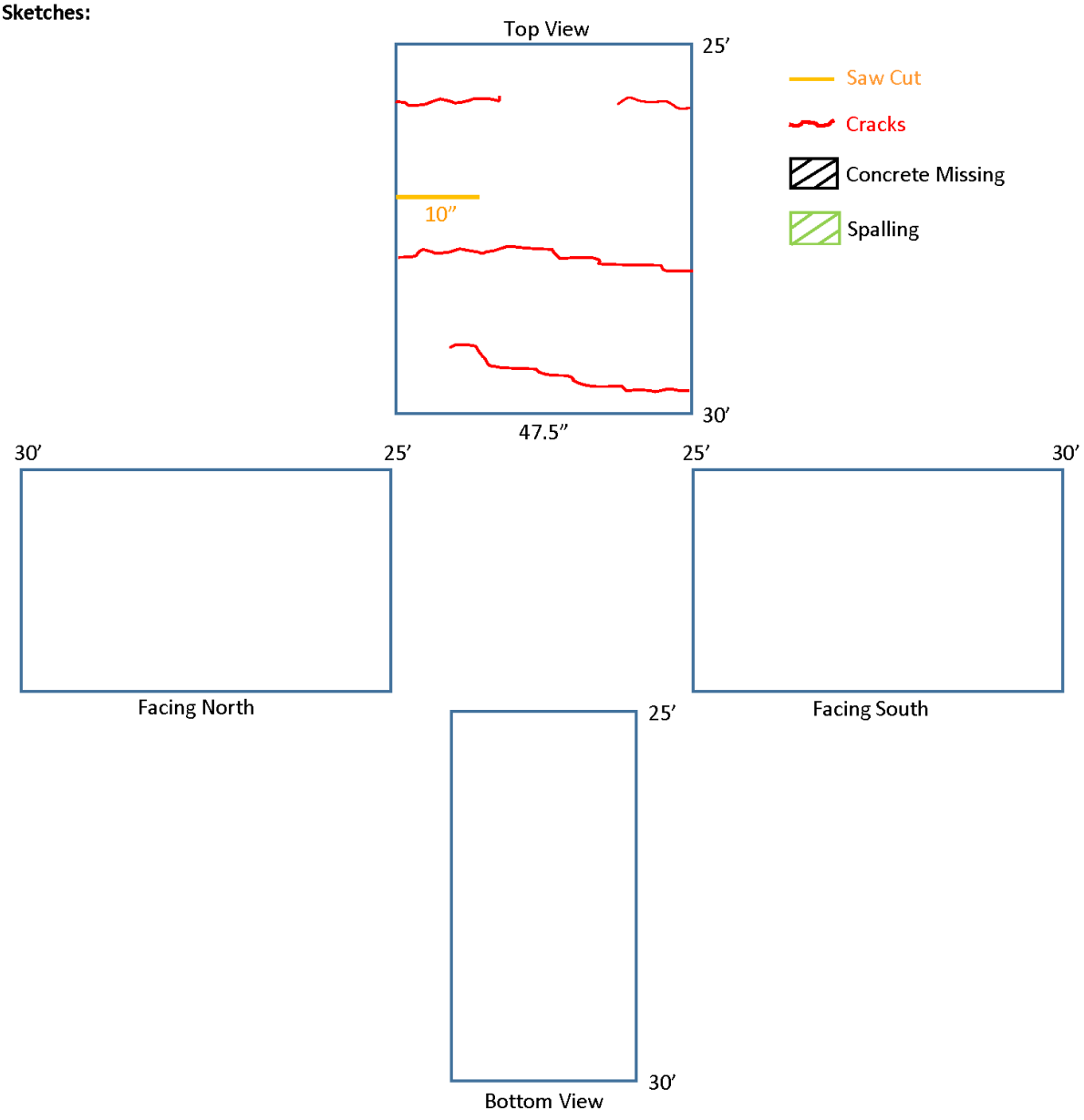

Girder ID: B **Section:** 30'-35'

Notes:

West End: 0' line
East End: Main Fire

Deck Thickness: 8.5"

Sketches:

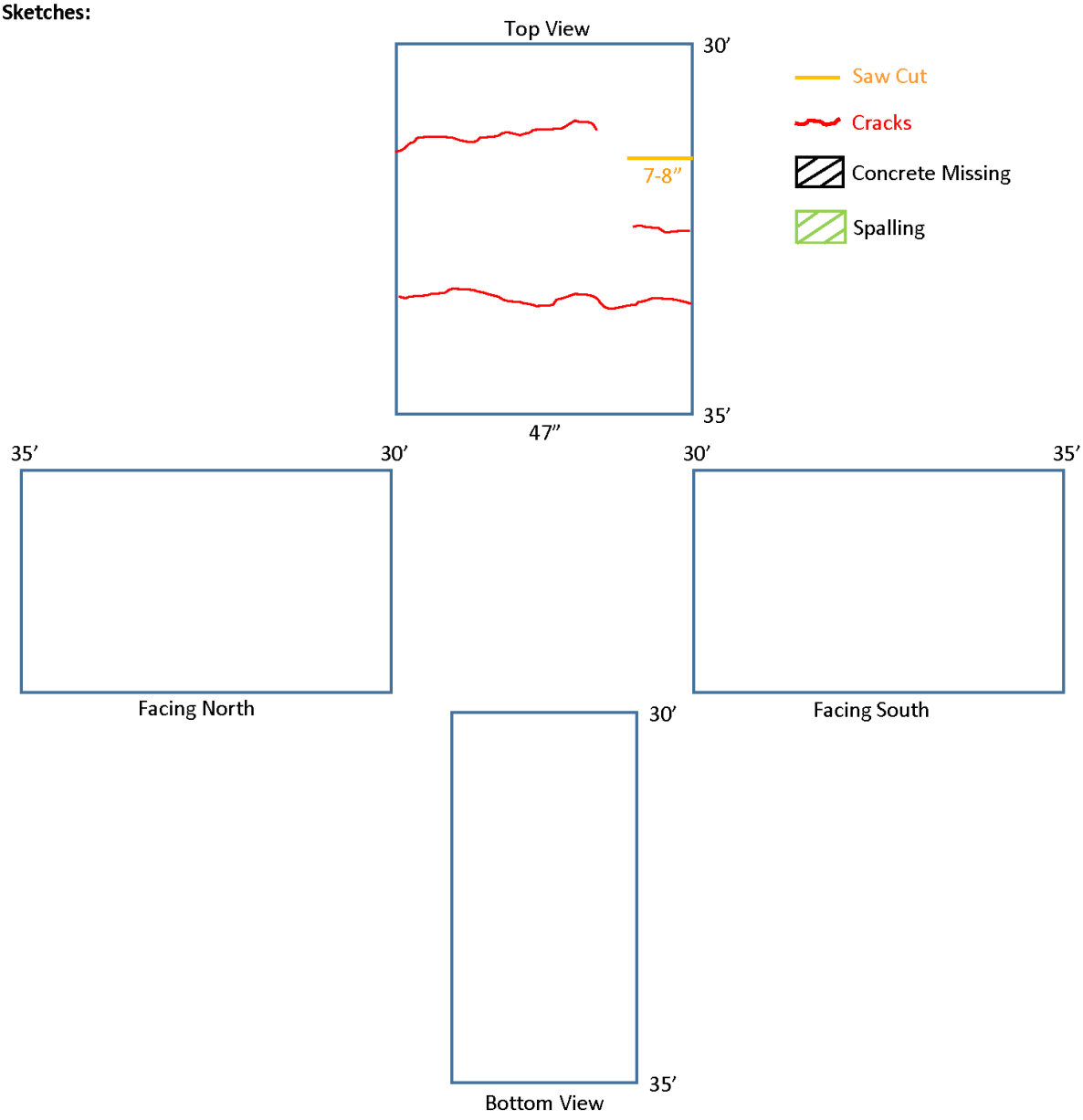

Girder ID: B **Section:** 35’-40’

Notes:

West End: 0’ line
East End: Main Fire

Deck Thickness: 8.25”

Sketches:

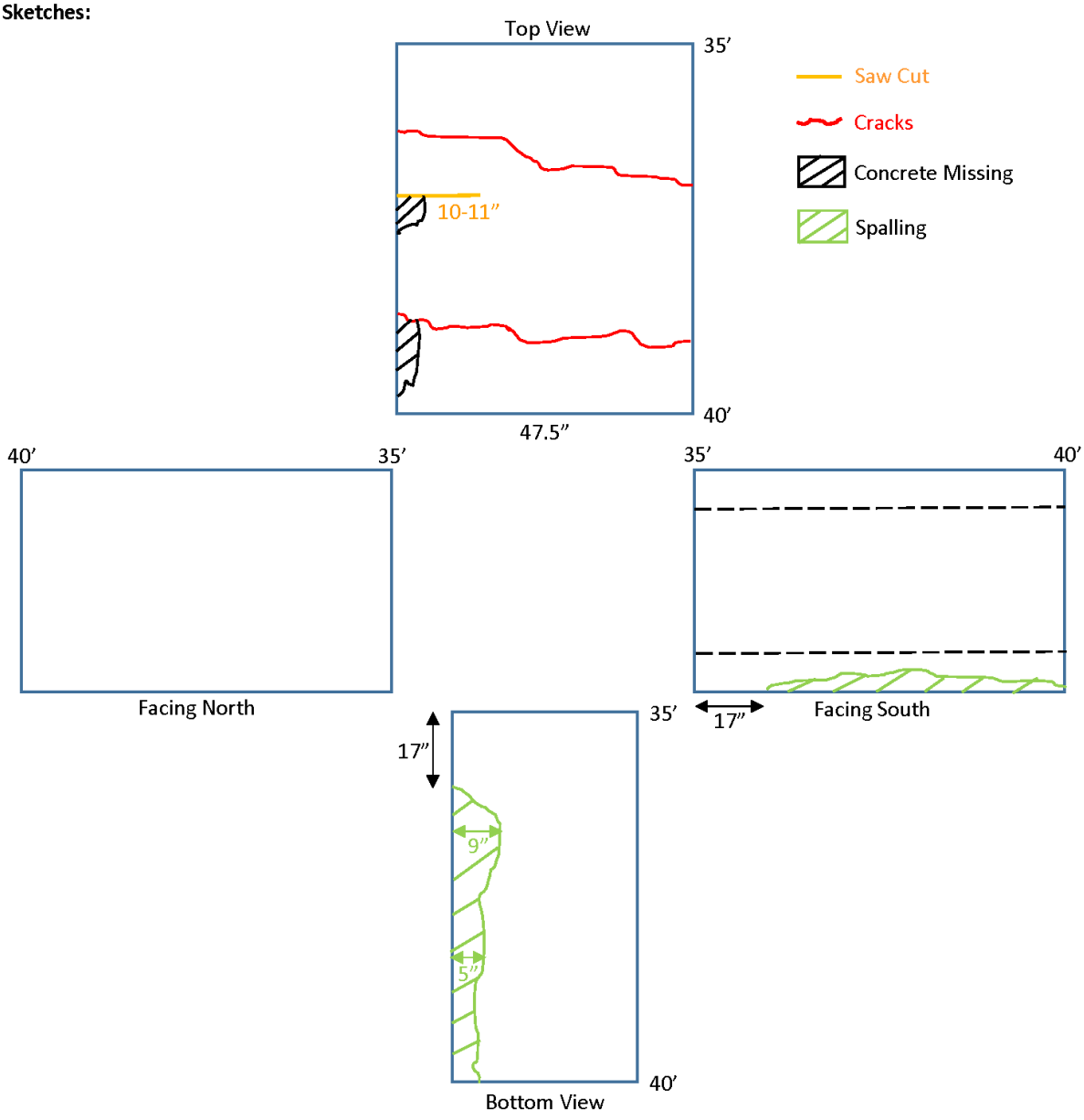

Girder ID: B **Section:** 40’-45’

Notes:

West End: 0’ line
East End: Main Fire

Deck Thickness: 8”

Sketches:

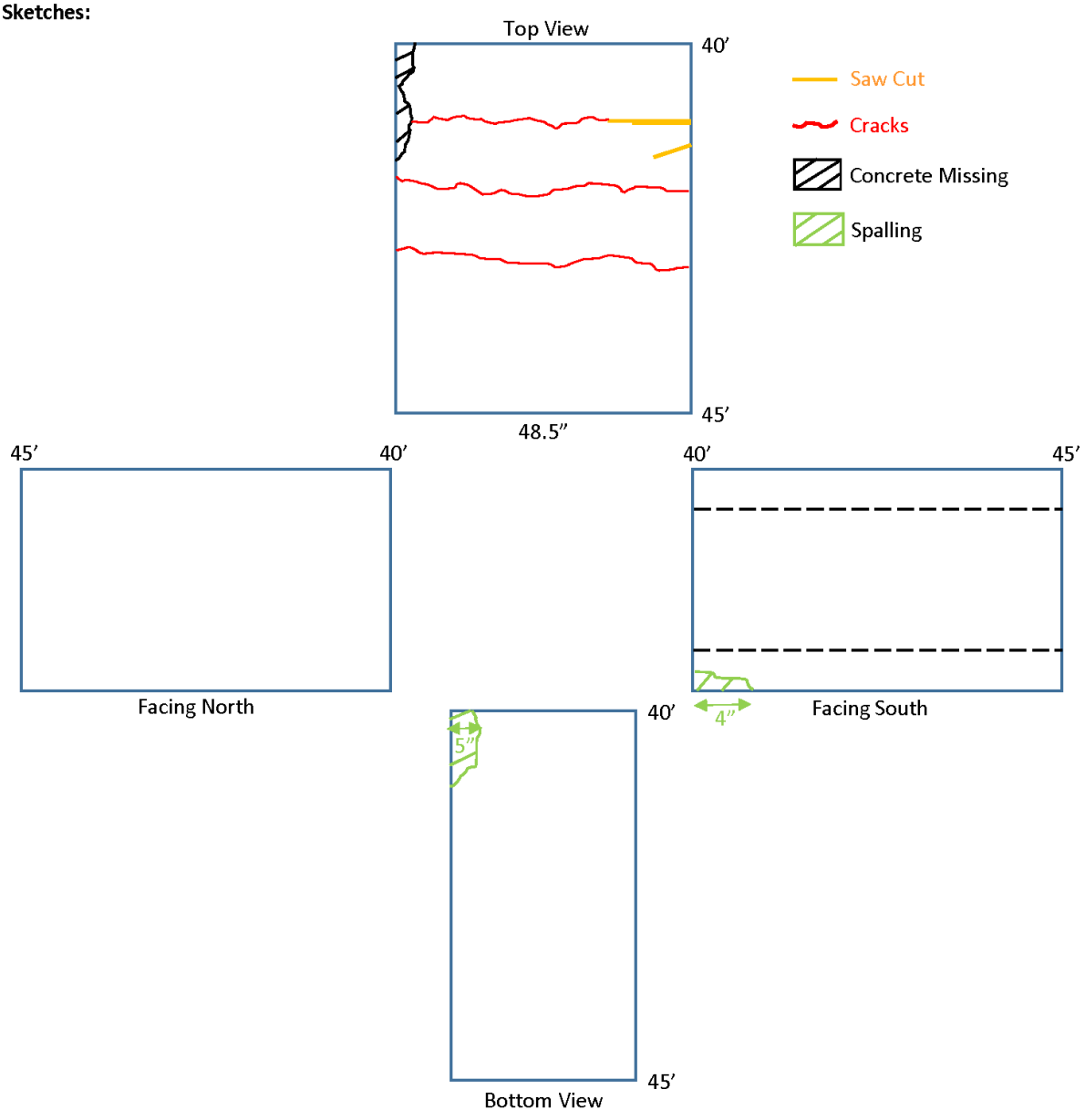

Girder ID: B **Section:** 45’-50’

Notes:

West End: 0’ line
East End: Main Fire

Deck Thickness: 8.25”

Sketches:

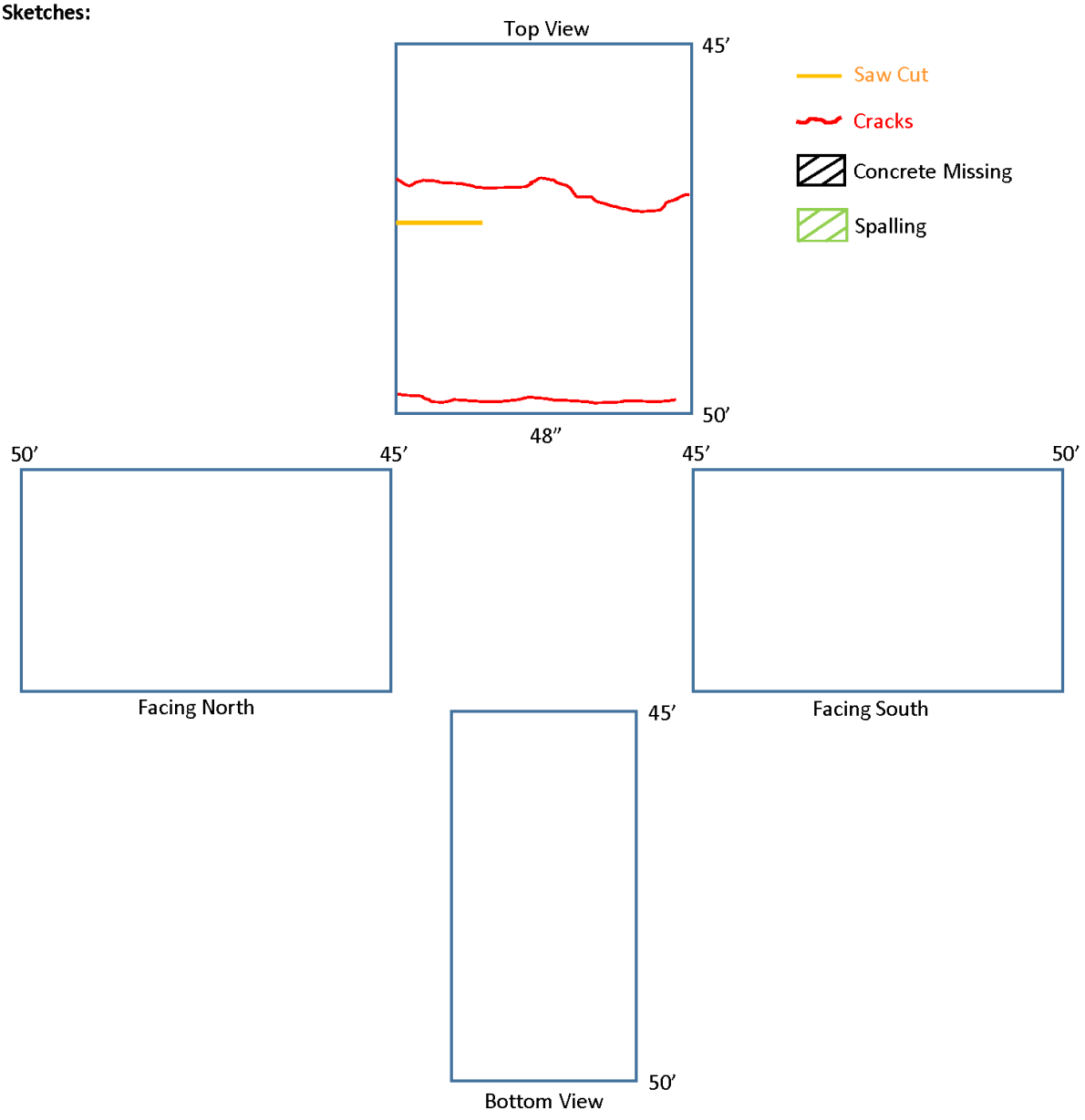

Girder ID: B **Section:** 50'-55'

Notes:

West End: 0' line
East End: Main Fire

Deck Thickness: 8.5"

Sketches:

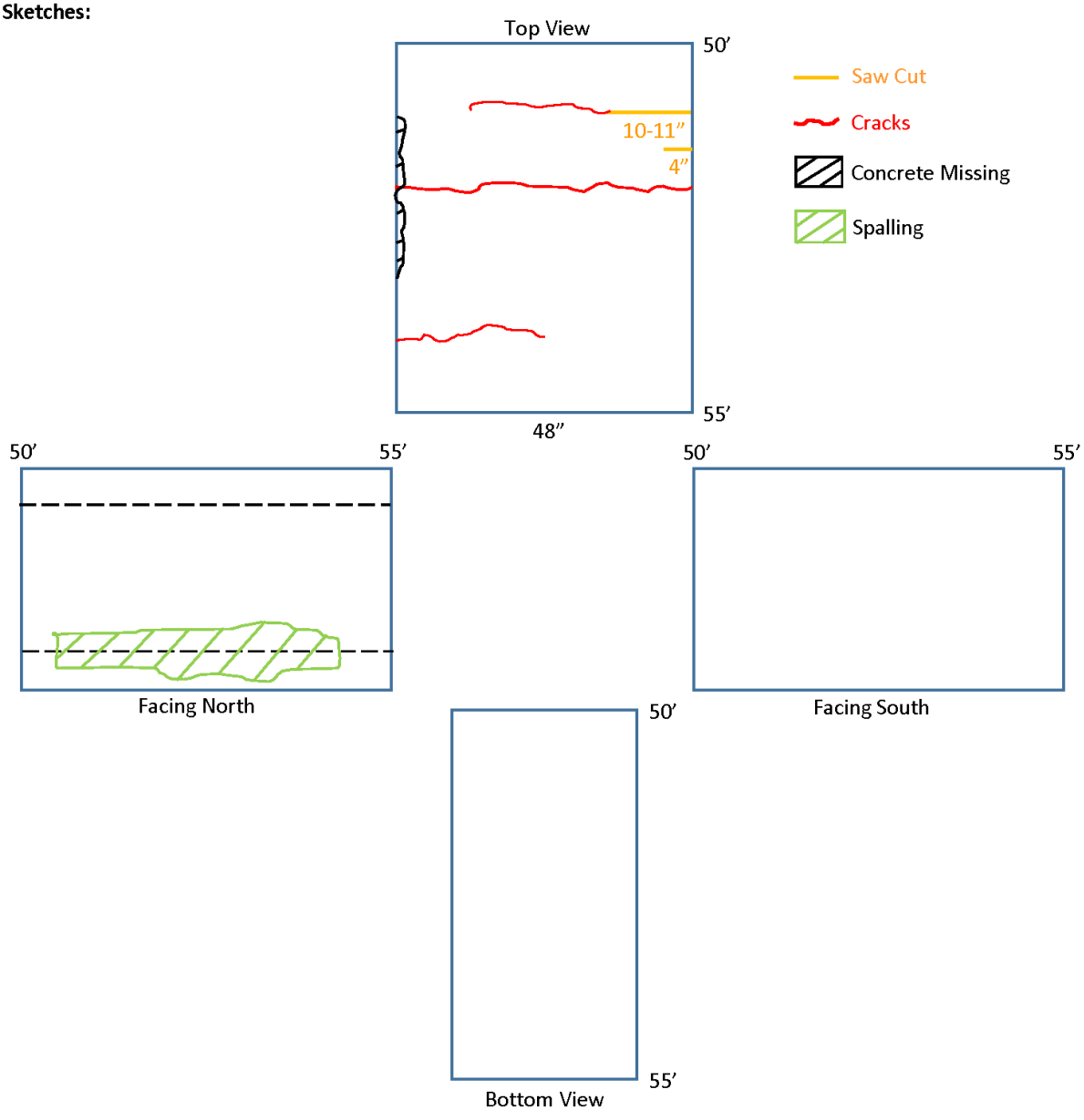

Girder ID: B **Section:** 55’-60’

Notes:

West End: 0’ line
East End: Main Fire

Deck Thickness: 8”

Sketches:

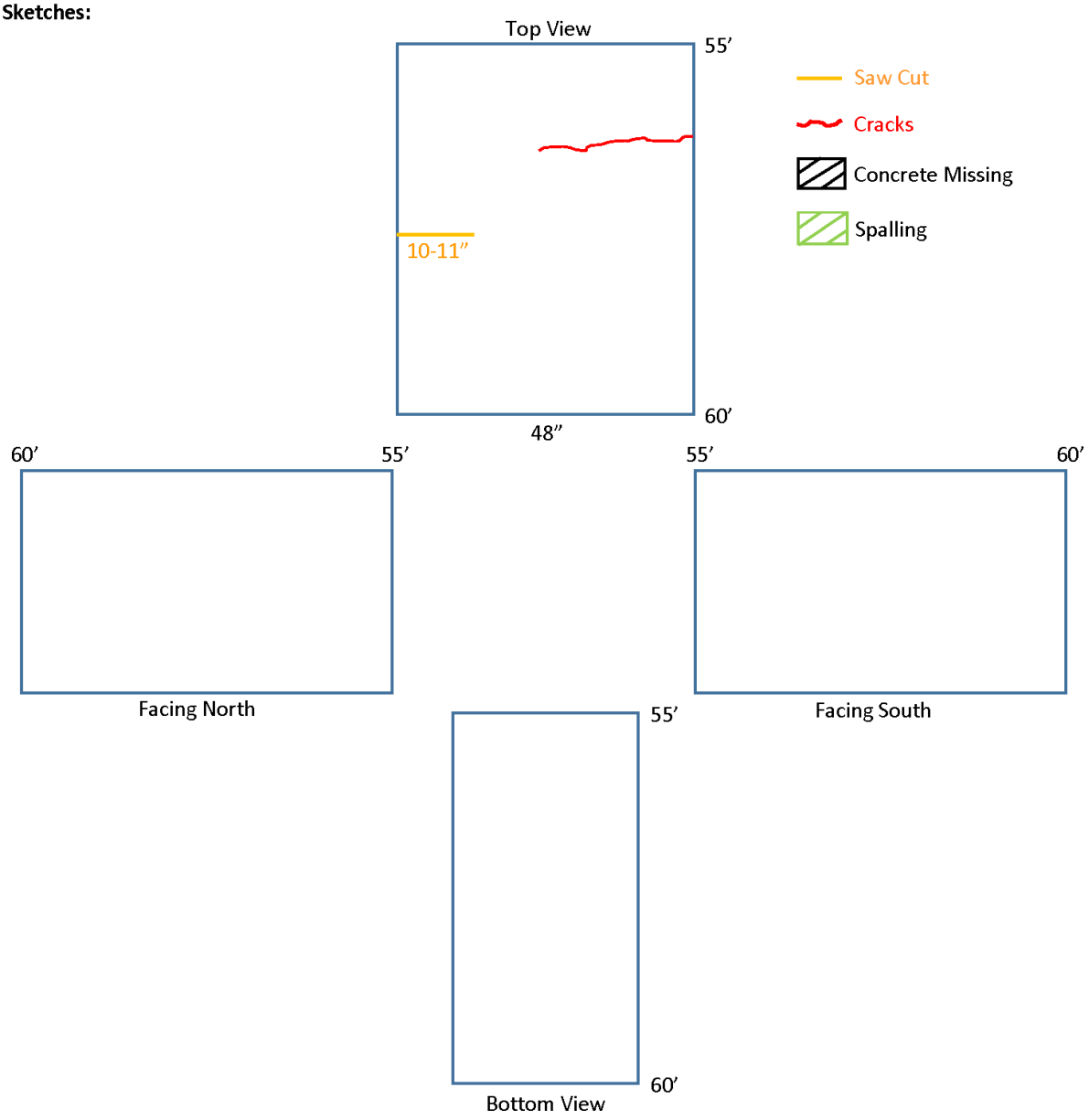

Girder ID: B **Section:** 60’-65’

Notes:

West End: 0’ line
East End: Main Fire

Deck Thickness: 8”

Sketches:

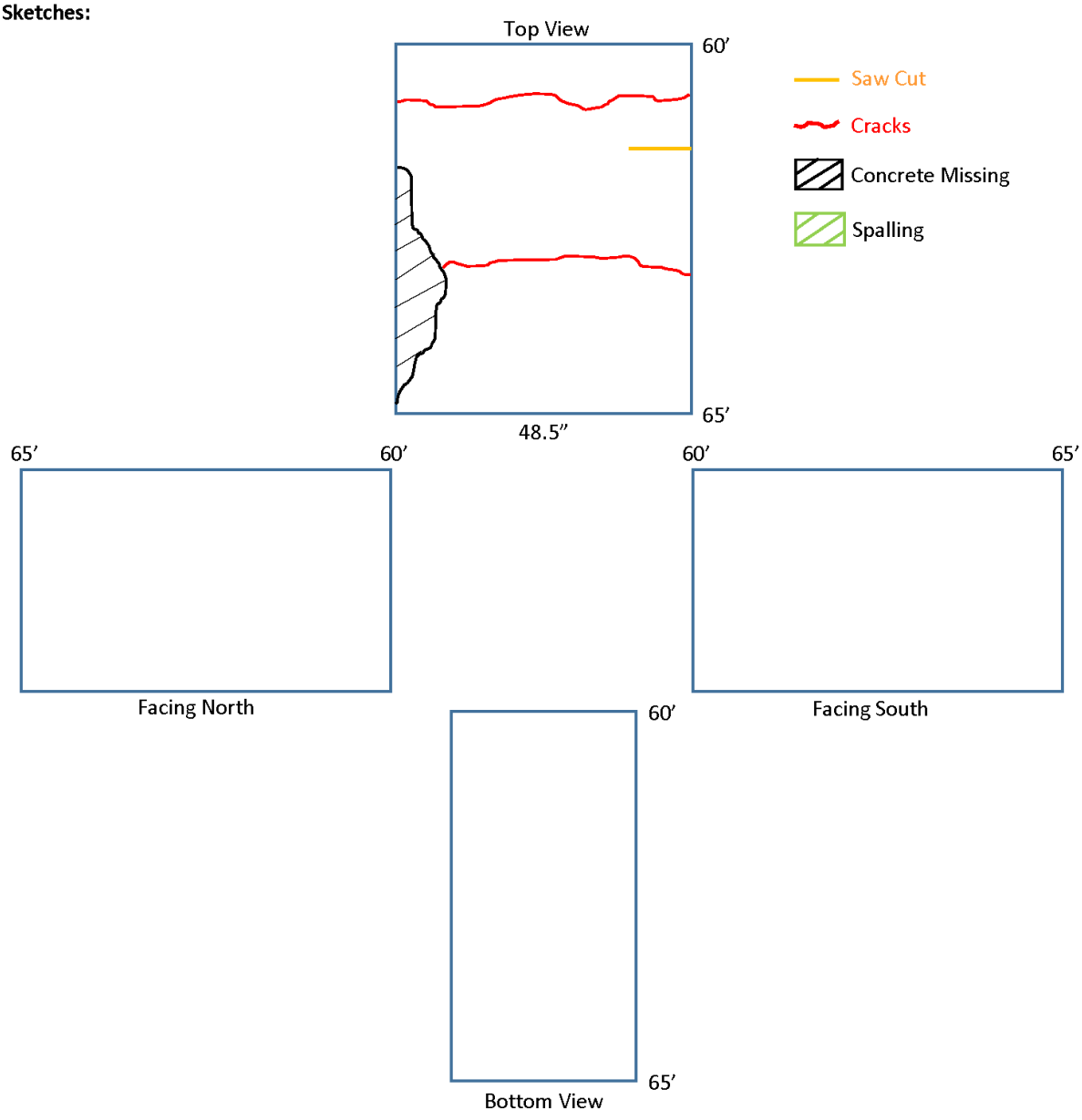

Girder ID: B **Section:** 65’-70’

Notes:

West End: 0’ line
East End: Main Fire

Deck Thickness: 8”

Sketches:

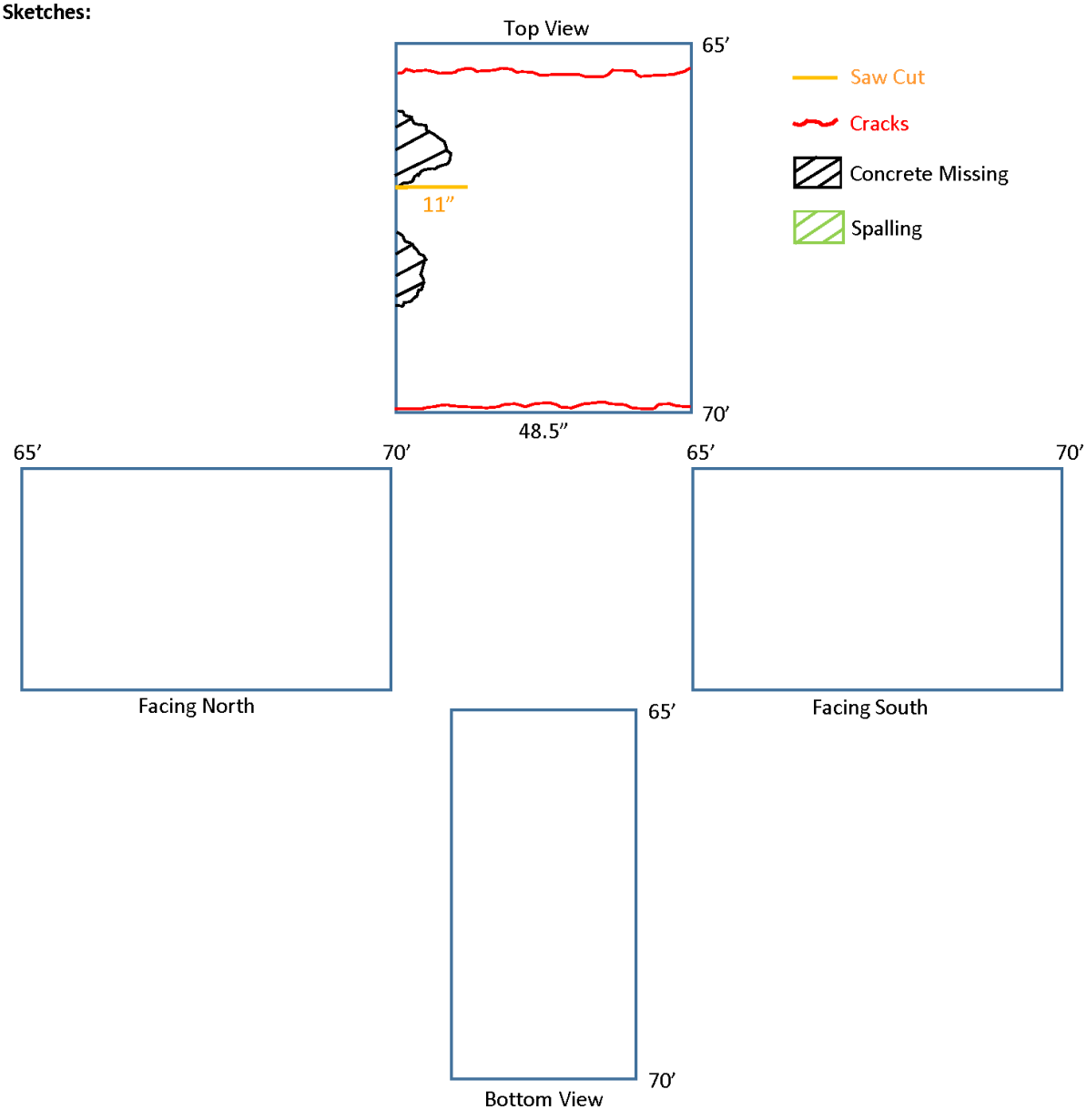

Girder ID: B **Section:** 70'-75'

Notes:

West End: 0' line
East End: Main Fire

Deck Thickness: 8"

Sketches:

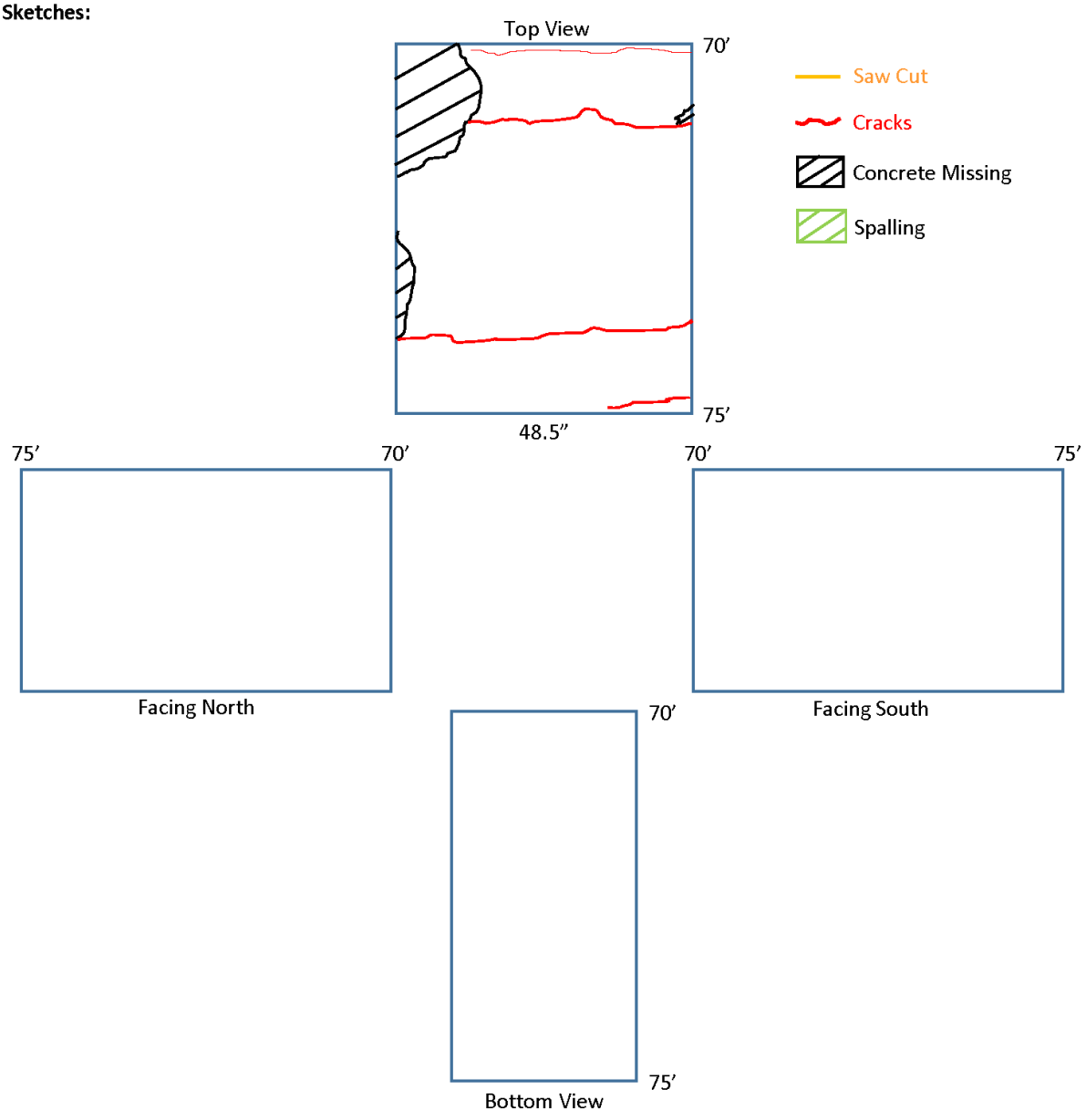

Girder ID: B **Section:** 75'-80'

Notes:

West End: 0' line
East End: Main Fire

Deck Thickness: 8"

Sketches:

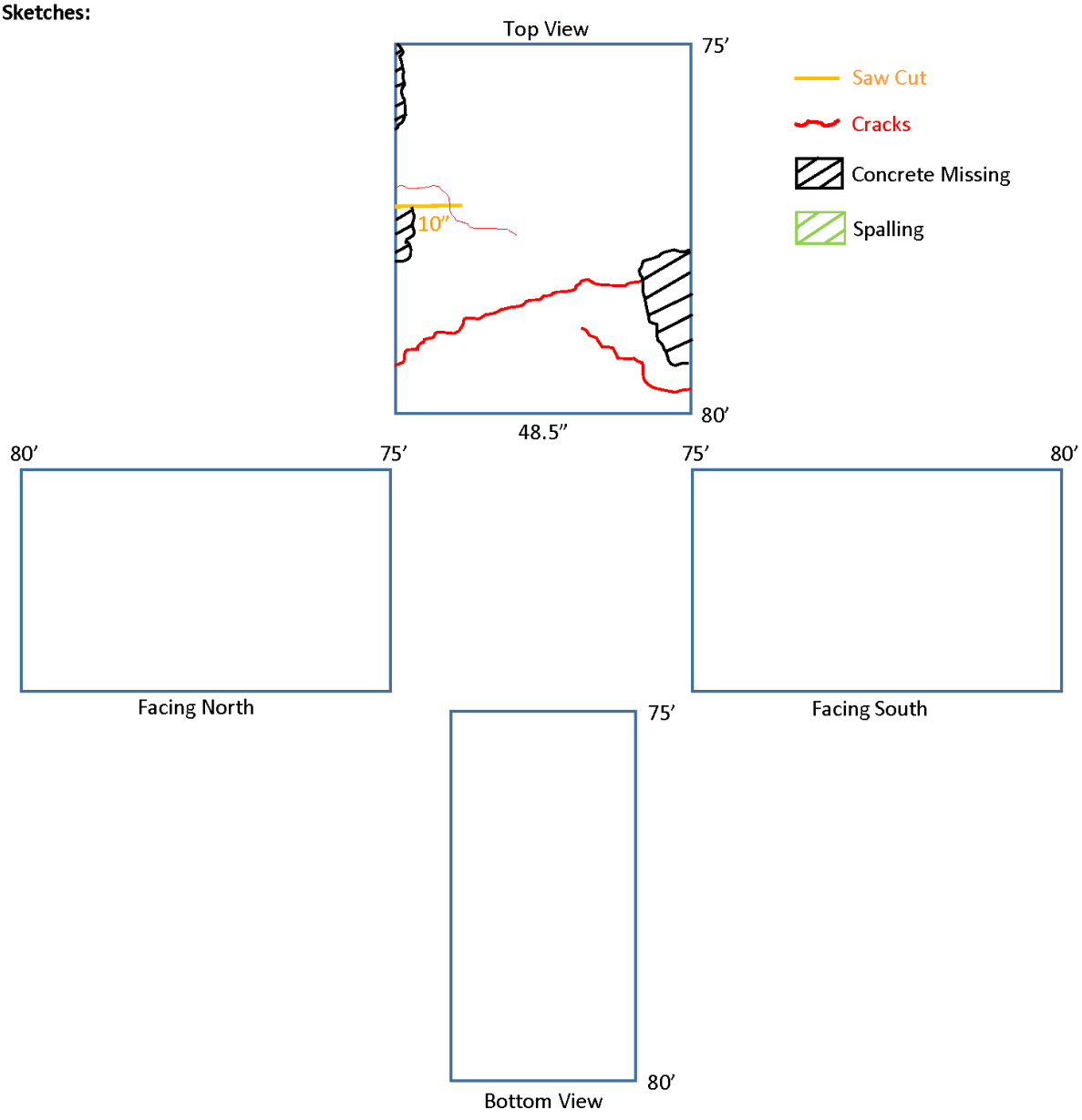

Girder ID: B **Section:** 80'-85'

Notes:

West End: 0' line
East End: Main Fire

Deck Thickness: 8"

Sketches:

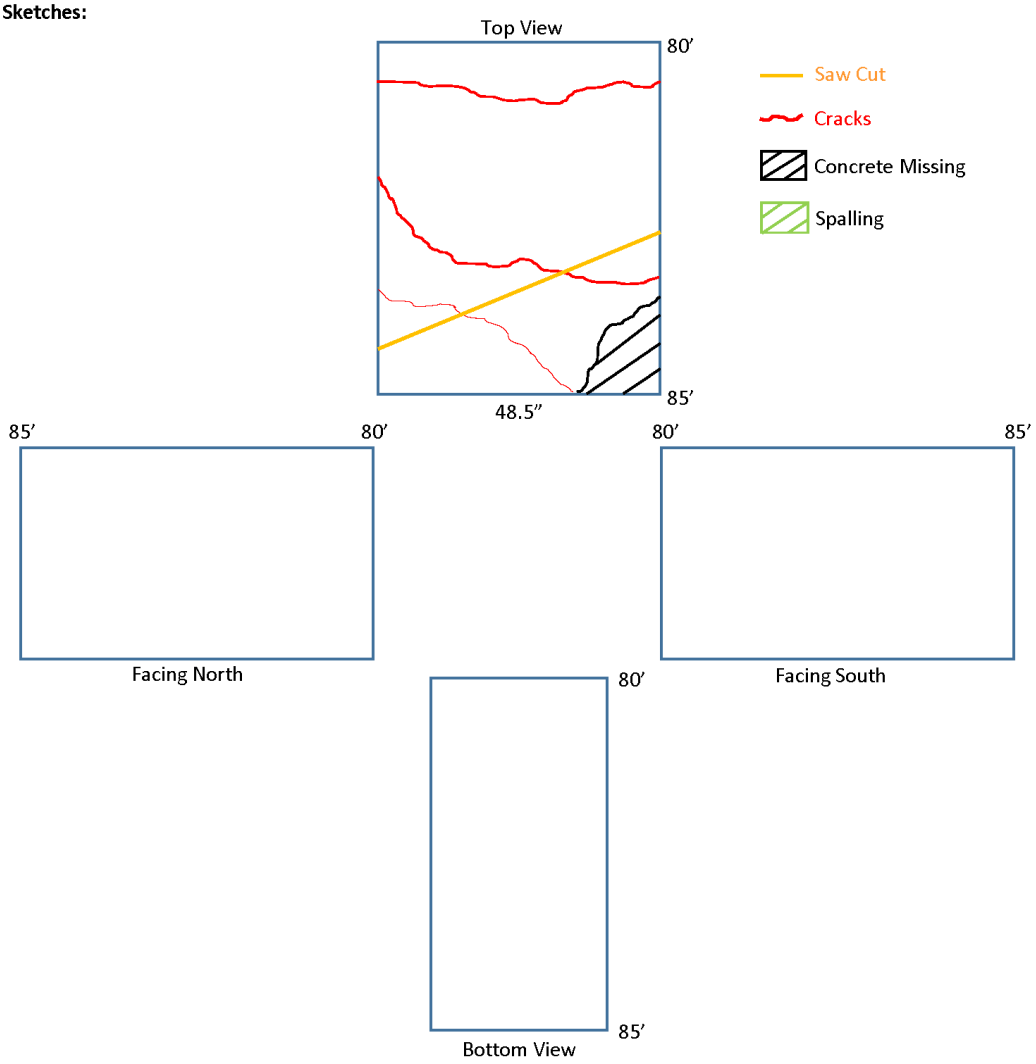

Girder ID: B **Section:** 85'-86.4'

Notes:

West End: 0' line
East End: Main Fire

Deck Thickness: 8"

Sketches:

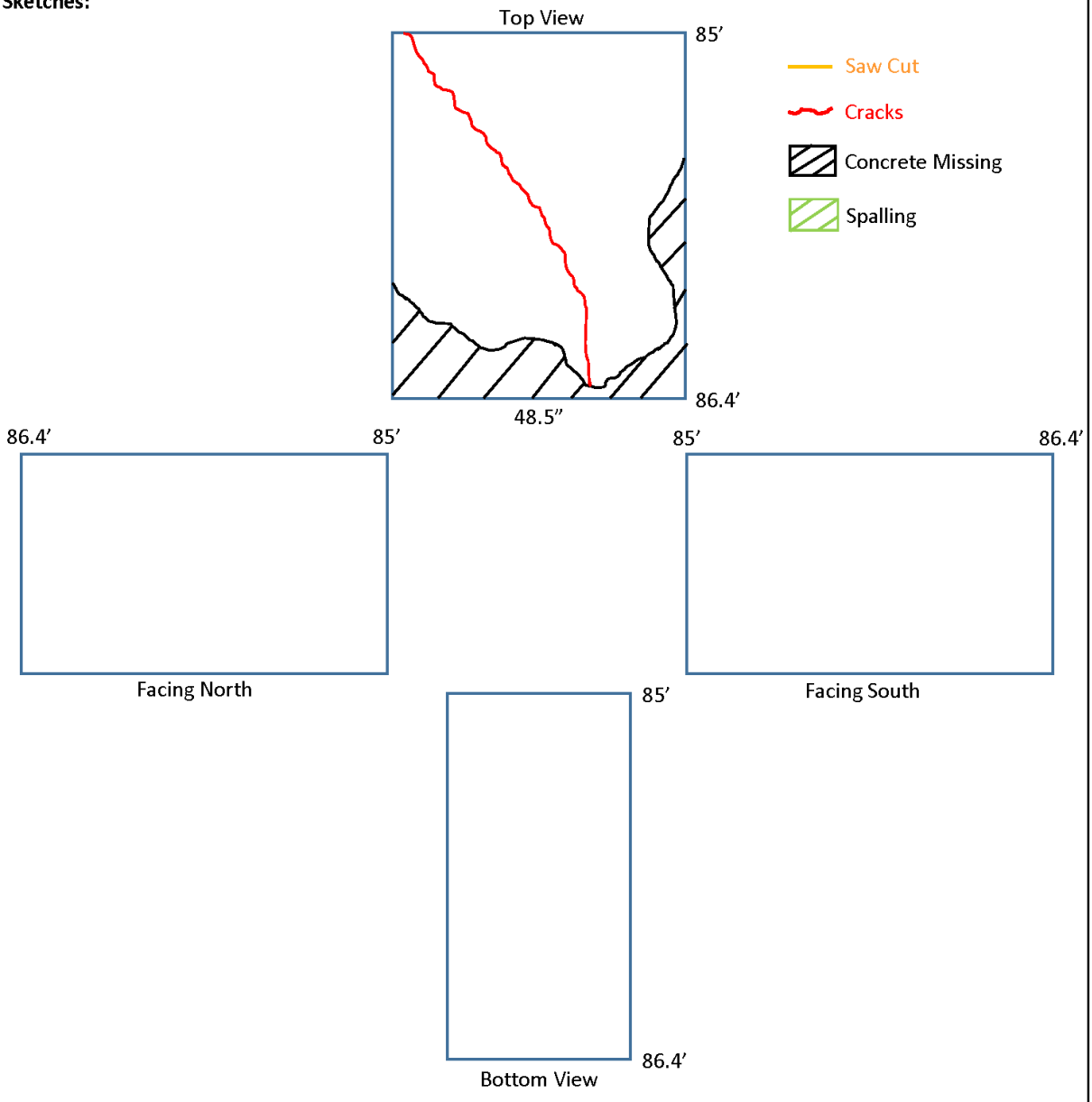

Girder E Condition Sheets

Girder ID: E **Section:** 0’-5’

Notes:

West End: 0’ line
East End: Main Fire

Deck Thickness:

Sketches:

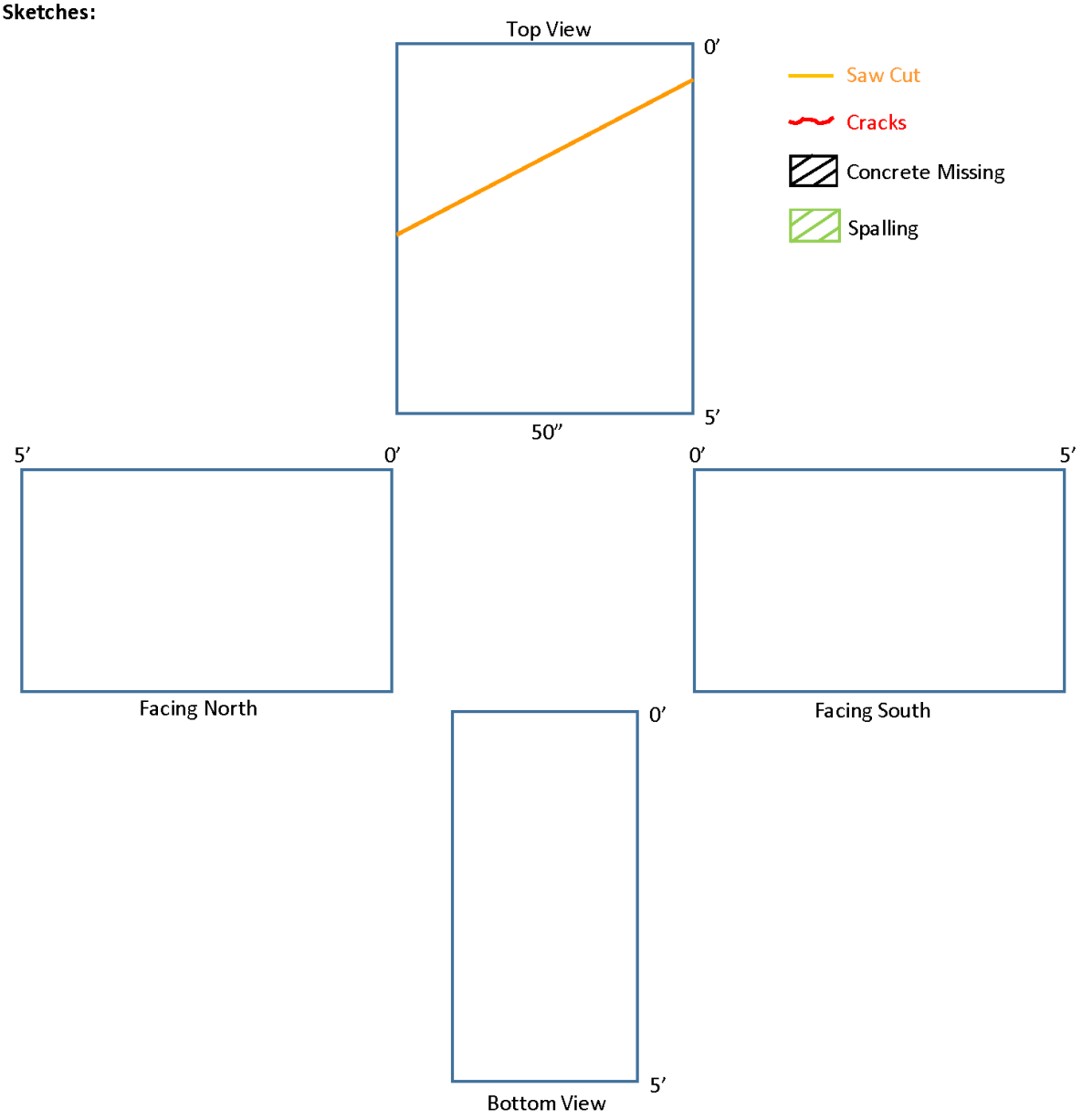

Girder ID: E **Section:** 5'-10'

Notes:

West End: 0' line
East End: Main Fire

Deck Thickness:

Sketches:

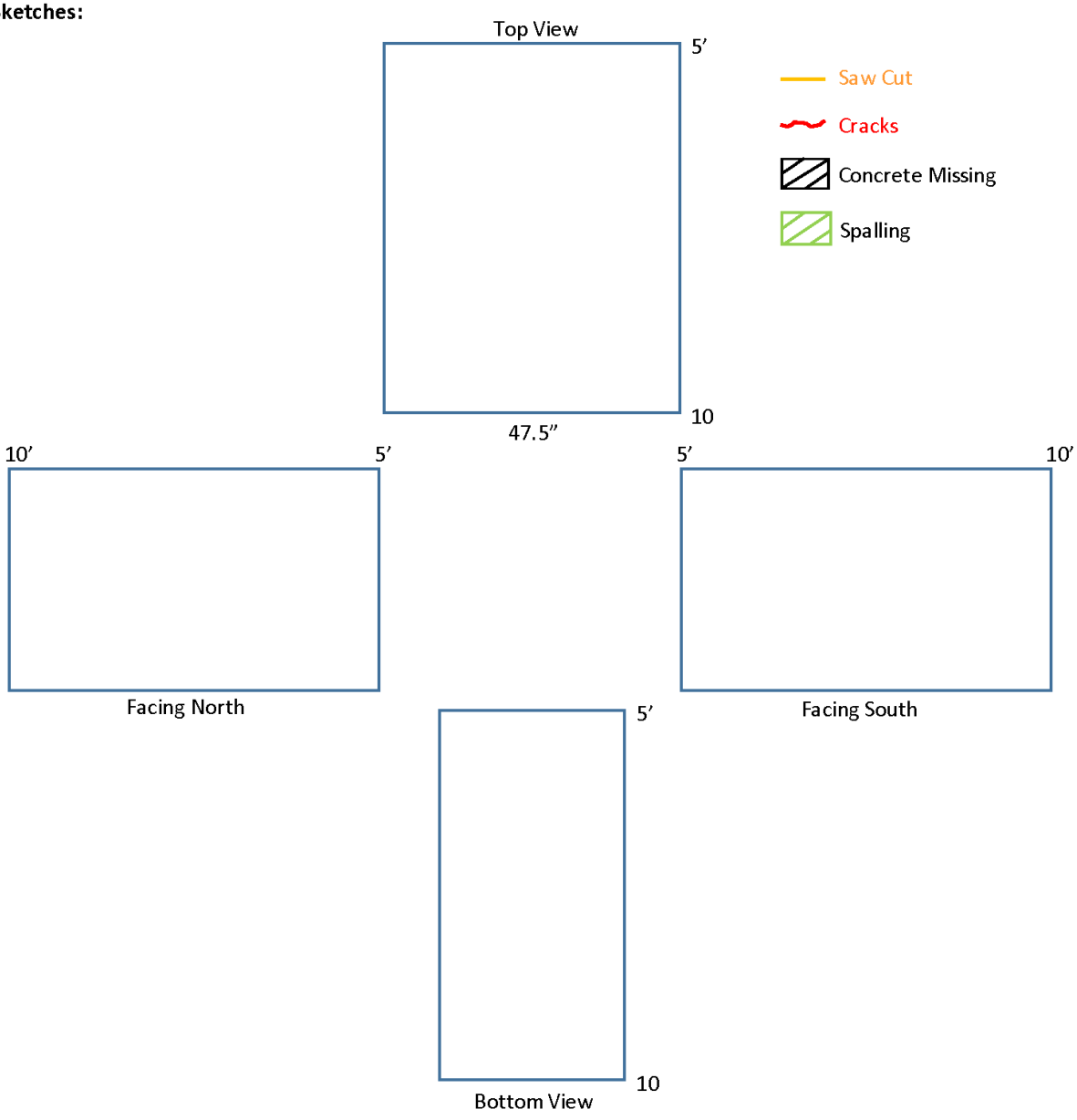

Girder ID: E **Section:** 10’-15’

Notes:

West End: 0’ line
East End: Main Fire

Deck Thickness: 8.5”

Sketches:

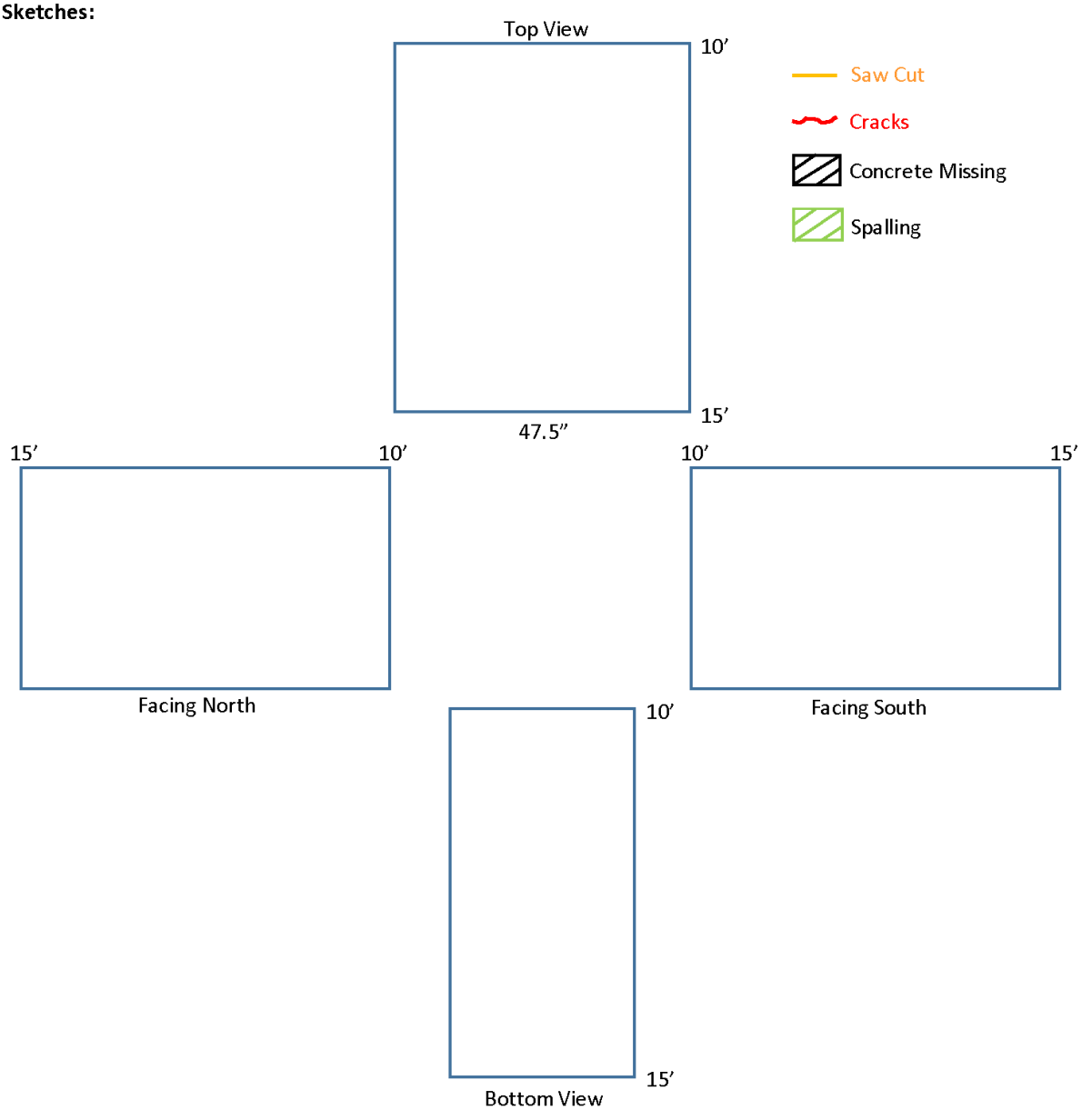

Girder ID: E **Section:** 15’-20’

Notes:

West End: 0’ line
East End: Main Fire

Deck Thickness: 8”

Sketches:

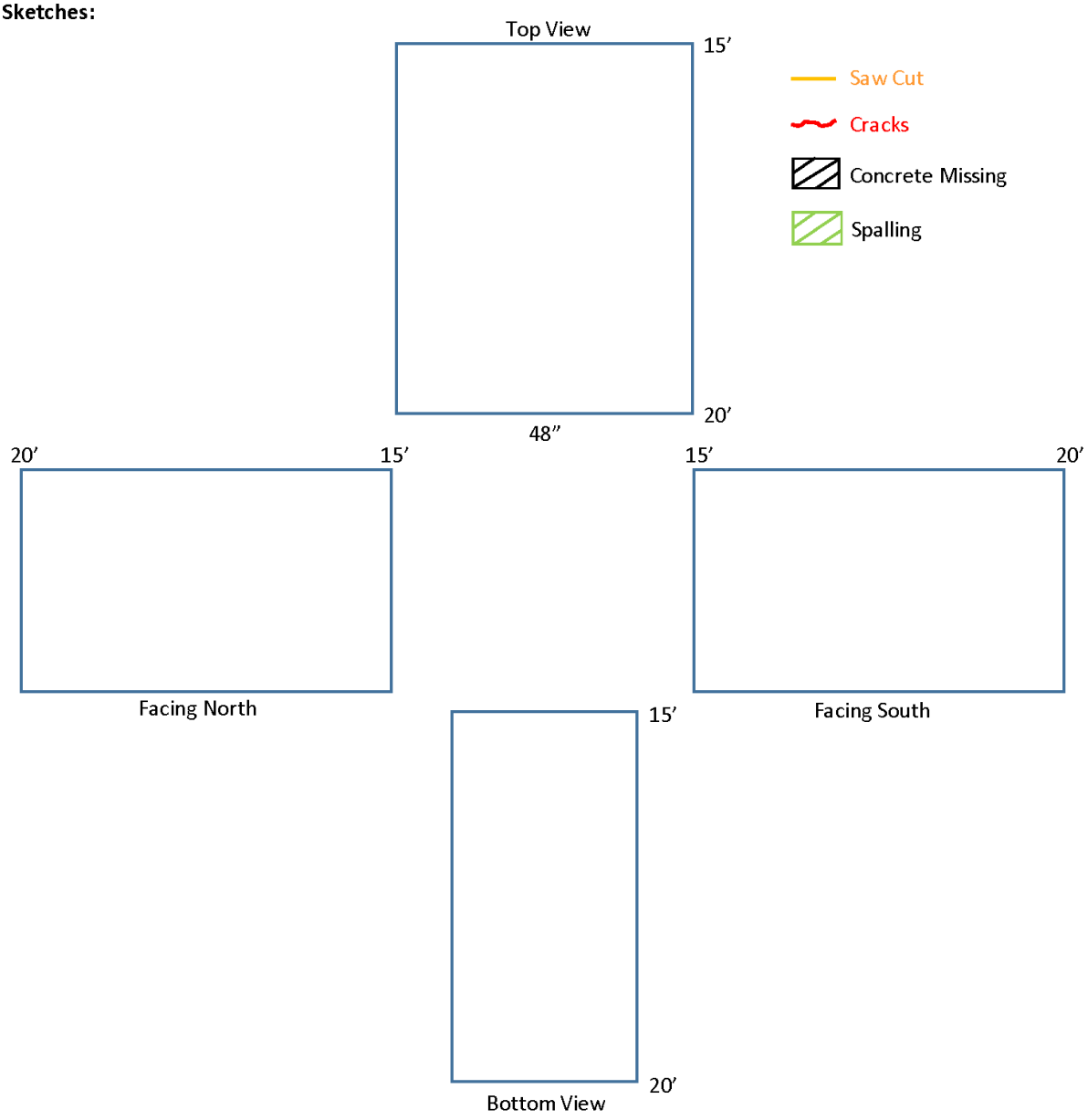

Girder ID: E **Section:** 20’-25’

Notes:

West End: 0’ line
East End: Main Fire

Deck Thickness: 8”

Sketches:

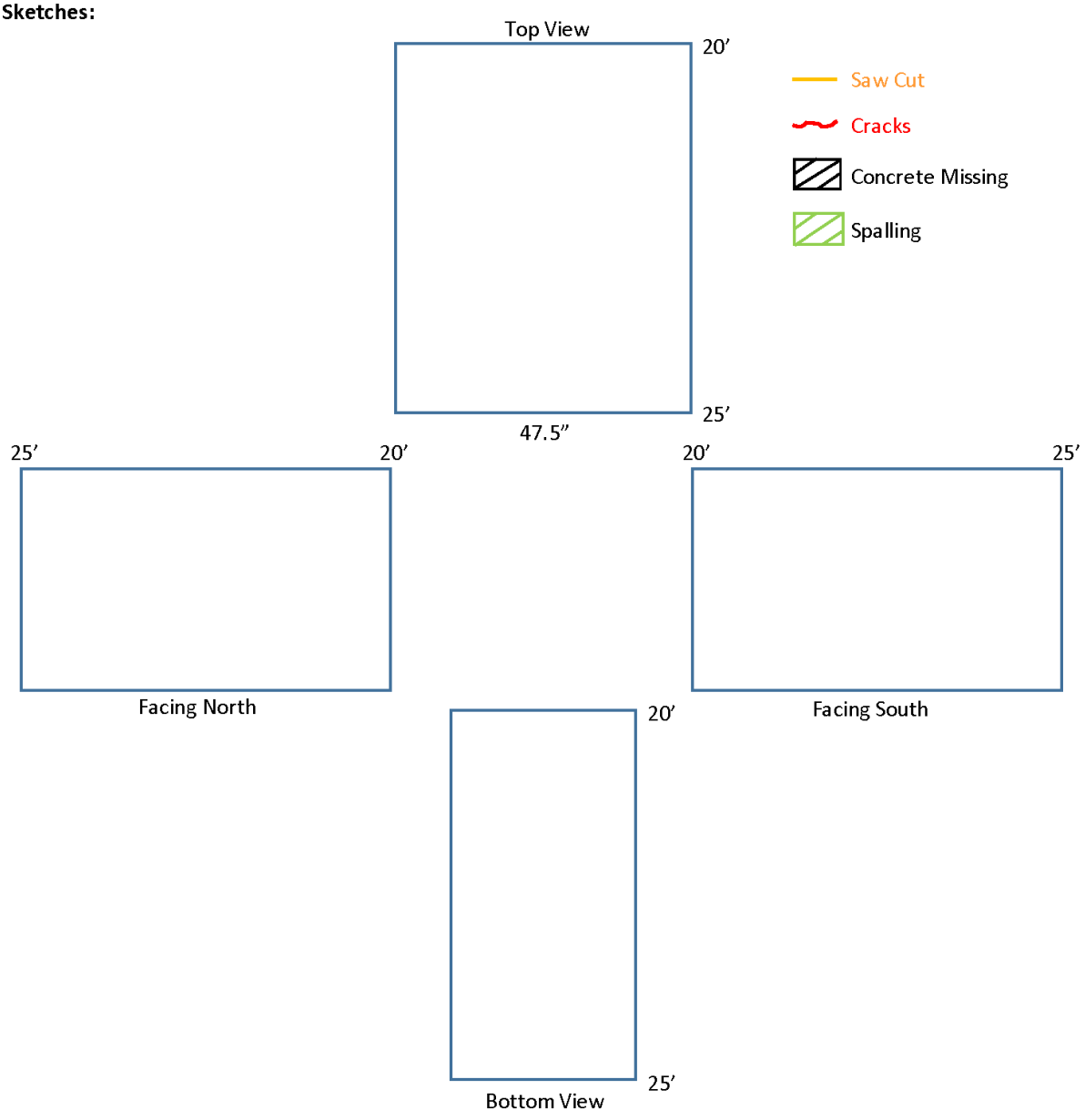

Girder ID: E **Section:** 25’-30’

Notes:

West End: 0’ line
East End: Main Fire

Deck Thickness: 8”

Sketches:

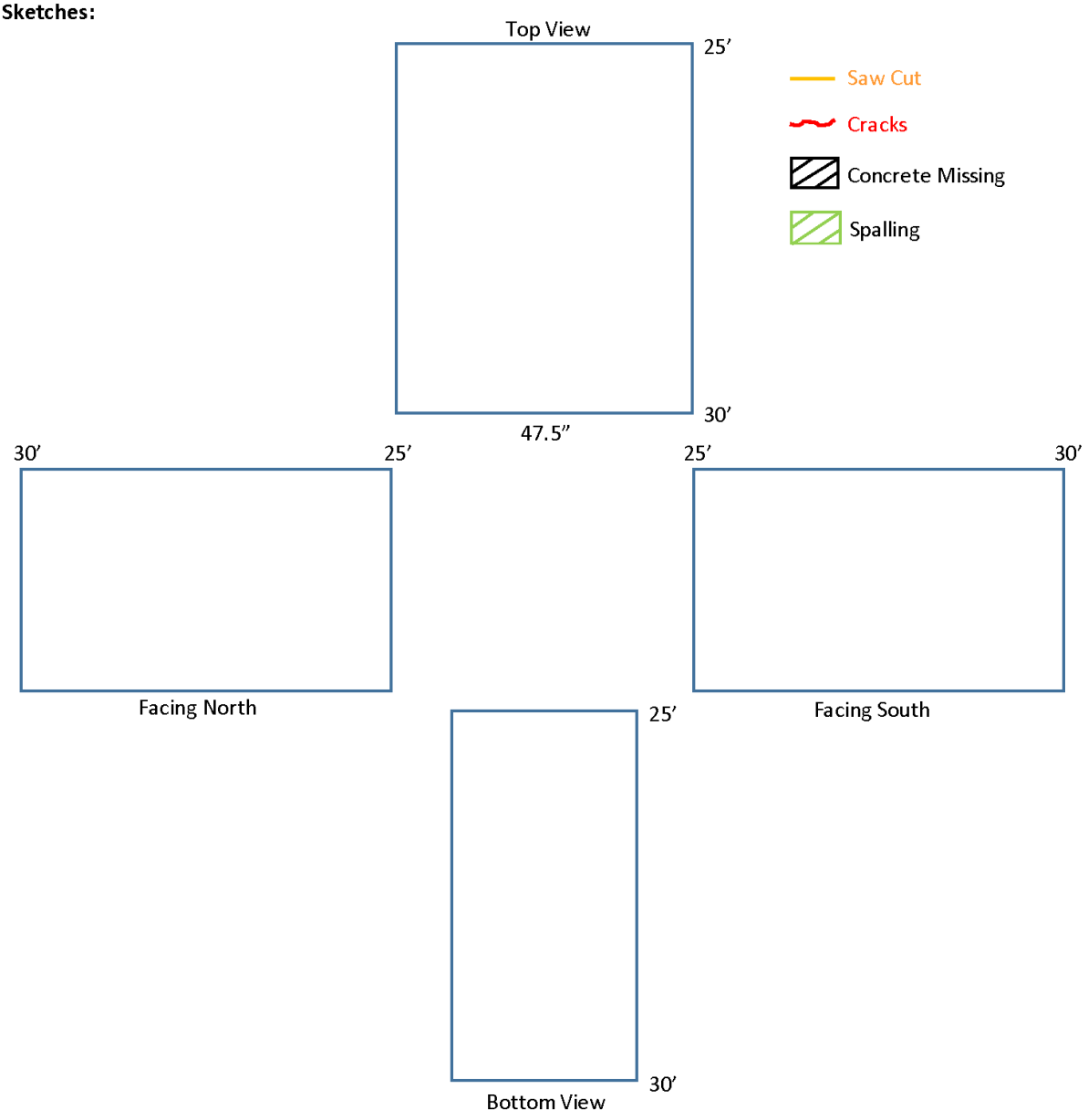

Girder ID: E **Section:** 30'-35'

Notes:

West End: 0' line
East End: Main Fire

Deck Thickness: 8.5"

Sketches:

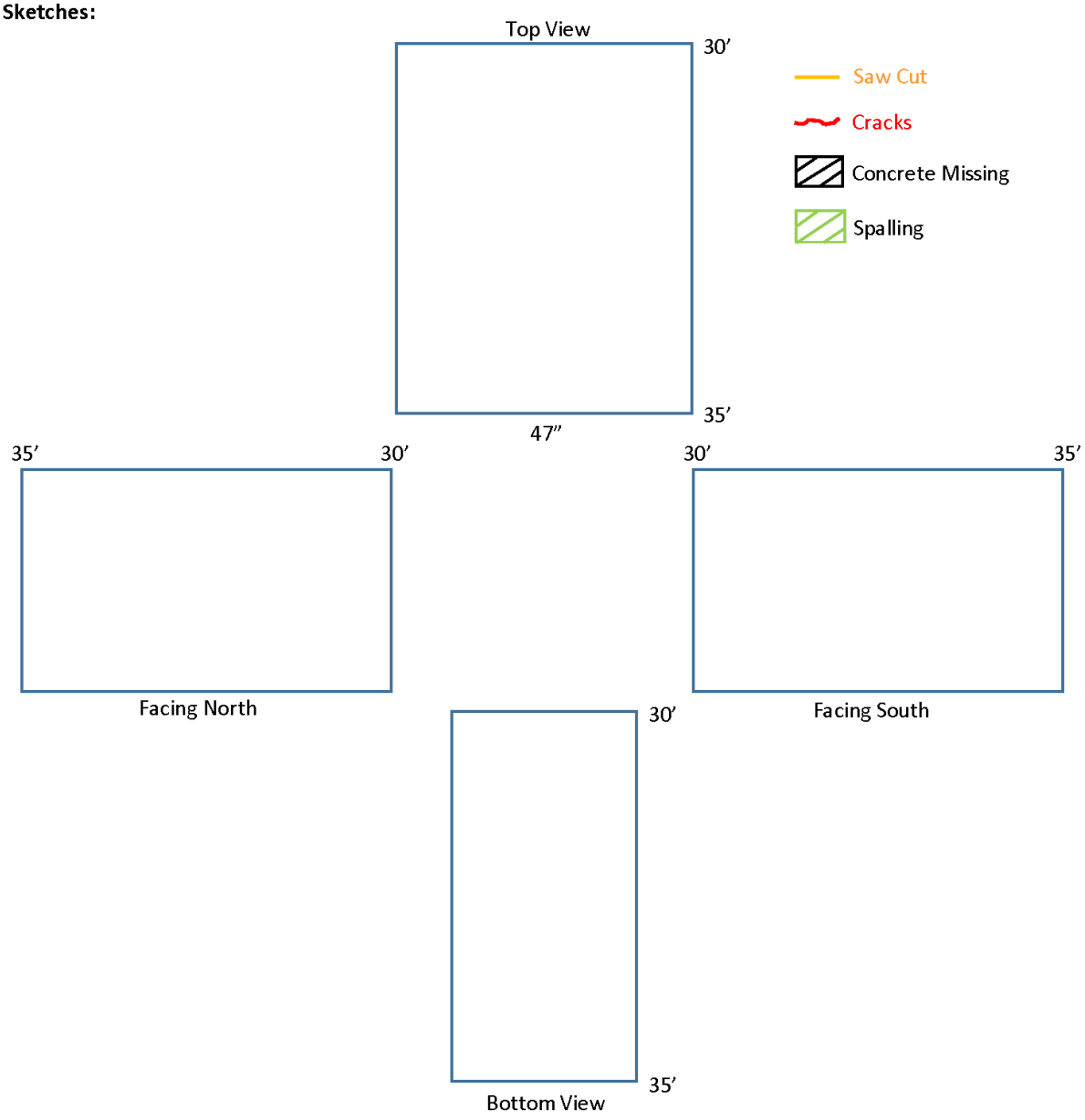

Girder ID: E **Section:** 35’-40’

Notes:

West End: 0’ line
East End: Main Fire

Deck Thickness: 8.25”

Sketches:

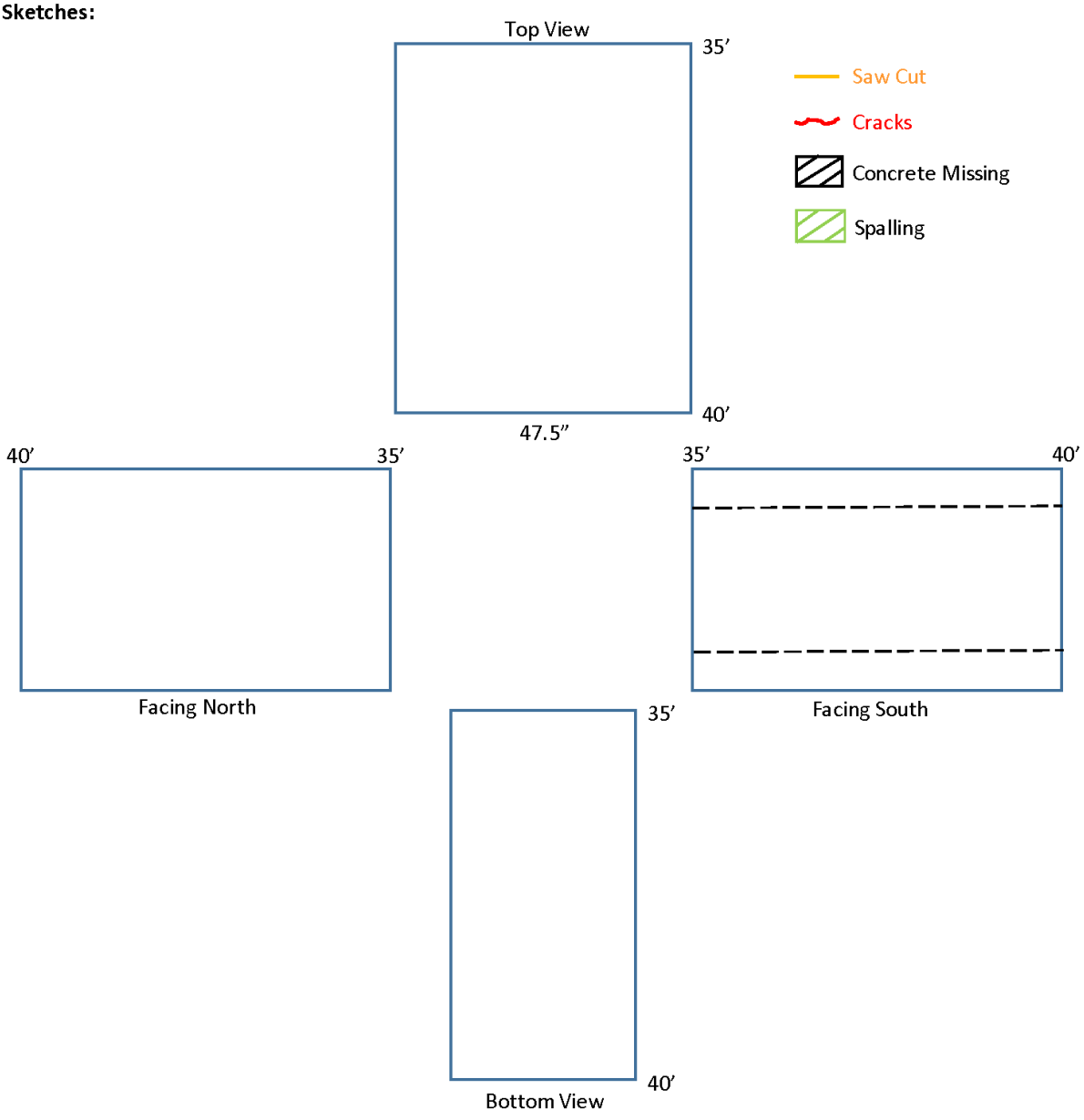

Girder ID: E **Section:** 40’-45’

Notes:

West End: 0’ line
East End: Main Fire

Deck Thickness: 8”

Sketches:

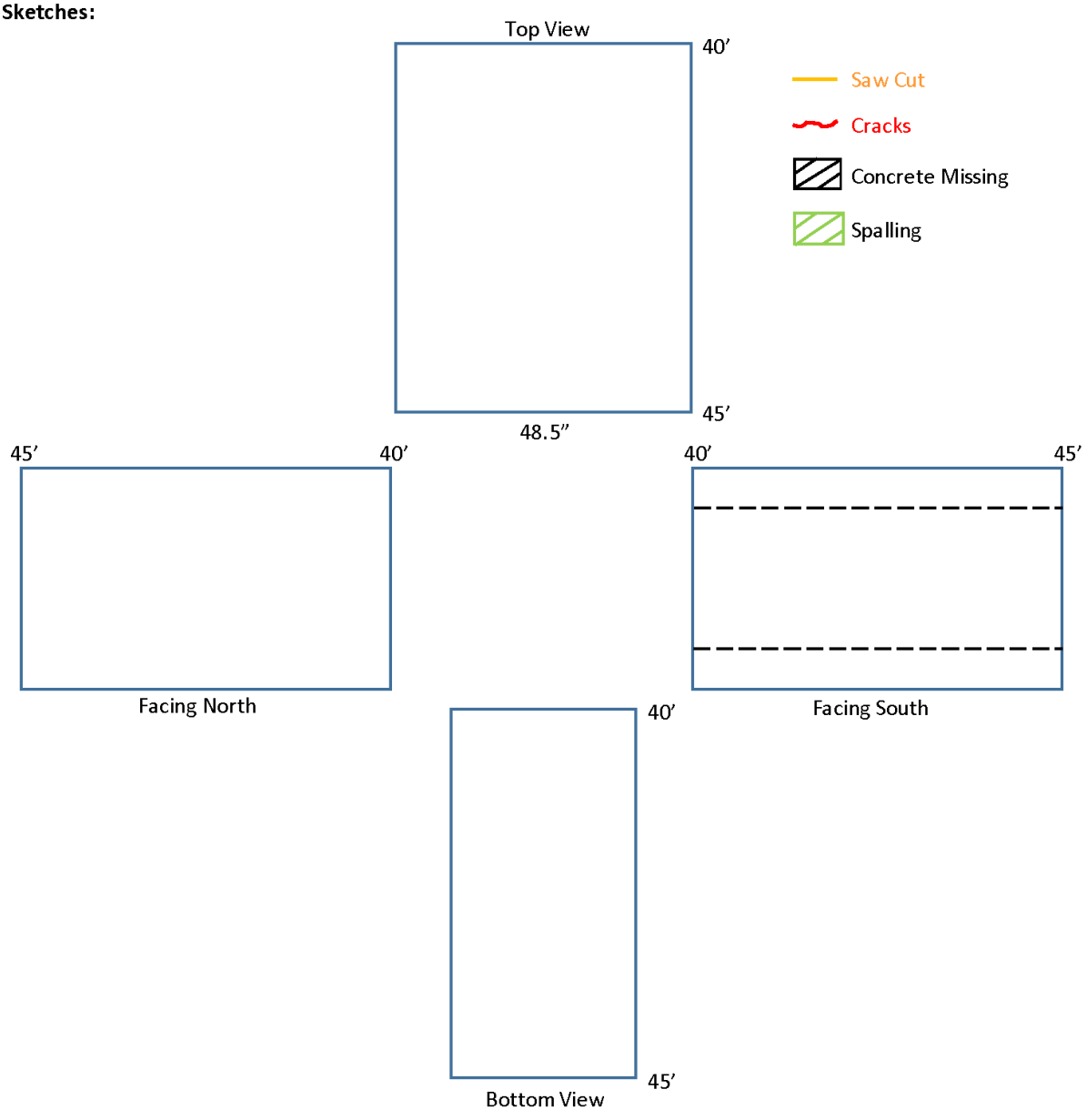

Girder ID: E **Section:** 45’-50’

Notes:

West End: 0’ line
East End: Main Fire

Deck Thickness: 8.25”

Sketches:

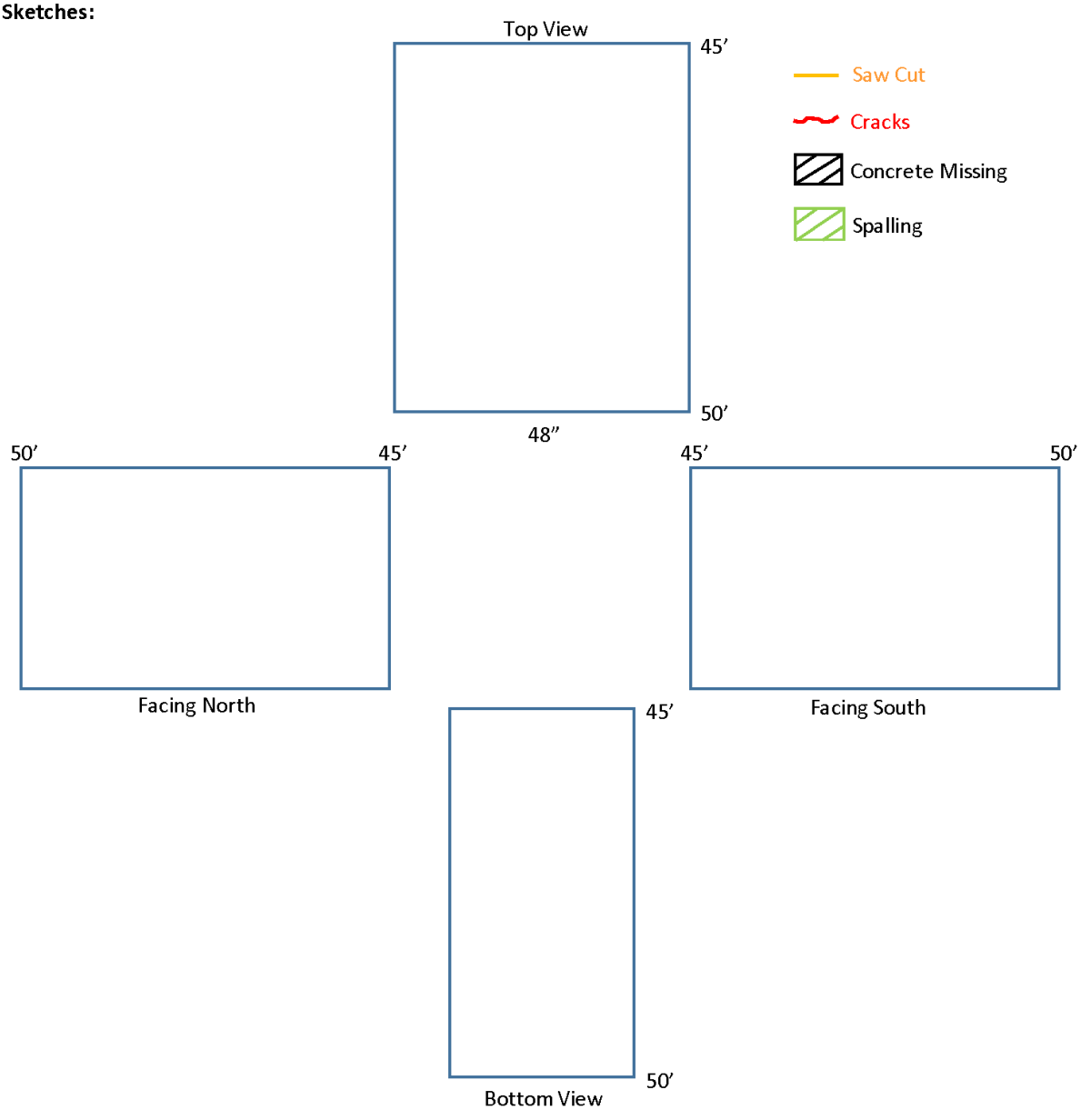

Girder ID: E **Section:** 50’-55’

Notes:

West End: 0’ line
East End: Main Fire

Deck Thickness: 8.5”

Sketches:

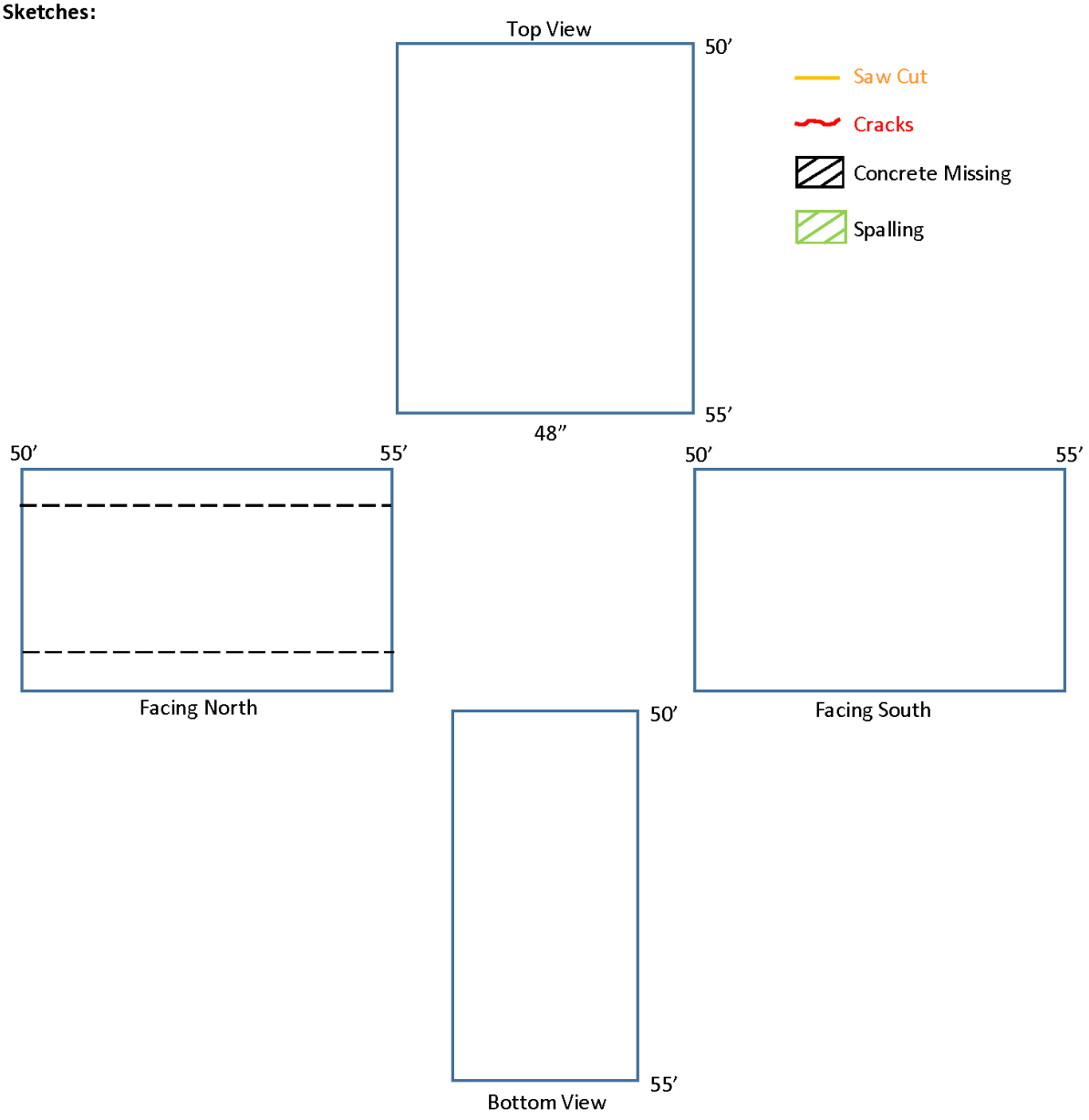

Girder ID: E **Section:** 55’-60’

Notes:

West End: 0’ line
East End: Main Fire

Deck Thickness: 8”

Sketches:

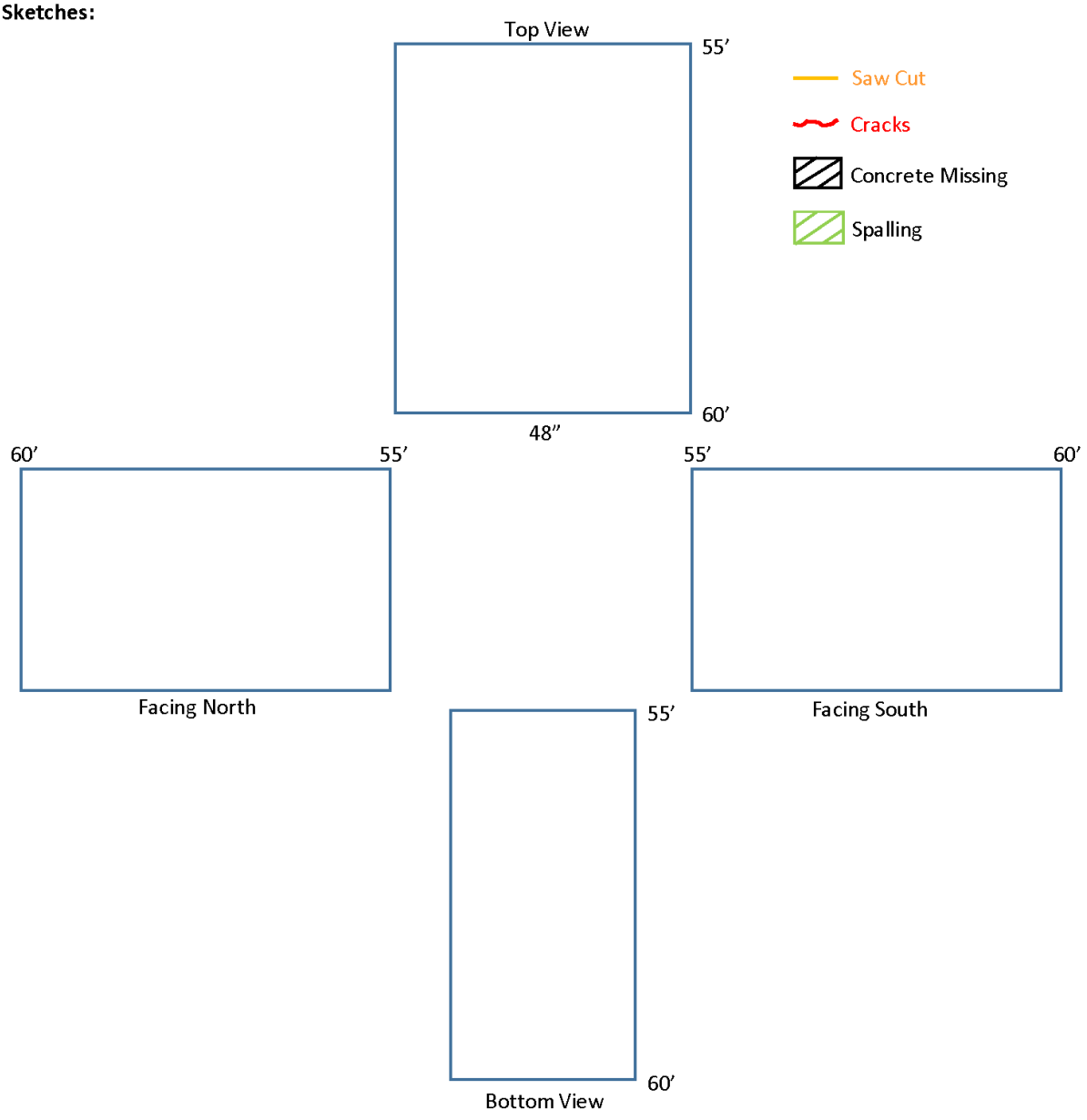

Girder ID: E **Section:** 60’-65’

Notes:

West End: 0’ line
East End: Main Fire

Deck Thickness: 8”

Sketches:

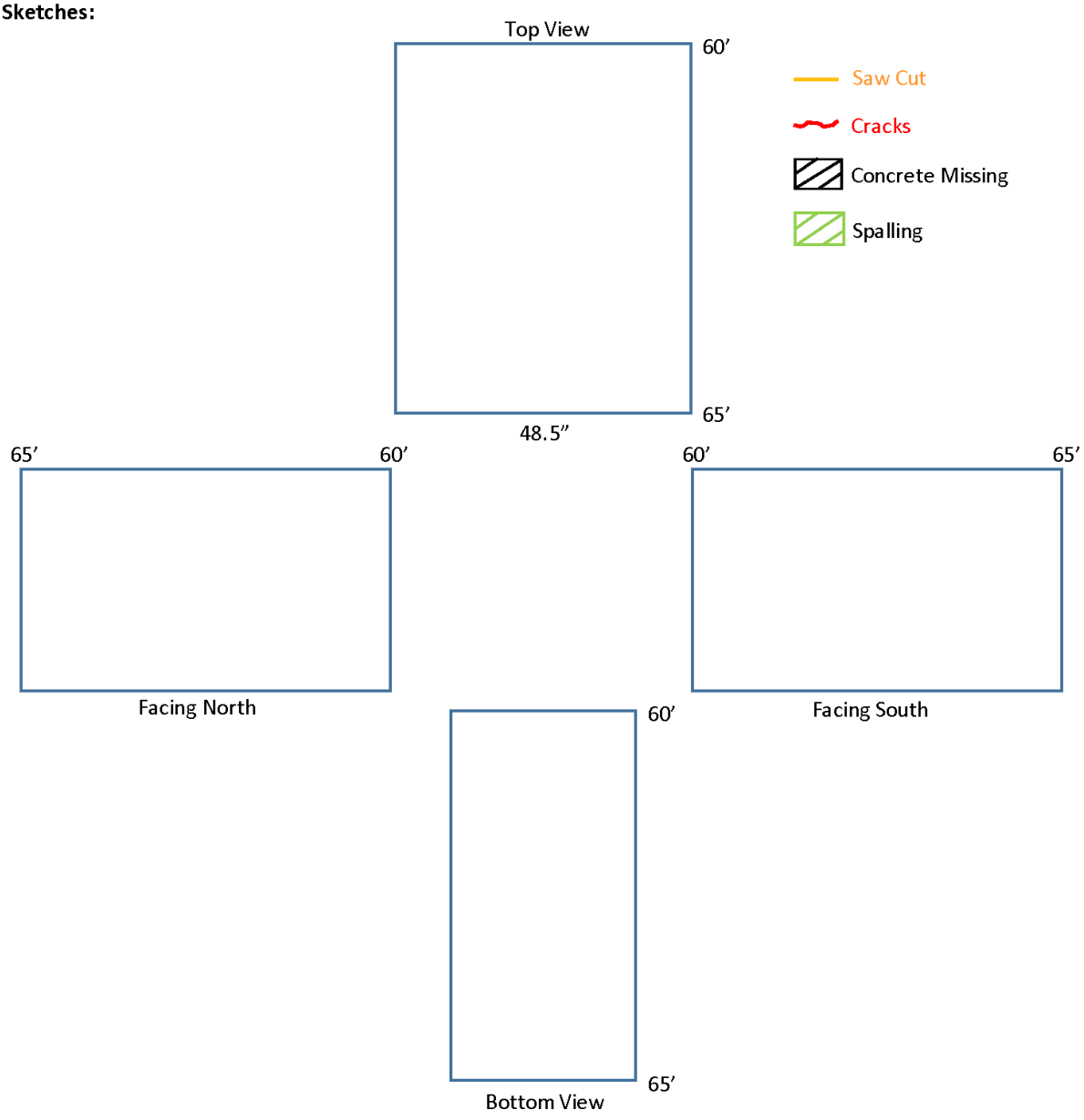

Girder ID: E **Section:** 65’-70’

Notes:

West End: 0’ line
East End: Main Fire

Deck Thickness: 8”

Sketches:

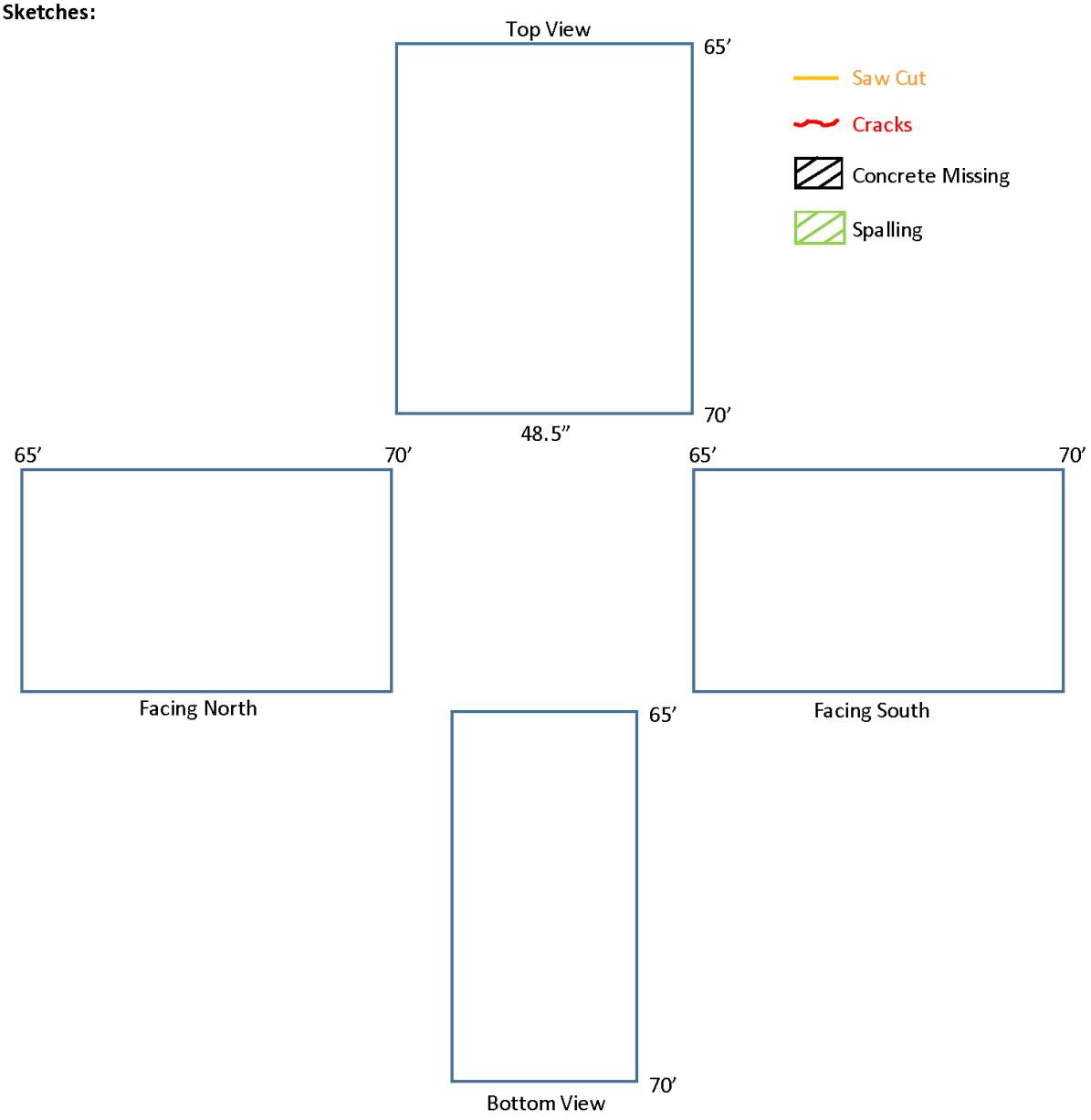

Girder ID: E **Section:** 70'-75'

Notes:

West End: 0' line
East End: Main Fire

Deck Thickness: 8"

Sketches:

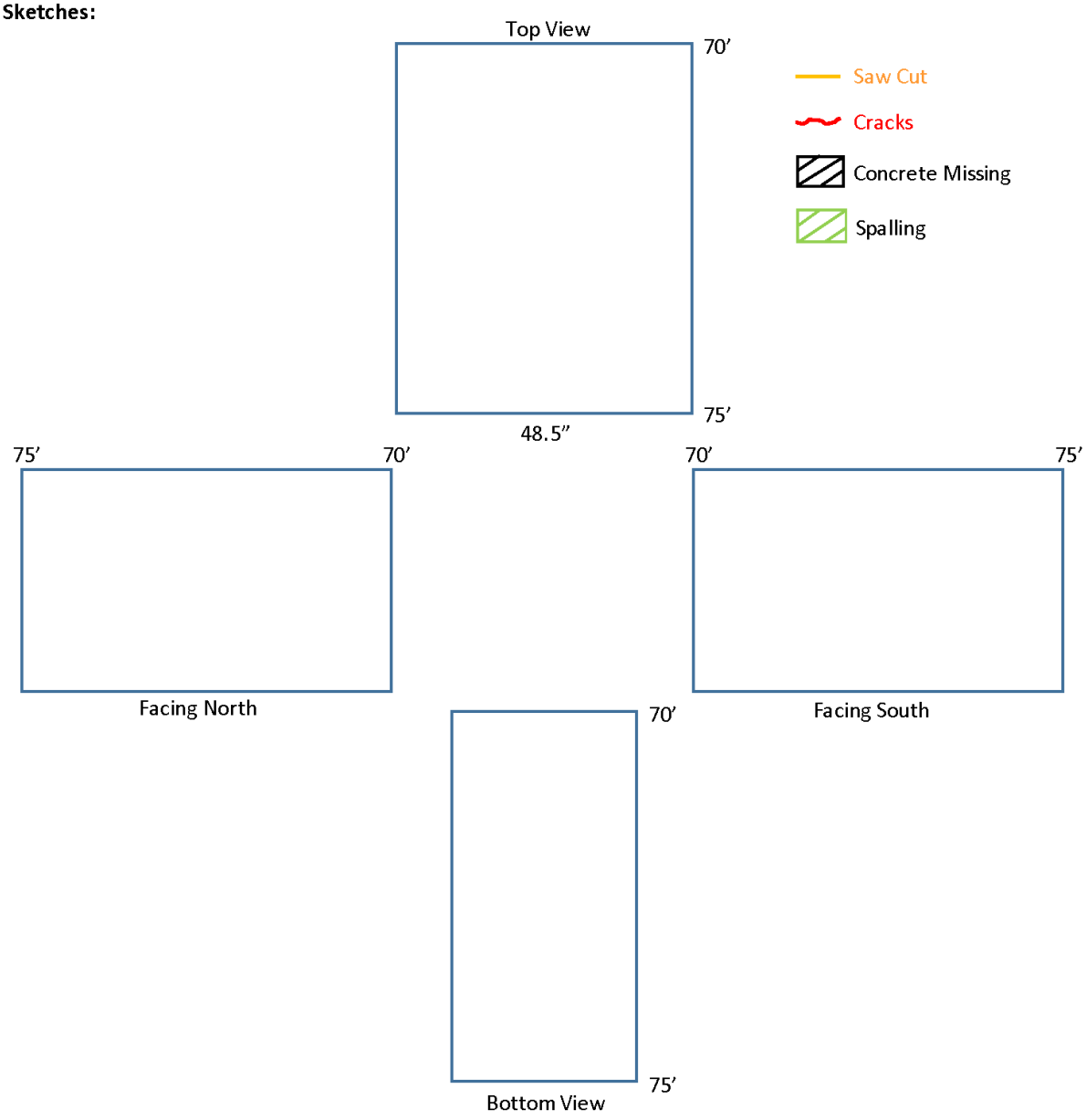

Girder ID: E **Section:** 75’-80’

Notes:

West End: 0’ line
East End: Main Fire

Deck Thickness: 8”

Sketches:

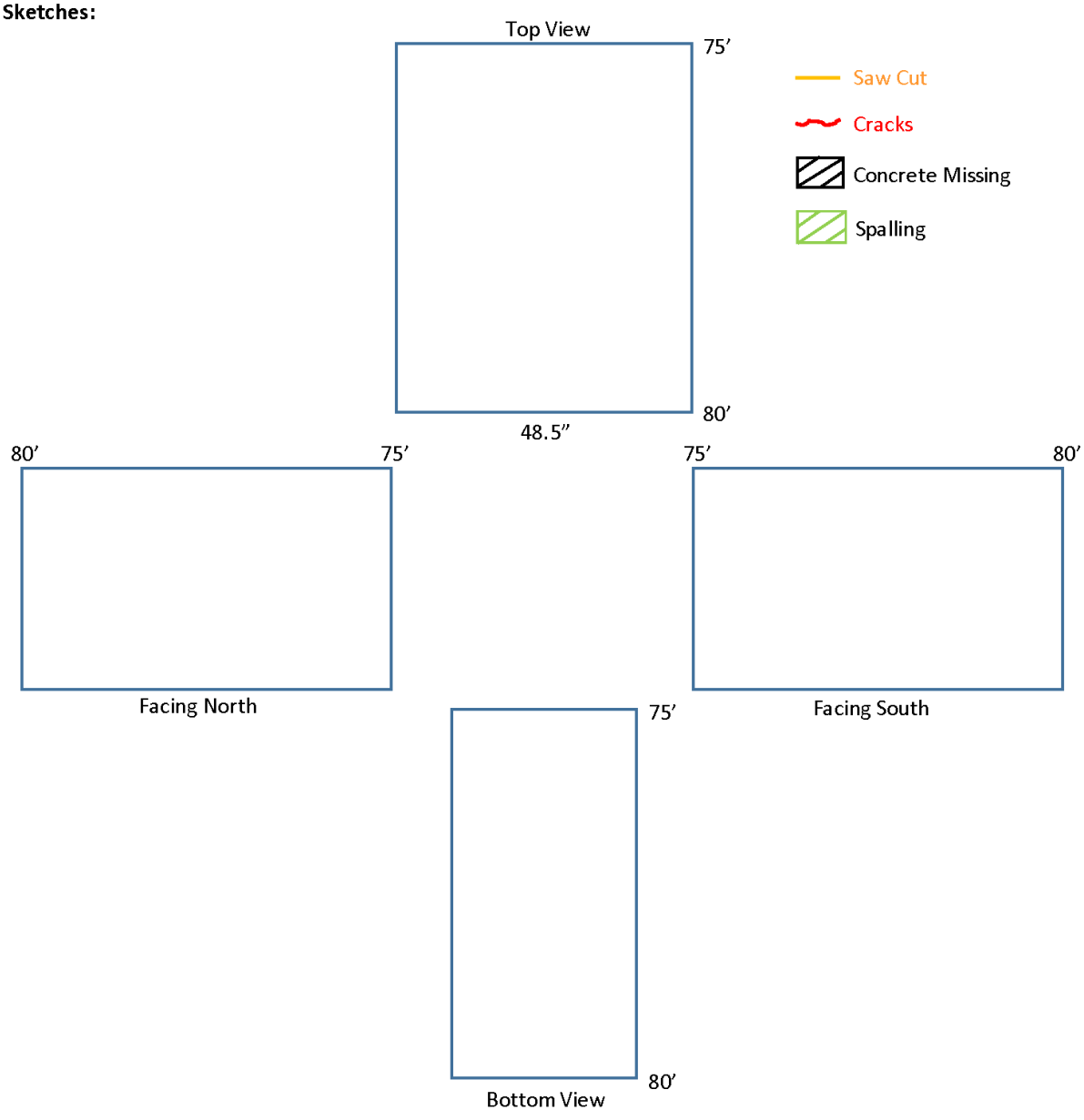

Girder ID: E **Section:** 80'-85'

Notes:

West End: 0' line
East End: Main Fire

Deck Thickness: 8"

Sketches:

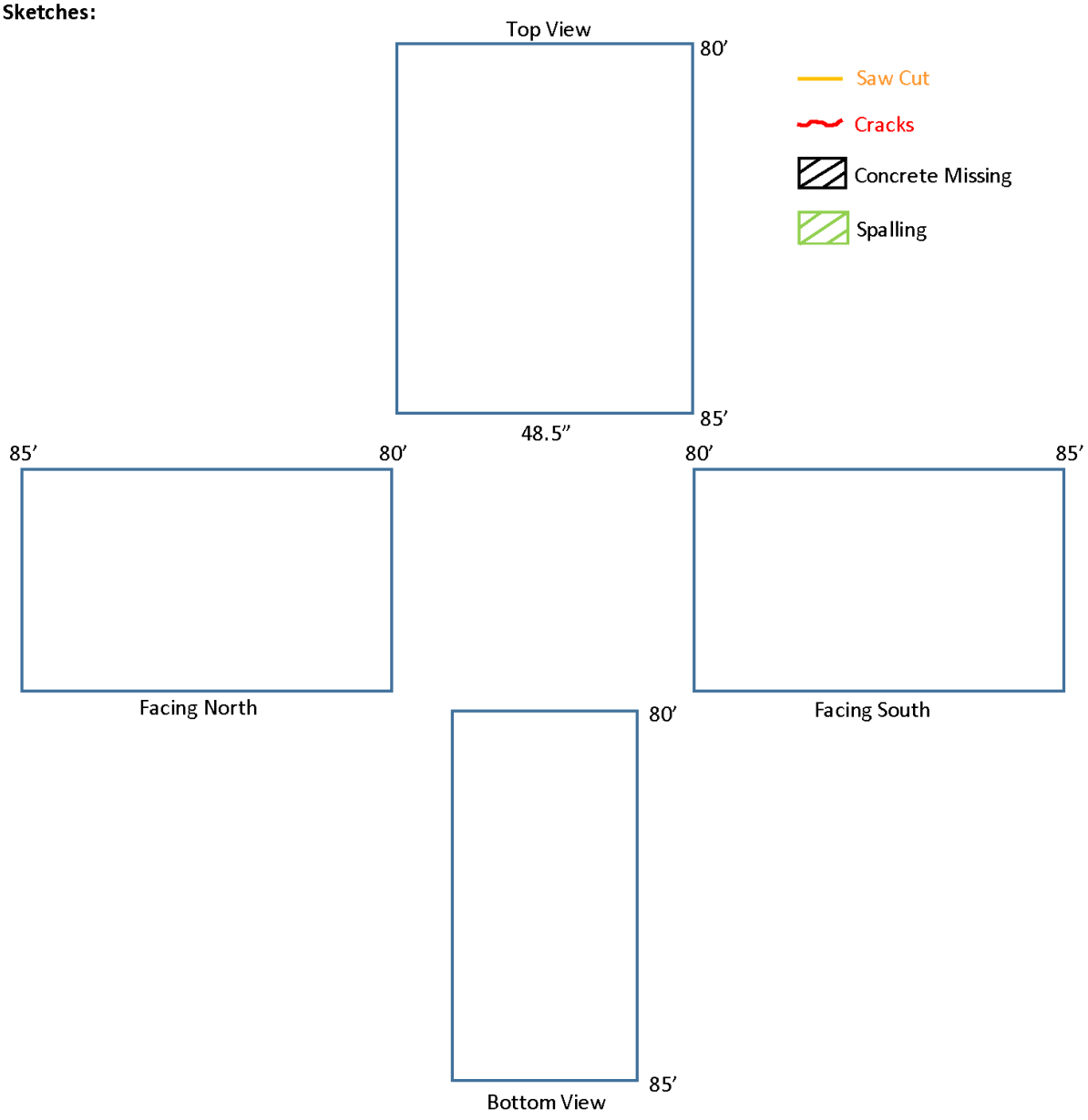

Girder ID: E **Section:** 85'-86.4'

Notes:

West End: 0' line
East End: Main Fire

Deck Thickness: 8"

Sketches:

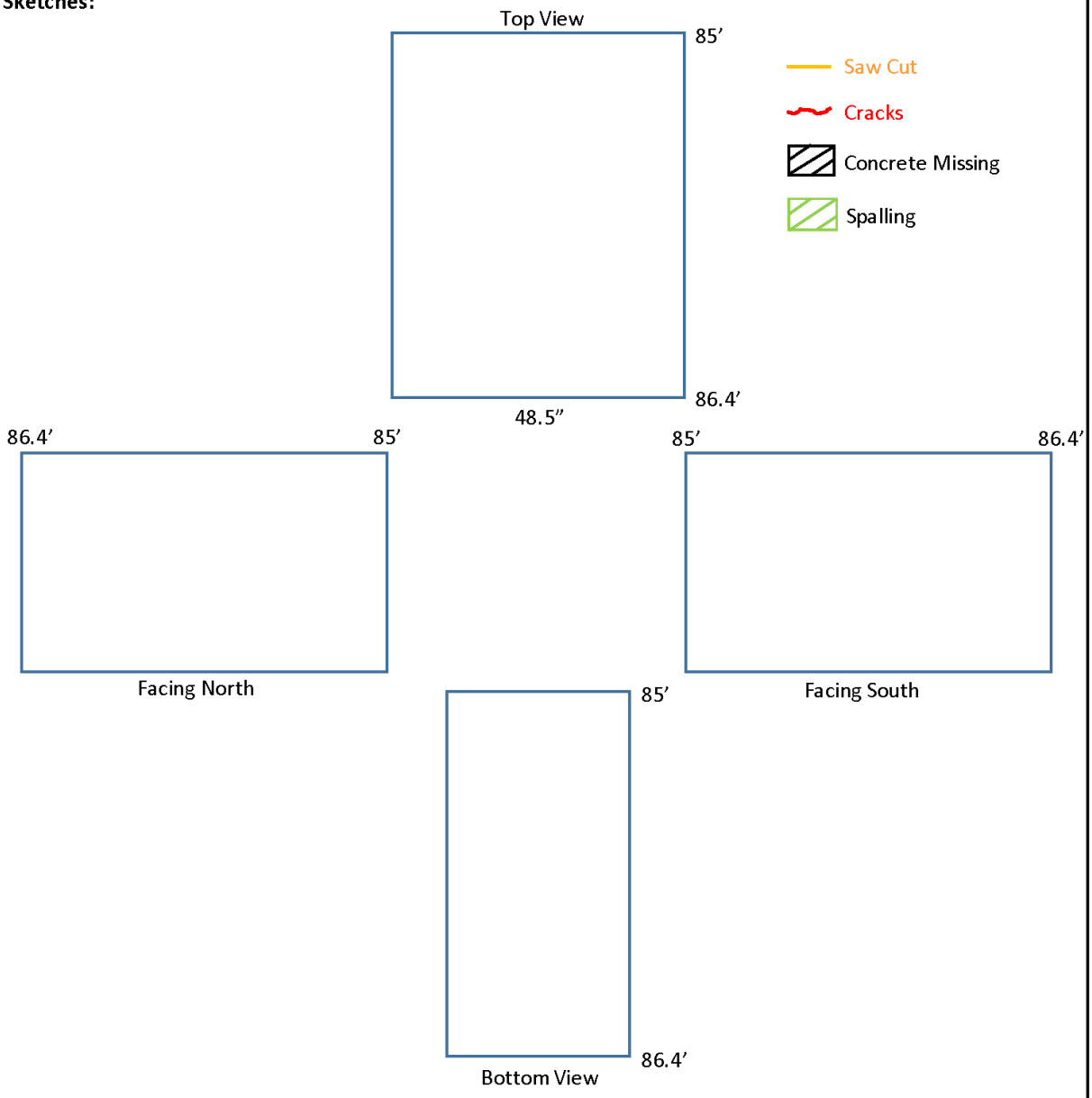

Girder G Condition Sheets

Girder ID: G **Section:** 0’-5’

Notes:

West End: 0’ line
East End: Main Fire

Deck Thickness:

Sketches:

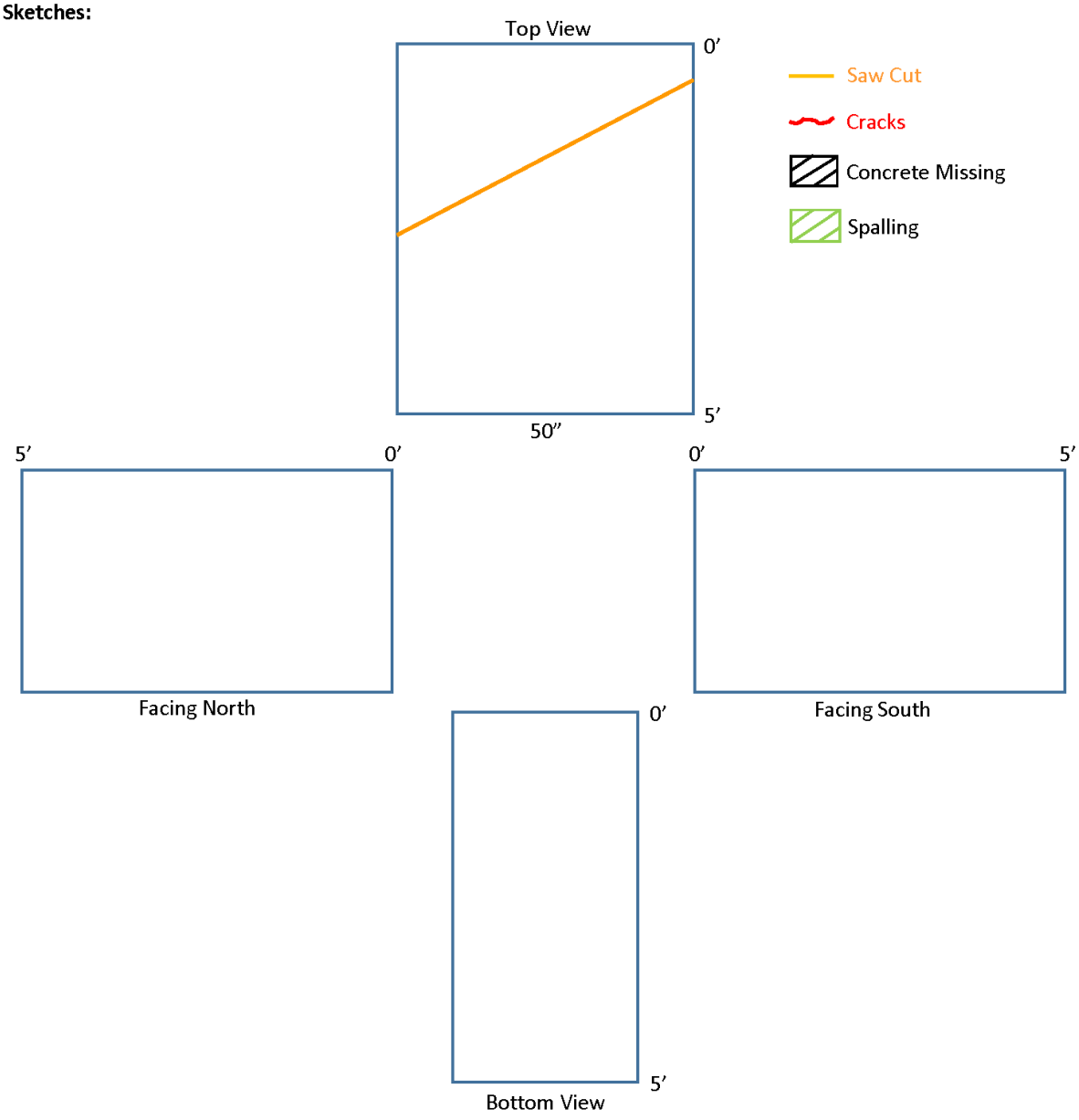

Girder ID: G **Section:** 5’-10’

Notes:

West End: 0’ line
East End: Main Fire

Deck Thickness:

Sketches:

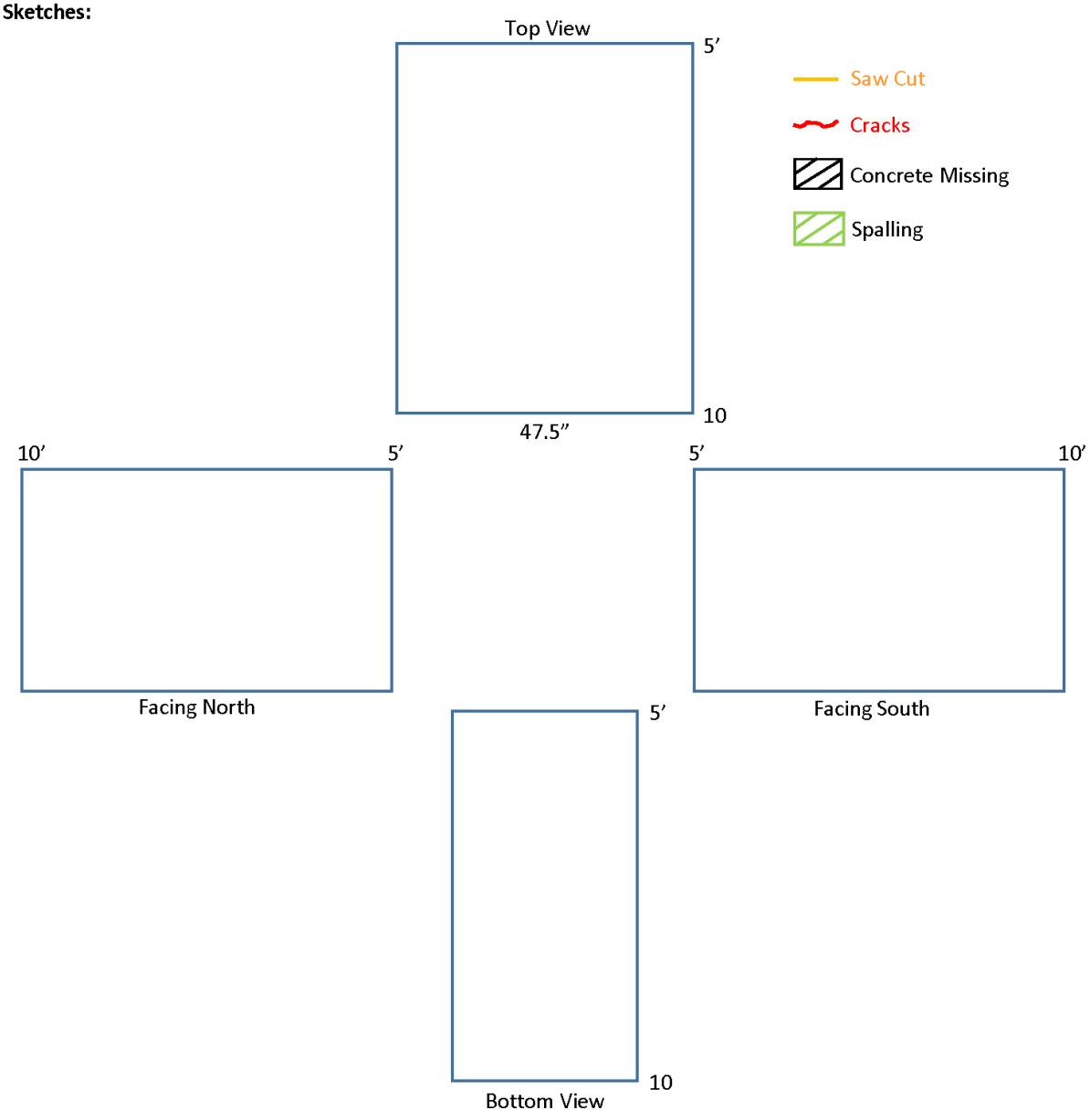

Girder ID: G **Section:** 10’-15’

Notes:

West End: 0’ line
East End: Main Fire

Deck Thickness: 8.5”

Sketches:

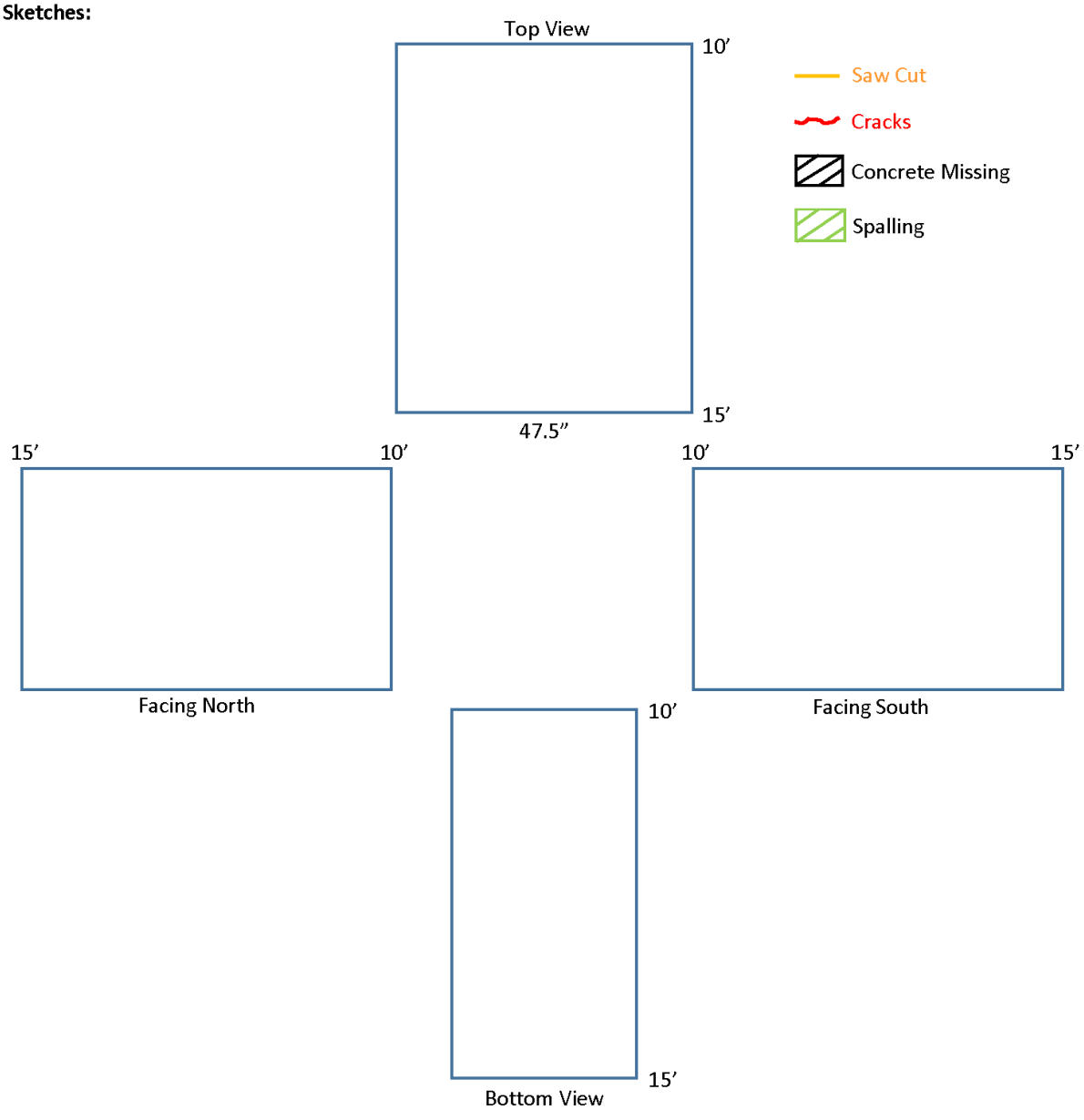

Girder ID: G **Section:** 15’-20’

Notes:

West End: 0’ line
East End: Main Fire

Deck Thickness: 8”

Sketches:

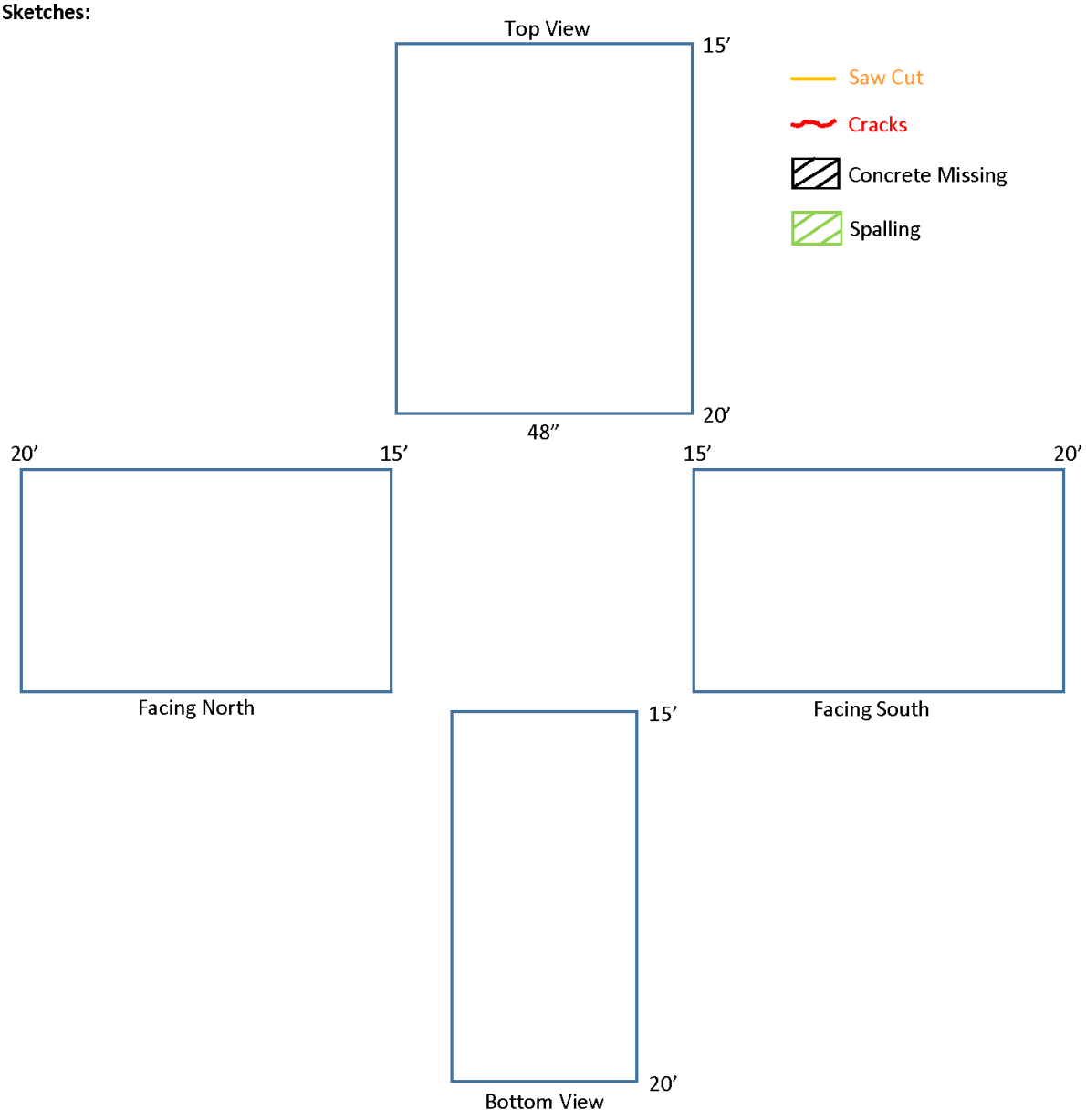

Girder ID: G **Section:** 20’-25’

Notes:

West End: 0’ line
East End: Main Fire

Deck Thickness: 8”

Sketches:

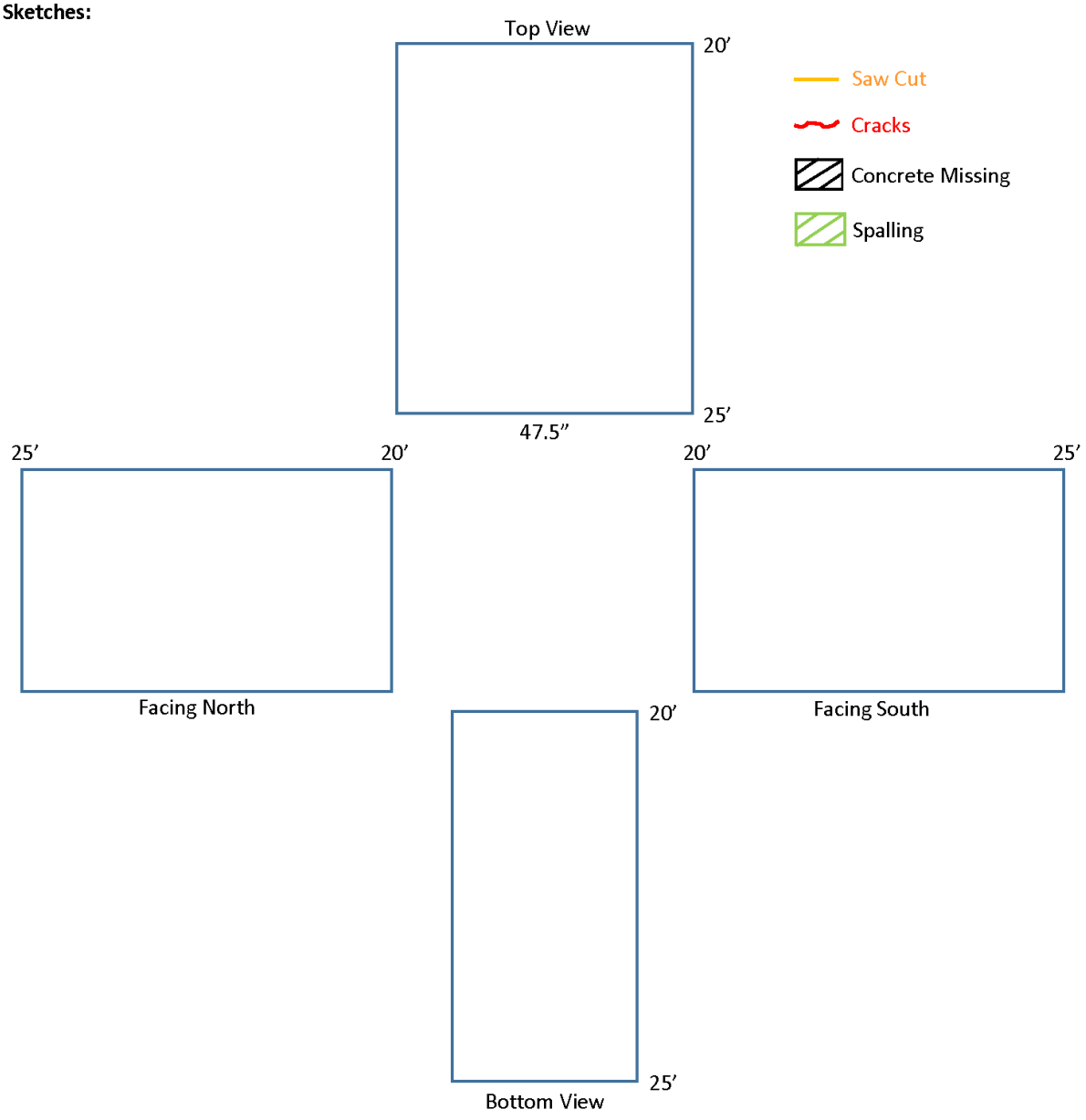

Girder ID: G **Section:** 25'-30'

Notes:

West End: 0' line
East End: Main Fire

Deck Thickness: 8"

Sketches:

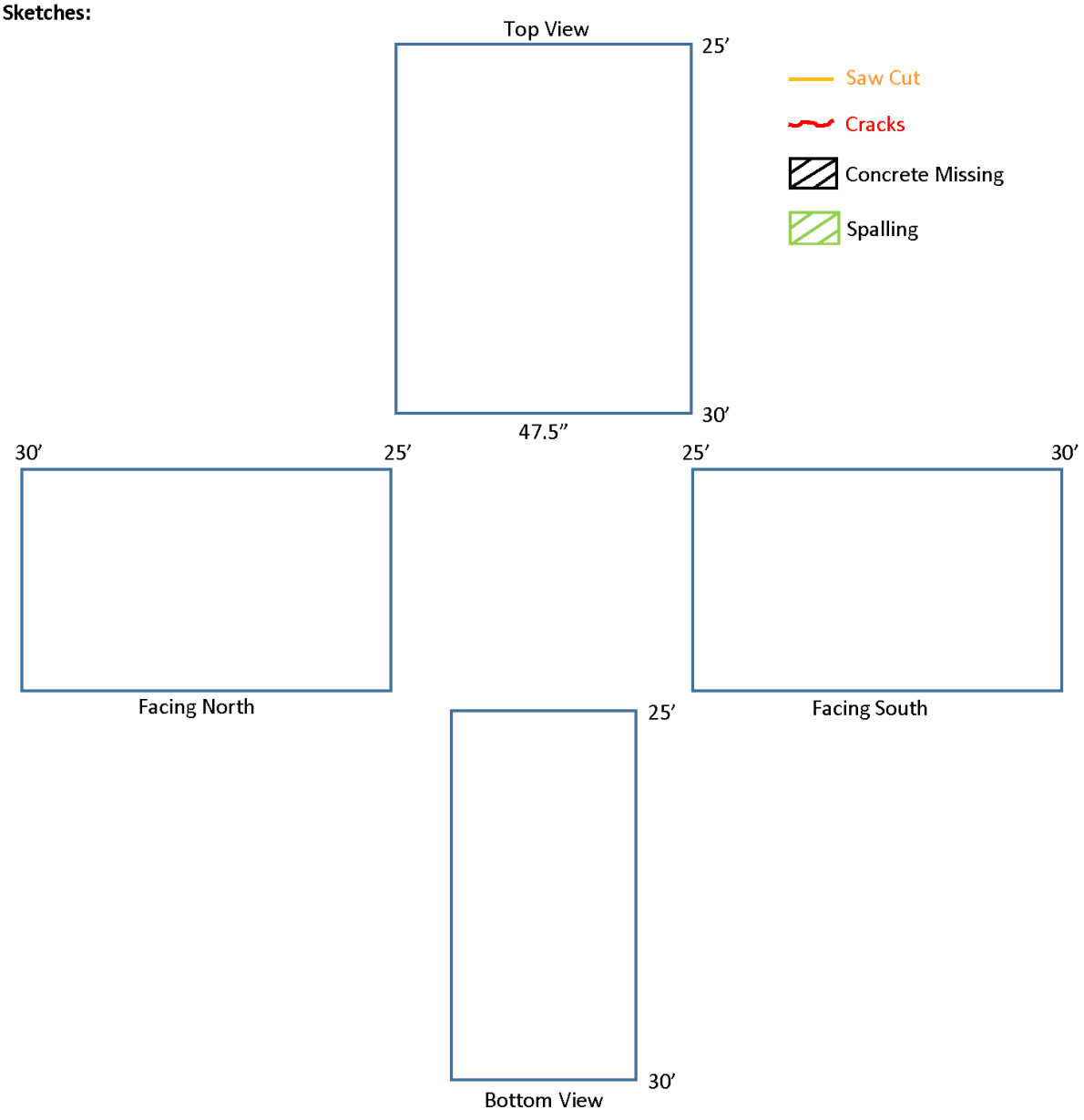

Girder ID: G **Section:** 30’-35’

Notes:

West End: 0’ line
East End: Main Fire

Deck Thickness: 8.5”

Sketches:

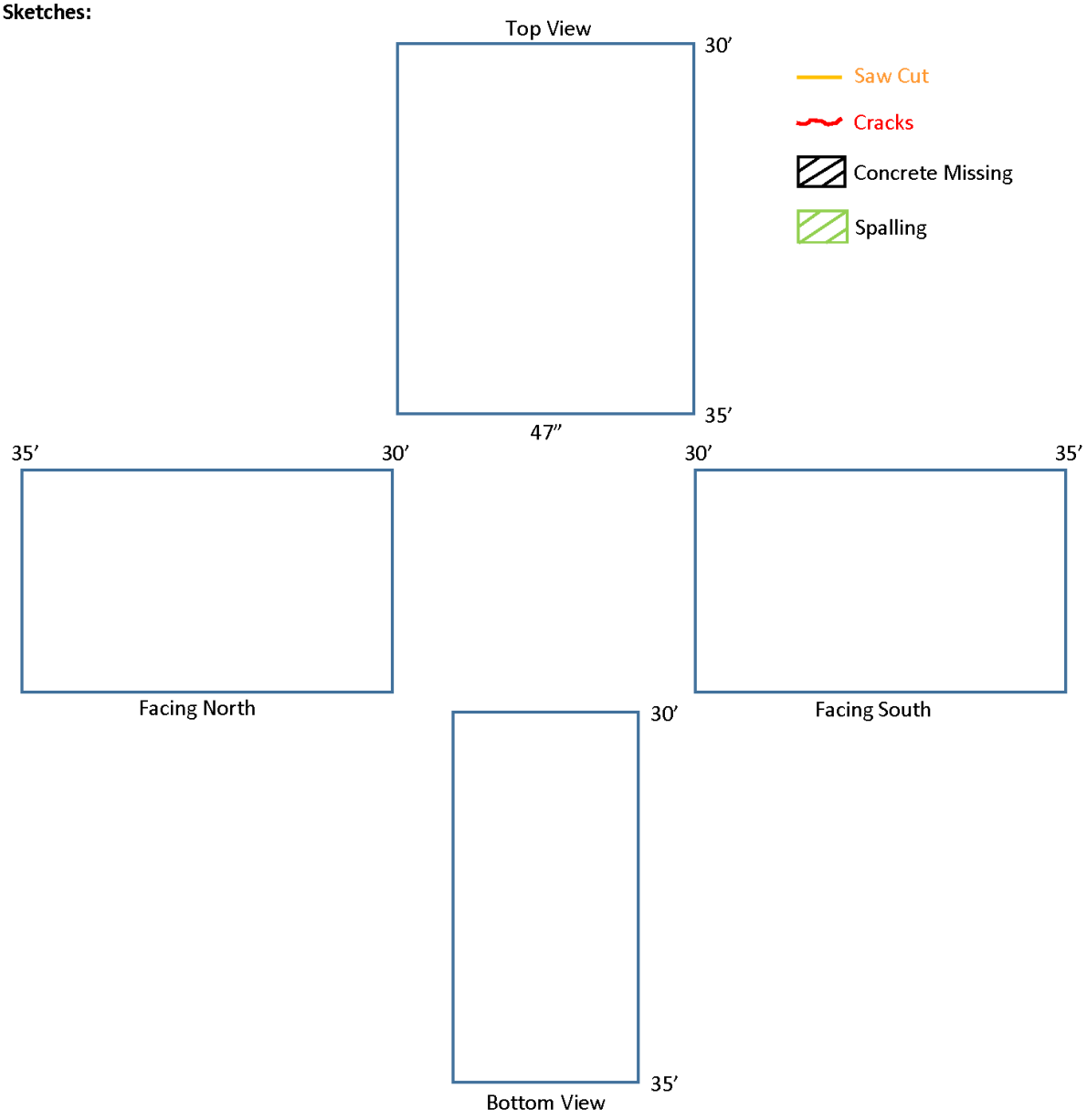

Girder ID: G **Section:** 35’-40’

Notes:

West End: 0’ line
East End: Main Fire

Deck Thickness: 8.25”

Sketches:

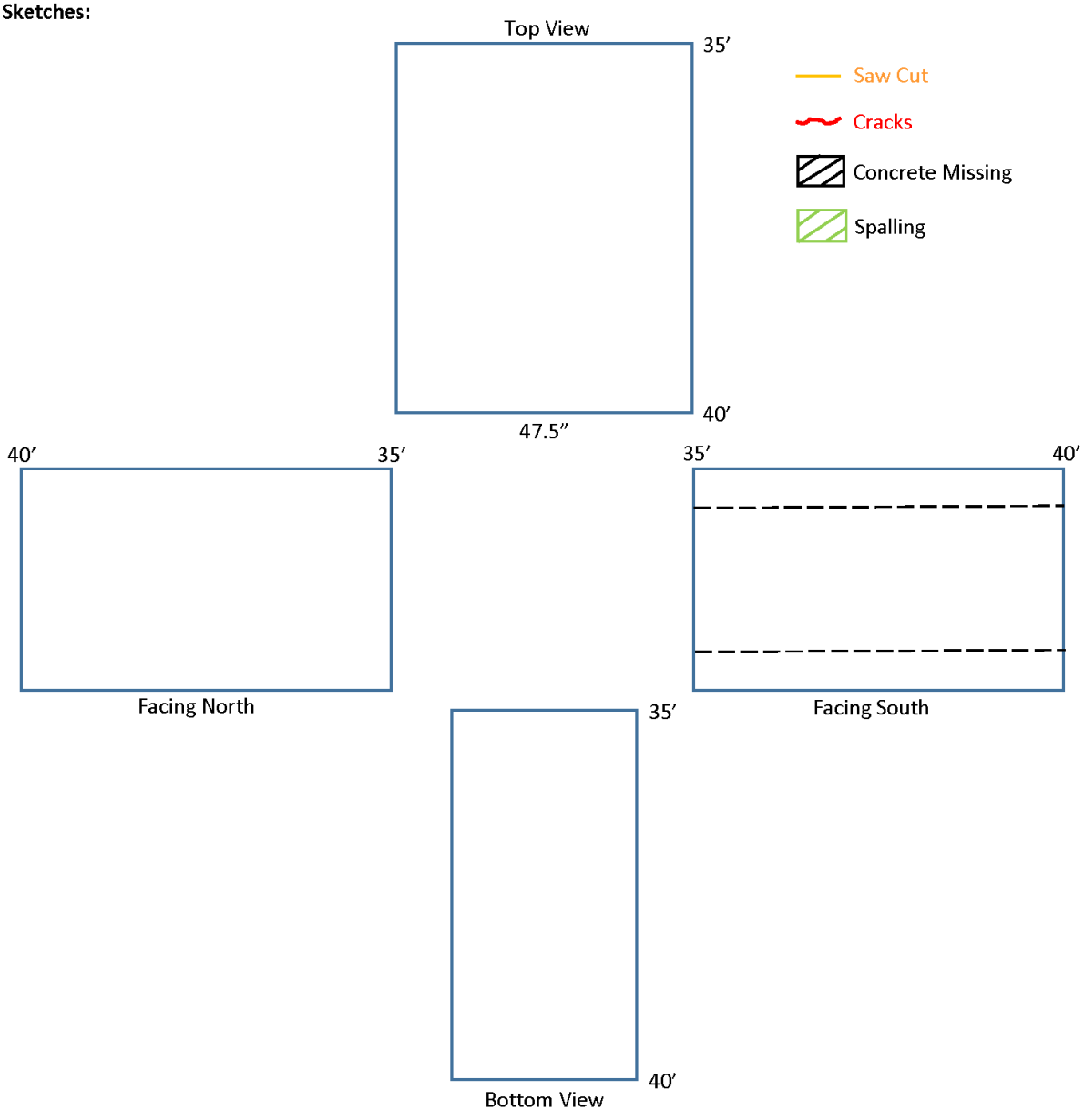

Girder ID: G **Section:** 40’-45’

Notes:

West End: 0’ line
East End: Main Fire

Deck Thickness: 8”

Sketches:

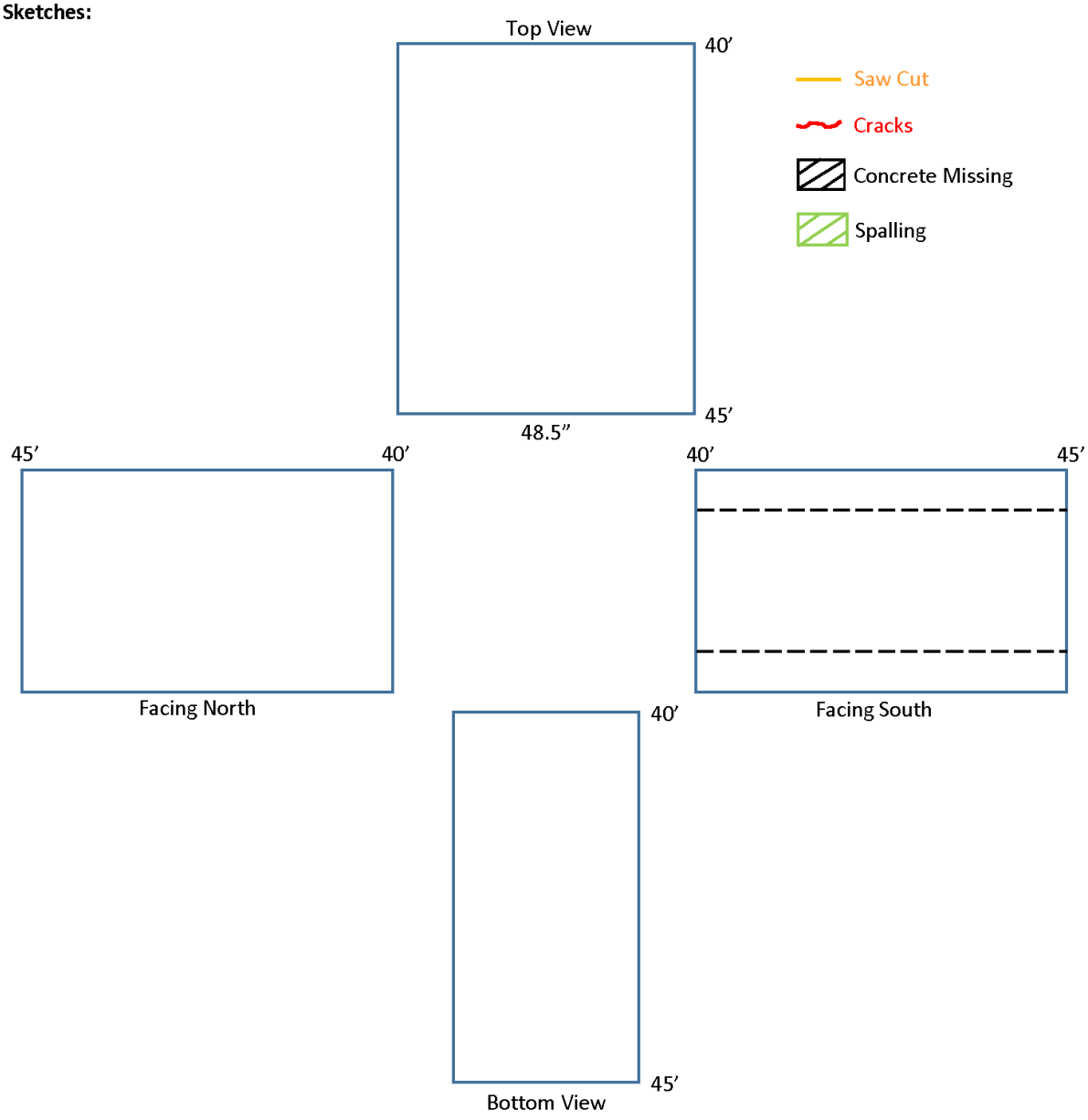

Girder ID: G **Section:** 45’-50’

Notes:

West End: 0’ line
East End: Main Fire

Deck Thickness: 8.25”

Sketches:

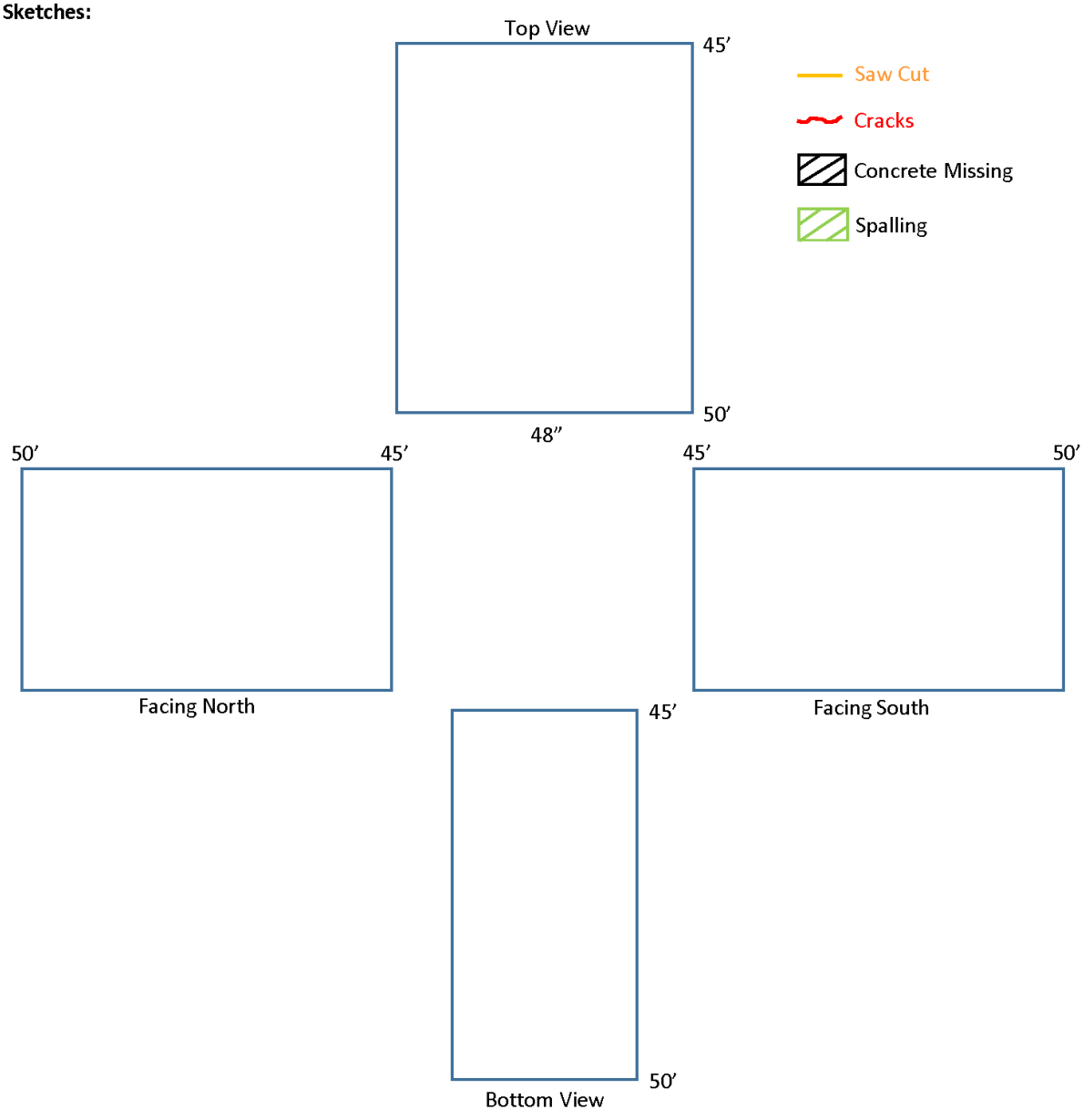

Girder ID: G **Section:** 50'-55'

Notes:

West End: 0' line
East End: Main Fire

Deck Thickness: 8.5"

Sketches:

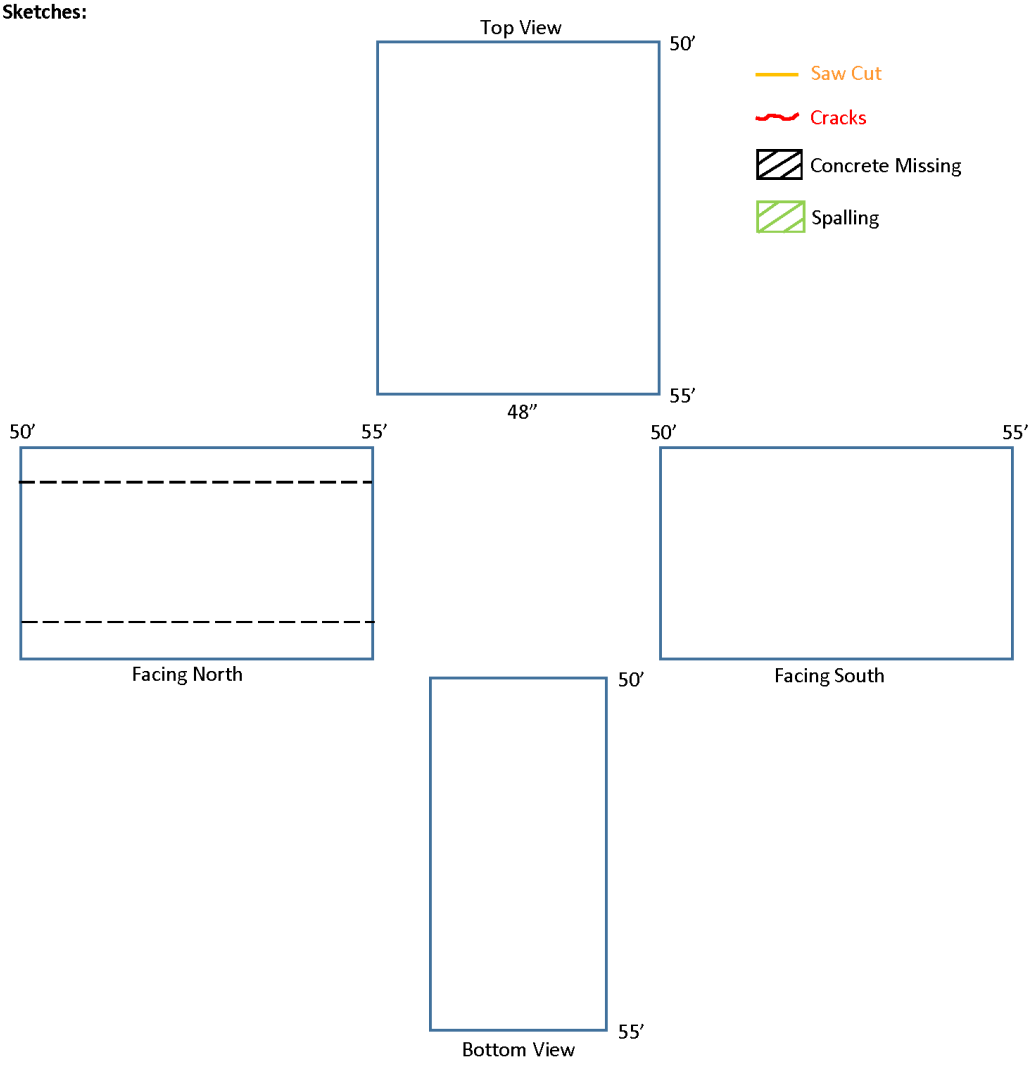

Girder ID: G **Section:** 55’-60’

Notes:

West End: 0’ line
East End: Main Fire

Deck Thickness: 8”

Sketches:

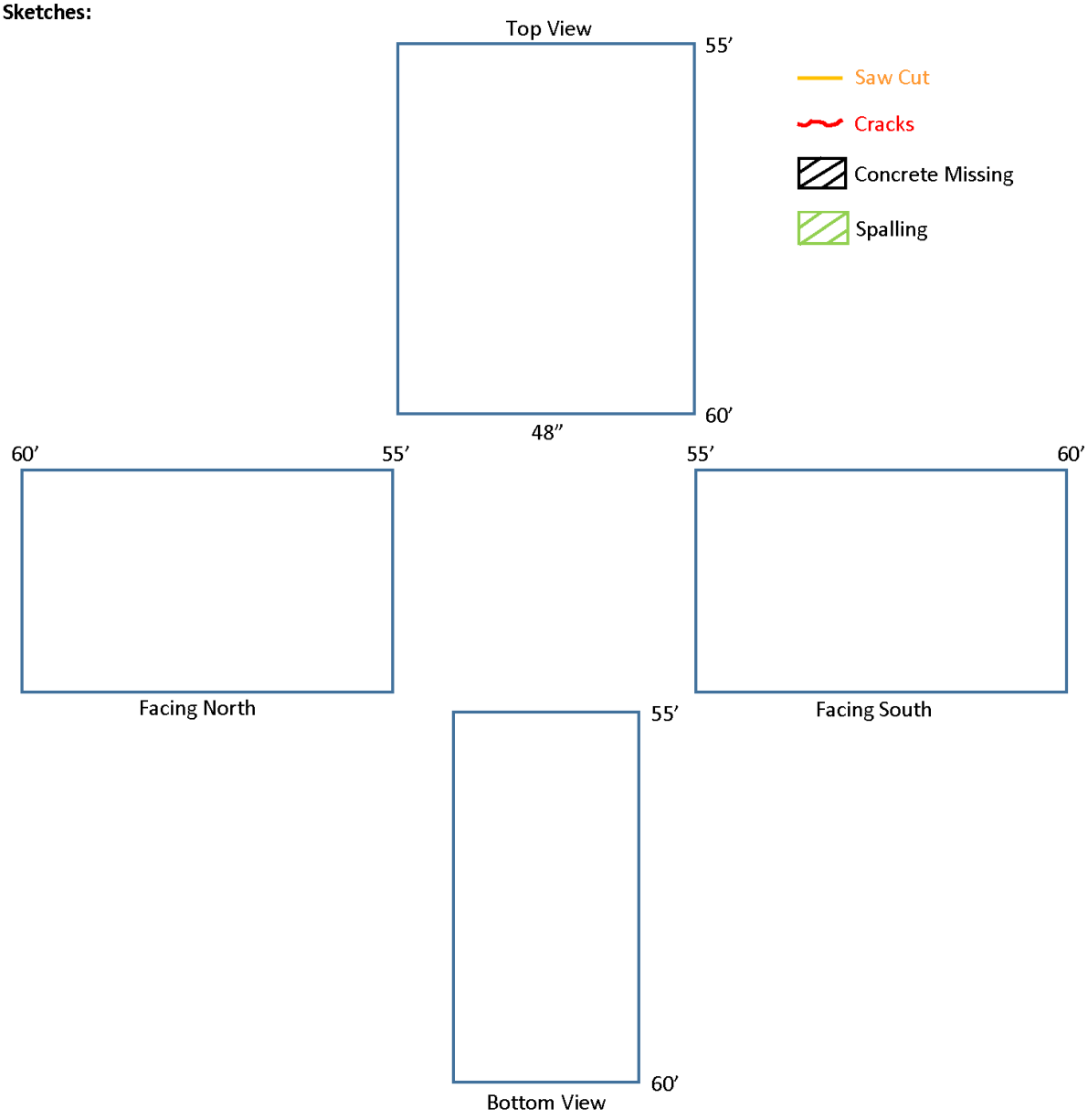

Girder ID: G **Section:** 60’-65’

Notes:

West End: 0’ line
East End: Main Fire

Deck Thickness: 8”

Sketches:

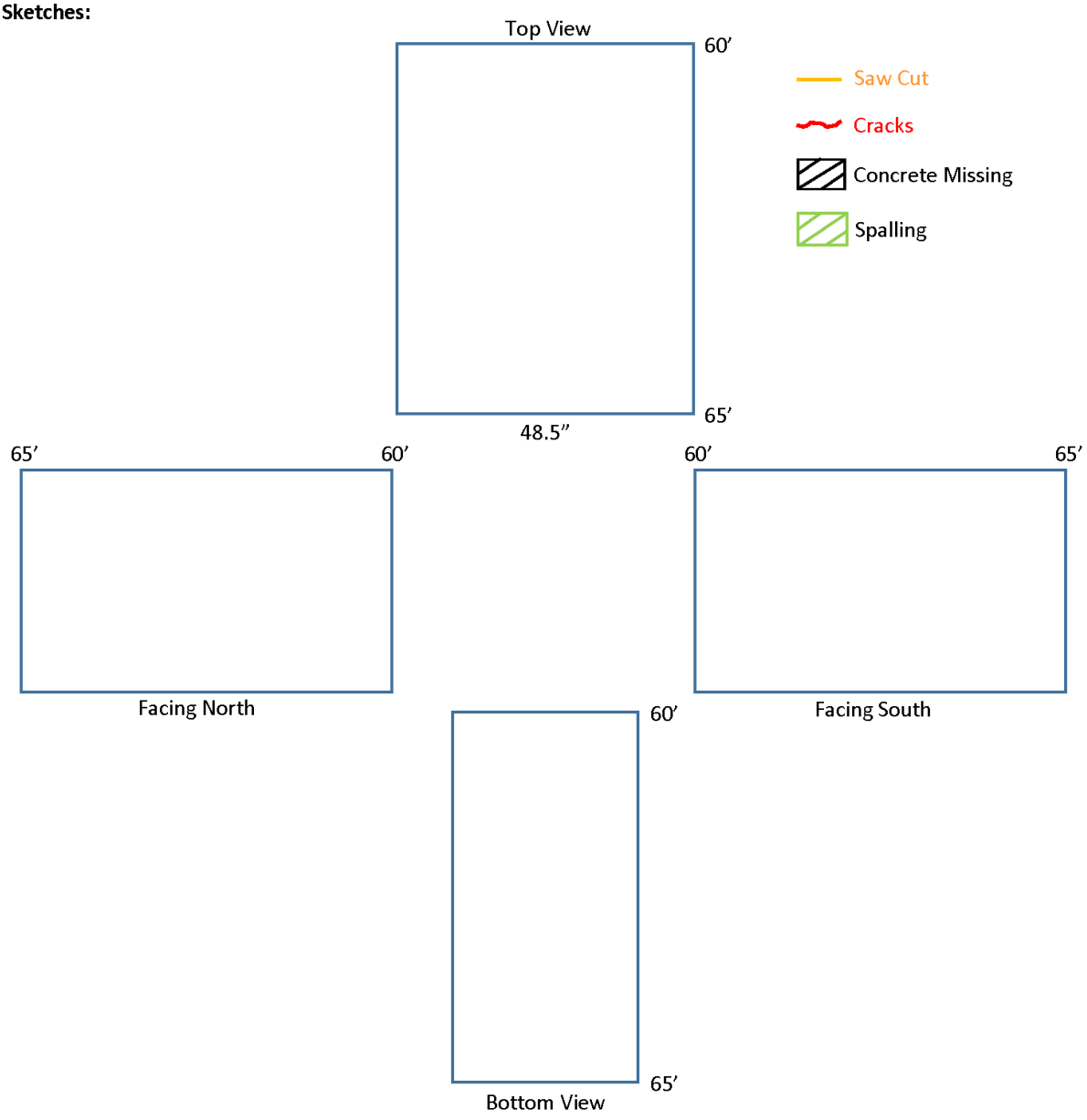

Girder ID: G **Section:** 65’-70’

Notes:

West End: 0’ line
East End: Main Fire

Deck Thickness: 8”

Sketches:

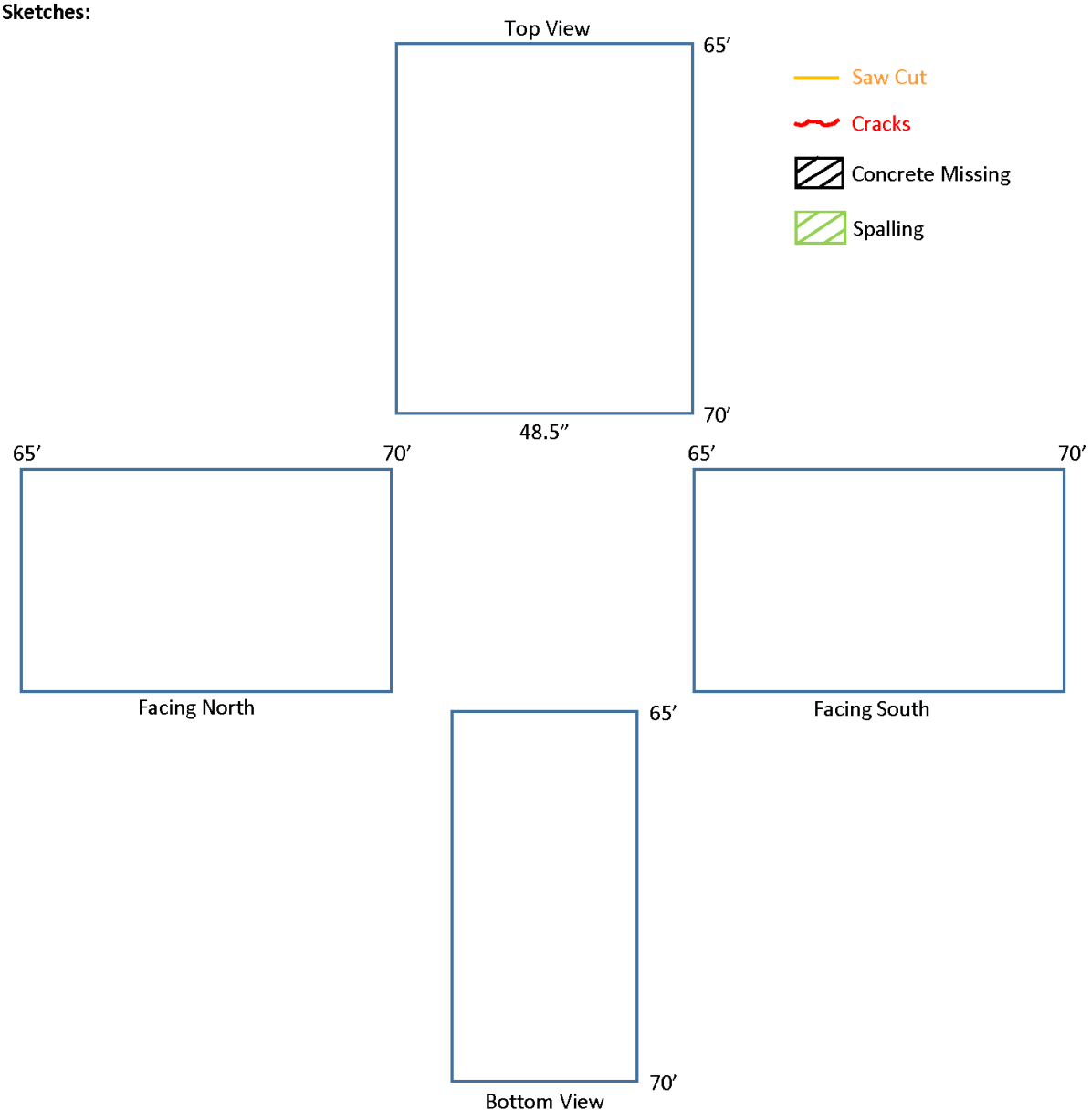

Girder ID: G **Section:** 70'-75'

Notes:

West End: 0' line
East End: Main Fire

Deck Thickness: 8"

Sketches:

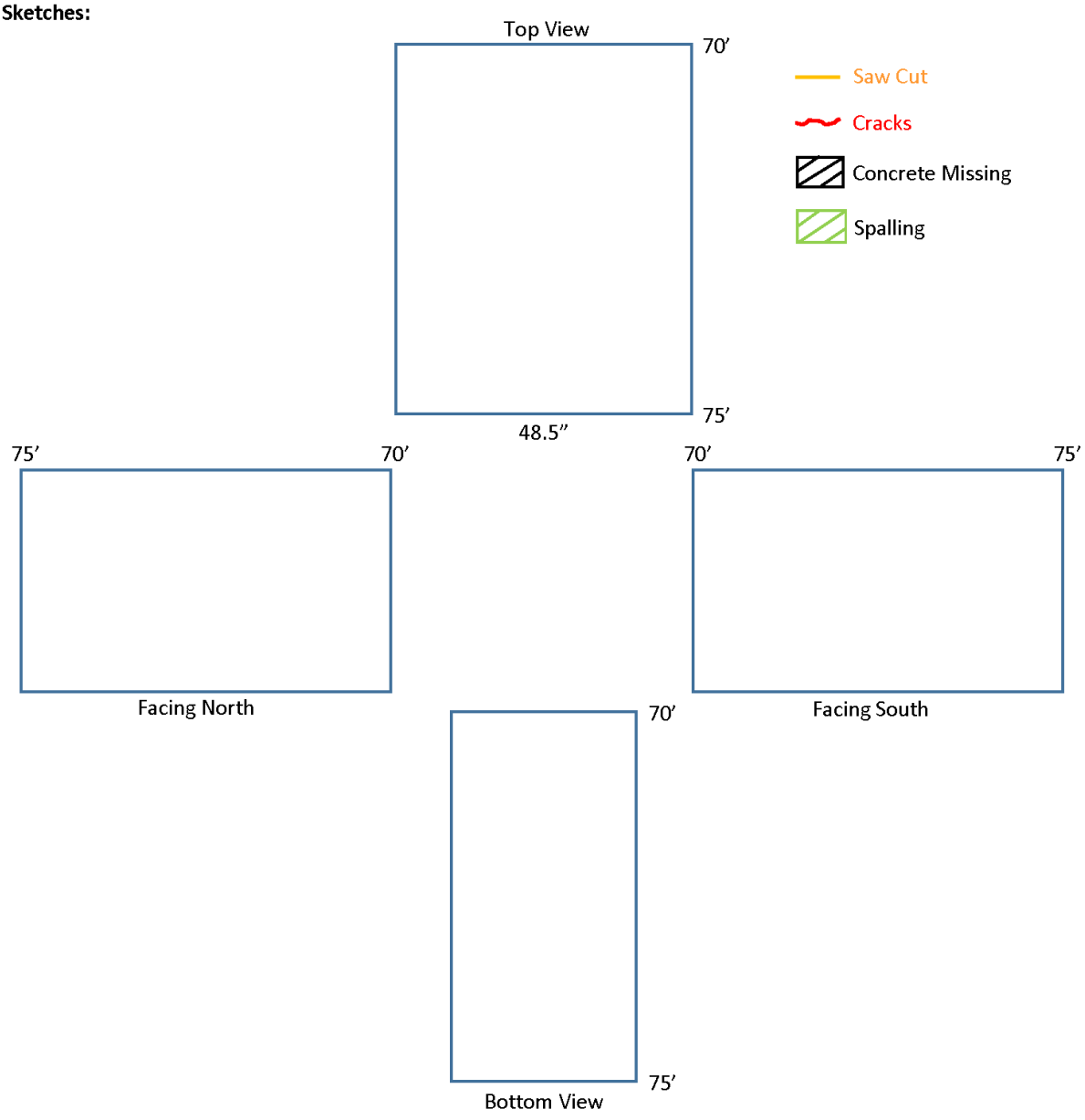

Girder ID: G **Section:** 75'-80'

Notes:

West End: 0' line
East End: Main Fire

Deck Thickness: 8"

Sketches:

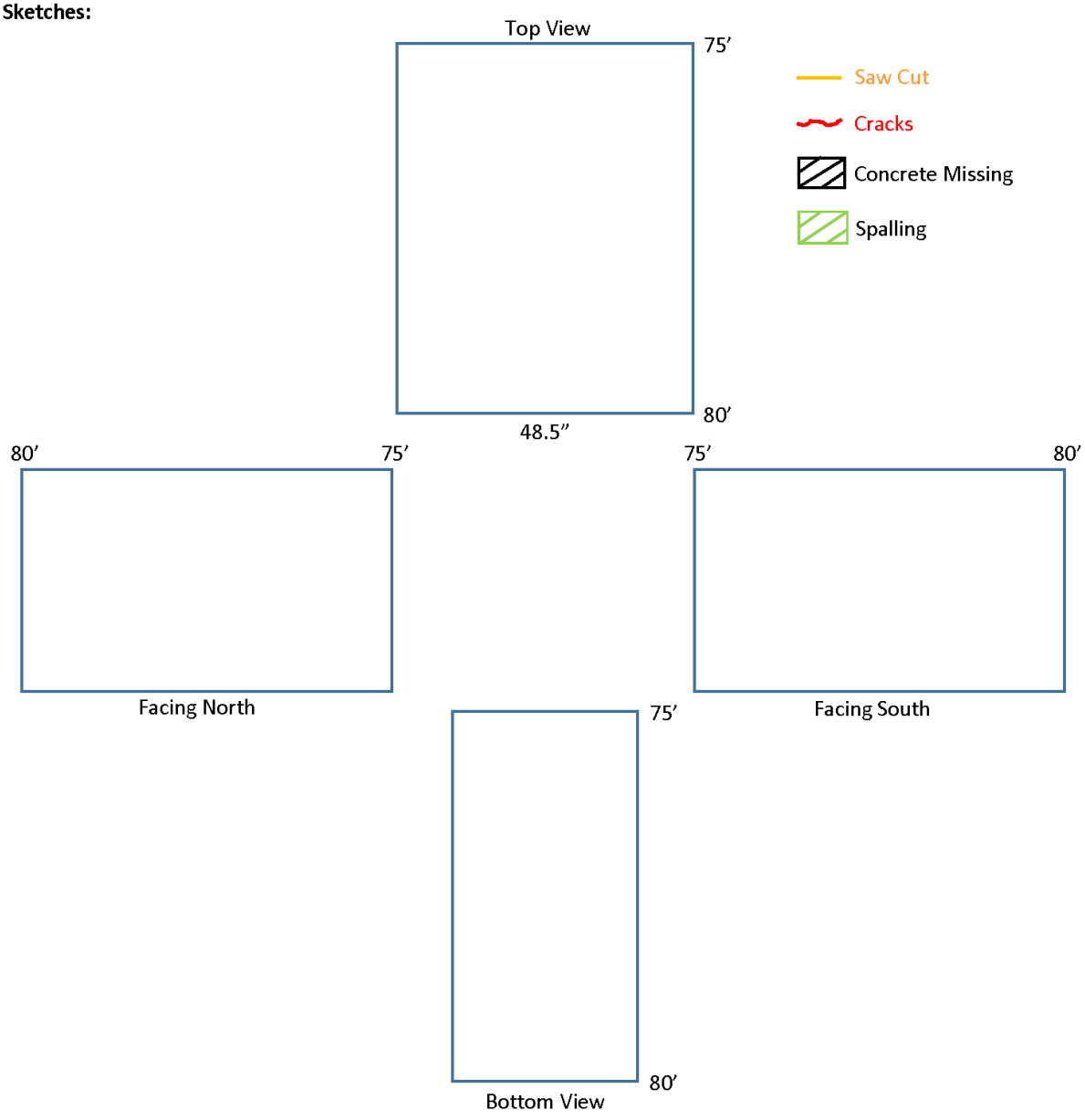

Girder ID: G **Section:** 80’-85’

Notes:

West End: 0’ line
East End: Main Fire

Deck Thickness: 8”

Sketches:

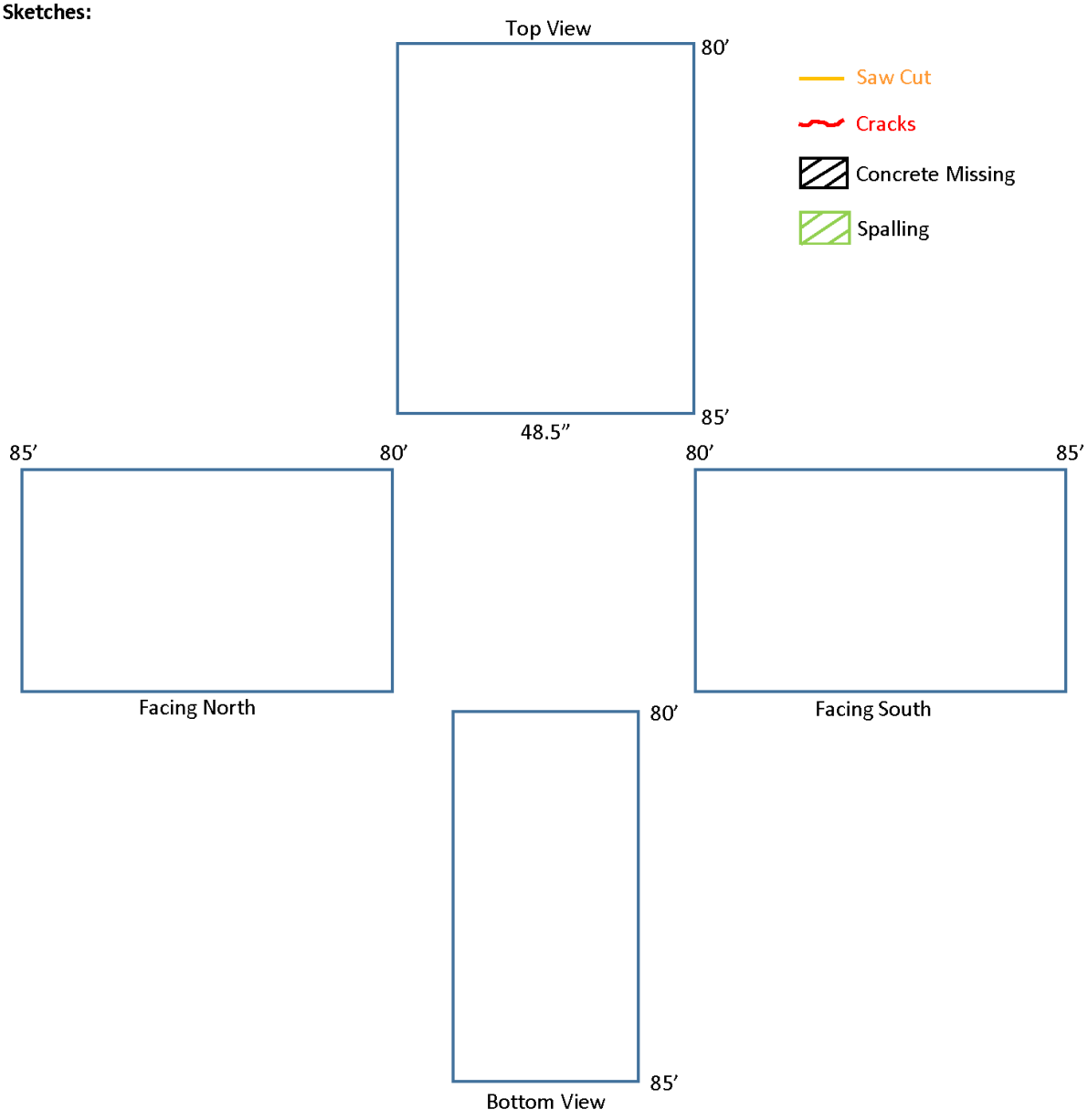

Girder ID: G **Section:** 85’-86.4’

Notes:

West End: 0’ line
East End: Main Fire

Deck Thickness: 8”

Sketches:

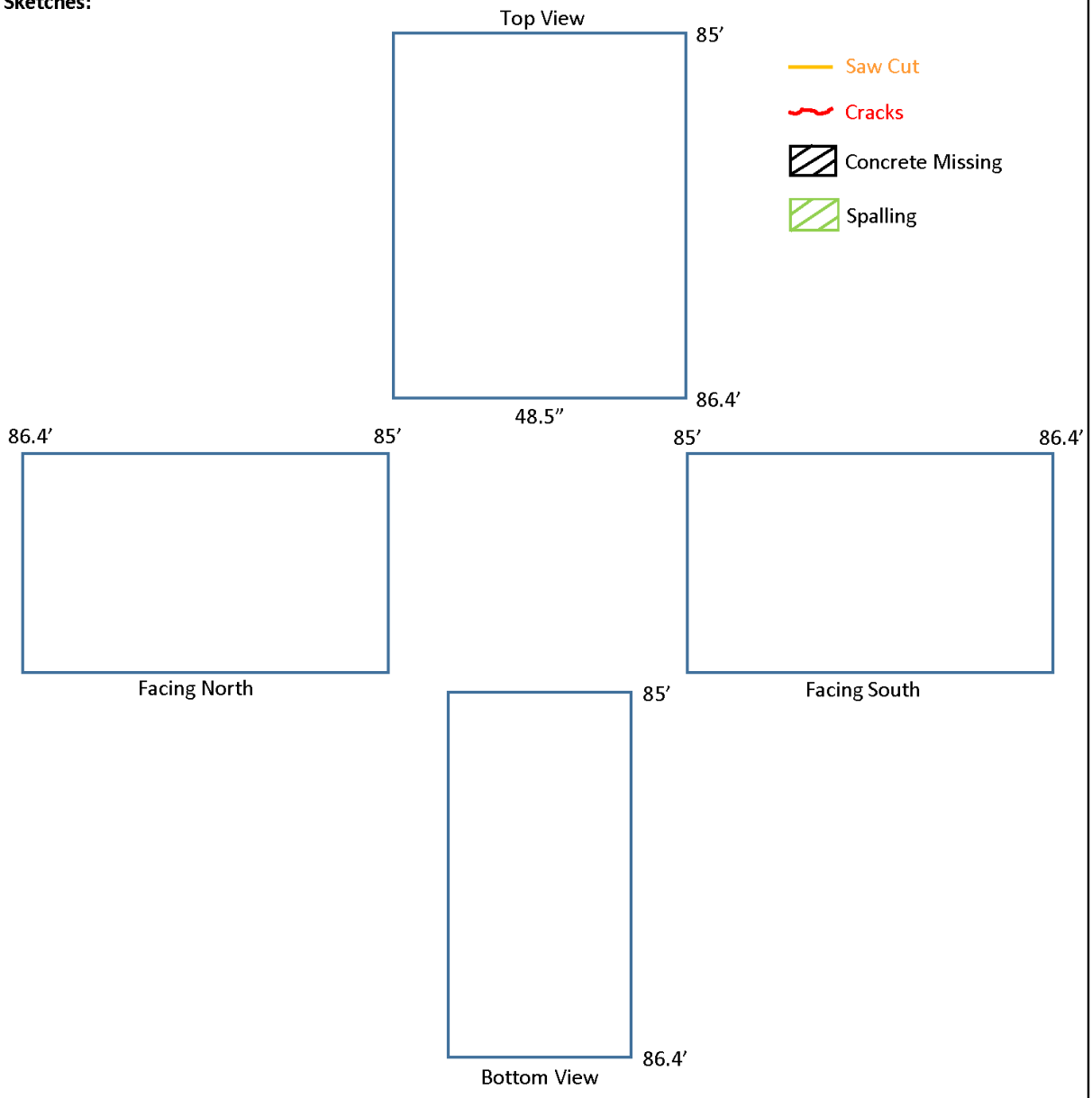

THE INSTITUTE FOR TRANSPORTATION IS THE FOCAL POINT FOR TRANSPORTATION AT IOWA STATE UNIVERSITY.

InTrans centers and programs perform transportation research and provide technology transfer services for government agencies and private companies;

InTrans contributes to Iowa State University and the College of Engineering's educational programs for transportation students and provides K–12 outreach; and

InTrans conducts local, regional, and national transportation services and continuing education programs.

IOWA STATE UNIVERSITY

Visit **InTrans.iastate.edu** for color pdfs of this and other research reports.